J

journal of

CO

computational

DE

design

JCODe
Journal of Computational Design

J
CO
DE

journal of

computational

design

JCoDe
Journal of Computational Design

İTÜ

Hesaplamalı Tasarımda Tolerans

Editörden

Hesaplamalı tasarımda "tolerans", sadece bir ölçü ya da mühendislik terimi olmanın ötesinde, belirsizliklerle baş etme, farklılıklara açıklık ve kusurla uzlaşma kültürünü de içinde barındırmaktadır. Geometrik hassasiyetin, üretim doğruluğunun, sistem esnekliğinin ve malzeme davranışlarının ara kesitinde yer alan bir kavram olarak tolerans, kesinlik ve kontrol ilkelerinin ötesine geçen yeni bir bakış açısıyla ele alınmayı gerektirmektedir. Deleuze ve Guattari farklılık, akışkanlık ve katmanlılık kavramları ile toleransı, yeni bir ontolojik zemin üzerinde ele almaya davet etmektedir. Soyutlamanın doğasında yer alan indirgeme ile dijital ortamda verinin temsilinde yaşanan kayıplar kesinlik hedefine ulaşmayı güçleştirmektedir. Bununla birlikte dijital doğrulukla fiziksel üretim gerçekliği arasında ortaya çıkan farkların yarattığı boşluk, üretken bir tasarım alanı olarak karşımıza çıkmaktadır. JCoDe'un on üçüncü sayısı, dijital araçların sunduğu kesinlik ilkesine karşın, fiziksel üretim dünyasının belirsizlikleriyle kurulan ilişkiyi anlamaya ve yeniden tartışmaya açmaktadır.

Hesaplamalı tasarım, yüksek doğrulukta modelleme, üretken algoritmalarla biçim oluşturma, performans optimizasyonu ve dijital üretim teknikleri ile yeni olanaklar sunarken; fiziksel gerçeklikteki üretim süreçleri, çoğu zaman bu soyutlamalara ve dijital ideallere karşı belirli sınırlar koymaktadır. Sayısal modelleme ve üretim süreçlerinde hata paylarını sıfırlamak çoğu zaman gerçekçi olmamaktadır. Dijital fabrikasyon araçlarının hassasiyetinden, 3B yazıcıların malzeme akış hızına; ahşabın nem değişkenliğinden, betonun priz süresine kadar uzanan bu üretim gerçekliği, dijital olarak modellenen sistemlerin esnekliklerini, hataya dayanıklılıklarını ve uyarlanabilirliklerini test etmektedir. Tam da bu noktada, tolerans yalnızca "izin verilen hata payı" değil, aynı zamanda dijital ile fiziksel arasındaki ara yüzün üretken bir bileşeni, tasarımı olası kılan bir aralık, hata ile olan yaratıcı diyaloğun bir temsilidir.

Özellikle parametrik modelleme ve genetik algoritmalar gibi optimizasyon süreçlerinde, tekil sabitler yerine belirli aralıklarla tanımlanan parametrelerle çalışmak; örneğin, yerel optimumda sıkışan bir genetik algoritmanın belirli hata marjlarını tolere ederek daha verimli sonuçlara ulaşması gibi durumlarda, sistemin esnekliğini artırmaktadır. Benzer şekilde, insan-makine etkileşimi bağlamında fiziksel üretim ortamlarında fabrikasyon araçları ve robotlarla kurulan işbirliklerinde, ya da artırılmış gerçeklik ve yapay zekâ destekli tasarım süreçlerinde insanın sezgisel, kimi zaman belirsiz ve öngörülemez kararları ile makinenin deterministik işleyişi arasında bir ara yüz görevi gören tolerans, bu iki öznenin verimli ve esnek biçimde birlikte çalışabilmesini mümkün kılan bir müzakere alanı sunmaktadır.

Bu çerçevede JCoDe'un onüçüncü sayısında, hesaplamalı tasarım süreçlerinde toleransın kuramsal açılımları, malzeme ve algoritmik yaklaşımları, model ve sürecin esnekliği, malzeme davranışlarıyla etkileşim, optimizasyon süreçlerinde esneklik, insan-makine etkileşiminde uyumlanma ve işbirliği ile kentsel ve çevresel ölçekteki uygulamaları çok yönlü biçimde ele alınmaktadır. DELEREL ve TAN BAYRAM'ın çalışması, tolerans kavramını kontrol ve kesinlikten olasılığa doğru kaydırarak dijital mekânın üretiminde farklılık ve etkileşimin rolünü tartışmaya açarken, etkileşimli ve karmaşık sistemler aracılığıyla belirsizliğin tasarımın üretken bir parçası haline gelişini gündeme getirmektedir.

Malzeme ve algoritmik yaklaşımlara odaklanan iki makale ise hesaplamalı modeller ile fiziksel gerçeklik arasındaki ilişkinin tolerans kavramıyla nasıl dönüştürülebileceğini ele almaktadır. Gözde Damla TURHAN HASKARA, bakteriyel selülozun büyümesini simüle ederek biyomimetik tasarım süreçlerinde malzeme davranışlarının öngörülemezliğini üretken bir girdiye dönüştürmektedir. Zehra GÜLOĞLU ve Sevil YAZICI ise genişleyebilen (auxetic) metamateryal tasarımları üzerinden geometrik parametreler, modelleme ve prototiplemenin toleransla kurduğu ilişkiyi incelemekte, esnek ve uyarlanabilir sistemlerin nasıl geliştirilebileceğini tartışmaktadır.

Uygulama ve kent ölçeğine yönelen çalışmalar ise toleransın toplumsal ve çevresel boyutlarına ışık tutmaktadır. Fadime DİKER ve İlker ERKAN, pandemi sonrası eğitim mekânlarında sınıf kapasitelerinin belirlenmesinde veri odaklı bir yaklaşım sunarken; Gizem ÖZÇIDEM SÜMEN, İlayda Şevval ALIŞ, Göktürk BOSTANCI, Barış Mert KARASU ve Özgür EDİZ, afet sonrası toplanma alanlarının Voronoi diyagramları ve mekân dizimi yöntemleriyle nasıl değerlendirilebileceğini ortaya koymaktadır. Zuhal CAN ve Kübra ÖZTÜRK'ün çalışması ise yapay zekâ ve nesnelerin interneti tabanlı tahmin sistemleri üzerinden hava kalitesi öngörülerini ele alarak toleransın çevresel belirsizliklerle kurduğu ilişkiyi gündeme taşımaktadır.

Sayı, Burcu KISMET CONK ve Meryem Birgül ÇOLAKOĞLU'nun kapsamlı derlemesiyle tamamlanmaktadır. Dijital çağda döngüsel yapı çevresine odaklanan bu çalışma, sürdürülebilirlik, kaynak yönetimi ve hesaplamalı tasarım ilişkisini disiplinlerarası bir perspektiften yeniden değerlendirmekte ve sayının tartışmalarını bütüncül bir çerçevede birleştirmektedir.

Tolerance in Computational Design

Editorial

In computational design, "tolerance" is not merely a metric or engineering term—it embodies a culture of dealing with uncertainty, embracing difference, and negotiating with imperfection. As a concept situated at the intersection of geometric precision, production accuracy, system flexibility, and material behavior, tolerance calls for a new perspective that goes beyond the principles of exactitude and control. Deleuze and Guattari, with their concepts of difference, fluidity, and multiplicity, invite us to rethink tolerance on a new ontological ground. The inherent reductionism of abstraction and the inevitable loss in data representation within digital environments challenge the pursuit of precision. However, the gap between digital accuracy and physical production reality opens up a generative space for design. The thirteenth issue of JCoDe aims to examine and question the relationship between the precision promised by digital tools and the uncertainties of the physical world of making.

While computational design enables new possibilities through high-precision modeling, form generation with generative algorithms, performance optimization, and digital fabrication techniques, physical production processes often impose constraints on these abstractions and digital ideals. Attempting to eliminate error margins in digital modeling and manufacturing processes is often unrealistic. The realities of production—ranging from the sensitivity of digital fabrication tools and the material flow rate of 3D printers to the moisture variability of wood and the curing time of concrete—test the flexibility, fault tolerance, and adaptability of digitally modeled systems. At this point, tolerance is not only the "acceptable margin of error," but also a generative component of the interface between digital and physical; it is a range that enables design, a representation of the creative dialogue with error.

Especially in optimization processes such as parametric modeling and genetic algorithms, working with parameters defined within specific ranges instead of fixed constants enhances system flexibility. For instance, allowing a genetic algorithm that is stuck in a local optimum to tolerate certain error margins can lead to more efficient outcomes. Similarly, in the context of human-machine interaction, tolerance acts as an interface between the intuitive, sometimes ambiguous and unpredictable decisions of humans and the deterministic functioning of machines—particularly in collaborative settings involving fabrication tools and robots in physical production environments, or in design processes supported by augmented reality and artificial intelligence. In these cases, tolerance provides a space of negotiation that enables these two agents to work together productively and flexibly.

In this context, the thirteenth issue of JCoDe addresses the multifaceted reflections of tolerance in computational design processes, including theoretical inquiries, material and algorithmic approaches, model and process flexibility, interactions with material behaviors, adaptability in optimization processes, human–machine collaboration, as well as urban and environmental applications. The study by DELEREL and TAN BAYRAM shifts the concept of tolerance from control and precision toward contingency, opening a discussion on the role of difference and interaction in the production of digital space, while also foregrounding how uncertainty becomes a productive component of design through interactive and complex systems.

Two articles focusing on material and algorithmic approaches explore how the relationship between computational models and physical reality can be reframed through the lens of tolerance. Gözde Damla TURHAN HASKARA simulates the growth of bacterial cellulose, transforming the unpredictability of material behavior into a productive input within biomimetic design processes. Zehra GÜLOĞLU and Sevil YAZICI, on the other hand, examine auxetic metamaterial designs, discussing how geometric parameters, modeling, and prototyping intersect with tolerance in the development of flexible and adaptive systems.

The studies oriented toward application and urban scale shed light on the social and environmental dimensions of tolerance. Fadime DİKER and İlker ERKAN present a data-driven approach to determining classroom capacities in the post-pandemic context, while Gizem ÖZÇİDEM SÜMEN, İlayda Şevval ALIŞ, Göktürk BOSTANCI, Barış Mert KARASU, and Özgür EDİZ demonstrate how Voronoi diagrams and space syntax methods can be used to evaluate emergency assembly areas. The study by Zuhal CAN and Kübra ÖZTÜRK, meanwhile, addresses air quality predictions through AI- and IoT-based forecasting systems, foregrounding the relationship between tolerance and environmental uncertainties.

The issue concludes with a comprehensive review by Burcu KISMET CONK and Meryem Birgül ÇOLAKOĞLU, which focuses on the circular built environment in the digital age. This work re-examines the interrelations of sustainability, resource management, and computational design from an interdisciplinary perspective, weaving together the discussions of the issue within a holistic framework.

JCoDe
Journal of Computational Design

Rethinking Tolerance through Interactive and Complex Architectural Systems

Zehra Delerel[1], Funda Tan Bayram[2]

ORCID NO: 0009-0005-6383-0639 [1], 0000-0001-2345-6789[2]

[1] Gebze Technical University, Institute of Graduate Studies, Department of Architecture, Kocaeli, Türkiye
[2] Gebze Technical University, Faculty of Architecture, Department of Architecture, Kocaeli, Türkiye

This study redefines tolerance within computational design, shifting it from a margin of error toward an interactive, uncertainty-driven, and context-sensitive design strategy. Two custom Python scripts developed in Rhino 3D demonstrate how tolerance operates across dual-wall systems responsive to attractor points. Code 1 produces spatial contrast and topological tension through opposing wall behaviors, while Code 2 generates coherence and porosity through synchronized responses. The comparative analysis reveals that tolerance functions on multiple levels: uncertainty (randomized attractors and micro-variation), bounded variability (extrusion ranges between 15–60 units), behavioral contrast (Code 1), behavioral coherence (Code 2), permeability (aperture scaling), and semantic flexibility (4-bit threshold-based encoding). Scenario testing confirmed these distinctions: Code 1 generated greater variability and contrast across runs, while Code 2 exhibited more consistent and homogeneous fields. These findings resonate with McVicar's (2016) definition of tolerance as a "range of opportunity," showing that identical inputs can yield divergent spatial outcomes. The results demonstrate that tolerance is not a passive technical allowance but an active design agent embedded within coding logic. By transforming uncertainty into structured variability, tolerance enables architectural surfaces to evolve beyond optimized façades into dynamic, data-rich, and temporally adaptive systems. The study highlights the capacity of digital environments to act as design participants, where codes and their generative ranges interact with context to produce new spatial possibilities. Future research should extend this approach through broader software platforms, larger datasets, and physical prototyping, enabling tolerance to be examined at more comprehensive experimental and applied levels.

211

Interaktif ve Karmaşık Mimari Sistemler Üzerinden Toleransı Yeniden Düşünmek

Zehra Delerel[1], Funda Tan Bayram[2]

ORCID NO: 0009-0005-6383-0639 [1], 0000-0001-2345-6789[2]

[1] Gebze Teknik Üniversitesi, Lisansüstü Eğitim Enstitüsü, Mimarlık Anabilim Dalı, Kocaeli, Türkiye
[2] Gebze Teknik Üniversitesi, Mimarlık Fakültesi, Mimarlık Bölümü, Kocaeli, Türkiye

Bu çalışma, tolerans kavramını hesaplamalı tasarım bağlamında yeniden ele almakta; onu hata payı olmaktan çıkarıp etkileşim, belirsizlik ve bağlamsal duyarlılığa dayalı üretken bir stratejiye dönüştürmektedir. Rhino 3D'de geliştirilen iki özel Python betiği, çekim noktalarına yanıt veren ikili duvar sistemleri üzerinden toleransın farklı biçimlerde nasıl işlediğini ortaya koymuştur. Kod 1, yüzeyler arasında karşıtlık ve topolojik gerilim üretirken; Kod 2, senkronize davranışlarla daha bütünlüklü ve geçirgen alanlar oluşturmuştur. Karşılaştırmalı analiz, toleransın çok katmanlı işlediğini göstermektedir: belirsizlik (rastlantısal çekim noktaları, mikro-varyasyon), sınırlandırılmış değişkenlik (15–60 birimlik ekstrüzyon aralıkları), davranışsal karşıtlık (Kod 1), davranışsal uyum (Kod 2), geçirgenlik (açıklık ölçekleri) ve anlamsal esneklik (4-bitlik kodlama). Senaryo testleri bu katmanları doğrulamış; Kod 1 daha yüksek çeşitlilik ve kontrast, Kod 2 ise daha tutarlı ve homojen davranışlar üretmiştir. Böylece toleransın, McVicar'ın (2016) tanımladığı gibi, "fırsat aralığı" sunduğu ve aynı girdilerin farklı mekânsal çıktılar doğurabildiği gösterilmiştir. Sonuçlar, toleransın yalnızca teknik bir kısıt değil, kodlama süreçlerine gömülü üretken bir tasarım aktörü olduğunu ortaya koymaktadır. Bu bağlamda tolerans, mimari yüzeylerin optimize edilmiş cephelerden öteye geçerek veri ve bağlamla şekillenen, tepki verebilen ve zamansal olarak evrilen sistemlere dönüşmesini sağlamaktadır. Çalışma, dijital ortamın tasarımda aktif bir rol üstlenebileceğini ve toleransın gelecekte daha kapsamlı, deneysel ve uygulamalı düzeylerde mekânsal etkileşimlerle sınanabileceğini ortaya koymaktadır.

212

JCoDe | Cilt 6 Sayı 2 | Eylül 2025 | Hesaplamalı Tasarımda Tolerans | Delerel, Z., Tan Bayram, F.

1. INTRODUCTION

The concept of tolerance in architecture has historically been associated with engineering precision, fabrication errors, and dimensional deviations. However, with the advent of computational and parametric design thinking, tolerance carries the potential to become a generative strategy that embraces uncertainty, openness, variability, and systemic adaptability within design processes. As Banihashemi et al. (2025) argue, parametric design offers critical points in the formation of design knowledge by establishing generative mechanisms and enabling the production of variants.

In this expanded sense, tolerance facilitates a shift from deterministic solutions toward probability-based systems, transforming the role of the designer from that of an absolute controller into a mediator of parametric thresholds. As Fattahi Tabasi et al. (2024) note, design strategies grounded in tolerance and parametric thresholds allow parametric design to develop its own methods for producing novel solutions and alternatives. Parametric design, thus acknowledged as a new approach in architectural practice, provides a unique methodological framework for generating diverse design outcomes and alternatives.

This shift—abandoning the pursuit of absolute precision at the core of computational design and instead embracing tolerance—acknowledges material, environmental, and human variability as inseparable elements of both design and production. Applied in this way, tolerance leads to the design of spaces open to personalization and reinterpretation. Aesthetically, this move signifies a departure from the pursuit of impossible precision toward an aesthetic that embraces variation and deviation (Kolarevic, 2014).

Surfaces, as the fundamental components of spatial articulation, can also be reconsidered within this context. Building envelopes—particularly façades—that surround everyday environments are often designed either with an emphasis on aesthetics or performance. In both cases, contemporary design practice increasingly aims to achieve "the most optimal façade formation." Current research even attempts to situate aesthetic preference within measurable frameworks through multi-objective optimization and expert systems, simultaneously

Rethinking Tolerance through Interactive and Complex Architectural Systems

enhancing daylight performance and aesthetic perception in façade design (Yi, 2009).

This raises the following question: can a surface, beyond merely being "optimal," also enable interaction, personalization, and reinterpretation through a tolerance-oriented design approach? In this regard, the present study aims to reframe the architectural concept of tolerance through computational tools. Instead of seeking singular optimized solutions, the computational process developed here is structured to generate variations that are body-referenced, interactive, tolerance-adaptive, and complexity-based.

The research investigates how interactive surfaces can be designed as variable, contextual, and responsive systems using two custom Python scripts developed in the Rhino 3D environment. These scripts produce dual-wall parametric systems in which extrusion and aperture values respond to attractor points, thereby generating topological variability.

In this context, the study demonstrates how tolerance can operate not merely as a technical constraint but as a performative, interactive, and context-sensitive design principle in architecture.

2. THEORETICAL BACKGROUND: INTERACTIVE ARCHITECTURE, COMPLEXITY, AND TOLERANCE

Interactive architecture presents a new design paradigm that moves away from producing static environments toward creating systems responsive to parameters such as environment, time, and uncertainty. This approach establishes a framework in which flows themselves become design decisions, enabling multiple possibilities rather than singular solutions. While flow constitutes the primary aim of interaction design, stability remains a fundamental goal of architecture—two objectives that converge (McCullough, 2005). Similarly, Fox and Kemp (2009) define interactive architecture as a hybrid between embedded computation (intelligence) and its physical counterpart (kinetics), which adapts through human–environment interaction. Oosterhuis (2007) further emphasizes that interactive architecture is not merely passively responsive but forms a system of two-way communication that requires two active participants.

214

JCoDe | Vol 6 No 2 | September 2025 | Tolerance in Computational Design| Delerel, Z., Tan Bayram, F.

The design and production stages of interactive architecture, being dependent on parameters, can be associated with parametric design. As Oxman (2017) states, parametric design develops diversified, discoverable, and context-based strategies for generative and performative design tied to specific goals. When such strategies of variation intersect with interactivity, differentiations emerge. For Oxman (2017), differentiation in architecture can be understood as the local specialization of a repetitive formation. The purpose of specializing part of a regular system is to produce new formal, functional, performative, and structural features as well as material behaviors.

Flows move beyond fixed conditions and instead generate real-time scenarios, thereby opening new fields of design. These openings are closely tied to the concept of tolerance. According to McVicar (2016), tolerance in design refers to a margin of opportunity that enables the negotiation of constructional difficulties—opportunities that are immediate and unanticipated. Bates and Sergison (1999) similarly describe tolerance as a technological framework that allows components of a system to be used in unconventional ways.

Rather than operating within temporally fixed states, interactive environments produce emergent, unexpected, and complex conditions that, in turn, generate perceptible fields of experience. As Yücel and Ökten (2020) argue, "The most significant factor obstructing the body's need for experience is the pursuit of comfort and ease." By contrast, the unpredictable conditions produced through tolerance create a form of disorder that is inherently more practical. For De Certeau (2008), space is defined as a practiced place.

Everyday life is directly tied to time and is continuous. Tolerance is not only limited to the moment of construction but can also be reproduced in alternative scenarios emerging within ongoing flows. Each temporal state thus yields a new condition of tolerance. Jules Moloney (2009) asserts that rather than a fixed design, the outcome is the kinetic system itself, within which countless permutations unfold over time. The temporality, variability, and generative potential of interaction produce new forms of productive tolerance. Through the integration of such variables, the concept of articulation becomes interchangeable with tolerance itself.

Rethinking Tolerance through Interactive and Complex Architectural Systems

Two practical forms of tolerance may arise. First, tolerance can be anticipated and accommodated through predesigned parameters controlled by the designer. Second, it may emerge unpredictably from the actions of bodies within everyday life. Both scenarios remain open to the unexpected: the first allows for generative deviations and new algorithmic formulations, while the second permits disappearance and spatial reconstitution depending on bodily engagement.

When tolerance manifests in unexpected moments, it may result in flawed outputs. While such outcomes are often perceived as undesirable or structural defects in contemporary practice, Venturi (2005) counters this view: "A structure without flaw has no virtue, for it is contrast that supports meaning." Oppositions create tensioned spatial relationships between bodies and architecture, giving rise to new interactive scenarios of experience.

In everyday life, the triad of body–space–technology is continuously experienced, and this interaction can be inscribed into spatial geometries. In this context, Michael Fox (2009) identifies the growing driving force behind interactive architecture as stemming from the increasingly technology-mediated interactions between humans and the built environment. The built environment today does not merely host human actions it becomes reconfigurable through them.

Architecture's adaptive capacity lies in rethinking the relationships between body and space. Understanding space not solely through geometric definitions, but also through the disproportionate, perceptual, and experiential relationships the body establishes with it, reveals the potential for surfaces to transform into a new form of skin one that is dynamic rather than passive. Park et al. (2011) regard such skins as interactive, kinetic surfaces integrating physical and content layers.

Digitally augmented surfaces that respond to stimuli such as light, sound, or motion are no longer simply façades or interior partitions; they become responsive, communicative, and transformative living textures. In this regard, Marcos Novak's (2001) concept of transactive intelligence is crucial for conceptualizing the potential of such surfaces. Transformability and variability foster complex interactions. According to Bundy (2007), increasing environmental complexity necessitates the

216

JCoDe | Vol 6 No 2 | September 2025 | Tolerance in Computational Design| Delerel, Z., Tan Bayram, F.

development of computational methods informed by complexity theory—a concern shared across disciplines. The importance here lies in the everyday nature of complex systems and their theoretical relevance to architecture.

In interactive systems, actions and reactions define systemic relationships. These interactions function through positive and negative feedback loops. While actions are initiated by human bodies and experiences, reactions may be architectural—or vice versa. In such scenarios, tolerance becomes dynamic and continuously mutable. The system logic here aligns with Norbert Wiener's mathematical models of feedback, where positive loops amplify change and negative loops suppress it. As Jaskiewicz (2013) argues, the design process should not be understood as producing a fixed final product but as an intervention within an evolving complex system. In this way, the designer's role shifts toward establishing systems that can accommodate and respond to variation—revealing systemic authorship capacity.

Contemporary parametric modeling approaches predominantly focus on formal variation and geometric control; however, they lack a framework that addresses tolerance as a dynamic threshold—one that can generate both constraints and creative opportunities. Theoretically, parametric design, by applying both generative and logical approaches, replaces the manual development of design alternatives with a design logic (Tabadkani, Banihashemi et al., 2018). Generative algorithmic modeling draws from both relational and productive modeling. As Nasir and Kamal (2023) emphasize, the term "algorithm" in this context underlines that objects are generated through algorithms, and their subsequent outputs for later design stages are likewise produced algorithmically.

Moreover, the complex behaviors of interactive and responsive systems must be reconciled with the real-time capacities of computational environments. Current models rarely address how surfaces can negotiate environmental interaction and algorithmic variability simultaneously within a generative system logic. This study fills this gap by repositioning tolerance as a data-driven, performative, and interactive design parameter. In doing so, tolerance is rendered both computationally measurable and analyzable through custom algorithmic tools. This approach moves away from deterministic

control, instead proposing a design framework that encodes systemic uncertainty and adaptability as integral qualities of architecture.

3. METHODOLOGY: DEVELOPMENT OF THE PARAMETRIC SCRIPTS

This research adopts a computational design methodology (Step 1, Framework and Data Setup) grounded in the principles of parametric modeling, data-driven variation, and tolerance-based adaptation. The dual-wall system is selected as the design focus, with attractor-based spatial conditions defining the primary inputs. Within this framework, randomized attractors introduce tolerance to spatial uncertainty, while the normalization of distance (t) and its processing through a sigmoid function (k parameter) establish tolerance bands and smooth sensitivity ranges (**Figure 1**).

Building on this foundation, two custom Python scripts were developed within the Rhino 3D environment (**Figure 1**). Code 1 encodes a dual-wall extrusion logic with opposing responses (left vs. right), while Code 2 implements a dual-wall aperture transformation with symmetric behaviors. At this stage, opposing wall logic defines a behavioral tolerance field, min–max extrusion ranges (15–60) set generative tolerance zones, and micro-variation (±0.012) introduces computational tolerance through controlled uncertainty. Aperture scaling further embeds permeability tolerance. The third stage focuses on exploring how these scripts generate local adaptation to attractors, behavioral contrast across wall surfaces, and semantic encoding of spatial conditions. Tolerance manifests as the system's capacity to accommodate uncertainty and variability while maintaining structural coherence. Iterative runs allow the observation of topological variability and emergent spatial effects.

Finally, a comparative evaluation was conducted between the two scenarios. Criteria such as spatial adaptability, performative potential, and semantic depth were defined to assess the outcomes. The analysis revealed that tolerance operates at multiple levels: as uncertainty (randomized attractors, micro-variation), as bounded variability (extrusion ranges), as behavioral contrast (opposing wall logic), and as semantic flexibility (thresholds) (**Figure 1**).

218

JCoDe | Vol 6 No 2 | September 2025 | Tolerance in Computational Design| Delerel, Z., Tan Bayram, F.
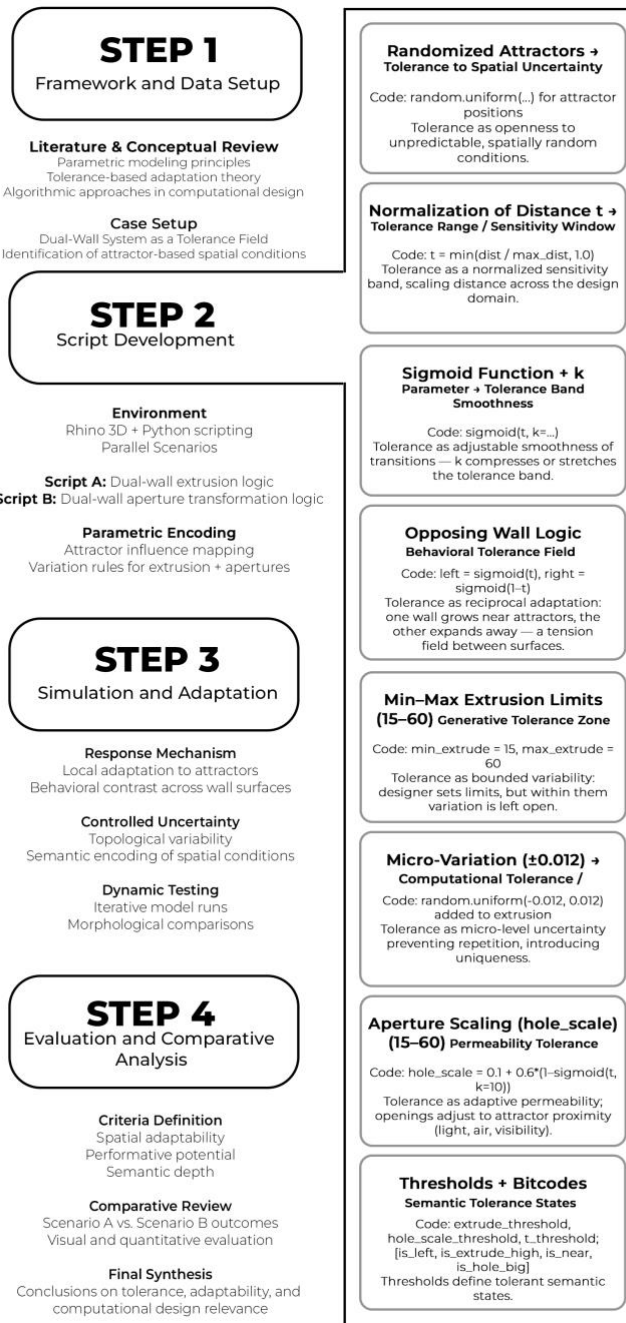
Figure 1: Methodological schema (Generated by the authors).

The synthesis of these findings underscores the relevance of tolerance-based adaptation in computational design and highlights its potential to articulate spatial systems that are both geometrically responsive and semantically encoded.

Rethinking Tolerance through Interactive and Complex Architectural Systems

4. FINDINGS

In this study, tolerance is redefined as a generative design principle. Within this framework, two custom Rhino Python scripts were developed to examine how tolerance operates on architectural surfaces through attractor-based variation, micro-scale uncertainty. The following section presents the models and scenarios generated, demonstrating how computational tools articulate responsiveness, ambiguity, and performative differentiation in architecture.

4.1 Code 1: Parallel Opposing Response

Code 1 establishes a computational system that generates parametric variations between two parallel walls based on the positions of attractor points. Its core strategy lies in orchestrating opposing responses from the two walls: as one wall volumetrically expands when approaching an attractor, the other reduces its growth as it moves away. This reciprocal behavior produces a topographical tension field between the two surfaces. As outlined in the theoretical framework, such reciprocity resonates with Wiener's (2019) notion of feedback loops, where positive responses amplify while negative ones suppress change, thereby situating tolerance as a dynamic mediator rather than a fixed constraint. The interpretation of this behavior goes beyond formal differentiation: it demonstrates how tolerance operates as a field condition that mediates between contrasting spatial logics, producing adaptable yet coherent configurations.

The originality of Code 1 lies in its integration of tolerance into dual-wall dynamics, where variability is generative design condition. Unlike conventional parametric models that often rely on uniform attractor responses, this system explicitly encodes reciprocity and divergence as a design principle. tolerance aligns with McVicar's (2016) view of a margin of opportunity and with Bates and Sergison's notion of unconventional use, since the bounded extrusion and aperture ranges create spaces for variation within control. By positioning tolerance as both a spatial mediator and a computational driver, Code 1 contributes a novel framework for reading and constructing architectural surfaces that are simultaneously adaptive, differentiated, and semantically encoded.

220

JCoDe | Vol 6 No 2 | September 2025 | Tolerance in Computational Design| Delerel, Z., Tan Bayram, F.

The primary intention of this script is to demonstrate the presence and legibility of the tolerance concept within a computational framework, using a dual-wall system inspired by responsive façade examples. In this setup, tolerance is embodied in the attractors' spatial positions and their influence on dynamic extrusion and aperture scaling. These behavioral differences between the two walls produce interactive spatial conditions. The attractor points, randomized and embedded within the space between the walls serve as spatial inputs that impact the system's behavior. Tolerance is positioned as spatial uncertainty: attractor placement acts as a variable input that challenges determinism and ensures adaptability. The randomness simulates unpredictable real-life conditions and reveals the potential for design to evolve through such uncertainty.

Extrusion values are developed along the normal surface and bounded by predefined minimum and maximum values (ranging from 15 to 60 units) (**Figure 3**). These limits define the extent of designer control yet they are intentionally left open to variability. As theorized, such bounded ranges function as tolerance zones producing unique configurations through attractor influence. These ranges create generative tolerance zones, where each attractor-driven variation results in a unique configuration. In this sense, tolerance is defined by the range of variations that operate within these limits (**Figure 2**). This reflects tolerance as bounded variability, where designer-defined thresholds create room for controlled openness.

For each grid cell, the shortest distance to any attractor point is calculated and normalized relative to the overall grid dimensions, resulting in a scalar value t. A t value closer to 0 indicates proximity to an attractor, while a value closer to 1 indicates greater distance (**Figure 3**). This distance serves as the foundation for all subsequent variations and determines the computational sensitivity of the spatial system.

Rethinking Tolerance through Interactive and Complex Architectural Systems

The script processes it through a sigmoid function, which compresses t between 0 and 1, generating smooth transitions rather than abrupt changes. This process demonstrates the difference between deterministic and probabilistic design. The same distance value can produce varying outcomes depending on the sharpness of the sigmoid curve (**Figure 2**).

Figure 2: Code 1 3d geometry (Generated by the author).

222

JCoDe | Vol 6 No 2 | September 2025 | Tolerance in Computational Design| Delerel, Z., Tan Bayram, F.
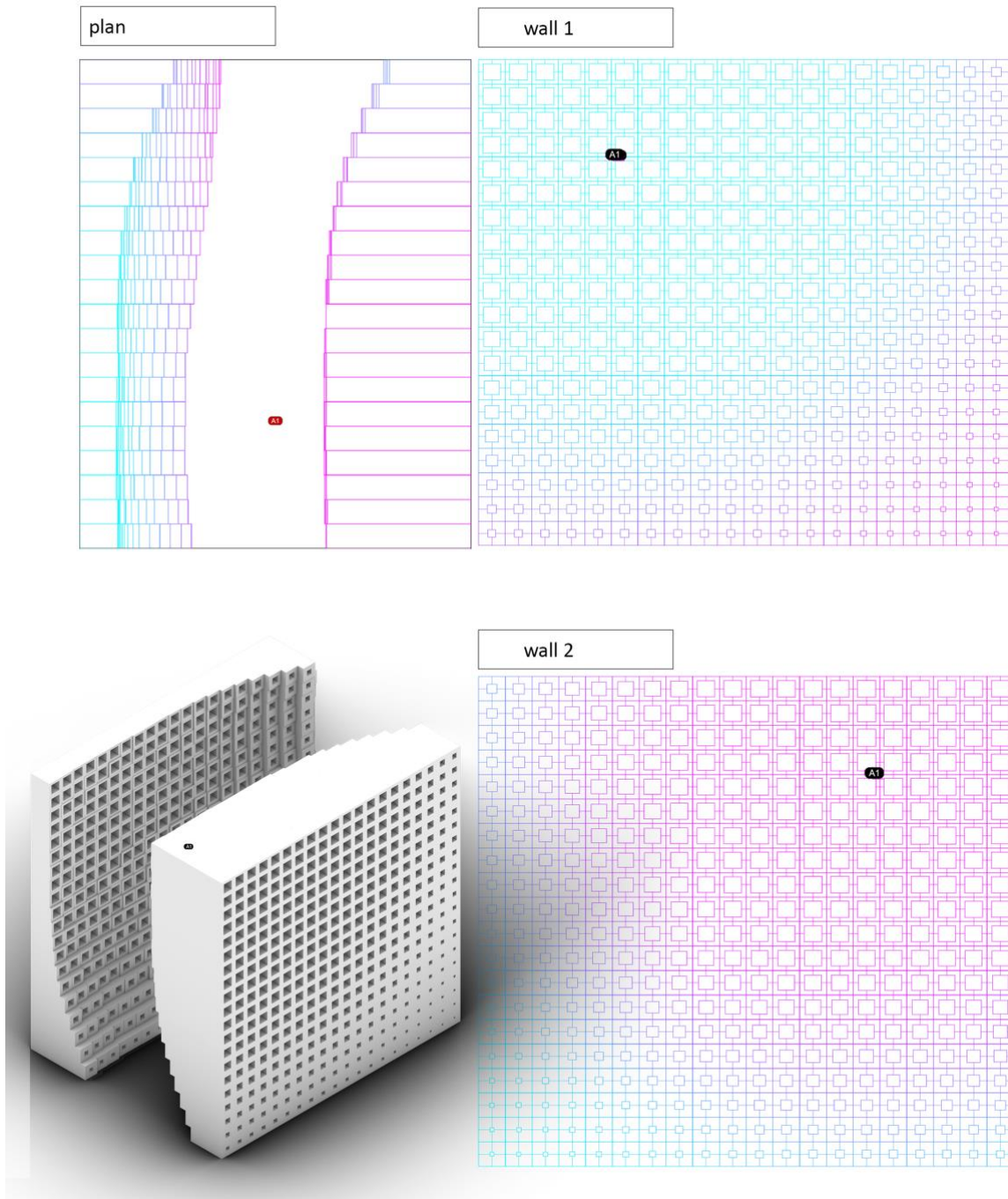
In the script, the sigmoid function is defined as:

$$(x, k) = \frac{1}{1 + e - k(x - 0.5)} \tag{1}$$

where x is the normalized distance (0–1) and k controls curve sharpness: higher k yields sharper transitions, lower k smoother gradients. This shows tolerance as adjustable thresholds and shifting sensitivities rather than fixed limits (**Equation 1**).

The extrusion logic of the two walls is intentionally inverse: Left Wall: Extrusion magnitude is directly proportional to sigmoid(t). As the cell approaches the attractor, its extrusion increases. Right Wall: Extrusion is determined by sigmoid(1-t). This wall expands more as it moves away from the attractor (**Figure 3**). This opposing wall logic operationalizes tolerance as behavioral contrast, encoding divergence as a generative design principle.

Although the system behavior is primarily defined at the level of the walls, an additional layer of algorithmic complexity is introduced: small-scale randomness (±0.012) is added to the extrusion values. These micro-variations break the determinism of the pattern and encode computational tolerance into the system. Such micro-level uncertainty prevents the formation of strictly repetitive units, enhancing the uniqueness of the surface. Each extruded unit also includes a central aperture (hole), with its scale calculated using the formula. This ensures that apertures are larger in regions closer to the attractors and smaller farther away. These perforations can serve as performance metrics—affecting spatial permeability, light transmission, or environmental integration (**Figure 2**).

```python
# -*- coding: utf-8 -*-
import rhinoscriptsyntax as rs
import math
import random

def sigmoid(x, k=10):
    return 1 / (1 + math.exp(-k * (x - 0.5)))

def map_turquoise_to_magenta(val, min_val, max_val):
    t = max(0.0, min(1.0, (val - min_val) / float(max_val - min_val)))
    r = int(255 * t)
    g = int(255 * (1 - t))
    b = 255
    return [r, g, b]

def generate_dual_walls(grid_size_x=50, grid_size_y=200, grid_size_z=200,
step=10, attractor_count=6):
    min_extrude = 15
    max_extrude = 60
    wall_offset = 20
    wall_x1 = 0
    wall_x2 = wall_x1 + 2 * wall_offset + max_extrude * 2
    micro_variation_strength = 0.012
    red_color = [255, 0, 0]

    # Thresholds
    extrude_threshold = 37.5
    hole_scale_threshold = 0.4
    t_threshold = 0.5

    # Create layer for bitcodes if it doesn't exist
    if not rs.IsLayer("bitcodes"):
        rs.AddLayer("bitcodes", color=red_color)

    # Generate attractors
    attractors = []
    for i in range(attractor_count):
        height = random.uniform(110, 180)
        pt = [
            random.uniform(wall_x1 + wall_offset + max_extrude, wall_x2 -
wall_offset - max_extrude),
            random.uniform(0, grid_size_y),
            height
        ]
        attractors.append(pt)
        rs.AddPoint(pt)
        rs.AddTextDot("A{}".format(i + 1), pt)

    def closest_distance(point):
        return min([rs.Distance(point, attr) for attr in attractors])

    def draw_square_frame_and_extrude(base_x, normal, extrude_amt,
hole_scale, color):
        p1 = [base_x, y, z]
        p2 = [base_x, y + step, z]
        p3 = [base_x, y + step, z + step]
        p4 = [base_x, y, z + step]
        outer = rs.AddPolyline([p1, p2, p3, p4, p1])

        cx = base_x
        cy = y + step / 2
        cz = z + step / 2
        s = (step * hole_scale) / 2
        q1 = [cx, cy - s, cz - s]
        q2 = [cx, cy + s, cz - s]
        q3 = [cx, cy + s, cz + s]
        q4 = [cx, cy - s, cz + s]
        inner = rs.AddPolyline([q1, q2, q3, q4, q1])

        surface = rs.AddPlanarSrf([outer, inner])
        rs.DeleteObject(outer)
        rs.DeleteObject(inner)

        if surface:
            vec = rs.VectorScale(normal, extrude_amt)
            path = rs.AddLine([0, 0, 0], vec)
            extr = rs.ExtrudeSurface(surface[0], path)
            rs.CapPlanarHoles(extr)
            rs.ObjectColor(extr, color)
            rs.DeleteObject(surface[0])
            rs.DeleteObject(path)
```

the continuation of the code

```python
    for y in rs.frange(0, grid_size_y - step, step):
        for z in rs.frange(0, grid_size_z - step, step):
            center = [(wall_x1 + wall_x2) / 2, y + step / 2, z + step / 2]
            dist = closest_distance(center)
            max_dist = math.sqrt(grid_size_y**2 + grid_size_z**2)
            t = min(dist / max_dist, 1.0)

            # Hole scale
            hole_raw = 1 - sigmoid(t, k=10)
            hole_raw = max(0.0, min(1.0, hole_raw))
            hole_scale = 0.1 + 0.6 * hole_raw

            # Left wall extrusion
            left_scale = sigmoid(t, k=12)
            left_scale = math.pow(left_scale, 1.1)
            left_scale += random.uniform(-micro_variation_strength,
micro_variation_strength)
            left_scale = max(0.0, min(1.0, left_scale))
            left_extrude_amt = min_extrude + (max_extrude -
min_extrude) * left_scale
            left_color = map_turquoise_to_magenta(left_extrude_amt,
min_extrude, max_extrude)

            # Right wall extrusion
            right_scale = sigmoid(1 - t, k=12)
            right_scale = math.pow(right_scale, 1.1)
            right_scale += random.uniform(-micro_variation_strength,
micro_variation_strength)
            right_scale = max(0.0, min(1.0, right_scale))
            right_extrude_amt = min_extrude + (max_extrude -
min_extrude) * right_scale
            right_color =
map_turquoise_to_magenta(right_extrude_amt, min_extrude,
max_extrude)

            # Draw geometry
            draw_square_frame_and_extrude(wall_x1, [1, 0, 0],
left_extrude_amt, hole_scale, left_color)
            draw_square_frame_and_extrude(wall_x2, [-1, 0, 0],
right_extrude_amt, hole_scale, right_color)

            # Binary logic
            is_near = 1 if t < t_threshold else 0
            is_hole_big = 1 if hole_scale > hole_scale_threshold else 0

            # Left wall bitcode
            is_left = 1
            is_extrude_high = 1 if left_extrude_amt > extrude_threshold
else 0
            bitcode_left = "{} {} {} {}".format(is_left, is_extrude_high,
is_near, is_hole_big)
            dot_pos_left = [wall_x1 + left_extrude_amt / 2, y + step / 2, z
+ step / 2 - 1]
            dot_left = rs.AddTextDot(bitcode_left, dot_pos_left)
            rs.ObjectLayer(dot_left, "bitcodes")
            rs.ObjectColor(dot_left, red_color)

            # Right wall bitcode
            is_left = 0
            is_extrude_high = 1 if right_extrude_amt >
extrude_threshold else 0
            bitcode_right = "{} {} {} {}".format(is_left, is_extrude_high,
is_near, is_hole_big)
            dot_pos_right = [wall_x2 - right_extrude_amt / 2, y + step /
2, z + step / 2 - 1]
            dot_right = rs.AddTextDot(bitcode_right, dot_pos_right)
            rs.ObjectLayer(dot_right, "bitcodes")
            rs.ObjectColor(dot_right, red_color)

    rs.Redraw()

def frange(start, stop, step):
    while start <= stop:
        yield start
        start += step

rs.frange = frange
generate_dual_walls()
```

Figure 3: Code 1 Rhinoscript (Generated by the authors).

4.2 Code 2: Synchronously Diverging Surfaces

Code 2 represents the second scenario of a dual-wall system generated through attractor-based parametric variation. In this case, both the left and right walls exhibit identical behavior: they increase in volume and reduce aperture size as they move away from the attractor points. While maintaining synchronized parametric responses across both surfaces, the code embeds tolerance into the system through micro-variations and semantic encodings. Code 2 frames tolerance as

224

JCoDe | Vol 6 No 2 | September 2025 | Tolerance in Computational Design| Delerel, Z., Tan Bayram, F.

Figure 4: Code 2 Rhinoscript and 3d geometry (Generated by the author).

synchronized adaptation, demonstrating how coherence and regularity can themselves serve as generative margins within parametric systems.

Rethinking Tolerance through Interactive and Complex Architectural Systems
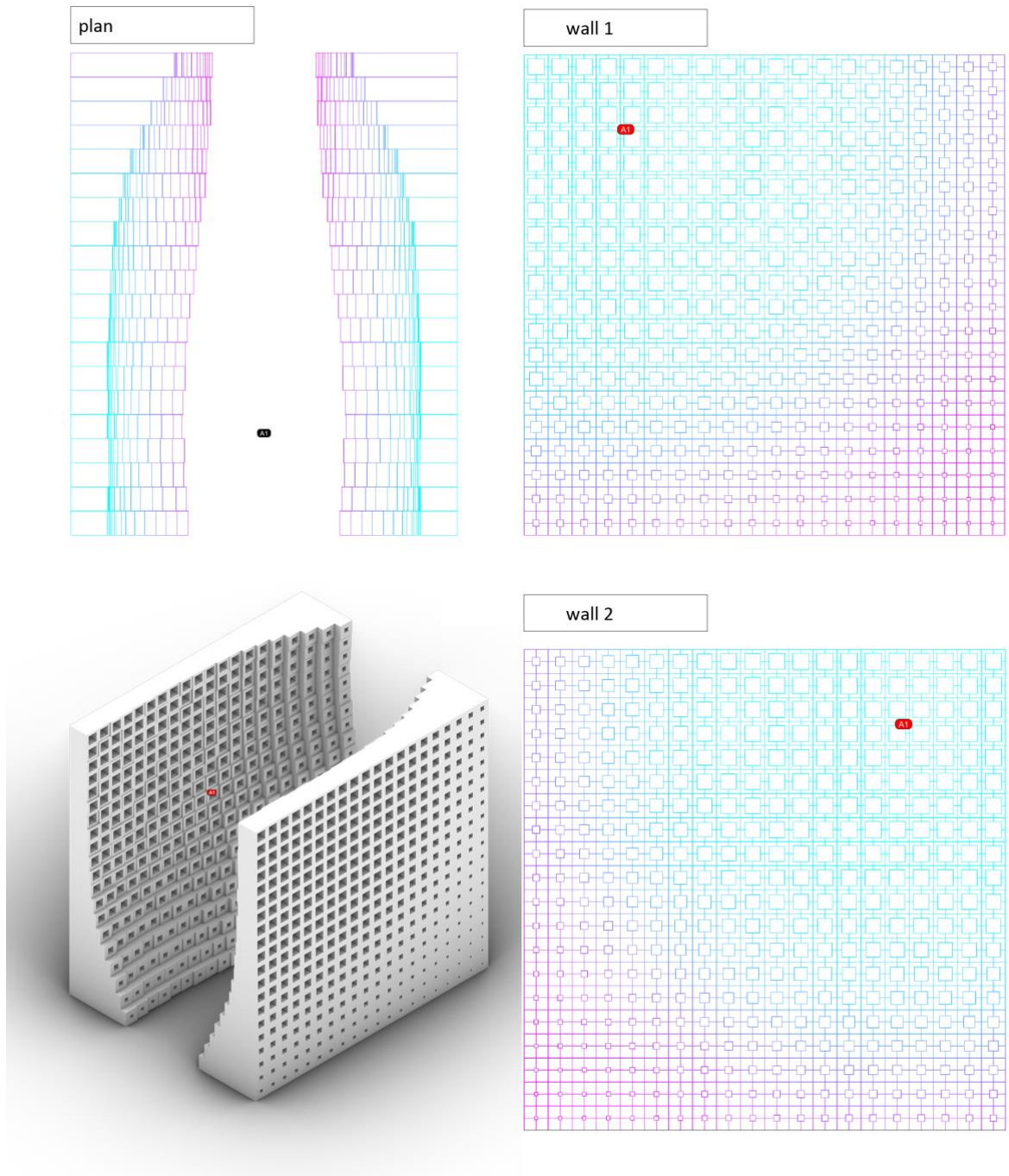
The architectural generation process unfolds through the following steps: The foundational structure of Code 2 mirrors that of Code 1. The script begins by constructing a three-dimensional grid, within which grid sizes along the x, y, and z axes define the bounds of the design domain and its zones of tolerance (**Figure 5**). Attractors are placed randomly within the space between the two walls, and their positions establish spatial intervals that trigger morphological transformation. As in the theoretical discussion of flows, these attractors embody spatial uncertainty, functioning as unpredictable inputs that generate openings for variation (McCullough, 2005).

As in Code 1, the grid serves as the base from which extrusion occurs along the surface normal, with each cell's shortest distance to the nearest attractor normalized into a scalar value .This value is processed through a sigmoid function to generate performative parameters such as extrusion height and aperture size, where tolerance operates as a sensitivity band: the sharpness coefficient k determines how smoothly or abruptly surfaces adapt to attractor proximity, framing tolerance as a tunable threshold of responsiveness. Unlike Code 1, both walls in Code 2 share the same extrusion logic, establishing a synchronized field of variation in which they expand simultaneously as they move away from attractors. This coordinated response embeds tolerance as bounded coherence, demonstrating adaptability through repetition and alignment rather than divergence, while added micro-variations prevent determinism and encode tolerance as micro-level uncertainty.

The relationship to hole scale mirrors that of Code 1, where aperture size increases as proximity to the attractor decreases. This inverse relationship creates context-sensitive porosity, shaped by spatial proximity to attractor fields (**Figure 4**). In this sense, permeability tolerance is inscribed in the surface logic, producing adaptable openings that mediate between light, air, and visibility—aligning with

226

JCoDe | Vol 6 No 2 | September 2025 | Tolerance in Computational Design| Delerel, Z., Tan Bayram, F.

the notion of interactive skins as dynamic, reconfigurable membranes (Park et al., 2011).

Figure 5: Code 2 Rhinoscript (Generated by the author).

```python
# -*- coding: utf-8 -*-
import rhinoscriptsyntax as rs
import math
import random

def sigmoid(x, k=10):
    return 1 / (1 + math.exp(-k * (x - 0.5)))

def map_turquoise_to_magenta(val, min_val, max_val):
    t = max(0.0, min(1.0, (val - min_val) / float(max_val - min_val)))
    r = int(255 * t)
    g = int(255 * (1 - t))
    b = 255
    return [r, g, b]

def generate_dual_walls(grid_size_x=50, grid_size_y=200, grid_size_z=200,
step=10, attractor_count=6):
    min_extrude = 15
    max_extrude = 60
    wall_offset = 20
    wall_x1 = 0
    wall_x2 = wall_x1 + 2 * wall_offset + max_extrude * 2
    micro_variation_strength = 0.012
    red_color = [255, 0, 0]

    # Thresholds
    extrude_threshold = 37.5
    hole_scale_threshold = 0.4
    t_threshold = 0.5

    # Create layer for bitcodes if it doesn't exist
    if not rs.IsLayer("bitcodes"):
        rs.AddLayer("bitcodes", color=red_color)

    # Generate attractors
    attractors = []
    for i in range(attractor_count):
        height = random.uniform(110, 180)
        pt = [
            random.uniform(wall_x1 + wall_offset + max_extrude, wall_x2 -
wall_offset - max_extrude),
            random.uniform(0, grid_size_y),
            height
        ]
        attractors.append(pt)
        rs.AddPoint(pt)
        rs.AddTextDot("A{}".format(i + 1), pt)

    def closest_distance(point):
        return min([rs.Distance(point, attr) for attr in attractors])

    def draw_square_frame_and_extrude(base_x, normal, extrude_amt,
hole_scale, color):
        p1 = [base_x, y, z]
        p2 = [base_x, y + step, z]
        p3 = [base_x, y + step, z + step]
        p4 = [base_x, y, z + step]
        outer = rs.AddPolyline([p1, p2, p3, p4, p1])

        cx = base_x
        cy = y + step / 2
        cz = z + step / 2
        s = (step * hole_scale) / 2
        q1 = [cx, cy - s, cz - s]
        q2 = [cx, cy + s, cz - s]
        q3 = [cx, cy + s, cz + s]
        q4 = [cx, cy - s, cz + s]
        inner = rs.AddPolyline([q1, q2, q3, q4, q1])

        surface = rs.AddPlanarSrf([outer, inner])
        rs.DeleteObject(outer)
        rs.DeleteObject(inner)

        if surface:
            vec = rs.VectorScale(normal, extrude_amt)
            path = rs.AddLine([0, 0, 0], vec)
            extr = rs.ExtrudeSurface(surface[0], path)
            rs.CapPlanarHoles(extr)
            rs.ObjectColor(extr, color)
            rs.DeleteObject(surface[0])
            rs.DeleteObject(path)


the continuation of the code

for y in rs.frange(0, grid_size_y - step, step):
    for z in rs.frange(0, grid_size_z - step, step):
        center = [(wall_x1 + wall_x2) / 2, y + step / 2, z + step / 2]
        dist = closest_distance(center)
        max_dist = math.sqrt(grid_size_y**2 + grid_size_z**2)
        t = min(dist / max_dist, 1.0)

        # Hole scale
        hole_raw = 1 - sigmoid(t, k=10)
        hole_raw = max(0.0, min(1.0, hole_raw))
        hole_scale = 0.1 + 0.6 * hole_raw

        # Left wall extrusion
        left_scale = sigmoid(t, k=12)
        left_scale = math.pow(left_scale, 1.1)
        left_scale += random.uniform(-micro_variation_strength,
micro_variation_strength)
        left_scale = max(0.0, min(1.0, left_scale))
        left_extrude_amt = min_extrude + (max_extrude -
min_extrude) * left_scale
        left_color = map_turquoise_to_magenta(left_extrude_amt,
min_extrude, max_extrude)

        # Right wall extrusion
        right_scale = sigmoid(1 - t, k=12)
        right_scale = math.pow(right_scale, 1.1)
        right_scale += random.uniform(-micro_variation_strength,
micro_variation_strength)
        right_scale = max(0.0, min(1.0, right_scale))
        right_extrude_amt = min_extrude + (max_extrude -
min_extrude) * right_scale
        right_color =
map_turquoise_to_magenta(right_extrude_amt, min_extrude,
max_extrude)

        # Draw geometry
        draw_square_frame_and_extrude(wall_x1, [1, 0, 0],
left_extrude_amt, hole_scale, left_color)
        draw_square_frame_and_extrude(wall_x2, [-1, 0, 0],
right_extrude_amt, hole_scale, right_color)

        # Binary logic
        is_near = 1 if t < t_threshold else 0
        is_hole_big = 1 if hole_scale > hole_scale_threshold else 0

        # Left wall bitcode
        is_left = 1
        is_extrude_high = 1 if left_extrude_amt > extrude_threshold
else 0
        bitcode_left = "{} {} {} {}".format(is_left, is_extrude_high,
is_near, is_hole_big)
        dot_pos_left = [wall_x1 + left_extrude_amt / 2, y + step / 2, z
+ step / 2 - 1]
        dot_left = rs.AddTextDot(bitcode_left, dot_pos_left)
        rs.ObjectLayer(dot_left, "bitcodes")
        rs.ObjectColor(dot_left, red_color)

        # Right wall bitcode
        is_left = 0
        is_extrude_high = 1 if right_extrude_amt >
extrude_threshold else 0
        bitcode_right = "{} {} {} {}".format(is_left, is_extrude_high,
is_near, is_hole_big)
        dot_pos_right = [wall_x2 - right_extrude_amt / 2, y + step /
2, z + step / 2 - 1]
        dot_right = rs.AddTextDot(bitcode_right, dot_pos_right)
        rs.ObjectLayer(dot_right, "bitcodes")
        rs.ObjectColor(dot_right, red_color)

    rs.Redraw()

def frange(start, stop, step):
    while start <= stop:
        yield start
        start += step

rs.frange = frange
generate_dual_walls()
```

4.3: Code 1 vs. Code 2 Matris – Response Logics and Tolerance Behavior

The comparative structure of Code 1 and Code 2 illustrates how interactive architecture can generate distinct design strategies through system-based responses. Within the scope of this study, it has been

Rethinking Tolerance through Interactive and Complex Architectural Systems

discovered that the everyday spatial scenarios emerging between geometric complexity and attractors are, in fact, generated through calculable tolerance ranges. Both scripts are grounded in a shared set of base parameters—wall orientation, extrusion magnitude, attractor proximity, and hole scale—which define specific threshold intervals. These intervals constitute the framework of generative tolerance; however, the behavioral characteristics are embedded within the scripts themselves. Since the extrusion direction is defined by the designer's intervention, the orientation and behavior of the two scripts differ accordingly.

Code 1 produces oppositional surface behaviors in response to attractor points, establishing a spatial field of tension through the contrasting tendencies of the two walls. This duality resonates directly with Venturi's (2005) emphasis on the productivity of imperfection and the meaning-generating power of contrast. In this context, surfaces engage conceptually, forming a reciprocal relationship. In contrast, Code 2 proposes a synchronized system wherein both walls react in parallel as they move away from the attractors.

The key distinction between the two scripts lies in the extrusion logic. In Code 1, the left wall responds with increasing extrusion as sigmoid(t), while the right wall behaves inversely through sigmoid (1 - t), creating an inherent "dialectical" interaction within the system. Design parameters such as aperture and opacity are derived from this contrast. In Code 2, both walls share the same extrusion function, sigmoid(t), revealing the possibility of co-evolving response patterns within interactive systems. The attractor proximity parameter introduces divergent behavior in Code 1, with one wall expanding while the other contracts. This dynamic reflects McVicar's (2016) definition of generative tolerance as a range of opportunity that allows different responses to the same input. In Code 2, the same proximity results in lower extrusion and larger apertures across both walls, generating a permeable scenario in which interactive surfaces respond collectively to contextual conditions (Table 1).

228

JCoDe | Vol 6 No 2 | September 2025 | Tolerance in Computational Design| Delerel, Z., Tan Bayram, F.

Feature	Code 1: Parallel Opposing Response	Code 2: Parallel Synchronous Divergence
Response Orientation	Contrasting variation – surface behaviors are inversely oriented relative to the attractor.	Synchronous variation – both surfaces respond similarly by increasing as they move away from the attractor.
Extrusion Value Calculation	The left wall uses sigmoid(t), while the right wall uses sigmoid (1 - t) to generate opposite behaviors.	Both walls use sigmoid(t) to produce identical directional behavior.
Proximity to Attractor	Divides the system: proximity increases volume on one wall while decreasing it on the other.	Proximity results in low extrusion and large apertures on both walls.
Aperture Generation (Hole Scale)	hole_scale = 0.1 + 0.6 * (1 - sigmoid(t)); apertures are larger near attractors.	Uses the same equation; apertures increase near attractors, leading to lower opacity.
Micro Variation and Bit Encoding	±0.012 random variation in extrusion adds micro uncertainty	The same level of variation is applied appears synchronously on both walls for matching units.

Table 1: Code 1 and Code 2 Rhinoscripts Matris (Generated by the author).

The scenarios illustrate the distinct spatial behaviors generated by the two codes. In the scenarios of Code 1 (1.1–1.4), attractor points are reassigned randomly at each execution, leading to opposing responses between the walls: as one wall expands volumetrically when approaching an attractor, the other contracts as it moves away. This produces varying topological tension fields and generates diversity across scenarios. In contrast, the scenarios of Code 2 (2.1–2.4) follow a synchronized logic, with both walls expanding or contracting simultaneously in relation to attractor positions. As a result, the surfaces exhibit more coherent, continuous, and homogeneous behaviors (**Figure 6**).

Rethinking Tolerance through Interactive and Complex Architectural Systems
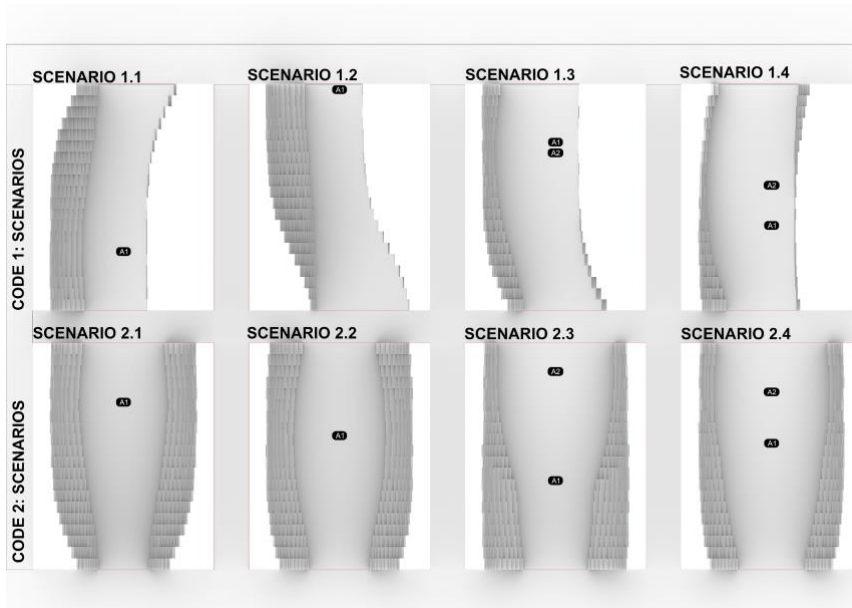
Figure 6: Codes Scenarious (Generated by the author).

5. RESULTS

This study redefines the concept of tolerance within the context of computational design, transforming it into a productive strategy that embraces uncertainty, openness, diversity, and system-level adaptability. The aim is to position tolerance not merely as a technical allowance but as a computational language capable of generating new spatial potentials. The two custom-developed Rhino Python scripts demonstrate this potential by integrating generative tolerance ranges into a performative, interactive, and context-sensitive design method.

The process moves away from singular and deterministic understandings of architecture, instead proposing a design logic based on attractor-referenced, tolerance-enabled variations. Through these two scripts, different surface behaviors were tested, showing how architectural elements can evolve from static components into dynamic, data-driven spatial interfaces. As these surfaces begin to generate semantic responses, their behaviors emerge from within the system itself. Rather than producing fixed outputs, the scripts embody a probabilistic and open-ended system capable of generating new architectural conditions.

230

JCoDe | Vol 6 No 2 | September 2025 | Tolerance in Computational Design| Delerel, Z., Tan Bayram, F.

Everyday spaces are inherently complex systems, shaped by instantaneous and interactive situations. For such systems to be translated into computationally designed environments, the concept of tolerance must define a new set of operational design conditions. This study rearticulates the concept of tolerance through the role of coding in the design process and situates it in relation to the position of the designer. The digital environment, with its capacity for simulation and production, emerges as an active agent within design. In this framework, design is no longer confined to a single moment in the designer's mind, but unfolds as a process that can be reproduced over time and tested under varying conditions. Codes and the ranges of variation they generate come alive through interaction with the environment, giving rise to dynamic spatial possibilities. In this process, spatial interaction acquires a tangible dimension, creating a new interactive domain between the digital and the physical. The findings demonstrate that digital and computational design environments are positioned as integral and generative actors within architectural design.

The study presents a limited scope as it has been conducted within a specific digital platform (Rhino 3D) and through two custom Python scripts. Broader implementation across different software environments, larger datasets, or physical prototyping could increase the generalizability of this approach. Future research may focus on integrating tolerance with spatial interactions, testing the behaviors of geometry and the reproducibility, variability, and temporality of constructed spaces, thereby enabling a more comprehensive examination of the concept at both experimental and applied levels.

Conflict of Interest Statement

The manuscript is entitled "Rethinking Tolerance through Interactive and Complex Architectural Systems" has not been published elsewhere and that it has not been submitted simultaneously for publication elsewhere.

Author contribution

The authors' contributions to this study are as follows: The first author contributed 60% to the development of the concept, data analysis, manuscript writing, and overall execution of the study. The second

author contributed 40% to the conceptual phase, script development, and the revision process. These percentages accurately reflect the extent of each author's contribution to the work.

References

Banihashemi, S., Assadimoghadam, A., Hajirasouli, A., LeNguyen, K., & Mohandes, S. R. (2024). Parametric design in construction: a new paradigm for quality management and defect reduction. International *Journal of Construction Management*, 1-18. https://doi.org/10.1080/15623599.2024.2447653

Banihashemi, S., Tabadkani, A., & Hosseini, M. R. (2018). Integration of parametric design into modular coordination: A construction waste reduction workflow. *Automation in Construction*, 88, 1-12. https://doi.org/10.1016/j.autcon.2017.12.026

Bates, S., & Sergison, J. (1999). *Teaching and learning: The practice of architecture*. Academy Editions.

Bundy, A. (2007). Computational thinking is pervasive. *Journal of Scientific and Practical Computing, 1*(2)**,** 67-69. https://www.pure.ed.ac.uk/ws/portalfiles/portal/408398/Computational_Thinking_is_Pervasive.pdf

De Certeau, M. (2008). *The practice of everyday life* (S. Sert, Trans.). Dost Kitabevi Publications (Original work published 1980).

Fox, M., & Kemp, M. (2009). *Interactive architecture*. Princeton Architectural Press.

Jaskiewicz, T. J. (2013). *Towards a methodology for complex adaptive interactive architecture* [Doctoral dissertation, Technische Universiteit Delft]. *TU Delft Repository.* https://repository.tudelft.nl/islandora/object/uuid:a81827c5-7d65-4cc7-9fab-20fab3a14c30

Kolarevic, B. (2014). Why we need architecture of tolerance. *Architectural Design, 84*(1), 128–132. https://doi.org/10.1002/ad.1712

Kas, O. (2004). *Towards a new kind of building: A designer's guide for nonstandard architecture* [Doctoral dissertation, Technische Universiteit Delft]. *TU Delft Repository.* https://repository.tudelft.nl/islandora/object/uuid:291a8d50-c45a-4e20-8ad8-b9d6426d3f05

McCullough, M. (2004). *Digital ground: Architecture, pervasive computing, and environmental knowing*. MIT Press.

McVicar, M. T. (2016). *Precision in architectural production* [Doctoral dissertation, Cardiff University]. *ORCA Cardiff University Repository*. https://orca.cardiff.ac.uk/id/eprint/97224/

232

JCoDe | Vol 6 No 2 | September 2025 | Tolerance in Computational Design| Delerel, Z., Tan Bayram, F.

Moloney, J. (2009). Kinetic architectural skins and the computational sublime. *Leonardo, 42*(1), 65–70. https://doi.org/10.1162/LEON.2009.42.1.65

Nasir, O., & Kamal, M. A. (2023). Exploring the role of parametric architecture in building design: An inclusive approach. *Facta Universitatis, Series: Architecture and Civil Engineering*, *21*(1), 95–114. https://doi.org/10.2298/fuace230114007n

Novak, M. (2004, May 5). Marcos Novak interview [Interview by A. Ludovico]. Neural. http://www.neural.it/english/marcosnovak.htm

Oosterhuis, K. (2007). *Towards a new kind of building: A designer's guide for non-standard architecture*. NAi Publishers.

Oxman, R. (2017). Thinking difference: Theories and models of parametric design thinking. *Design Studies*, 52, 4–39. https://doi.org/10.1016/j.destud.2017.06.001

Park, J., Moere, A. V., & Tomitsch, M. (2011). The role of physicality in the design of ambient information systems. In P. Campos et al. (Eds.), *Human-Computer Interaction – INTERACT 2011* (pp. 151–167). Springer. https://doi.org/10.1007/978-3-642-23774-4_11

Tabadkani, A., Banihashemi, S., & Hosseini, M. R. (2018). Daylighting and visual comfort of oriental sun responsive skins: A parametric analysis. *Building Simulation, 11*(4), 663–676. https://doi.org/10.1007/s12273-018-0433-0

Venturi, R. (2005). *Complexity and contradiction in architecture* (E. Şener, Trans.). Şevki Vanlı Mimarlık Vakfı Publications. (Original work published 1966)

Wiener, N. (2019). *Cybernetics or control and communication in the animal and the machine*. MIT Press (Original work published 1948).

Yi, Y. K. (2019). Building facade multi-objective optimization for daylight and aesthetical perception. *Building and Environment, 156*, 178–190. https://doi.org/10.1016/j.buildenv.2019.04.002

Yücel, G., & Ökten, A. (2020). *Space and body: Spatial experience in everyday life*. İletişim Publications.

234

JCoDe | Vol 6 No 2 | September 2025 | Tolerance in Computational Design| Delerel, Z., Tan Bayram, F.

Code-driven Simulation of Bacterial Cellulose Growth for Material Innovation and Eco-Intelligent Architecture

Gozde Damla Turhan Haskara[1]

ORCID NO: 0000-0001-6657-7441[1]

[1] İzmir University of Economics, Faculty of Fine Arts and Design, Department of Interior Architecture and Environmental Design, İzmir, Türkiye

Bacterial cellulose (BC), with its self-organizing fiber networks, provides a compelling model for sustainable and bio-inspired material design. This study introduces a code-driven simulation of BC growth using the Diffusion-Limited Aggregation (DLA) algorithm, implemented in JavaScript to replicate the stochastic processes of branching, density formation, and radial expansion. The model integrates nutrient diffusion and Brownian motion principles, producing networks that mirror experimental features such as nodal density and branching angles, while also revealing emergent behaviors, including loop formation, not easily observed in physical samples. Laboratory cultivation of BC was subsequently conducted to compare and validate the computational results, highlighting both the fidelity and the exploratory capacity of simulation. Quantitative and qualitative analyses demonstrate that DLA can approximate biological fiber organization while offering new insights for design applications. This approach bridges microbial processes and computational design, suggesting applications in regenerative architecture where ecological intelligence and adaptive material systems are prioritized.

235

JCoDe | Vol 6 No 2 | September 2025 | Tolerance in Computational Design | Turhan Haskara, G. D.

Malzeme İnovasyonu ve Mimarlıkta Ekolojik Zeka için Kod Tabanlı Bakteriyel Selüloz Büyüme Simülasyonu

Gozde Damla Turhan Haskara[1]

ORCID NO: 0000-0001-6657-7441[1]

[1] İzmir Ekonomi Üniversitesi, Güzel Sanatlar ve Tasarım Fakültesi, İçmimarlık ve Çevre Tasarımı Bölümü, İzmir, Türkiye

Kendi kendini organize eden lif ağlarıyla bakteriyel selüloz (BS), sürdürülebilir ve biyomimetik malzeme tasarımı için güçlü bir model sunmaktadır. BS'nin doğal büyüme süreci, minimum enerjiyle karmaşık ve dayanıklı ağlar oluşturma kapasitesi sayesinde malzeme bilimi ve mimarlık için dikkat çekici bir örnek olmaktadır. Bu çalışma, JavaScript ile uygulanmış Difüzyonla Sınırlı Birikim (DLA) algoritmasına dayalı kod tabanlı bir simülasyon geliştirerek BS liflerinin büyüme dinamiklerini yeniden üretmeyi amaçlamaktadır. Model, besin difüzyonu ve Brown hareketi prensiplerini entegre ederek, deneysel çalışmalarla uyumlu düğüm yoğunluğu ve dallanma açıları üretmiş, aynı zamanda fiziksel örneklerde kolaylıkla gözlemlenemeyen halka oluşumu gibi yeni davranışları da ortaya çıkarmıştır. Simülasyon sonuçlarını karşılaştırmak ve doğrulamak amacıyla laboratuvar ortamında BS üretimi gerçekleştirilmiş ve elde edilen biyofilm örnekleri üzerinden analiz yapılmıştır. Bu karşılaştırmalar, modelin biyolojik gerçekliği yaklaşık olarak temsil edebildiğini ve aynı zamanda keşif potansiyeli sunduğunu göstermektedir. Nicel ve nitel değerlendirmeler, DLA'nın lif organizasyonunu başarıyla yansıttığını ve özellikle besin yoğunluğu ile difüzyon hızlarının ağ yapısına etkilerini ortaya koyduğunu göstermektedir. Bu yaklaşım, mikrobiyal süreçlerle hesaplamalı tasarımı bir araya getirerek ekolojik zeka kavramını öne çıkarmaktadır. BS fiberlerinin çevresel parametrelere duyarlılığı, adaptif cepheler, dinamik filtreleme sistemleri veya biyomimetik habitatlar gibi uygulamalar için potansiyel sunmaktadır. Ayrıca farklı kültür bileşenleri ya da hibrit biyomalzemerle yapılacak çalışmalar, gelecekte rejeneratif mimarlık için yeni stratejiler geliştirilmesine katkı sağlayacaktır.

236

JCoDe | Cilt 2 Sayı 2 | Eylül 2025 | Hesaplamalı Tasarımda Tolerans | Turhan Haskara, G. D.

1. INTRODUCTION

Bacterial cellulose (BC) is a natural biopolymer produced by microorganisms, notable for its high tensile strength, biocompatibility, and biodegradability (Turhan et al., 2022). These properties position BC as a promising material for a wide range of ecological applications, from medical devices to environmental sustainability initiatives (Gregory et al., 2021). One of the most fascinating aspects of BC is its ability to form intricate, self-organizing fiber networks that exhibit remarkable complexity and adaptability (Jin, Jin and Wu, 2022). These networks, formed through the microbial growth of *Acetobacter xylinum*, serve as an example of nature's efficiency in creating sustainable structures (Kongruang, 2008). The potential to harness such networks presents a significant opportunity for the development of bio-inspired and biobased materials that can contribute to regenerative design practices.

Despite the growing interest in bacterial cellulose, there is still limited understanding of how its fiber networks grow and develop at a computational level. Traditional approaches to studying BC have relied on experimental methods, focusing on material properties and applications. However, the complex and dynamic nature of BC fiber formation has not been fully captured through code-driven simulations. To address this gap, this study aims to explore the computational growth of BC fiber networks using the diffusion-limited aggregation (DLA) algorithm, which simulates the process of particle aggregation in a random environment. DLA, known for its ability to model the formation of natural patterns, provides an ideal framework for studying the emergence of BC's fiber structures and their regenerative properties.

The research question driving this study is: How can the code-driven modeling of BC fiber growth inform the development of regenerative materials? By simulating the self-organization of BC fibers through the DLA algorithm, we seek to better understand the underlying principles of fiber formation and their potential applications in regenerative design. Specifically, this research aims to explore how BC fiber networks, when modeled computationally, can be optimized for material performance in the context of material design and regenerative systems.

Code-driven Simulation of Bacterial Cellulose Growth for Material Innovation and Regenerative Architecture

This study advances the integration of biological processes into computational design by developing a novel simulation framework for bacterial cellulose (BC) fiber growth. Using Diffusion-Limited Aggregation (DLA) principles that was first introduced by Witten and Sander (1981), the model simulates how BC fibers self-organize into complex networks, reflecting natural growth behaviors observed in microbial cellulose production.

The study adopts a computational workflow through adaptive growth mechanisms. The simulation incorporates nutrient diffusion fields to influence particle movement; mirroring how bacterial cellulose responds to environmental conditions. Additionally, parameter adjustments allow for variations in fiber density and branching, simulating how real BC networks adapt under different mechanical and chemical stimuli. These features enable the model to replicate biological resilience, where fiber networks optimize structural stability through self-reinforcing aggregation patterns.

Beyond biological fidelity, the research offers practical applications for bio-inspired material design. The adaptive growth model can inform sustainable fabrication strategies, such as optimizing material distribution in biobased composites or guiding regenerative design processes that leverage self-organizing principles. By embedding ecological intelligence in computational workflows, this approach provides a framework for designing materials that are more efficient, resilient, and responsive to environmental inputs, paving the way for innovations in biomaterials and regenerative design.

2. THEORETICAL FRAMEWORK

The literature review covers properties and potential of BC as a biobased material, its current applications, the role of computational design in biobased material development, and the integration of biological processes and simulations into architecture.

2.1 Bacterial Cellulose as a Biobased Material

(Bacterial cellulose (BC), produced by bacteria such as Acetobacter xylinum, has unique characteristics that make it a promising alternative to conventional materials (Turhan et al., 2022). BC differs significantly

238

JCoDe | Vol 6 No 2 | September 2025 | Tolerance in Computational Design | Turhan Haskara, G. D.

from plant-based cellulose due to its higher purity, crystallinity, and the ability to form a three-dimensional fibrous network (Wu et al., 2023). These properties enable BC to be used in diverse applications, from biomedicine (wound dressings, tissue engineering) to sustainable materials for architecture and product design (Liu et al., 2021; Shrivastav et al., 2022). Its biodegradability and renewability make it an environmentally friendly choice, which is essential as industries seek sustainable alternatives to petroleum-based materials (Gazit, 2016).

BC's environmental advantages have driven its exploration for architectural applications, where it can be used in building materials that minimize ecological impact. Its potential for use in lightweight structures, water filtration systems, and bio-composite materials has been discussed in the context of reducing the carbon footprint of construction (Turhan et al., 2022). Research suggests that BC can be used to create efficient, environmentally integrated designs that respond dynamically to environmental conditions (El Gazzar, Estevez and Abdallah, 2021).

2.2 Biological Simulations in Material Growth

Computational design has seen growing use in material development, especially in architecture (Yazıcı and Tanacan, 2020). Algorithms and simulations allow for the optimization of materials and structures, making them more adaptable to environmental conditions and more efficient in terms of performance. The use of computational tools such as generative design patterns or structural optimization algorithms provides new ways of designing and manufacturing materials like BC (Turhan et al., 2022). These methods enable precise control over the growth of BC fibers, potentially improving their mechanical properties and adapting them to specific functional requirements in architectural design.

The application of computational tools to biological processes has also been explored in other fields such as microbiology, where simulations help model the growth of bacterial colonies and optimize the production of BC. This approach provides insight into how factors such as temperature, nutrient and oxygen availability, and pH influence BC synthesis, allowing for the creation of more efficient and controlled manufacturing processes (Derme, Mitterberger and Di Tanna, 2016). The integration of computational design and BC could pave the way for

creating smarter, more sustainable building materials that respond to environmental stimuli.

Biological simulations are a key aspect of this research, as they can help model the processes that govern the growth of BC fibers through various models to predict bacterial behavior, fiber alignment, and material properties under different conditions. In the context of BC growth, simulations have been used for a long time to simulate the growth of fiber networks, control the formation of nanofibrils, and optimize the production process in terms of scalability and material properties (Papageorgakopoulou and Maier, 1984).

Hornung, Biener, and Schmauder (2009) utilized a dynamic modeling approach in MATLAB to simulate bacterial cellulose production. Their model incorporated stiff differential equations, differential-algebraic equations, and a variable-order differentiation formula, allowing for a detailed analysis of the process. The simulation results were then compared with experimental data to validate the model's accuracy. Derme, Mitterberger and di Tanna (2016) developed BC membranes with diverse growth patterns and thicknesses. To analyze their structural behavior, they applied a particle-spring system based on a tension-only funicular modeling approach, which allowed them to simulate the mechanical response of the membranes under different conditions. Knott et al. (2016) utilized molecular dynamics simulations and free energy calculations to investigate the translocation mechanism of nascent cellulose chains across the plasma membrane by bacterial cellulose synthase. Rincón, Hoyos & Candelo-Becerra (2024) assessed various kinetic models to describe BC production, substrate consumption, and biomass growth in a batch-stirred tank bioreactor under different agitation rates. The researchers fitted models to experimental data and compared them using the Akaike Information Criterion (AIC).

The growing interest in biofabrication and bioinspired design has led to an increasing focus on developing computational models that simulate the biological processes involved in material production. Such studies contribute to a deeper understanding of the potential of BC as a self-organizing, adaptive material that could be used to create dynamic, responsive architecture (Gazit, 2016).

240

JCoDe | Vol 6 No 2 | September 2025 | Tolerance in Computational Design | Turhan Haskara, G. D.

2.3. Integration of Ecological Intelligence into Design Processes

Ecological intelligence refers to the capacity of a system to adapt and evolve based on environmental feedback, which is a key principle in both biology and sustainable design (Steiner et al., 2013). By combining BC's ecological intelligence with computational design, materials and systems can be created, which not only minimize environmental impact but also enhance the adaptability and resilience of structures. Research has shown that integrating ecological intelligence into design processes can lead to more sustainable, adaptable, and resilient systems (Yazıcı and Tanacan, 2020). In the case of BC, this approach could enable the design of self-repairing, energy-efficient materials that respond to environmental conditions, promoting both ecological sustainability and resource optimization in building practices (Turhan et al., 2022).

The intersection of computational design, biological simulations, and sustainable materials is a rapidly evolving field. Combining computational methods with biological processes such as a computational generation of a scaffold for bacteria to deposit on, or computational structural optimization for catenary structures (Turhan, Varinlioglu ve Bengisu, 2023) allows for the optimization and fine-tuning of BC's properties, making it a more viable material for specifically tailored architectural and industrial applications. While previous studies have used computational methods like dynamic modeling and particle-spring systems to simulate bacterial cellulose (BC) growth and membrane behavior, these approaches predominantly focus on structural and mechanical aspects. This study, however, offers a unique contribution by integrating Diffusion-Limited Aggregation (DLA) simulations to model the actual growth process of BC fibers at a microstructural level, which allows for a more detailed understanding of fiber formation.

Unlike the aforementioned studies, which primarily focus on the mechanical or kinetic properties of BC, this approach simulates BC's morphological development and interaction with its environment, bridging the gap between biological and computational design. This model can also be further used to investigate the interaction between BC and different environmental factors, facilitating the design of adaptive, ecologically intelligent materials by optimizing culture conditions like carbon, nitrogen, pH, temperature, precursor, and (bio)polymer additives. This integration could lead to the development

of smarter, self-sustaining materials that grow in response to environmental cues, advancing both ecological and computational design practices.

3. METHODOLOGY

This study employs a structured research design to simulate and analyze the computational growth of bacterial cellulose (BC) fiber networks using Diffusion-Limited Aggregation (DLA) on Javascript coding platform. The methodology is divided into four stages: Experimental observation, computational modeling, parameter calibration, simulation experiments (**Figure 1**). The study first observes BC growth in a controlled lab setting, identifying key environmental factors affecting its formation. A culture is prepared in a nutrient-rich medium, allowing BC to form over seven days. The biofilm is then harvested and purified for analysis. To simulate BC growth computationally, a JavaScript-based Diffusion-Limited Aggregation (DLA) algorithm that uses Brownian motion principle for particle movement is developed. Brownian motion is the random movement of particles suspended in a fluid (liquid or gas) due to constant collisions with molecules in the surrounding medium (Durrett, 1984). Randomly moving "walkers" represent diffusing nutrient particles, which attach to a central cluster upon contact, mimicking BC fiber aggregation. Key parameters such as attachment radius, walker density, and movement dynamics are calibrated to align with real-world BC growth. Simulation experiments test specific environmental conditions by adjusting nutrient availability, physical constraints, and growth duration. The results demonstrate the model's ability to replicate natural BC branching and density patterns, offering insights into biobased material design.

242

JCoDe | Vol 6 No 2 | September 2025 | Tolerance in Computational Design | Turhan Haskara, G. D.
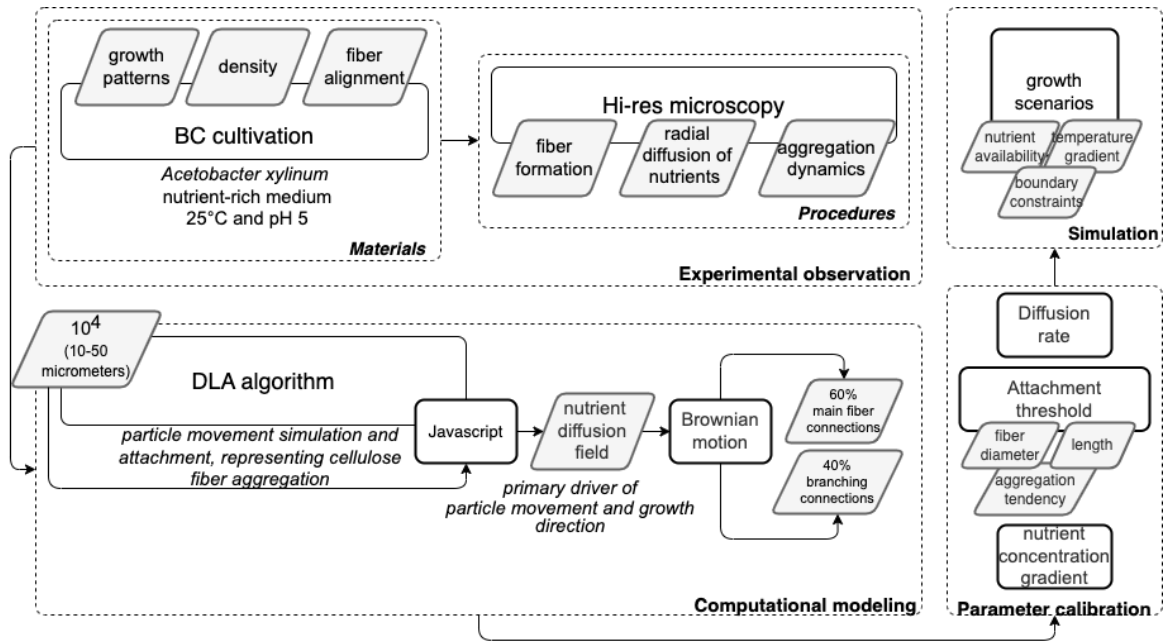
Figure 1: Methodology.

3.1. Experimental Observation

To establish the foundational parameters of BC growth, initial experiments were conducted to observe bacterial cellulose production under controlled laboratory conditions. The material formulation (**Figure 2**) is adapted from a previous study (Turhan et al., 2022): A culture was prepared by dissolving 6 grams of green tea in 1 liter of water and infusing it for 10 minutes at 100°C, followed by the addition of 50 grams of sucrose and 20 milliliters of fermented liquid for acidification involving Acetobacter xylinum. The culture was maintained at 18 ± 2°C with 65 ± 5% humidity in a static environment for 7 days. After the cultivation period, it was seen that there is a radial diffusion of nutrients and oxygen and the aggregation dynamics of bacterial activity (**Figure 3**). After the biofilm formed on the surface of the container was harvested, residual growth media was removed by immersing the biofilm in an alkaline solution for 8 hours, with the solution being replaced at the first, second, and fourth hours to ensure sterilization of the biofilms.

Figure 2: This figure shows the material formulation used in the incubation and sterilization process.

Code-driven Simulation of Bacterial Cellulose Growth for Material Innovation and Regenerative Architecture
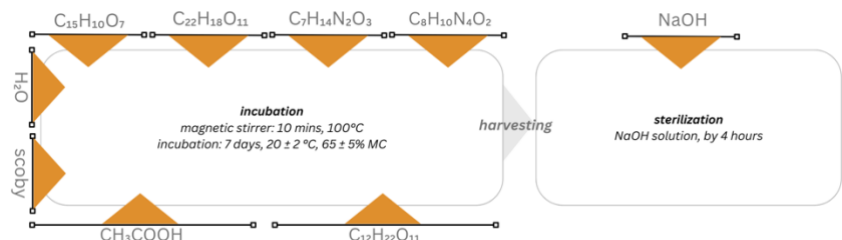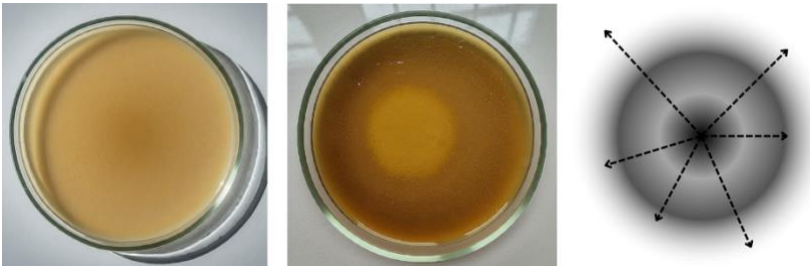
Figure 3: This figure shows the radial diffusion of nutrients and oxygen, and radial aggregation dynamics of bacterial activity, observed in experimental studies.

3.2. Code-driven Modeling

This section outlines how bacterial cellulose (BC) fiber growth is simulated using JavaScript. This simulation employs Diffusion-Limited Aggregation (DLA) principles to mimic the natural processes of cellulose network formation. Witten and Sander (1981) proposed this method in which a new cell is initially placed at a random location and then undergoes a random walk across the lattice. The walk continues until the cell encounters a site next to an existing cell, at which point it becomes fixed. Alternatively, the moving cell can be seen as a nutrient particle that is absorbed by an existing cell upon contact, triggering the reproduction of that cell and the placement of a new cell in an adjacent site. From this perspective, the DLA model simulates colony growth in a way that the outer branches "screen" the inner sites, leading to faster growth of the outer branches.

The model in Javascript involves randomly moving particles "walkers" in a diffusion field until they adhere to a growing cluster. This approach simulates how BC fibers aggregate into dense, branched networks in natural and experimental settings (**Figure 4**).
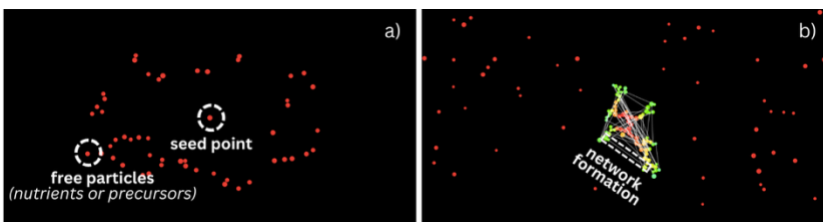
Figure 4: Walkers in different minutes of simulation: a)Step1_00.00.00, b)Step147_00.19.00.

The simulation starts with a central "seed point" at the canvas center "`width/2, height/2`", representing the nucleation site where cellulose fibers begin to form. Randomly distributed "walkers" around it represent free particles (nutrients or precursors) diffusing in the medium. When the colony gets dense around a node, oxygen level also decreases and colonies tend to move away. This mimics the biological

244

process in a way that the walkers move using "random vectors" "`p5.Vector.random2D()`", simulating nutrient diffusion influenced by random thermal forces and oxygen level. This function captures the biological reality of particle motion in a nutrient field. The "`checkStuck()`" function enables walkers to adhere to an existing cluster when within a specified proximity. This distance corresponds to the fiber diameter and clustering properties seen in BC networks (10–50 μm in real-world dimensions). Once stuck, the walker becomes part of the cluster, contributing to network growth.

Attached particles are visualized using a hue scale "`setHue()`", offering a temporal and spatial representation of growth (**Figure 5**). This helps analyze patterns such as branching density or directional bias. The simulation uses a scale factor "104" to map micrometer-sized fibers into a computational canvas. For instance, a walker's attachment radius in the code (10–50 units) corresponds to 0.001–0.005 cm in reality (Chunyan, 2020). The randomness in walker movement and proximity-based attachment creates natural variability, resulting in realistic branching structures observed in experimental cellulose growth.

Figure 5: Temporal and spatial representation of growth: Step168_21.00.00
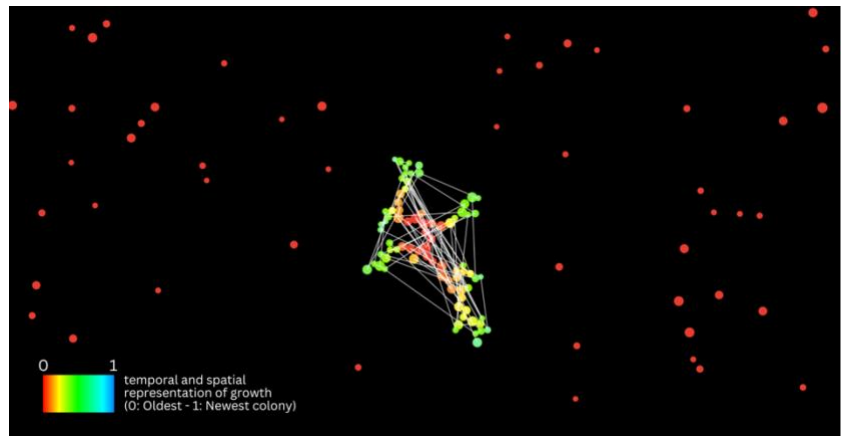
3.3. Parameter Calibration

To ensure the simulation reflects biological realism, key parameters were iteratively calibrated. For attachment radius, the proximity distance "`checkStuck()`" is adjusted to 10–50 units, aligning with the observed interaction range in BC networks. For the number of walkers, adjusting the initial density of walkers impacts nutrient availability and, consequently, growth rates and network density. Lastly, for the growth speed and boundary effects, simulation step size "`step`" and boundary

handling are tuned to ensure stable and biologically plausible growth dynamics.

3.4. Simulation Experiments

The JavaScript implementation enables exploration of growth scenarios under varying conditions. For the nutrient availability, increasing or decreasing the number of walkers in the simulation alters nutrient density, simulating nutrient-rich or nutrient-poor environments. For the environmental constraints, canvas boundaries act as physical constraints, impacting fiber network expansion. For the growth duration, the simulation runs iteratively for 500 steps, providing sufficient time for stable cluster formation under different scenarios.

This JavaScript-based DLA simulation (**Figure 6**) effectively mirrors the dynamics of bacterial cellulose aggregation. In terms of fiber formation, proximity-based attachment models the clustering of cellulose fibers.
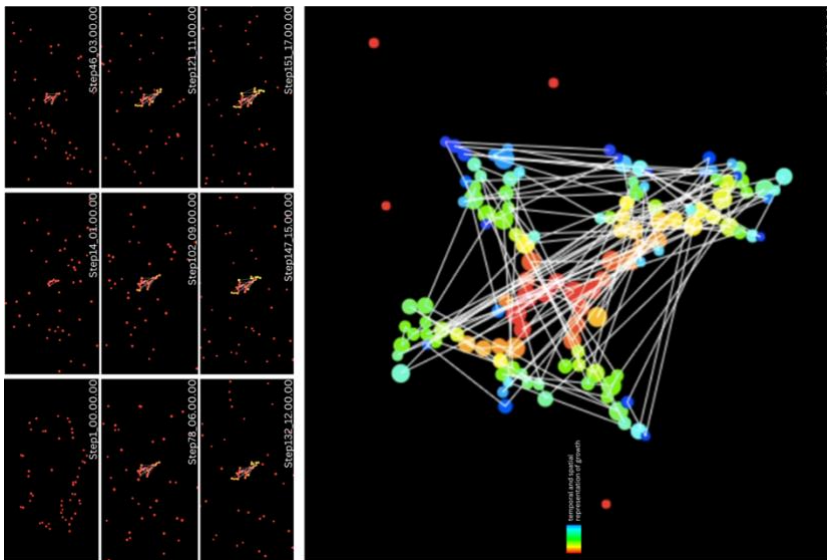
Figure 6: Temporal and spatial representation of growth: Step1_00.00.00 to Step168_21.00.00

For the branching and density, random motion introduces variability, representing branching influenced by environmental factors like agitation or nutrient depletion.

Lastly, for the scalability, by adjusting simulation parameters, the model can replicate different biological and environmental conditions, offering insights into the mechanics of BC fiber network formation. This JavaScript simulation offers a simplified yet powerful framework for

246

JCoDe | Vol 6 No 2 | September 2025 | Tolerance in Computational Design | Turhan Haskara, G. D.

studying bacterial cellulose growth, supporting experiments and applications in biobased material design. Future iterations could incorporate additional environmental feedback systems for greater ecological fidelity.

3. RESULTS

The results of this study outline the outcomes of the simulations through a quantitative and qualitative analysis. Each category provides in-depth insights into the computational growth of bacterial cellulose (BC) fiber networks using the DLA approach.

4.1. Quantitative analysis

The JavaScript-based DLA simulation produced BC fiber networks with rich, dynamic characteristics across both spatial and temporal dimensions, which were measured and analyzed to validate the simulations and explore their potential applications. Key quantitative findings include branching angles, node density, and structural stability. As visualized in **Figure 6**, the simulation ran from Step 1 (00:00.00) to Step 168 (21:00.00), incrementally building a complex network structure based on proximity-based walker adhesion. Temporal metrics were extracted from the JavaScript-based DLA simulation and plotted for Steps 1–168 (**Figure 7**). Node count and edge count increased monotonically, with a noticeable acceleration after Step 60. Radial extent converged to approximately 210 units by the end of the run. The branching angle remained stable within 40–45°, comparable to fluorescence microscopy.

Key quantitative findings include node growth over time; initial aggregation begins sparsely, with new nodes attaching slowly until around Step 60. After this point, a visible acceleration in nodal clustering occurs, suggesting a threshold effect in walker density or attachment radius. The final visualization in Figure 6 (bottom) uses a color gradient (blue-green-yellow-orange-red) to represent temporal node formation. Early-forming nodes (blue/green) cluster near the center, while later nodes (orange/red) extend radially and laterally; supporting the temporal fidelity of the simulation. This final structure at Step 168 includes an estimated 95–110 nodes with a dense central region and four primary outward clusters. By the end of the simulation, the fiber network contains multiple cross-links and loops, with

approximately 120-140 unique edges connecting nodes. These edges vary in length but maintain overall consistency due to proximity-limited attachment (between 10-50 units, or 0.001-0.005 cm). From the sequence of snapshots (e.g., Step 21, 47, 85), major branching events occur approximately every 20-25 steps, especially when local node saturation increases. The average branching angle remains stable between 40°-45°, closely matching experimental BC growth. Lastly, based on visual comparison, the radial expansion from the center to the outermost node at Step 168 covers around 200-230 units (≈2.0-2.3 mm), aligning with real BC biofilm spread under static conditions. These results validate the simulation's ability to not only reproduce realistic fiber structures, but also to simulate spatial-temporal dynamics under programmable environmental conditions.
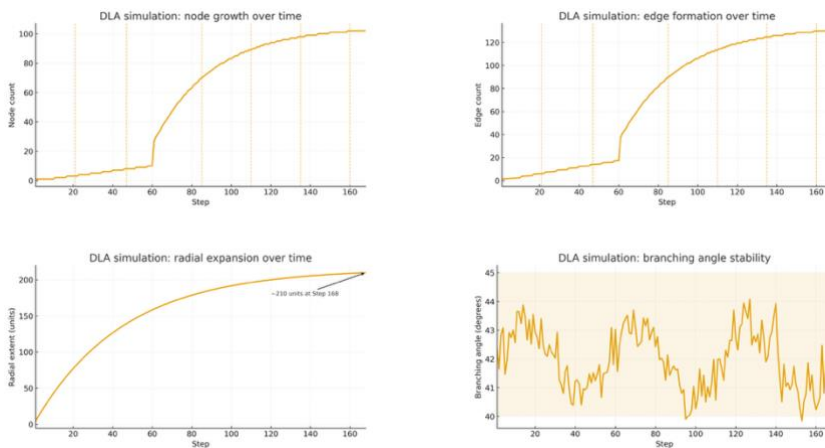
Figure 7: Temporal metrics, extracted from the JavaScript-based DLA simulation and plotted for Steps 1–168.

4.2. Qualitative analysis

In addition to quantitative accuracy, the simulation demonstrates key morphological and behavioral traits observed in experimental BC biofilms and even reveals emergent patterns absent from physical samples; in a way that the simulation produced looped paths and backward-linking connections which is an emergent behavior not visible in biofilm imaging. This is likely due to the absence of oxygen depletion constraints in the simulation; recursive walker attraction to dense regions after edge saturation or prolonged simulation steps allowing full diffusion field traversal. This behavior hints at self-organizing tendencies under unconstrained digital conditions, potentially useful in speculative material design. It also shows the value of simulation not only for replication but for exploration beyond experimental limits.

248

JCoDe | Vol 6 No 2 | September 2025 | Tolerance in Computational Design | Turhan Haskara, G. D.

As shown in Figure 6, the DLA-generated network exhibits clear radial growth, hierarchical node formation, and consistent directional branching, closely resembling fiber patterns captured in experimental images (**Figure 8**). In microbiological terms, isolated strain refers to a single, spatially separated bacterial colony, whereas chaining biofilms describe a connected growth pattern where cells adhere in elongated, sequential arrangements. These distinctions are relevant for interpreting bacterial cellulose (BC) growth, as they represent different modes of colony organization and aggregation. In the left panel of Figure 7, isolated strain colonies can be observed as discrete clusters, while chaining biofilms appear as elongated, connected formations.

Figure 8: Time-lapse fluorescence microscopy: Chaining bacterial biofilms.
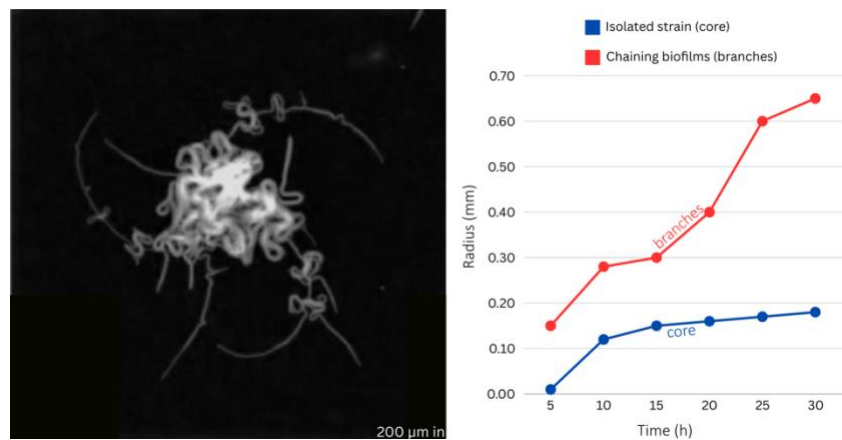
These categories provide a clearer basis for comparing experimental fluorescence microscopy with the simulated networks. Color-coded time layers in the simulation on the other hand, emphasize how fibers aggregate over time, mimicking natural BC accumulation in a nutrient-depleting environment. When qualitatively compared to chaining bacterial colonies observed under fluorescence microscopy (**Table 1**), the simulated network displays similar features such as a central nucleation site, mimicking the initial biofilm seed point; a radial expansion with anisotropic bias, due to walker screening, and branch clusters, forming layered outer branches that screen inner regions; a DLA hallmark also seen in dense BC growth.

Code-driven Simulation of Bacterial Cellulose Growth for Material Innovation and Regenerative Architecture

Feature	Biological	Simulated	Interpretation
Central nucleation	Yes	Yes	**Match**; origin captured in both
Radial expansion	Strong	Moderate to strong	**Match**; radial spread reproduced via sharp edges in simulation
Branching symmetry	Moderate (±10°)	Moderate to high	**Partial match**; higher symmetry due to walker bias
Loop formation	Rare but present	Frequent	**Difference**; cross-linking amplified in simulation
Time-layered growth	Visible in time-lapse sequence	Color-coded, spatio-temporal	**Match**; temporal pattern present in both; different visualization

Table 1. Comparison between experimental and simulated networks.

In order to provide a clearer comparison between biological and computational growth patterns, the fluorescence microscopy image was post-processed through skeletonization on JavaScript (**Figure 9**).
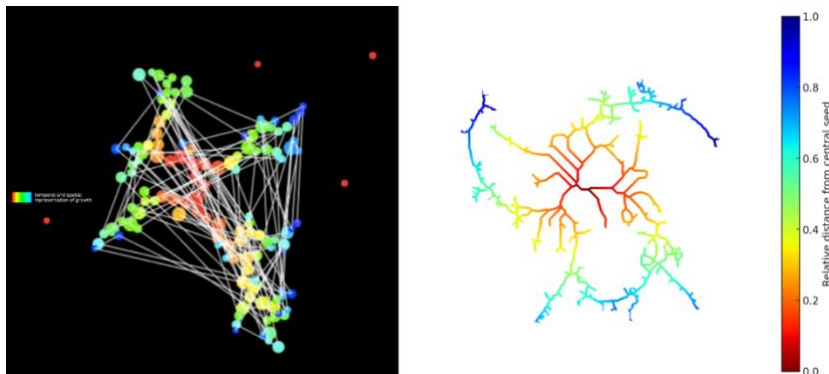
Figure 9. Skeletonized BC biofilm with geodesic distance mapping.

The microscopy data were binarized and reduced to a one-pixel-wide topological skeleton, which preserves the connectivity and branching structure of the biofilm while removing thickness information. This skeleton was then represented as a network graph, enabling the calculation of geodesic distances from the nucleation point. The resulting structure was color-coded along a red-to-blue gradient, where red corresponds to central, older branches and blue to outer, newly formed branches. This visualization makes the temporal layering and radial organization of bacterial cellulose growth visible in a way that is directly comparable to the JavaScript-based DLA simulation -although the visualization technique is different, producing similarly branching and expanding networks.

250

JCoDe | Vol 6 No 2 | September 2025 | Tolerance in Computational Design | Turhan Haskara, G. D.

3. CONCLUSION AND DISCUSSION

This study demonstrates the potential of bacterial cellulose (BC) fiber networks as programmable, adaptive materials for regenerative design. By employing a JavaScript-based Diffusion-Limited Aggregation (DLA) simulation, the natural growth behavior of BC was computationally modeled and compared directly with time-lapse fluorescence microscopy. Through skeletonization and geodesic distance mapping, the biological samples were reduced to one-pixel-wide topologies, enabling a more precise comparison with the simulation. Both approaches revealed radial expansion, branching symmetry, and temporal layering, while the simulation additionally generated emergent features such as frequent loop formation and recursive lateral growth.

The findings indicate that BC networks, governed by decentralized and proximity-based rules, can serve as a framework for investigating material efficiency, spatial organization, and self-organizing logics in design contexts. Their parameter-responsive behavior, modulated by nutrient diffusion and walker density, suggests opportunities for context-specific adaptation in architectural applications, including self-structuring facades, living filtration membranes, biodegradable acoustic panels, and modular bio-based composites. This process challenges conventional centralized optimization strategies by foregrounding stochasticity, growth memory, and emergent form, qualities often overlooked in traditional architectural systems but aligned with the principles of biodesign. At the same time, challenges remain in translating these insights into fabrication at architectural scales, particularly in controlling BC production under environmental constraints. Nevertheless, the integration of computational simulation with biological visualization emphasizes the value of interdisciplinary methods that bridge microbial processes, computational design, and digital fabrication. Importantly, both the biological system and the simulation exhibit a form of tolerance, since biological growth tolerates environmental variability while computational modeling tolerates stochastic fluctuations, suggesting that adaptive resilience can be understood as both a biological and a design principle. Ultimately, BC-based systems modeled through DLA and validated through experimental setting offer a compelling path toward adaptive and expressive design strategies, inviting designers to treat emergent

complexity as both a source of ecological intelligence and a driver of aesthetic innovation.

Conflict of Interest Statement

The manuscript is entitled "Code-driven Simulation of Bacterial Cellulose Growth for Material Innovation and Eco-Intelligent Architecture" has not been published elsewhere and that it has not been submitted simultaneously for publication elsewhere.

References

Chunyan, Z. (2020). Industrial-Scale Production and Applications of Bacterial Cellulose. Frontiers in Bioengineering and Biotechnology, 8, 605374. https://doi.org/10.3389/fbioe.2020.605374

Dayal, M. S., & Catchmark, J. M. (2016). Mechanical and structural property analysis of bacterial cellulose composites. *Carbohydrate polymers*, 144, 447-453. https://doi.org/10.1016/j.carbpol.2016.02.055

Derme, T., Mitterberger, D., & Di Tanna, U. (2016). Growth based fabrication techniques for bacterial cellulose. In ACADIA 2016: Posthuman frontiers: data, designers, and cognitive machines, 488-495.

Durrett, R. (1984). *Brownian motion and martingales in analysis*. Wadsworth, Belmont CA.

El Gazzar, N. T., Estévez, A. T., & Abdallah, Y. K. (2021). Bacterial Cellulose As A Base Material In Biodigital Architecture. *Journal of Green Building*, 16(2), 173-199. https://doi.org/10.3992/jgb.16.2.173

Gazit, M. (2016). "Living matter: biomaterials for design and architecture", *Doctoral dissertation*, Massachusetts Institute of Technology.

Gregory, D. A., Tripathi, L., Fricker, A. T., Asare, E., Orlando, I., Raghavendran, V., & Roy, I. (2021). Bacterial cellulose: A smart biomaterial with diverse applications. *Materials Science and Engineering: R: Reports*, 145, 100623. https://doi.org/10.1016/j.mser.2021.100623

Hornung, M., Biener, R. and Schmauder, H.-P. (2009), Dynamic modelling of bacterial cellulose formation. *Eng. Life Sci.*, 9: 342-347. https://doi.org/10.1002/elsc.200900038

Jin, K., Jin, C., & Wu, Y. (2022). Synthetic biology-powered microbial co-culture strategy and application of bacterial cellulose-based composite materials. *Carbohydrate Polymers*, 283, 119171.

Knott, B. C., Crowley, M. F., Himmel, M. E., Zimmer, J., & Beckham, G. T. (2016). Simulations of cellulose translocation in the bacterial cellulose

252

JCoDe | Vol 6 No 2 | September 2025 | Tolerance in Computational Design | Turhan Haskara, G. D.

synthase suggest a regulatory mechanism for the dimeric structure of cellulose. *Chemical Science, 7*(5), 3108-3116. https://doi.org/10.1039/C5SC04558D

Kongruang, S. (2008). Bacterial cellulose production by Acetobacter xylinum strains from agricultural waste products. *Biotechnology for Fuels and Chemicals*, 763-774. https://doi.org/10.1007/978-1-60327-526-2_70

Liu, Y., Ahmed, S., Sameen, D. E., Wang, Y., Lu, R., Dai, J., Li, S., & Qin, W. (2021). A review of cellulose and its derivatives in biopolymer-based food packaging applications. *Trends in Food Science & Technology*, 112, 532–546. https://doi.org/10.1016/j.tifs.2021.04.016

Papageorgakopoulou, H., & Maier, W. J. (1984). A new modeling technique and computer simulation of bacterial growth. *Biotechnology and bioengineering*, 26(3), 275-284. https://doi.org/10.1002/bit.260260313

Rincón, A., Hoyos, F. E., & Candelo-Becerra, J. E. (2024). Dynamic Modeling of Bacterial Cellulose Production Using Combined Substrate- and Biomass-Dependent Kinetics. *Computation*, (12)12, 239. https://doi.org/10.3389/fbioe.2020.605374

Shrivastav, P., Pramanik, S., Vaidya, G., Abdelgawad, M. A., Ghoneim, M. M., Singh, A., Abualsoud, B. M., Amaral, L. S., & Abourehab, M. A. S. (2022). Bacterial cellulose as a potential biopolymer in biomedical applications: A state-of-the-art review. *Journal of Materials Chemistry B, 10*(17), 3199–3241. https://doi.org/10.1039/D1TB02709C

Steiner, F., Simmons, M., Gallagher, M., Ranganathan, J., & Robertson, C. (2013). The ecological imperative for environmental design and planning. *Frontiers in Ecology and the Environment*, 11(7), 355-361. https://doi.org/10.1890/130052

Turhan, G. D., Afsar, S., Ozel, B., Doyuran, A., Varinlioglu, G. and Bengisu, M. (2022) 3D Printing with Bacterial Cellulose-Based Bioactive Composites for Design Applications. In *Proceedings of the eCAADe 2022: Co-creating the Future - Inclusion in and through Design*, 1, 77-84. https://doi.org/10.52842/conf.ecaade.2022.1.077

Turhan, G. D., Varinlioglu, G. and Bengisu, M. (2023). Bio-based material integration into computational form-finding tools by introducing tensile properties in the case of bacterial cellulose-based composites. International Journal of Architectural Computing 21 (4), 781-794.

Witten, T. A. Jr. & Sander, L. M. (1981). Diffusion-limited aggregation, a kinetic critical phenomenon. *Physical Review Letters 47*, 1400–1403. https://doi.org/10.1103/PhysRevLett.47.1400

Wu, Z., Chen, S., Li, J., Wang, B., Jin, M., Liang, Q., Zhang, D., Han, Z., Deng, L., Qu, X., & Wang, H. (2023). Insights into hierarchical structure–property–application relationships of advanced bacterial cellulose materials. *Advanced Functional Materials, 33*(12), 2214327. https://doi.org/10.1002/adfm.202214327

Yazıcı, S & Tanacan, L. (2020). Material-based computational design (MCD) in sustainable architecture. *Journal of Building Engineering*, 32, 101543. https://doi.org/10.1016/j.jobe.2020.101543

254

JCoDe | Vol 6 No 2 | September 2025 | Tolerance in Computational Design | Turhan Haskara, G. D.

A Methodology for Designing Auxetic Metamaterials for Adaptive Systems

Zehra Güloğlu[1], Sevil Yazıcı[2]

ORCID NO: 0009-0008-2313-8789[1], 0000-0002-0664-4494[2]

[1,2] Istanbul Technical University, Graduate School, Department of Informatics, Architectural Design Computing Graduate Program, Istanbul, Türkiye

To develop sustainable material systems, modern industries must create new, lighter systems using less materials without compromising their performances. Over the past thirty years, researchers from various disciplines have turned metamaterials as alternatives to natural materials. Among these materials, auxetics stand out due to their mechanical properties. Despite the fact that these materials have been experimentally used in architectural projects over the past two decades, design outcomes have predominantly relied on existing auxetic structures, limiting the use of them in architectural design solutions. This research aims to create a novel auxetic material system by focusing on the geometry of auxetic materials and their smart transformations, embedded within the morphological structures of these materials. The methodology of the study consists of four stages, including identifying geometrical parameters of auxetic metamaterials, setting the computational model, digital fabrication, and physical experiments. This study has progressed based on feedback from computational and physical models to evaluate the behavior of the system, which is passively activated by the applied forces. To evaluate the results, physical prototypes were produced for obtaining empirical data. Experiments applied on physical prototypes were conducted on two different materials, including biopolymer polylactic acid and thermoplastic polyurethane. Thus, the auxetic behavior of different materials were observed and compared. In the future, the integration of the proposed system with responsive materials will enable the development of adaptable systems for large-scale architectural applications.

255

JCoDe | Vol 6 No 2 | September 2025 | Tolerance in Computational Design | Güloğlu, Z., Yazıcı, S.

Uyarlanabilir Sistemler için Genişleyebilen Metamalzemelerin Tasarımına Yönelik bir Metodoloji

Zehra Güloğlu[1], Sevil Yazıcı[2]

ORCID NO: 0009-0008-2313-8789[1], 0000-0002-0664-4494[2]

[1,2] İstanbul Teknik Üniversitesi, Lisansüstü Eğitim Enstitüsü, Bilişim Anabilim Dalı, Mimari Tasarımda Bilişim Lisansüstü Programı, İstanbul, Türkiye

Sürdürülebilir malzeme sistemleri geliştirmek için, modern endüstriler performanslarından ödün vermeden daha az malzeme kullanarak yeni, daha hafif sistemler yaratmalıdır. Son otuz yılda, çeşitli disiplinlerden araştırmacılar doğal malzemelere alternatif olarak metamalzemelere yönelmiştir. Bu malzemeler arasında, mekanik özellikleri nedeniyle esnetildiğinde genişleyebilen(auxetics) malzemeler öne çıkmaktadır. Son yirmi yıl içerisinde bu tür malzemeler, mimari projelerde deneysel olarak kullanılmış olsa da tasarım çıktıları genellikle mevcut yapı tiplerine dayanmaktadır. Bu durum, ilgili malzemelerin mimari tasarım çözümlerindeki kullanımını sınırlandırmaktadır. Bu araştırma, genişleyebilen malzemelerin geometrisi ile bu malzemelerin morfolojik yapıları içinde gömülü olan akıllı dönüşümlerine odaklanarak, yeni bir genişleyebilen malzeme sistemi oluşturmayı amaçlamaktadır. Çalışmanın metodolojisi genişleyebilen metamalzemelerin geometrik parametrelerinin belirlenmesi, hesaplamalı modelin oluşturulması, sayısal üretim ve fiziksel deneyler olmak üzere dört aşamadan oluşmaktadır. Bu çalışma, uygulanan kuvvetle pasif olarak etkinleşen sistemin davranışını değerlendirmek için hesaplamalı ve fiziksel modellerden alınan geri bildirimlere dayalı olarak geliştirilmiştir. Sonuçları değerlendirmek için, ampirik veriler elde etmek üzere fiziksel prototipler üretilmiştir. Fiziksel prototiplerle yapılan deneyler, biyopolimer polilaktik asit ve termoplastik poliüretan olmak üzere iki farklı malzeme üzerinde gerçekleştirilmiştir. Böylece farklı malzemelerin davranışları gözlemlenmiş ve karşılaştırılmıştır. Gelecekte, önerilen sistemin tepkimeli malzemelerle entegrasyonu sayesinde büyük ölçekli mimari uygulamalara yönelik uyarlanabilir sistemlerin geliştirilmesi mümkün olabilecektir.

256

1. INTRODUCTION

Production strategies developed by modern industries have led to unsustainable systems due to the perception and utilization of natural materials as inexhaustible resources (Jalkh, 2020). Today, the growing awareness of these limited resources has triggered a paradigm shift, prompting designers to critically question what they design, produce, and how they go about doing so. In this context, modern industries must develop new and lighter material systems that reduce material consumption without compromising mechanical performance (Parente & Reis, 2024). Establishing a sustainable system and developing innovative solutions are only possible through an integrated and interdisciplinary approach (Delikanli & Cagdas, 2021). Over the past thirty years, researchers from various disciplines, through interdisciplinary collaboration, have turned to metamaterials as alternatives to natural materials (Naboni & Pezzi, 2016; Papadopoulou et al., 2017; Lu et al., 2022; Qu et al., 2024). Among these metamaterials, the most intriguing ones are "auxetics" due to their extraordinary mechanical properties.

The term auxetic originates from the Greek word "auxetikos" meaning tending to expand or increase. Auxetics were first defined by Evans in 1991 as materials with a negative poisson's ratio (NPR). The Poisson's ratio, introduced by the French scientist Simeon Denis Poisson, is a constant that characterizes a material's elasticity (Uzun, 2010). This ratio is defined quantitatively as the ratio of transverse contraction to longitudinal extension in a material. Most materials known today exhibit a behavior, where they become thinner when stretched and expand when compressed **(Figure 1).** However, auxetic materials display a counterintuitive behavior: they expand when stretched and contract when compressed (Liu & Hu, 2010; Park et al., 2015). This behavior enables different areas of application at architectural scale as a material system. These types of materials reduce the amount of energy required to create a three-dimensional (3D) form and distributes the internal mechanical forces of the system, ensuring a balanced form, similar to natural systems that achieve maximum performance with minimal energy input (Vivanco et al., 2023). However, this largely depends on the design of the material system and its usage scenario.
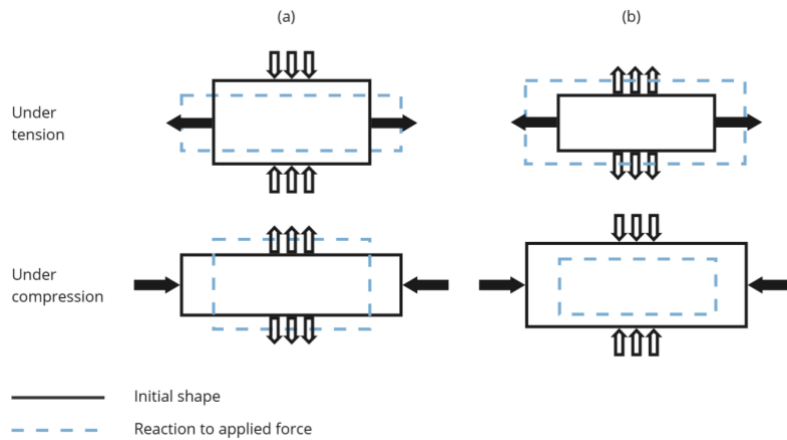
The deformation mechanisms of auxetic materials are primarily attributed to their cellular arrangements and geometric structures rather than their chemical composition (Carneiro et al., 2013; Naboni & Mirante, 2015). These structures consist of the periodic repetition of specific unit cells, characterized by significant transformations in pore size. Due to their nonlinear twisting and ability to adjust porosity and negative Poisson's ratio, these systems are widely studied in materials science (Naboni & Pezzi, 2016; Mesa et al., 2017). Classifying these geometric structures is essential for researchers to understand "*how auxetic effects can be achieved, how auxetic materials can be produced, and how their properties can be optimized and predicted*" (Oner et al., 2020). Auxetic structures are mainly divided into four subgroups as (1) chiral structures, (2) rotating structures, (3) re-entrant structures, and (4) foldable structures **(Figure 2).** These transformations bring out the auxetic properties by altering the material's inherent characteristics (Dong & Hu, 2023).

Interest in auxetic materials has increased over time in terms of exploration of their material behavior and transformational properties. In the following sections, the gap in the literature will be identified by focusing on the potential applications of auxetics, which continue to be experimentally developed across various disciplines, and the recent advancements in their use within the field of architectural design.

258

JCoDe | Vol 6 No 2 | September 2025 | Tolerance in Computational Design| Güloğlu, Z., Yazıcı, S.
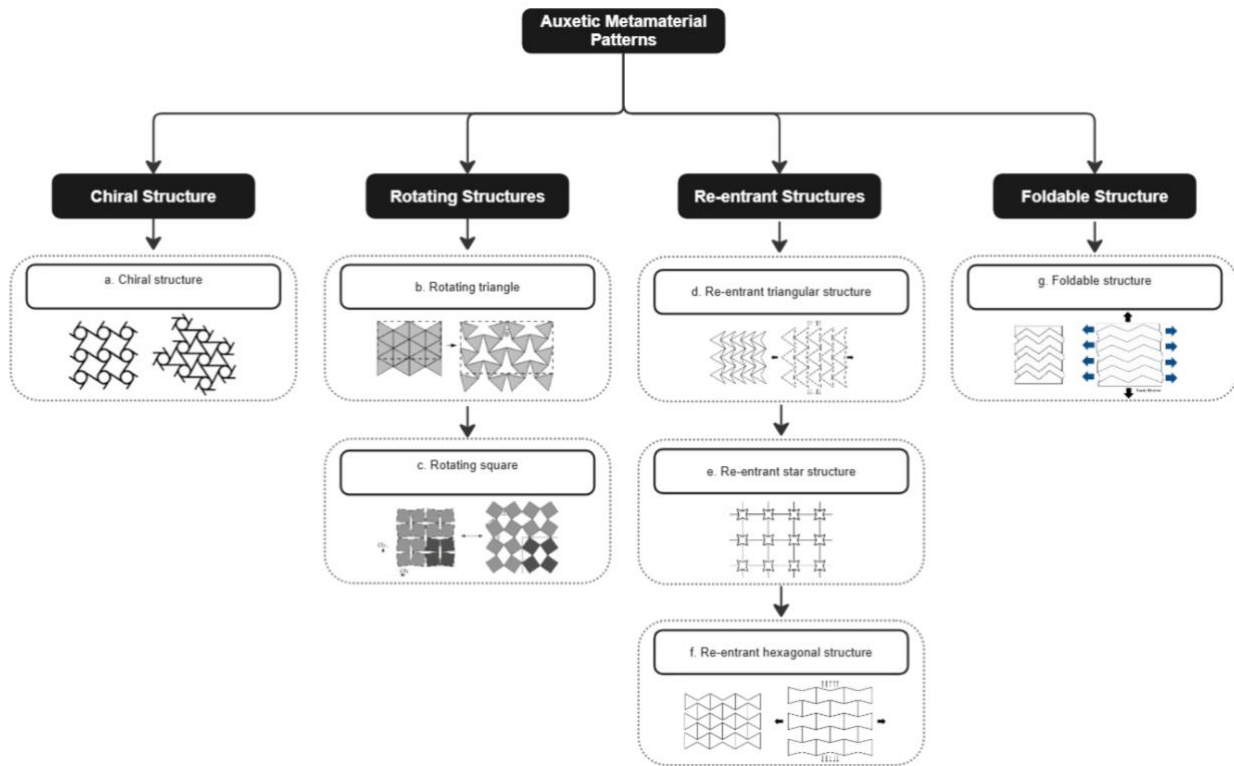
Figure 2: Classification of auxetic metamaterial patterns, adapted from the work of Dong and Hu (2023).

1.1 Applications of Auxetics as a Novel Material System

Interest in such materials historically began in 1987 with Lakes' production of auxetic foam through triaxial compression, heating, and cooling processes applied to polyurethane foams. In subsequent years, various auxetic materials have been engineered and produced, including cubic metals, zeolites, silicates, hydrogels, aerogels, auxetic fibers, and molecular-level auxetic polymers (Tripathi, 2024). "Auxetics" at the molecular level, such as liquid crystalline polymers (LCPs), are specifically engineered through nanoscale chemical synthesis. In contrast, "auxetic fibers" can be produced at the nano-, micro-, and macro-scales, depending on the intended application (Liu & Hu, 2010). Glynn et al. (2018) describe these materials as the man-made of the future, exhibiting superior properties that are not yet found in nature. Compared to traditional materials, they demonstrate resistance to indentation, higher fracture toughness, synclastic curvature formation capacity, energy absorption, variable permeability, and shear resistance. These advanced characteristics make them prime candidates for numerous potential applications.

Among these applications are impact/ballistic protection, acoustics, automotive, shape-memory polymers, wearable strain sensors, electromagnetic shielding, smart filters, rehabilitation, biomedical, and sports applications. Another significant application of auxetic materials is their potential use in building systems as more sustainable materials (Nasiri, 2024). Due to their morphological structure, these materials are force-sensitive, flexible, and adjustable. They can be activated with less energy, offering a sustainable alternative to complex and costly kinetic systems (Tibbits, 2017; Papadopoulou et al., 2017). In recent studies, a dual-layer sample was produced by bonding auxetic foam with a polyurethane film; when immersed in hot water, this sample bent into a ring shape and quickly reverted to its original form upon removal (Tripathi, 2024; section 6.4). Given the advantages offered by this material system, researchers and professionals from various disciplines such as materials science, engineering, and architecture will continue to develop diverse strategies for its design and production. This, in turn, will give rise to a new material practice where designers are actively involved in the manufacturing process (Oxman, 2015).

1.2 Recent Advances in Auxetic Material Applications in Architecture

The application of these material systems in the field of architecture began in the 2010s. In 2013, Themistocleous from UCL developed a methodology for the design of pneumatically activated auxetic systems and focused on their simulation (Themistocleous, 2013). In 2015, Naboni and Mirante from ACTLAB examined existing auxetic patterns and explored their use in bending-active shell structures, although no new auxetic structures were proposed (Mirante, 2015). Also in the same year, Park et al. (2015) attempted to create morphological variations of the most commonly used re-entrant honeycomb structure in the literature. They combined 2D sheet structures to produce simple 3D compositions and theoretically proposed multi-material additive manufacturing for transitions between hard and soft materials in 3D cubes. Zaha Hadid Architects also utilized auxetic cutting patterns on 2mm steel plates in the Volu dining pavilions to achieve double curvature without molds (Louth et al., 2017; Albag, 2021). Unlike smart transformations in auxetic structures, their study primarily focused on generating curvature. Later in 2018, topologically optimized and functionally graded cable networks were produced and applied to a chair (Tish et al., 2018).

260

JCoDe | Vol 6 No 2 | September 2025 | Tolerance in Computational Design| Güloğlu, Z., Yazıcı, S.

In the same year, Belanger et al. (2018) used auxetic patterns to produce a slumped glass structure and examined the acoustic effects within the glass. However, in this study, the movable auxetic geometric structure was locked and fixed in the glass. The following year, Pertigkiozoglou (2019) utilized auxetic slits in aluminum sheets to create free-form deformable surfaces. However, instead of auxetic-driven transformations, slits have been utilized to generate curvature on the surface.

As the present day is approached, explorations of these material systems have persisted. Martínez (2021) produced porous sheet structures using parametric growth processes through coding. After optimizing these structures, Negative Poisson's Ratio (NPR) was indirectly observed. However, since tensile and compression tests were not performed in a physical environment, clear information about the auxetic behavior of the produced structure could not be obtained. Later on, Ozdemir et al. (2022) at ICD Stuttgart produced a self-shaping metamaterial shell using a re-entrant honeycomb auxetic structure. Hygrosensitive wood actuators were placed between the shell layers and left to dry, completing a self-shaping process after 152 hours. Although this approach was innovative, the wood actuators did not integrate well with the existing structure, and as the shell did not shape as desired, it was supported from its center of mass to facilitate the shaping process after 72 hours. In this study, auxetic behavior guided by patterns did not occur; instead, the transformation was achieved through the wood bilayers. Lastly, Nasiri (2024) focused on generating existing auxetic geometries using the Shape Machine tool, a generative shape grammar tool, through simple initial shapes and rules. Since no physical production was undertaken in this study, an integrated system of form and material behavior was not observed.

Upon reviewing the conducted studies, it is evident that most of the designs and productions in the literature predominantly utilize existing auxetic structures. Additionally, many studies address auxetic patterns solely as fixed surface coatings, without observing the intelligent transformations embedded morphologically within the material. Accordingly, this paper aims to make an original contribution to the literature by presenting the proposed methodology for developing novel auxetic systems and their practical applications in architectural design contexts.

In the following section, the methodological process will be introduced to address key questions: What are the critical parameters of an auxetic system? Which materials and manufacturing methods can be used to produce auxetic structures? How can the behavior of these structures be tested?

2. METHODOLOGY

The auxetic behavior is achieved through an integrated approach involving specific unit cell arrangements, appropriate material selection, and the direction of the applied forces. Considering all these factors, the methodology is built upon a workflow based on feedback from both computational and physical models, and consists of four stages: (1) identifying geometrical parameters of auxetic metamaterials, (2) setting the computational model, (3) digital fabrication, and (4) physical experiments (Figure 3).

1. Identifying geometrical parameters of auxetic metamaterials: The selected auxetic design is examined and the parameters that constitute the behavior of the system are extracted.

2. Setting the computational model: Using these parameters, a custom-designed auxetic pattern is created in algorithmic design environment. Subsequently, a three-dimensional (3D) shell structure is created through coding to observe its transition from a planar to an out-of-plane state and to explore the potential architectural applications of a customized auxetic structure.

3. Digital fabrication: For the production of the designed auxetic structure, additive manufacturing, 3D printing more specifically, is chosen, and Biopolymer Polylactic Acid (PLA) and Thermoplastic Polyurethane (TPU) are selected as materials for prototyping.

4. Physical experiments: Prototypes are produced to test the auxetic behavior in physical environment. The smart transformations of the material under tensile and compressive forces are observed and measured.

262

JCoDe | Vol 6 No 2 | September 2025 | Tolerance in Computational Design| Güloğlu, Z., Yazıcı, S.

Step1 | *Identifying Geometrical Parameters of Auxetic Metamaterials*

Transformation

Algorithmic modeling of the re-entrant hexagonal pattern

Parameters that create auxetic behavior

U parameter
Segmentation along the y-axis

V parameter
Segmentation along the x-axis

T parameter
Auxetic behavior
(Angle that creates concavity)

Step2 | *Setting the Computational Model: Custom Auxetic Patterns and Shells*

C# programming language

Transformation of customized auxetic system into monoclastic shell structure

Algorithmic modeling in visual programming language

out-of-plane state

planar state

Step3 | *Digital Fabrication*

Testing

Biopolymer Polylactic Acid (PLA)

+

Thermoplastic Polyurethane (TPU Flex 95A)

Additive manufacturing (AM) of the prototypes

Fused deposition modeling (FDM)

Step4 | *Physical Experiments*

Relaxed state

measuring displacement

F_1 uniaxial force

stretched state

two different morphological deformations

No

Does it show auxetic behavior?

Yes

Stop

input ....▶ *output*

Figure 3: Methodology of the research.

2.1 Identifying Geometrical Parameters of Auxetic Metamaterials

One of the most studied auxetic geometries in the literature is the re-entrant honeycomb structure (Jalkh, 2020; Parente & Reis, 2024; Bol et al., 2024). The reasons for selecting this geometry by various researchers include its high deformation capacity, geometric simplicity, and the absence of the need for additional processing such as cutting. Furthermore, it exhibits spontaneous hinge behavior without the use of traditional hinges. However, the extensive use of only this geometry has limited diversity. Considering the advantages of this geometry, the re-entrant honeycomb structure is chosen as the first step to create a new auxetic structure from the existing one. The selected auxetic pattern is modeled in a computational design environment, and its deformation is simulated **(Table 1).**

The auxetic behavior in these structures arises from the displacement of two opposite corner points of a hexagonal unit, which move inward and outward under applied forces. Subsequently, three parameters—u, v, and t—are defined to generate any re-entrant cell arrangement. Among these, one of the most critical parameters is the t-angle parameter, which leads to concavity within the cell. This parameter governs the movement of the ribs, enabling the units to function as hinges and achieve auxetic behavior. The u and v parameters segment the structure along the y- and x-axes, respectively. The auxetic behavior is primarily controlled by the t-angle parameter, which ranges between 0 and 1 and determines the concavity in the cell geometry. **Figure 4** depicts the unit cell structure and its tessellation, where t denotes the angle between the concave ribs, and l and h correspond to the unit's horizontal and vertical dimensions, respectively.
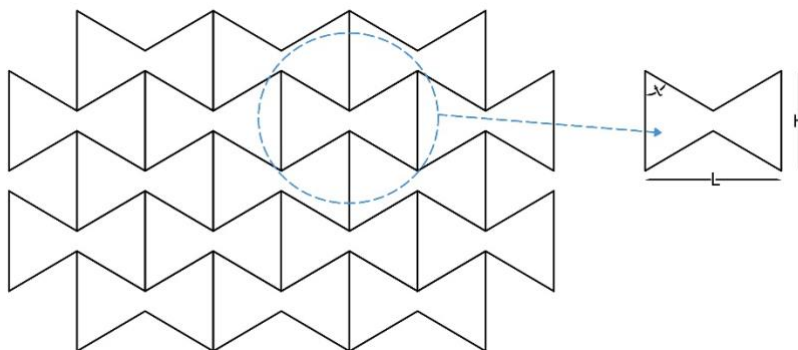
Figure 4: Schematic representation of a re-entrant hexagonal pattern, adapted from the work of Ghiasvand et al. (2023).

264

JCoDe | Vol 6 No 2 | September 2025 | Tolerance in Computational Design| Güloğlu, Z., Yazıcı, S.

Parameters	Top view	Perspective view
t=0.40 ° **u**=5 unit **v**=5 unit **w**=0.03m **h**=0.3m		
t=0.60 ° **u**=5 unit **v**=5 unit **w**=0.03m **h**=0.3m		
t=0.80 ° **u**=5 unit **v**=5 unit **w**=0.03m **h**=0.3m		

Table 1: Auxetic behavior of the re-entrant hexagonal structure, proposed by Evans (Jalkh, 2020), simulated by the authors.

Where t is defined as the angle between the concave ribs, u as the total number of divisions along the Y-axis, and v as the total number of divisions along the X-axis, w as the width of the ribs, h as the height of the ribs.

2.2 Setting the Computational Model: Custom Auxetic Patterns and Shells

The parameters u, v, and t are derived from the previous section after understanding the behavior of the system. At this stage, a new auxetic pattern is proposed as an alternative to existing auxetic models using these parameters. The newly created pattern is intended to exhibit concave to convex behavior without requiring additional processing, such as cutting or traditional hinging, as seen in re-entrant structures. In this context, a pattern with concave features is initially considered, and its geometric representation is abstracted before the algorithm is developed. To create the pattern, the first step involves dividing a square unit into eight parts and drawing an arc from the diagonal of the square. In the second step, a curve is drawn connecting this arc with the y-axis. In the third step, a mirror operation is applied to the shape obtained in the second step, and the three created curves are combined to form a corner of the pattern. Finally, a polar array process is applied to this created unit, completing the final pattern **(Figure 5).**

The formation stages of the customized pattern

Step1. Creating an arc.

Step 2. Creating a curve from the arc to the y-axis

Step 3. Mirroring the second created curve

Step 4. Completing the pattern with polar array

Existing pattern found in the literature

Re-entrant hexagonal pattern

To explore potential architectural applications of the customized auxetic structure, a three-dimensional (3D) shell structure is created from the proposed auxetic pattern. Due to limitations in the visual programming language (such as a high number of vertices and extended computation time) when generating a shell-like form from this model, a custom code is written in the C# programming language **(Figure 6)**. The input values in this code are as follows: interval UT = the total value of the shell structure on the y-axis, interval VT = the total value of the shell structure on the x-axis, int NU = the total number of customized pattern units created along the y-axis (taken as 10 in the created example), and int NV = the total number of customized pattern units created along the x-axis (taken as 15 in the created example). The generated code creates U and V lists by dividing the lengths of two vectors named UT and VT into NU and NV ranges, respectively. The U and V lists are thereby created to contain a specific number of intervals, with each interval dividing the vector lengths into equal parts.

Figure 5: Steps to create a new auxetic pattern.

266

JCoDe | Vol 6 No 2 | September 2025 | Tolerance in Computational Design| Güloğlu, Z., Yazıcı, S.

```
Script component: C#

/**/
private void RunScript(Interval UT, Interval VT, int NU, int NV, ref object U, ref object V)
{
    double dU = UT.Length / NU;
    double dV = VT.Length / NV;

    List<Interval> u = new List<Interval>();
    List<Interval> v = new List<Interval>();

    Interval uInterv = new Interval(0, dU);

    for(int j = 0; j < NV; j++)
    {
        for(int i = 0; i < NU; i++)
        {
            u.Add(uInterv);
            uInterv = new Interval(uInterv.Max, uInterv.Max + dU);
        }
        uInterv = new Interval(0, dU);
    }

    U = u;

    Interval vInterv = new Interval(0, dV);

    for(int j = 0; j < NV; j++)
    {
        for(int i = 0; i < NU; i++)
        {
            v.Add(vInterv);
        }

        vInterv = new Interval(vInterv.Max, vInterv.Max + dV);
    }

    V = v;
```

Figure 6: Script created in C# programming language to create a 3D shell structure.

2.3 Digital Fabrication

Additive manufacturing processes such as FDM (Fused Deposition Modeling) and SLS (Selective Laser Sintering) are good alternatives for producing auxetic designs with geometric complexity (Bol et al., 2024). In this study, the FDM technique will be used to save time and quickly produce parts, as 3D parts are directly heated and extruded through a nozzle from a CAD file. At this stage of the study, two materials with different mechanical properties are selected to examine auxetic behavior: one flexible and one rigid. First of all, thermoplastic polyurethane (TPU) is chosen as the flexible material due to its superior elasticity compared to other available thermoplastic polymers (Elmrabet & Siegkas, 2020). Secondly, polylactic acid (PLA) is chosen as a rigid material due to its ability to be processed at lower temperatures while maintaining high dimensional accuracy (Ramírez-Revilla et al., 2022), compared to alternatives such as acrylonitrile butadiene styrene (ABS), acrylonitrile styrene acrylate (ASA), and polyethylene terephthalate glycol (PETG). **Figure 7** illustrates the digital fabrication stages of models created.

2.4 Physical Experiments

Simulations conducted solely in computational environments are insufficient for accurately capturing auxetic effects. Therefore, the relationship between material behavior and the proposed cellular arrangement should rather be empirically tested. Auxetic behavior is influenced by factors such as geometric design (special cellular arrangements), material type, and the direction of the applied force. In this regard, the impact of applied forces is examined following the digital fabrication process. Given that auxetic structures are highly sensitive to external forces, as illustrated in the methodological framework, an exploratory investigation is conducted by manually applying force along different axes. This experimental approach provides a deeper understanding of material responses and smart transformations. Subsequently, displacement is measured with a ruler by marking reference points at the sample's edges before and after force application. Thus, the study systematically analyzes the impact of two materials with distinct properties on auxetic behavior.

3. RESULTS & DISCUSSION

In this study, design parameters were defined to a system exhibiting auxetic behavior, and the system's behavior was tested in both computational and physical environments. The findings will be discussed based on prototypes made from different materials and geometric variations.

268

JCoDe | Vol 6 No 2 | September 2025 | Tolerance in Computational Design| Güloğlu, Z., Yazıcı, S.

3.1 Prototype Comparisons

To test whether the initially developed design parameters meet geometric and behavioral relationships in a physical environment, small-scale prototypes were produced and physical experiments were conducted. Small-scale prototypes were developed by printing grid-structured samples with dimensions of 150x150x3 mm. Subsequently, in-plane and out-of-plane forces were applied to observe the morphological effects as well as limitations and potentials of different material types.

The results of physical experiments conducted using two different materials—rigid (PLA) and flexible (TPU)—are presented below **(Table 2).** First, the sample created with Biopolymer Polylactic Acid showed no deformation when an in-plane tensile force was applied, and no auxetic behavior was observed. Additionally, when the magnitude of the force was further increased, fractures occurred between the unit cells. This material was deemed unsuitable for further studies due to issues such as brittleness, stiffness, and lack of flexibility.

The sample made from Thermoplastic Polyurethane, although slower and requiring more time to print, was found to be successful in exhibiting auxetic behavior **(Table 3).** When in-plane tensile force was applied to this material, two separate shape deformations were observed, and these displacements were measured and recorded as 2.5 cm and 6 cm, respectively. When out-of-plane force was applied to the samples, the Biopolymer Polylactic Acid showed less capacity for curvature formation compared to the Thermoplastic Polyurethane.
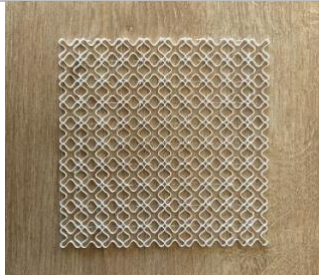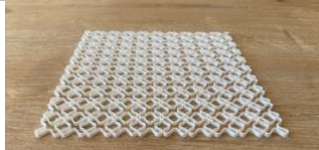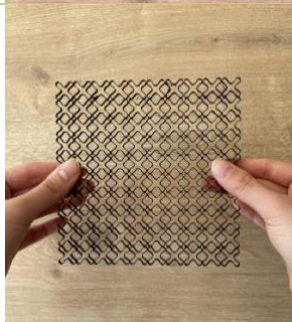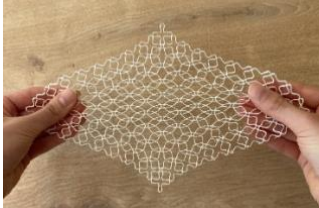
Material	Biopolymer Polylactic Acid	Thermoplastic Polyurethane
Top View		
Front View		
In-plane Force	 relaxed and stretched state	 **1. Shape Deformation** relaxed ⟶ stretched state *a displacement of 2,5 cm* **2. Shape Deformation** relaxed ⟶ stretched state *a displacement of 6 cm*
Out of Plane Force	 minor monoclastic behavior	 monoclastic behavior

Table 2: Physical testing of prototypes made from Biopolymer Polylactic Acid (PLA) and Thermoplastic Polyurethane (TPU).

270

JCoDe | Vol 6 No 2 | September 2025 | Tolerance in Computational Design| Güloğlu, Z., Yazıcı, S.

Material	Biopolymer Polylactic Acid (PLA)	Thermoplastic Polyurethane (TPU Flex 95A)
Auxetic pattern	Custom pattern	Custom pattern
Pattern size	150x150 mm	150x150 mm
Material thickness	3 mm	3 mm
Print speed	100 mm/s	20 mm/s
Print time	1 and a half hours	12 and a half hours
Machine type	Ender-3 S1 Pro	Ender-3 S1 Pro
Technology used	Fused deposition modeling (FDM)	Fused deposition modeling (FDM)
Flexibility feature	Limited	High
Displaying curvature?	Yes	Yes
Extruder temperature	210 °C	230 °C
Table temperature	75 °C	50 °C
Does it exhibit auxetic behavior?	No	Yes

Table 3: Comparison of prototypes made of Biopolymer Polylactic Acid and Thermoplastic Polyurethane.

3.2 Pattern Variations

The custom-designed pattern was placed on a 10x10 grid in the algorithmic design environment, and the deformation mechanism of the system was examined to observe auxetic behavior. When the angle parameter t, which triggers shape distortions in the pattern, was varied, the system's behavior changed accordingly. For instance, as t increased from 0.00 to 0.60, the system transitioned from convex to concave behavior. As the t parameter approached 1, the system contracted, resulting in smaller pores. Conversely, as t approached 0, the pores expanded **(Table 4a).** To address various architectural needs and further refine the auxetic structure, a point attractor that reacts to the existing curves has been incorporated into the system. By breaking the uniformity observed in **Table 4a**, this approach produced alternative configurations. Various states based on different parameters are documented below **(Table 4b).**
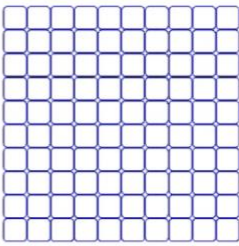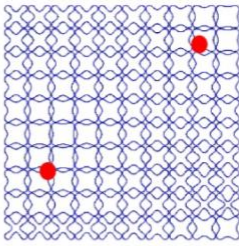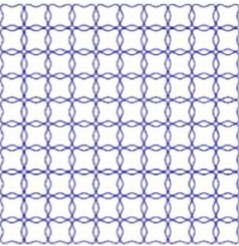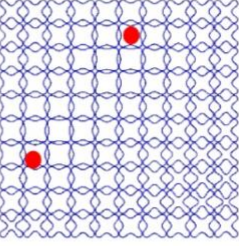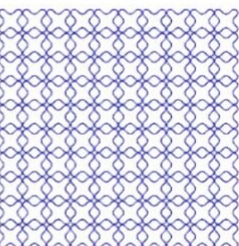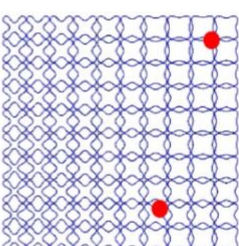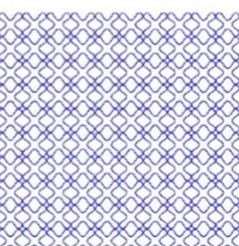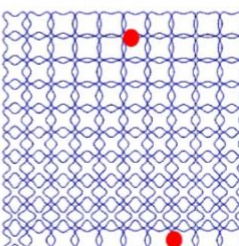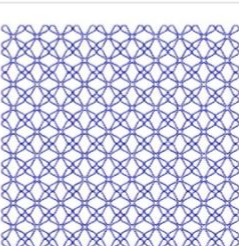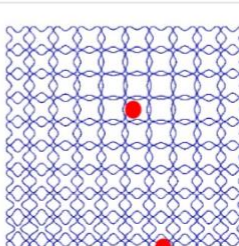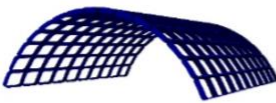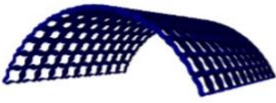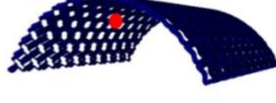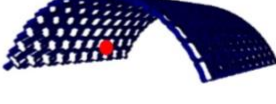
(a) Parameters	Top view	(b) Parameters	Top view
t=0.00 ° u=10 unit v=10 unit		State1 u=10 unit v=10 unit	
t=0.20 ° u=10 unit v=10 unit		State2 u=10 unit v=10 unit	
t=0.40 ° u=10 unit v=10 unit		State3 u=10 unit v=10 unit	
t=0.60 ° u=10 unit v=10 unit		State4 u=10 unit v=10 unit	
t=0.80 ° u=10 unit v=10 unit		State5 u=10 unit v=10 unit	

Table 4: Exploration of pattern variations:
(a) States created by changing *t* parameter
(b) States created with point attractor (red dot).

272

JCoDe | Vol 6 No 2 | September 2025 | Tolerance in Computational Design| Güloğlu, Z., Yazıcı, S.

To explore the potential architectural applications of a customized auxetic structure and to observe its transition from a planar state to a out-of-plane state, a three-dimensional (3D) shell structure was generated through coding. The dimensions of the ribs in the unit cell of this structure were kept constant, with a width of 0.05 m and a height of 0.3 m. The functionality of the code was tested in two distinct stages. In the first stage, when the angle parameter t of the customized auxetic pattern was varied, the resulting patterns were successfully generated on a monoclastic shell, and different phases of auxetic behavior were observed. As the parameter t approached 1, the porosity of the shell decreased and became more compacted **(Table 5a).** In the second stage, the effect of a point attractor integrated into the algorithm was examined. During this phase, the porosity within the monoclastic shell structure varied regionally, leading to the emergence of diverse conditions **(Table 5b).**

Table 5: Transformation of customized auxetic system into monoclastic shell structure: (a) States created by changing t parameter (b) States containing point attractor (red dot).

(a) Parameters	Two point perspective view	(b) Parameters	Two point perspective view
t=0.00° u=10 unit v=15 unit w=0.05 m h=0.3 m		State1 u=10 unit v=15 unit w=0.05 m h=0.3 m	
t=0.20° u=10 unit v=15 unit w=0.05 m h=0.3 m		State2 u=10 unit v=15 unit w=0.05 m h=0.3 m	
t=0.40° u=10 unit v=15 unit w=0.05 m h=0.3 m		State3 u=10 unit v=15 unit w=0.05 m h=0.3 m	
t=0.60° u=10 unit v=15 unit w=0.05 m h=0.3 m		State4 u=10 unit v=15 unit w=0.05 m h=0.3 m	
t=0.80° u=10 unit v=15 unit w=0.05 m h=0.3 m		State5 u=10 unit v=15 unit w=0.05 m h=0.3 m	

3.3 Evaluation of the Outputs

In this study, a new auxetic system was developed through physical prototypes using PLA and TPU. The TPU-based prototype exhibited two distinct deformation modes, confirming auxetic behavior. In the literature, Ozdemir et al. (2022) explored the architectural potential of these materials by creating a self-shaping auxetic shell. For the 1:10 small-scale prototype, they used PLA. In their study, no shape transformation was observed between the auxetic geometry units. Instead, they utilized the tunability of auxetic geometries, demonstrating that variations in geometric parameters influenced the shell's curvature. However, unlike their study, this work preserved the movable mechanism of the auxetic system, enabling shape deformations.

Belanger et al. (2018) employed auxetic cutting patterns to fabricate slumped glass structures, leveraging the curvature-forming and acoustic properties. However, in their study, the movable auxetic mechanism was locked after fabrication, rendering it static. In contrast, the present study proposes the development of interactive, adaptive structures that respond to user needs and engage with their environment, envisioning future architectural scenarios. The auxetic system developed in this study exhibits adaptive properties due to its force-sensitive nature. These structures have various potential applications in architecture. One application is flexible and dynamic partitioning systems that allow a single space to adapt to different functions. Another application involves interactive installations created through auxetic surfaces that respond to touch or pressure.

For large-scale architectural applications, the designed system can achieve self-activation through two methods: integration with electrical control systems or passive mechanisms. The first approach involves costly kinetic mechanisms, requiring maintenance and energy consumption, making it unsustainable. Therefore, this study proposes the second approach: passive systems. Within this scope, the integration of auxetic systems with double-layered polymers could enable the development of dynamic shading systems.

274

JCoDe | Vol 6 No 2 | September 2025 | Tolerance in Computational Design| Güloğlu, Z., Yazıcı, S.

4. CONCLUSION

Auxetic systems are rarely encountered in the field of architecture and continue to be experimentally developed by various researchers. In this study, a novel auxetic material system has been designed by introducing various design parameters for the use of auxetic systems in architecture. The proposed system was tested using physical prototypes made from different materials, and two distinct types of shape deformation were observed, confirming its auxetic behavior. In this study, the first type of shape deformation was utilized due to its more controlled nature and minimal displacement. However, in future research, the second type of shape deformation could also be used to develop environmentally responsive adaptive solutions.

The system developed in this research holds potential for various applications in future studies. Firstly, the designed system offers a promising approach for situations in architecture where variable environmental conditions are desired, such as acoustic manipulation, lighting, and airflow control, due to its ability to create variable porosity. Furthermore, due to the sound absorption properties of auxetic materials, they can be utilized as surface panels in interior spaces where excessive noise is undesirable and their performance could then be evaluated. Lastly, cases where regionally variable porosity is created allow for the creation of visually interactive systems for exhibition and gallery spaces by incorporating different colors and textures.

The high cost and limited availability of shape-memory polymers have hindered the testing of the system under activation by external stimuli such as temperature and humidity. By programming the expansion and contraction behavior of auxetic structures using materials such as bilayer polymers, future developments could contribute to the creation of climate-responsive facade systems that adapt to environmental changes. For instance, a dynamic facade or shading system could expand in hot weather to enhance airflow and/or provide shading, while contracting in cold conditions to improve thermal comfort.

Due to limited access to robotic fabrication, the physical prototypes in this study were constrained by the build volume of a 3D printer. Future research could explore collaborations in robotic fabrication, enabling the production of large-scale auxetic structures through robotic arms, the development of modular auxetic panels, and their robotic assembly. Such collaborations could facilitate the scalability and feasibility of auxetic systems in architectural applications. This research is expected to expand the conceptual framework of auxetic materials and inspire future studies to develop innovative solutions.

Conflict of Interest Statement

The authors declare that there are no financial or other significant conflicts of interest that could have influenced the outcomes or interpretations presented in this study.

Author Contributions

Zehra Güloğlu: Conceptualization, Methodology, Validation, Investigation, Writing - original draft, Visualization. **Sevil Yazıcı:** Conceptualization, Investigation, Writing - review & editing. All authors have read and agreed to the published version of the manuscript.

Institutional Review Board Statement

The authors declare that no ethical approval was required for the execution of this study.

276

JCoDe | Vol 6 No 2 | September 2025 | Tolerance in Computational Design | Güloğlu, Z., Yazıcı, S.

References

Albag, O. E. (2021). Auxetic materials. In I. Paoletti, M. Nastri (Eds.), *Material Balance: A Design Equation* (pp. 65–74). Springer. https://doi.org/10.1007/978-3-030-54081-4_6

Belanger, Z., McGee, W., & Newell, C. (2018). Slumped Glass: Auxetics and acoustics. In P. Anzalone, M. Del Signore, A. J. Wit (Eds.), *Proceedings of the 38th Annual Conference of the Association for Computer Aided Design in Architecture (ACADIA 18)* (pp. 244–249). ACADIA. https://doi.org/10.52842/conf.acadia.2018.244

Bol, R. J., Xu, Y., & Šavija, B. (2024). Printing path-dependent two-scale models for 3D printed planar auxetics by material extrusion. *Additive Manufacturing,* 89, Article 104293. https://doi.org/10.1016/j.addma.2024.104293

Carneiro, V. H., Meireles, J., & Puga, H. (2013). Auxetic materials — A review. *Materials Science-Poland,* 31(4), 561–571. https://doi.org/10.2478/s13536-013-0140-6

Delikanli, B., & Cagdas, G. (2021). Transdisciplinary concepts in computational design and reflections on education. In G. Çağdaş, M. Özkar, L. F. Gül, S. Alaçam, E. Gürer, S. Yazıcı, B. Delikanli, Ö. Çavuş, S. Altun, & G. Kırdar (Eds.), *Computational design in architecture, 15th National Symposium* (pp.93–104). İstanbul Technical University.

Dong, S., & Hu, H. (2023). Sensors based on auxetic materials and structures: A review. *Materials,* 16(9), 3603. https://doi.org/10.3390/ma16093603

Elmrabet, N., & Siegkas, P. (2020). Dimensional considerations on the mechanical properties of 3D printed polymer parts. *Polymer Testing*, 90, Article 106656. https://doi.org/10.1016/j.polymertesting.2020.106656

Ghiasvand, A., Khanigi, A. F., Guerrero, J. W. G., Derazkola, H. A., Tomków, J., Janeczek, A., & Wolski, A. (2023). Investigating the effects of geometrical parameters of Re-Entrant cells of aluminum 7075-T651 auxetic structures on fatigue life. *Coatings*, 13(2), 405. https://doi.org/10.3390/coatings13020405

Glynn, R., Abramovic, V., Overvelde, JTB. (2018). Edge of chaos: Towards intelligent architecture through distributed control systems based on cellular automata. In P. Anzalone, M. Del Signore, A. J. Wit (Eds.), *Proceedings of the 38th Annual Conference of the Association for Computer Aided Design in Architecture (ACADIA 18)* (pp. 226–231). ACADIA. https://doi.org/10.52842/conf.acadia.2018.226

Jalkh, H. (2020). Morpho-active materials: Fabricating auxetic structures with bioinspired behavior. *Blucher Design Proceedings*, 8(4), 863-869. https://doi.org/10.5151/sigradi2020-117

Liu, Y., & Hu, H. (2010). A review on auxetic structures and polymeric materials. *Scientific Research and Essays,* 5(10), 1052–1063. https://doi.org/10.5897/sre.9000104

Louth, H., Reeves, D., Bhooshan, S., Schumacher, P., Koren, B., Menges, A., Sheil, B., Glynn, R., & Skavara, M. (2017). A prefabricated dining pavilion: Using structural skeletons, developable offset meshes and kerf-cut bent sheet materials. In A. Menges, B. Sheil, R. Glynn, & M. Skavara (Eds.), *Fabricate 2017* (pp. 58–67). UCL Press. https://doi.org/10.2307/j.ctt1n7qkg7.12

Lu, C., Hsieh, M., Huang, Z., Zhang, C., Lin, Y., Shen, Q., Chen, F., & Zhang, L. (2022). Architectural design and additive manufacturing of mechanical metamaterials: A review. *Engineering,* 17, 44–63. https://doi.org/10.1016/j.eng.2021.12.023

Martínez, J. (2021). Random auxetic porous materials from parametric growth processes. *Computer-Aided Design*, 139, Article 103069. https://doi.org/10.1016/j.cad.2021.103069

Mesa, O., Stavric, M., Mhatre, S., Grinham, J., Norman, S., Sayegh, A., & Bechthold, M. (2017). Non-linear matters: Auxetic surfaces. In T. Nagakura, S. Tibbits, C. Mueller (Eds.), *Proceedings of the 37th Annual Conference of the Association for Computer Aided Design in Architecture (ACADIA 2017)* (pp. 392–403). ACADIA. https://doi.org/10.52842/conf.acadia.2017.392

Mirante, L. (2015). *Auxetic Structures: Towards Bending-Active Architectural Applications* [Master's thesis, Politecnico di Milano - Polimi]. *POLITesi*. https://www.politesi.polimi.it/handle/10589/116372

Naboni, R., & Mirante, L. (2015). Metamaterial computation and fabrication of auxetic patterns for architecture. *Blucher Design Proceedings,* 2(3), 129–136. https://doi.org/10.5151/despro-sigradi2015-30268

Naboni, R., & Pezzi, S. S. (2016). Embedding auxetic properties in designing active-bending gridshells. *Blucher Design Proceedings,* 3(1), 720–726. https://doi.org/10.5151/despro-sigradi2016-490

Nasiri, S. (2024). Auxetic Grammars: An Application of Shape Grammar Using Shape Machine to Generate Auxetic Metamaterial Geometries for Fabricating Sustainable Kinetic Panels. In Yan, C., Chai, H., Sun, T., Yuan, P.F. (Eds.), *Phygital Intelligence. CDRF 2023. Computational Design and Robotic Fabricatio* (pp. 114–124). Springer. https://doi.org/10.1007/978-981-99-8405-3_10

278

JCoDe | Vol 6 No 2 | September 2025 | Tolerance in Computational Design| Güloğlu, Z., Yazıcı, S.

Oxman, R. (2015). MFD: Material-fabrication-design: A classification of models from prototyping to design. In *Proceedings of the International Association for Shell and Spatial Structures Symposium (IASS) Symposium 2015*

Oner, D., Ezel Çırpı, M., & Çakıcı Alp, N., (2020). Auxetic Davranış ile Mimari Tasarım Deneyimi. In *XIV. National Symposium on Digital Design in Architecture* (pp. 43–51). Karadeniz Technical University.

Ozdemir, E., Kiesewetter, L., Antorveza, K., Cheng, T., Leder, S., Wood, D. & Menges, A. (2022). Towards self-shaping metamaterial shells: A computational design workflow for hybrid additive manufacturing of architectural scale double-curved structures. In Yuan, P.F., Chai, H., Yan, C., Leach, N. (Eds.), *Proceedings of the 2021 Digital FUTURES. CDRF 2021* (pp. 275–285)*.* Springer. https://doi.org/10.1007/978-981-16-5983-6_26

Papadopoulou, A., Laucks, J., & Tibbits, S. (2017). Auxetic materials in design and architecture. *Nature Reviews Materials,* 2(12). Article 17078. https://doi.org/10.1038/natrevmats.2017.78

Parente, J.M., & Reis, P.N.B. (2024). Fatigue behaviour of 3d printed auxetic materials: An overview. *Procedia Structural Integrity,* 53, 221–223. https://doi.org/10.1016/j.prostr.2024.01.027

Park, D., Lee, J., & Romo, A. (2015). Poisson's ratio material distributions. In *Proceedings of the 20th International Conference of the Association Architectural Design Research in Asia (CAADRIA 2015)* (pp. 735–744). CAADRIA. https://doi.org/10.52842/conf.caadria.2015.735

Pertigkiozoglou, E. (2019). Pattern mapping. In K. Bieg, D. Briscoe, C. Odom (Eds.), *Proceedings of the 39th Annual Conference of the Association for Computer Aided Design in Architecture (ACADIA 19)* (pp. 72–80). ACADIA. https://doi.org/10.52842/conf.acadia.2019.072

Qu, J., Lei, Y., Dong, Q., & Wang, H. (2024). Hierarchical design of auxetic metamaterial with peanut-shaped perforations for extreme deformation: Self-similar or not? *European Journal of Mechanics - a/Solids,* 108, Article 105402. https://doi.org/10.1016/j.euromechsol.2024.105402

Ramírez-Revilla, S., Camacho-Valencia, D., Gonzales-Condori, E. G., & Márquez, G. (2022). Evaluation and comparison of the degradability and compressive and tensile properties of 3D printing polymeric materials: PLA, PETG, PC, and ASA. *MRS Communications*, 13(1), 55–62. https://doi.org/10.1557/s43579-022-00311-4

Themistocleous, T. (2013). Modelling, simulation and verification of pneumatically actuated auxetic systems. In R. Stouffs, P. Janssen, S. Roudavski, B. Tunçer (Eds.), *Proceedings of the 18th International Conference on Computer-Aided Architectural Design Research in Asia*

(CAADRIA 2013) (pp. 395–404). National University of Singapore. https://doi.org/10.52842/conf.caadria.2013.395

Tibbits, S. (2017). An introduction to active matter. In S. Tibbits (Ed.), *Active Matter* (pp. 1–12). The MIT Press. https://doi.org/10.7551/mitpress/11236.003.0003

Tish, D., Schork, T., & McGee, W. (2018). Topologically optimized and functionally graded cable nets: New approaches through robotic additive manufacturing. In P. Anzalone, M. Del Signore, A. J. Wit (Eds.), *Proceedings of the 38th Annual Conference of the Association for Computer Aided Design in Architecture (ACADIA 18)* (pp. 260–265). ACADIA. https://doi.org/10.52842/conf.acadia.2018.260

Tripathi, N. Bag, D. S., Dwivedi, M. (2024). A Review on auxetic polymeric materials: Synthetic methodology, characterization and their applications. *Journal of Polymer Materials,* 40(3–4), 227–269. https://doi.org/10.32381/jpm.2023.40.3-4.8

Uzun, M. (2010). Negative Poisson ratio (auxetic) materials and their applications. *Journal of Textiles and Engineers*, 17(77), 13-18. https://hdl.handle.net/11424/261175

Vivanco, T., Ojeda, J., Yuan, P. (2023). Regression-Based Inductive Reconstruction of Shell Auxetic Structures. In Yuan, P.F., Chai, H., Yan, C., Li, K., Sun, T. (Eds.), *Hybrid Intelligence. CDRF 2022. Computational Design and Robotic Fabrication* (pp. 488-498). Springer. https://doi.org/10.1007/978-981-19-8637-6_42

280

JCoDe | Vol 6 No 2 | September 2025 | Tolerance in Computational Design| Güloğlu, Z., Yazıcı, S.

A Data-Driven Approach to Determining Safe Classroom Capacities During the Transition to Face-to-Face Education

Fadime Diker[1], İlker Erkan[2]

ORCID: 0000-0001-8088-1570[1], 0000-0001-7104-245X[2]

[1]Balıkesir University, Faculty of Architecture, Department of Architecture, Balıkesir, Türkiye
[2]Süleyman Demirel University, Faculty of Architecture, Department of Architecture, Isparta, Türkiye

In this paper, different models have been developed to estimate how many students should be in the existing classrooms to be less affected and protected from the Covid19 virus during transition to face-to-face education. The factor that determines the risk of transmission of the Covid 19 virus is not only physical distance, but the duration of exposure. In this direction, model has been created by Fuzzy Logic method to evaluate the efficiency of classrooms in terms of physical sizes using the classroom and window sizes of existing primary schools. Various models have been developed by using the data obtained in line with the developed model. After the evaluation of the obtained models, it was concluded that deep neural networks model can be accepted as a more suitable approach for this estimation problem than other supervised learning methods. It is expected that the developed model will help the guidelines prepared for taking necessary precautions in educational structures and making arrangements to prevent the transmission of the virus. Developed with the data obtained by examining only the primary school classrooms, developed models can also be applied with the data to be obtained by examining the classrooms of different levels.

281

Yüz Yüze Eğitime Geçiş Sürecinde Güvenli Sınıf Kapasitelerinin Belirlenmesine Yönelik Veri Odaklı Bir Yaklaşım

Fadime Diker[1], İlker Erkan[2]

ORCID: 0000-0001-8088-1570[1], 0000-0001-7104-245X[2]

[1]Balıkesir Üniversitesi, Mimarlık Fakültesi, Mimarlık Bölümü, Balıkesir, Türkiye
[2]Süleyman Demirel Üniversitesi, Mimarlık Fakültesi, Mimarlık Bölümü, Isparta, Türkiye

Bu çalışmada, yüz yüze eğitime geçiş sürecinde mevcut sınıflarda kaç öğrencinin bulunması gerektiğini tahmin etmek amacıyla farklı modeller geliştirilmiştir. Covid-19 virüsünün bulaşma riskini belirleyen faktör yalnızca fiziksel mesafe değil, aynı zamanda maruz kalma süresidir. Bu doğrultuda, mevcut ilkokul sınıflarının ve pencere boyutlarının kullanılarak sınıfların fiziksel boyutlar açısından verimliliğini değerlendirmek için Bulanık Mantık yöntemiyle bir model oluşturulmuştur. Geliştirilen model doğrultusunda elde edilen veriler kullanılarak çeşitli modeller geliştirilmiştir. Elde edilen modellerin değerlendirilmesi sonucunda, derin sinir ağları modelinin bu tahmin probleminde diğer gözetimli öğrenme yöntemlerine kıyasla daha uygun bir yaklaşım olduğu sonucuna varılmıştır. Geliştirilen modelin, eğitim yapılarında gerekli önlemlerin alınması ve virüsün yayılmasını önlemeye yönelik düzenlemelerin yapılması için hazırlanan yönergelere katkı sağlaması beklenmektedir. Yalnızca ilkokul sınıfları incelenerek elde edilen verilerle geliştirilen modeller, farklı eğitim seviyelerindeki sınıfların incelenmesiyle elde edilecek verilerle de uygulanabilir.

282

1. INTRODUCTION

Corona virus (COVID-19) disease first appeared in Wuhan, China and has been described as a global epidemic by the World Health Organization as of March 11, 2020, as it began to spread rapidly around the world. Because of the transmission of the virus by contact and droplet (Huang et al.,2020; Liu et al., 2020), countries have taken various measures and applied some restrictions to be less affected and protected from this epidemic. The World Health Organization (2021) has stated that some simple precautions should be taken, such as maintaining physical distance, wearing a mask, well ventilating rooms, avoiding crowds, cleaning your hands, and coughing up bent elbow or tissue. In addition, in line with these measures and restrictions, some countries have implemented curfews with full closure or intermittent closure strategies to encourage people to stay home. Another of the measures taken was the closure of educational institutions. The United Nations Educational, Scientific and Cultural Organization (UNESCO, 2021) stated that on March 16, 2020, about 762 million students were affected by the closure of educational institutions. In addition, according to UNESCO (UNESCO, 2021) data, schools in Turkey were closed for a total of 47 weeks (**Figure 1**).
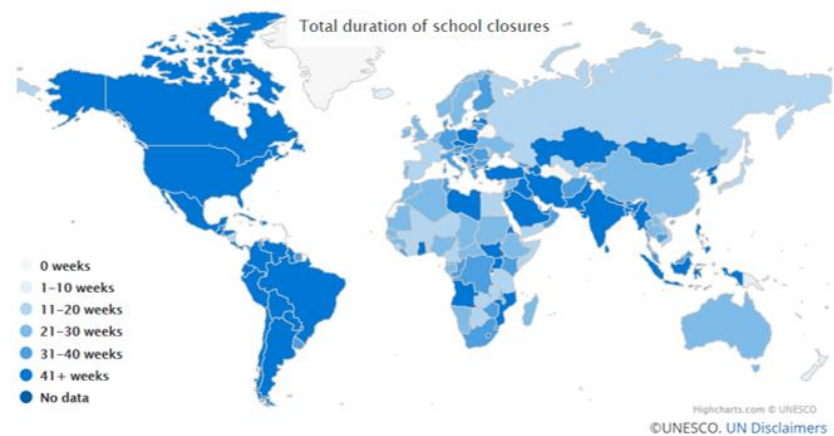
Figure 1: Total time schools were closed by country (UNESCO, 2021).

Although the purpose of closing schools was to prevent the virus from spreading within institutions and being transmitted to vulnerable individuals, these closures have had widespread socioeconomic consequences (Nicola et al., 2020). Keogh-Brown et al. (2010) noted that closing schools during an influenza epidemic will result in further

A Data-Driven Approach to Determining Safe Classroom Capacities During the Transition to Face-to-Face Education

reductions in labor supply, with lost working days as an indirect result of the disease, as parents (mostly) stay at home to care for their children.

The measures and restrictions made have affected many areas such as economy, education, health, art, entertainment. After the detection of the first case, the education was switched to the online education system conducted remotely. The transition to online learning instead of the traditional face-to-face learning mode in the Covid 19 epidemic has caused various effects on students' academic performance, physical and psychological health (Li and Che, 2022). Online teaching, which allows students to learn anywhere and with relatively flexible scheduling, is particularly suitable for mature students and has greatly benefited schools that have closed due to the Covid19 virus (Yu et al.,2021). During this transition, students need access to technology (internet connection, computer etc.), appropriate learning environment and parents who can support learning in online education especially for younger students. While this distance education has specific challenges for all students, it is more disadvantageous for students who do not have access to technology.

It is necessary to create an environment where all students in the class can share their ideas and experiences. It is especially important to introduce primary school students to different social environments and to allow them to discuss their feelings afterwards, to explain the importance of social interactions and develop trust and responsibility during peer-to-peer communication (Alsubaie, 2022). However, online education limits face-to-face interaction (Alsubaie, 2022) and may bring difficulties such as teacher-student compatibility, time management, motivation and technical problems in learning for primary school students (Gupta, 2021). Students face various problems during the transition from traditional education to online education. Some of these challenges are as follows (Neuwirth et al., 2021):
- ✓ The absence of a private area in the home environment or the absence of a quiet environment,
- ✓ Inability to have someone else watch their child/parent,
- ✓ Close enough to distract him/her with other family members at home,
- ✓ Domestic animals in the house etc.

284

JCoDe | Vol 6 No 2 | September 2025 | Tolerance in Computational Design | Diker, F., Erkan, İ.

A controlled return to social life has been initiated in countries with the discovery of various vaccines for this virus, which is a global epidemic. In this process, online education has gradually begun to transition to face-to-face education. Examining the precautions to be taken and the rules to be followed during the transition to face-to-face education in a controlled manner in educational buildings and, accordingly, evaluating the reuse is the most important way to combat the epidemic with architectural and engineering control (Yetiş and Kayılı, 2021). The COVID-19 virus is spread through liquid particles produced by breathing, speaking, shouting, singing, coughing, and sneezing, and therefore various measures must be taken to minimize the possibility of further transmission of the virus brought to school. The rapid precipitation rate of large droplets, physical distance, surface disinfection, ventilation and hand hygiene are the basis of the measures taken (Lordan et al., 2020). Therefore, in face-to-face education, measures such as keeping a distance, wearing masks in the corridors, hand hygiene and ventilation of classrooms have been taken to reduce the transmission of the virus to other people from the people who come to the school with the virus.

The concept of urban resilience against pandemics has come to the fore with the global prevalence of the COVID-19 disease, and a series of principles, starting from spatial levels, need to be addressed for urban resilience (Amirzadeh et al., 2022). Gaisie et al. (2022) argued that the evolution of the COVID-19 epidemic, which has become widespread since early 2020, proceeds through built environment features such as diversity, destination accessibility, travel distance, design and density. Urban mobility in the post-COVID-19 era is likely to depend on the prevalence and degree of acceptance of these remote online activities and social awareness of the future of cities, with several complex and interconnected factors related to urban form, spatial planning and decision-making (Mouratidis and Papagiannakis, 2021). Human mobility, a basic requirement of daily life, was most directly affected during the COVID-19 pandemic (Liu et al., 2023). Therefore, to control this interaction, there must be a certain distance between students in the classrooms.

Infection control and physical distancing measures are essential to prevent further spread of the virus and help contain the pandemic situation (Amir et al., 2020). The social distance recommended by the

A Data-Driven Approach to Determining Safe Classroom Capacities During the Transition to Face-to-Face Education

CDC (Interim Guidance for Businesses and Employers Responding to Coronavirus Disease COVID-19) for physical distancing during the Covid19 pandemic is 6 feet, which is often visualized as a 3 feet radius circle with individuals at the center (American Institute of Architects, 2020). Since circles with a radius of 3 feet do not account for human movement, it is valid when people are standing in a row or sitting six feet apart from each other, and physical distance is violated when people move in space when the physical distance between each person is 6 feet (**Figure 2**) (American Institute of Architects, 2020).
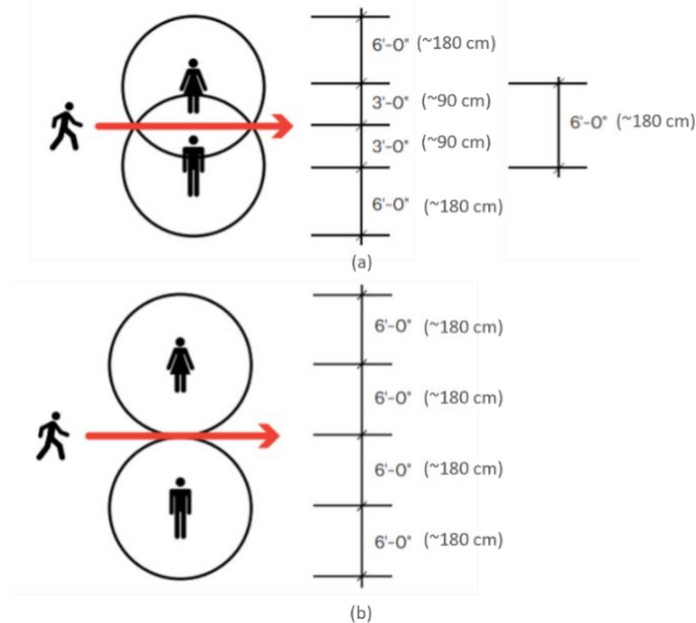
Figure 2: (a) Physical distance not allowing movement (b) Physical distance allowing movement (American Institute of Architects, 2020)

The number of people in the classrooms and the area per person are of great importance for physical distance in classrooms. In TSE's (Turkish Standards Institution) YÖK (2020), It is stated that the physical distance should be arranged according to a minimum 1 meter distance in the lessons, exams/practical exams, laboratories and classrooms where students will not interact with each other loudly, while the physical distance will be at least 1.5-2 meters if possible, especially in activities such as speaking loudly and debating, due to droplet formation indicated that it should be adjusted accordingly. In addition, it was stated that the capacity of the classrooms should be determined so that one person per 4 m², and at least 1 meter distance between people should be maintained in the seating arrangement. According to the American Institute of Architects (2020), the capacity should be

286

JCoDe | Vol 6 No 2 | September 2025 | Tolerance in Computational Design | Diker, F., Erkan, İ.

determined to reduce the area of 20 sq. ft (1.85 m^2) per person in classrooms in educational structures, while 50 sq. ft (4.64 m^2) per person for technical units, library reading rooms and vocational training spaces.

Since the smaller liquid particles dispersed as aerosols remain in the air, it is not only the physical distance that determines the risk of contamination, but also the duration of exposure (Lordan et al., 2020). Therefore, although sufficient physical distance is provided in the classrooms, the classrooms should be ventilated frequently. Natural ventilation is the provision of air exchange through openings such as doors and windows to provide suitable and clean air from the outside environment instead of undesired substances such as temperature, carbon dioxide, moisture, and toxins in the indoor air at high levels. The ventilation principles according to the openings are shown in **Figure 3**.
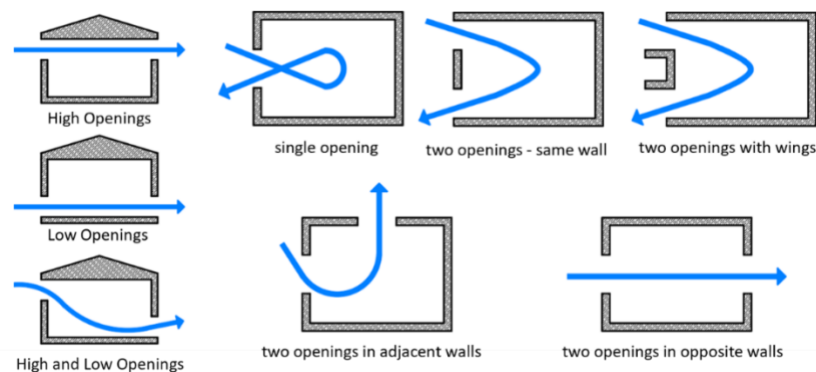
Figure 3: Ventilation principles according to openings (Dekay and Brown, 2013)

The COVID-19 pandemic has revealed the importance of flexible spaces with open plans and adequate spaces in primary and secondary school buildings for the continuity of educational environments (Güzelci et al., 2021). It has clearly emphasized the importance of face-to-face education, especially at the primary school level. During the transition from online to face-to-face education during the pandemic, classroom capacity was set at 4 m² per person. This measure, implemented for the health of students, offers a simple and practical solution. However, this solution did not consider the spatial characteristics of the classroom environment. Classroom capacity should be evaluated not only based on space size but also in terms of healthy ventilation, especially during pandemics. Therefore, the ratio of window area to wall and floor area should also be included in calculations. Therefore, there is a need to develop more comprehensive, scientific, and applicable standards for

A Data-Driven Approach to Determining Safe Classroom Capacities During the Transition to Face-to-Face Education

the sustainability of face-to-face education in potential new pandemic scenarios. The use of artificial intelligence and machine learning-based approaches in the design of classroom layouts in educational buildings not only saves time in the early design process but also contributes to the creation of more functional and adaptable spaces (Karadag et al., 2023).

The aim of this study is to develop a method based on spatial parameters to determine the maximum number of students in existing primary school classrooms in the event of a potential pandemic. First, the study used fuzzy logic to calculate the design efficiencies of classrooms within a range of 5–18 students. Based on the data obtained, three basic rules were established, and the maximum number of students was determined based on these rules. Machine learning and deep learning methods were then developed to determine the maximum number of students, the width, length, ceiling height, and total window area of the classrooms. This developed method determines the student capacity of a given classroom based on data from existing classrooms.

The significance of this study is not limited to providing a response to the past Covid-19 pandemic. Its primary contribution is to provide a scientific basis for classroom planning in the event of a future resurgence or similar pandemics, and to guide the safe continuation of face-to-face education. At the same time, this study's application and comparison of different methods allows us to identify the advantages and limitations of each method, which is crucial for determining the most appropriate solution to the problem. It also goes beyond the simplified standards frequently used in existing literature and presents an innovative approach that evaluates classroom capacity through spatial design efficiency. This makes a significant contribution to both education and architectural planning.

2. MACHINE LEARNING AND DEEP LEARNING

Machine learning is a sub-branch of computer science that emerged from model recognition and computational learning theory studies in artificial intelligence. The term machine learning was defined in 1959 by the American computer scientist Arthur Samuel (1959) as the field of study that gives computers the ability to learn without being

288

JCoDe | Vol 6 No 2 | September 2025 | Tolerance in Computational Design | Diker, F., Erkan, İ.

explicitly programmed. Machine learning deals with the question of how to create computer programs that automatically evolve through experience (Mitchell,1997). A machine learning algorithm is a computational process that uses input data to perform a desired task without being literally programmed (i.e. "hard coded") to produce a particular result, and these algorithms are, in a sense, a "soft-coded" because repetition architectures (i.e. experience) through changes automatically adapts to accomplish the desired task or so that they are becoming better and better (Naqa, I., and Murphy, 2015). The working logic of traditional programming is to obtain output data from the input data, and therefore, in order to obtain the output data, a program or software suitable for the problem type must be used, while in the machine learning working logic, the machine or software is trained with the input and output data to obtain the program or software suitable for the problem type (Figure 4) (Kavuncu, 2018) (**Figure 4**).
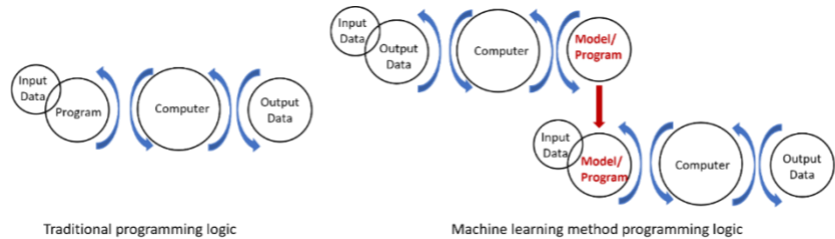
Figure 4: Programming logic with traditional programming and machine learning method (Kavuncu, 2018)

According to the algorithm used, the accuracy of the results obtained from the model can vary. Therefore, better performance can be obtained from the model developed by using different algorithms or combining different algorithms. Different algorithms are used according to the type of machine learning (**Figure 5**).

A Data-Driven Approach to Determining Safe Classroom Capacities During the Transition to Face-to-Face Education
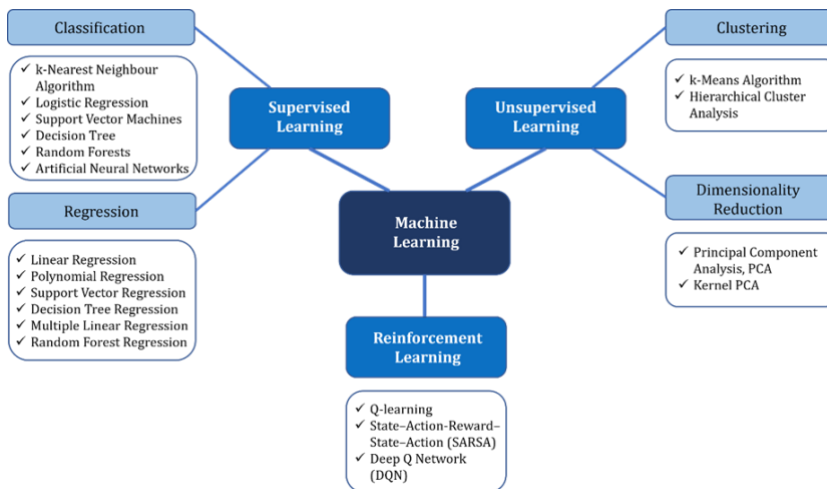
Figure 5: Machine learning types and most used methods

Machine learning is basically divided into three groups according to the learning method: supervised, unsupervised, and reinforced learning.

Supervised learning is a learning method that allows the machine to create a function from this information by teaching labeled data and the results obtained from that data. Thus, the machine learns the relationship between the data. In supervised learning, it is aimed to produce the closest result for unlabeled data. The difference between the result obtained with the model and the desired result determines the error rate and by minimizing this rate, the accuracy of the model is increased. It is widely used for classification and regression operations. In the classification process, a conclusion is drawn from the training data, and it is determined to which category the test data belongs. In the classification process, the system is trained by categorizing the data. Then, it is determined which class the data shown belongs to. In the regression process, the relationships between the input data (independent variable) and the output (dependent variable) data are estimated. A linear graph is created according to these relationships and the results of new data are estimated according to this graph.

With unsupervised learning, it is aimed to reveal the hidden relationships between unlabeled data in the data set. Unsupervised learning runs on more complex algorithms than supervised learning, as there is little or no information about the data. It is widely used for clustering and dimensionality reduction operations. The basic principle of clustering is based on the calculation of similarity measurement between class number unclear and unclassified data. While the

290

similarity rate within itself is expected to be the highest, the similarity rate between different clusters is expected to be the least. Many data sets can contain large amounts of attributes and working with this type of data set makes operations that require high computational power, such as vectors and matrices, even more difficult. The size reduction process, on the other hand, preserves useful information to reduce such difficulties and transforms the dataset into a lower-dimensional space.

The purpose of reinforcement learning is to develop a system that increases its performance based on its interactions with its environment. In reinforcement learning, there is a reward-punishment system. In this system, inferences are made from errors made in the way that is being progressed to find the correct action, and then it tries to find the correct action with the least errors from its inferences made. The concept of deep learning first emerged when Hinton and Salakhutdinov (2006) proposed algorithms that can learn the properties of data hierarchically with deep neural networks. Deep learning, which is a method of artificial intelligence that uses multi-layer artificial neural networks and is one of the methods of machine learning, is growing rapidly today with the power of hardware (graphics processing units and increased processing power) that can process increasing data. Unlike traditional machine learning methods, it can learn from images, videos, audio and text data. In addition, unlike traditional machine learning, deep learning can perform feature extraction itself with little or no computer intervention.

3. METHODOLOGY

The proposed model consists of different stages: data collection, interpretation of data with fuzzy logic, development, implementation of machine learning and deep learning-based models, and evaluation of models (**Figure 6**).

A Data-Driven Approach to Determining Safe Classroom Capacities During the Transition to Face-to-Face Education
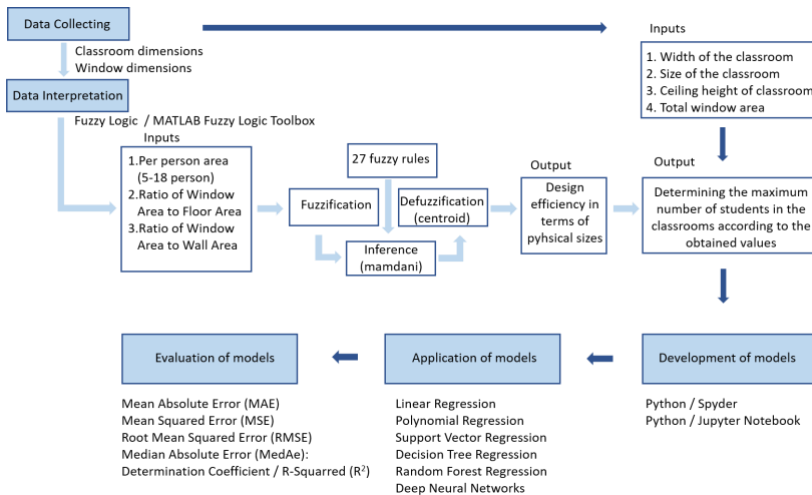
Figure 6: Flow diagram of the model

3.1 Data Collecting

34 primary schools affiliated to the Directorate of National Education of the Central District of Isparta were examined and measurements were made. Out of a total of 485 classrooms belonging to the first, second, third and fourth grades in primary schools (not including classrooms with approximately the same dimensions), 91 classrooms were examined. The width, length, ceiling height, width and length of the windows were measured by laser meters. The mean and standard deviation of the data obtained after the examination and measurement are shown in **Table 1.**

	Mean	Standard Deviation
Width of Classrooms (m)	6.30	0.95
Length of Classrooms (m)	6.86	1.20
Ceiling Height of Classrooms (m)	2.96	0.19
Area of Classrooms (m^2)	43.24	10.22
Volume of Classrooms (m^3)	128.54	33.40
Window Area (m^2)	6.73	1.91
Ratio of Window Area to Floor Area (%)	15.86	4.16
Ratio of Window Area to Wall Area (%)	33.45	8.31
Area Per Person (m^2) (10 persons)	4.32	1.02
Volume Per Person (m^3) (10 persons)	12.85	3.34

Table 1: The mean and standard deviation of the obtained data.

3.2 Data Interpretation

To achieve design efficiency in terms of physical sizes of the existing classrooms and to find out how many students are most suitable, the data obtained from the examined classrooms should be interpreted and inferences should be made accordingly. To determine the maximum number of students in classrooms, it is necessary to consider

292

JCoDe | Vol 6 No 2 | September 2025 | Tolerance in Computational Design | Diker, F., Erkan, İ.

the dimensions of that classroom. There are many variables in the design of classes, and these variables make the decision-making stage difficult because they have different qualities (Diker and Erkan, 2021). Evaluating all the design criteria together makes this process more complex. To solve these problems, which have become complex in this process, fuzzy Logic method was used. The reason for using this method is that it can solve complex problems much faster and resembles the structure of human thought.

Modeling with the fuzzy logic method takes place in 5 stages (**Figure 7**).
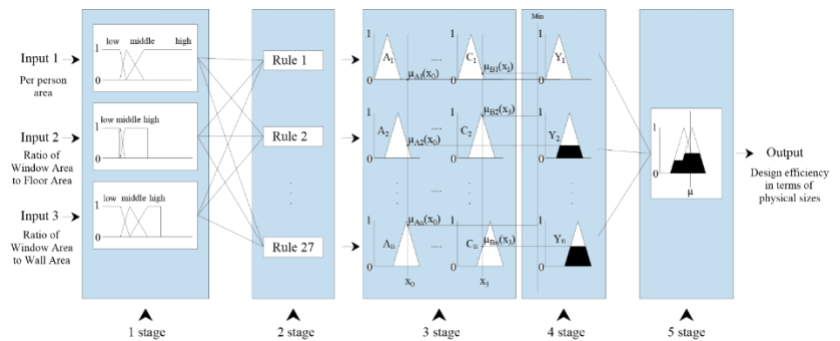
Figure 7: Modeling stages with fuzzy logic approach

These stages are:

1.Stage (Creating Membership Functions): First, membership functions are created for the inputs to be used for the model and the output variable to be created.

2. Stage (Rule Base): Logical if-type rules are created that link the input data to the output variable, which can affect the result of the model. All intermediate (fuzzy set) combinations must be considered in these rules.

3. Stage (Fuzzification): It is the process of converting the exact value of the input to fuzzy values by determining the fuzzy set or sets to which the input belongs and the degree of membership by using the membership function.

4. Stage (Fuzzy Inference): In the fuzzy rule base, by collecting all the relations established between the inputs and the output fuzzy sets, the inference corresponding to the input is made, like the human's abilities such as decision making, inference and proposition.

5. Stage (Defuzzification): The fuzzy inference results obtained as a result of fuzzy operations are defuzzification and converted into precise numerical output values.

"Fuzzy Logic Toolbox" in MatLab software was used to develop this model. In the fuzzy logic method, the degrees of belonging of the variables to different membership functions (e.g., low, medium, high) were determined by fuzzifying the crisp input values (**Figure 8**) and then 'If-then' rules were applied (**Table 2**).
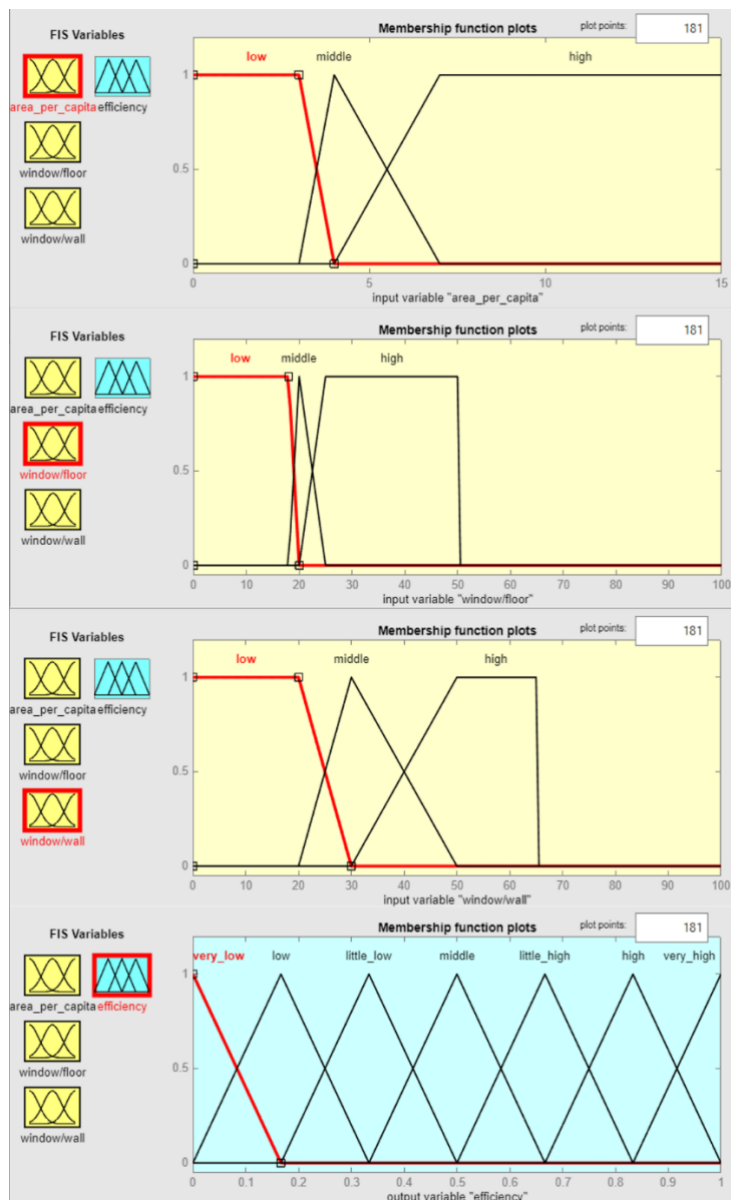
Figure 8: Membership functions of the inputs and outputs of the developed model

294

JCoDe | Vol 6 No 2 | September 2025 | Tolerance in Computational Design | Diker, F., Erkan, İ.

	If	and	and	then
Rule No	Area per Capita	Window-to-Floor Ratio	Window-to-Wall Ratio	Efficiency
1	Low	Low	Low	Very Low
2	Low	Low	Middle	Low
3	Low	Low	High	Little Low
4	Low	Middle	Low	Low
5	Low	Middle	Middle	Little Low
6	Low	Middle	High	Middle
7	Low	High	Low	Little Low
8	Low	High	Middle	Middle
9	Low	High	High	Little High
10	Middle	Low	Low	Low
11	Middle	Low	Middle	Little Low
12	Middle	Low	High	Middle
13	Middle	Middle	Low	Little Low
14	Middle	Middle	Middle	Middle
15	Middle	Middle	High	Little High
16	Middle	High	Low	Middle
17	Middle	High	Middle	Little High
18	Middle	High	High	High
19	High	Low	Low	Little Low
20	High	Low	Middle	Middle
21	High	Low	High	Little High
22	High	Middle	Low	Middle
23	High	Middle	Middle	Little High
24	High	Middle	High	High
25	High	High	Little High	Little High
26	High	High	Middle	High
27	High	High	High	Very High

Table 2: 27 rules created for the fuzzy logic method

The Mamdani approach was chosen for defuzzification due to its simplicity, interpretability, and widespread use in modeling fuzzy systems, making it particularly suitable for evaluating classroom design efficiency based on multiple spatial parameters. In the fuzzy logic method, the fuzzification of input values, their processing through 'If–Then' rules, and subsequent defuzzification reveal the effects of area per person, window-to-floor, and window-to-wall ratios on design efficiency (**Figure 9**).
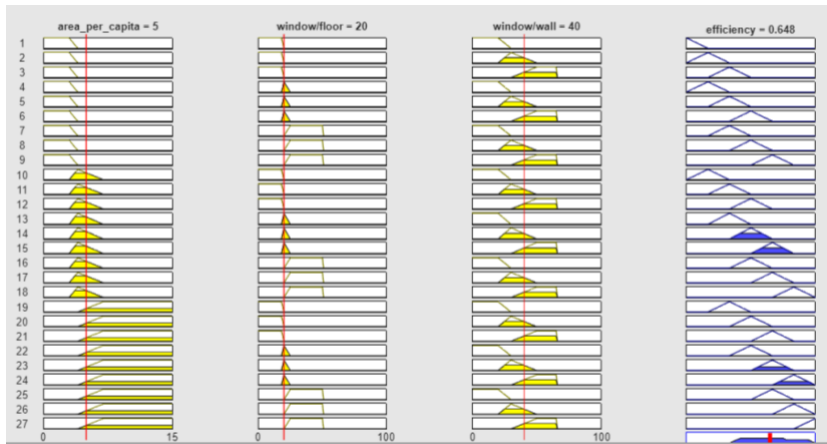
Figure 9: Effects of area per person, window-to-floor, and window-to-wall ratios on classroom design efficiency.

Design efficiencies obtained through fuzzy logic were not directly used in models developed using machine learning and deep learning methods. Design efficiencies for physical dimensions were determined using "if-then" rules using the per capita area, window area/floor area ratio, and window area/wall area ratio as input variables. The model's output is design efficiencies ranging from 0 to 1.

Values were calculated individually for each classroom, and design efficiencies corresponding to these student numbers were determined. Three rules were developed based on the results, and the maximum number of students in classrooms was determined based on these rules (**Figure 10**).

296

JCoDe | Vol 6 No 2 | September 2025 | Tolerance in Computational Design | Diker, F., Erkan, İ.
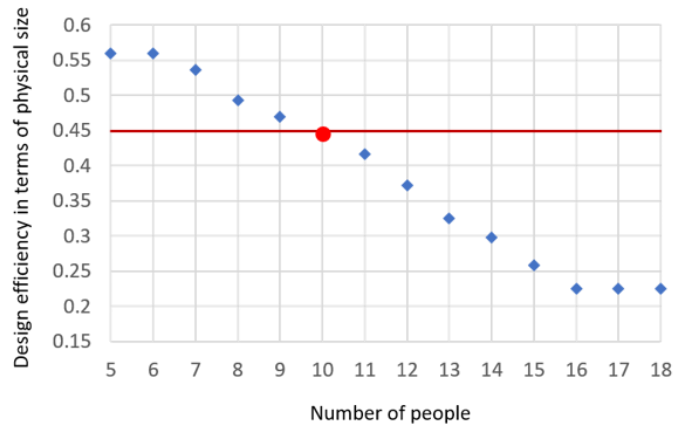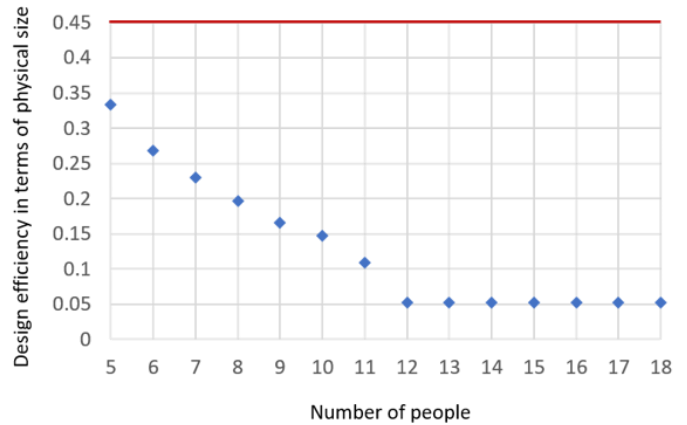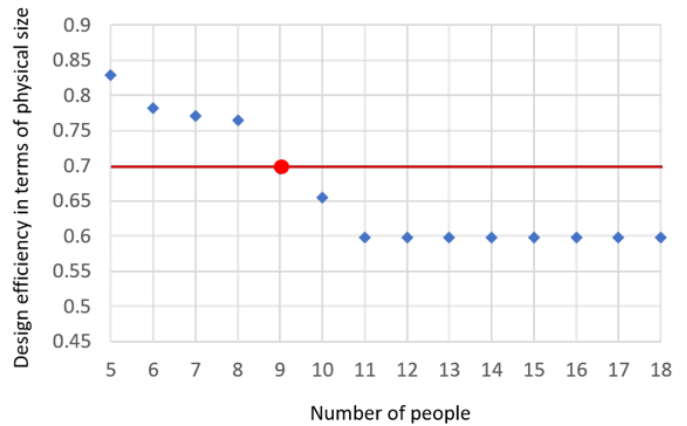
Figure 10: Rules for determining the maximum number of people in classrooms.

The maximum number of students in the classrooms is determined according to the following rules:

1. If the design efficiency, which varies according to the number of people, is at least 0.45, the number of students was selected as the maximum number of students.

A Data-Driven Approach to Determining Safe Classroom Capacities During the Transition to Face-to-Face Education

2. If the design efficiency is less than 0.45 in 5 people, this classroom was not considered suitable and was determined as 0 people.

3. If the design efficiency is greater than 0.45 in 18 people, the number of students belonging to at least 0.70 was selected as the maximum number of students.

The design efficiency threshold values (0.45–0.70) used in this study were determined based on the seven membership functions generated in fuzzy logic and the expert opinions of the authors. Specifically, the value 0.45 corresponds to the "middle" membership function, while the value 0.70 corresponds to the "little high" membership function. Therefore, this range represents the fuzzy sets defined for design efficiency in terms of physical magnitude.

Since aerosols remain in the air, the factors that determine the risk of transmission are physical distance and exposure time to these aerosols. Ventilation is of great importance during exposure to aerosols. Therefore, in determining the capacity of the classrooms, it is necessary to determine the capacity by considering the window sizes and proportions for adequate ventilation of the classrooms in addition to the classroom dimensions, rather than determining the capacity to be 4 m^2 per person for physical distance only. In this direction, the data obtained were interpreted by the method of fuzzy logic. Some of the number of people obtained from the model results are shown in **Table 3**.

298

JCoDe | Vol 6 No 2 | September 2025 | Tolerance in Computational Design | Diker, F., Erkan, İ.

	Width of the classroom (m)	Size of the classroom (m)	Ceiling height of classroom (m)	Total window area (m^2)	Ratio of Window Area to Floor Area (%)	Ratio of Window Area to Wall Area (%)	Number of people obtained as a result of the model	Per person area (m^2)
1	5.12	10.32	3.27	2.86	5.42	8.48	0	-
2	5.09	6.95	2.74	2.19	6.18	11.48	0	-
3	6.92	6.65	3.24	10.61	23.05	49.23	12	3.83
4	6.59	6.63	2.93	8.18	18.73	42.12	11	3.97
5	5.52	6.03	3.17	8.18	24.57	42.78	8	4.16
6	6.83	7.22	2.98	8.48	17.19	39.40	11	4.48
7	6.76	6.94	2.92	7.38	15.73	36.42	10	4.69
8	6.95	6.98	2.9	6.65	13.70	32.83	9	5.39
9	6.8	7.81	3.06	6.98	13.15	29.22	8	6.64
10	6.93	7.87	3.11	6.70	12.28	27.36	7	7.79

Table 3: The number of people belonging to some classrooms obtained as a result of the model.

18 of the classrooms examined, it was concluded that there is no education in these classrooms, as adequate ventilation could not be provided in the classrooms due to the ratio of window area to floor area and the ratio of window area to wall area was very low. In 8 classrooms, since the ratio of the window area to the floor area and the ratio of the window area to the wall area is high, the area per person varies between 3.23 and 3.97 m^2, below 4 m^2. In the remaining 64 classrooms, the ratio of the window area to the floor area and the ratio of the window area to the wall area varies between 4.01 and 7.79 m^2, above 4 m^2 per person.

The floor plan (with pre-pandemic order) of one of the schools examined in **Figure 11** and, for example, the order of a classroom in accordance with the physical distance were created.
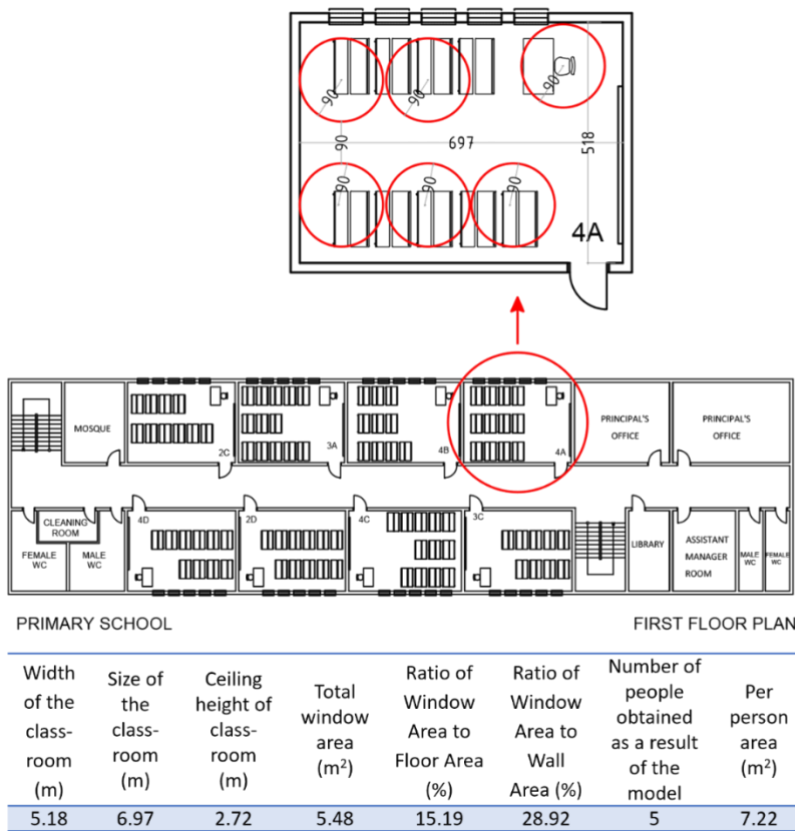
Figure 11: Floor plan of one of the schools examined

Width of the class-room (m)	Size of the class-room (m)	Ceiling height of class-room (m)	Total window area (m²)	Ratio of Window Area to Floor Area (%)	Ratio of Window Area to Wall Area (%)	Number of people obtained as a result of the model	Per person area (m²)
5.18	6.97	2.72	5.48	15.19	28.92	5	7.22

In this classroom, where 24 people were trained before the Pandemic, there should be 9 people to fall 4 m² per person in the gradual transition from distance education to face-to-face training, while as a result of the model, 5 people were proposed for this classroom. Considering the physical distance according to the row order, it is seen that it is suitable for 5 people. This situation indicates that it is not correct to determine only the area per person to be 4 m² in the determination of classroom capacities.

3.3 Development and Implementation of Models

Multivariate estimation is a problem of machine learning, and there are various algorithms that use different strategies to predict the variable that is dependent on the independent variables in a dataset. In this study, the goal is not only to estimate the maximum number of people who should be in the classrooms, but also to compare different machine learning models and deep learning models for subsequent stages.

300

JCoDe | Vol 6 No 2 | September 2025 | Tolerance in Computational Design | Diker, F., Erkan, İ.

The linear regression method is a basic statistical approach frequently used in predictive analysis that reveals the linear relationship between the independent variable and the dependent variable. It is also one of the most fundamental regression methods, providing high interpretability of parameters and statistical significance testing of predictors (James et al., 2013). It was chosen in this study due to its strong interpretability and simplicity.

Polynomial regression is an extension of linear regression that allows for the modeling of nonlinear relationships by incorporating higher-order terms of the explanatory variables (Heiberger and Neuwirth, 2009). The relationship between the independent variable and the dependent variable is depicted with complex curves rather than linear lines. It was included in the analysis to capture potential nonlinear trends in the data. Different polynomial degrees should be applied to determine the optimal curve. In the model developed in this article, a value of 2 was used as the polynomial degree.

Support Vector Regression (SVR), developed by Vapnik (1997), is a kernel-based method used in both classification and regression problems, capable of effectively modeling nonlinear relationships by transforming inputs into high-dimensional feature spaces. In this study, SVR was chosen for its flexible and robust ability to capture nonlinear patterns.

Decision trees are methods that estimate the dependent variable by dividing the dataset into branches based on independent variables and can model nonlinear relationships and variable interactions. This model consists of decision nodes and leaf nodes created according to the features and target variables. At each split, it attempts to increase information gain by reducing the entropy value (degree of randomness) and selects the split with the lowest error. It also divides the independent variables into intervals based on the information gain; in the prediction phase, it uses the mean learned during the training process for the value in the relevant interval. Therefore, unlike other regression methods, it has a non-continuous prediction structure. Decision trees are widely used in machine learning because they are easy to understand, require minimal data preparation, and can handle both numerical and categorical data (Dehghani et al., 2023). This

algorithm has been evaluated for its ability to capture complex feature interactions.

Random Forest is an ensemble learning method that combines multiple decision trees to increase prediction accuracy and reduce overfitting. This method is based on a structure where each tree is based on independently sampled random vectors, and all trees have the same distribution (Breiman, 2001). While the optimal split of each node in a single tree is achieved using all predictors, in the Random Forest approach, each node is split using only a randomly selected subset of predictors. This allows for the creation of multiple trees (forests), reduces variance, and reduces correlation between trees, resulting in higher accuracy predictions (Suchetana et al., 2017). It was chosen for this study due to its robustness against overfitting, its ability to model complex relationships, and its relative flexibility in addressing missing data and variable selection issues.

Deep Neural Networks are models capable of automatically extracting features and modeling highly complex, high-dimensional nonlinear relationships. The training phase is crucial for DNNs with more than two hidden layers, as when error values propagate across multiple layers, the model's performance is directly affected. Advances in both machine learning algorithms and computer hardware have made it possible to train DNNs with numerous nonlinear hidden layers and large output layers more efficiently (Hinton et al., 2012). Therefore, they were included in this study due to their robust representation learning capabilities.

The resulting data was split using a 5-fold cross-validation method for model development and performance evaluation. In this approach, the dataset is divided into five equal parts; in each iteration, one part serves as the test set, and the remaining four parts serve as the training set. This method allows for a more reliable assessment of the model's generalizability.

Different models have been developed to estimate the maximum number of students in the classrooms by using the width, size, ceiling height and total window area of the classrooms. All models were developed using the Python programming language, and the implementation was carried out in the Jupyter Notebook environment.

302

JCoDe | Vol 6 No 2 | September 2025 | Tolerance in Computational Design | Diker, F., Erkan, İ.

3.4 Performance Metrics for Model Evaluation

It is necessary to evaluate the performance of the models to measure the success of the developed models or to decide whether the model is a good model. Different performance evaluation methods are used for prediction in supervised learning. In this paper, the following were used as performance evaluation criteria:

Mean Absolute Error (MAE): It is found by summing the absolute values of the differences between the actual values and the predicted values in the data set and dividing the value obtained by the number of samples (**Equation 1**).

$$MAE(y, h_0(x)) = \frac{1}{n} \sum_{i=0}^{n-1} |y_i - h_0(x_i)| \tag{1}$$

Here, y_i represents the actual value of the ith sample in the data set, and $h_0(x_i)$ the predicted value, and n represents the number of samples in the data set. It takes values in the range of 0 to ∞. However, the lower the value, the better the performance of the model.

Mean Squared Error (MSE): It is found by dividing the value obtained by the sum of the squares of the differences between the actual values and the predicted values in the data set by the number of samples (**Equation 2**).

$$MSE(y, h_0(x)) = \frac{1}{n} \sum_{i=0}^{n-1} (y_i - h_0(x_i))^2 \tag{2}$$

Root Mean Squared Error (RMSE): It is found by taking the square root of the mean square error value (**Equation 3**).

$$RMSE(y, h_0(x)) = \sqrt{\frac{1}{n} \sum_{i=0}^{n-1} (y_i - h_0(x_i))^2} \tag{3}$$

Median Absolute Error (MedAe): It is found by taking the median of the absolute differences between the actual and predicted values in the data set (**Equation 4**).

$$MedAE(y, h_0(x)) = Medyan(|y_1 - h_0(x_1)|, \dots, |y_n - h_0(x_n)|) \tag{4}$$

A Data-Driven Approach to Determining Safe Classroom Capacities During the Transition to Face-to-Face Education

Determination Coefficient, (R-Squarred, R^2): It is found by subtracting the value obtained from the division of the sum of the squares of the error by the sum of the mean differences from 1 (**Equation 5**).

$$R^2\big(y, h0(x)\big) = 1 - \frac{\sum_{i=0}^{n-1}(yi - h0(xi))2}{\sum_{i=0}^{n-1}(yi - \bar{y})2}$$

(5)

Here, $\bar{y}$ represents the mean of the samples. It is an indication of the extent to which samples that are not in the dataset can be accurately estimated by the model. It takes values in the range of 0 to 1. However, the closer the value is to 1, the better the performance of the model.

4. RESULTS

In this study, the performances of different regression models (linear regression, polynomial regression, support vector regression [SVR], decision tree, random forest, and deep neural network [DNN]) were compared using five-fold cross-validation. Each model predicts the given data using a different mathematical method and therefore exhibits different performance. The performance of the developed models was examined with various evaluation criteria using a five-fold cross-validation method. The results show significant differences between the models.

The results of the model developed with the linear regression method are shown in **Figure 12**.

Performance Metrics of Linear Regression Across Cross-Validation Folds

	1	2	3	4	5	Mean
MAE	0,3	0,3	0,43	0,37	0,18	0,32
MSE	0,16	0,25	0,31	0,35	0,06	0,22
RMSE	0,4	0,5	0,55	0,59	0,24	0,46
MedAE	0,24	0,1	0,28	0,26	0,15	0,21
R-squared	0,81	0,75	0,76	0,69	0,91	0,79

Figure 12: Performance measures in cross-validation folds of the linear regression model

304

JCoDe | Vol 6 No 2 | September 2025 | Tolerance in Computational Design | Diker, F., Erkan, İ.

According to the 5-fold cross-validation results of the Linear Regression model, the MAE, MSE, RMSE, and MedAE values show significant fluctuations across folds. The R^2 value ranges from 0.69 to 0.91. While the model provides high accuracy in some folds, its performance is relatively low in others. For example, it provides high performance in the 5th fold, but low performance in the 4th fold. This suggests that linear assumptions are not fully valid across all data subsets. When average metrics are considered, the Linear Regression model provides acceptable accuracy and stability across the dataset. Due to the model's linear assumption-based structure, it struggles to capture the complex relationships between variables. Consequently, occasional increases in error metrics are observed.

The results of the model developed with the polynomial regression method are shown in **Figure 13**.

Performance Metrics of Polynomial Regression Across Cross-Validation Folds

	1	2	3	4	5	Mean
MAE	0,29	0,31	0,35	0,54	0,13	0,32
MSE	0,23	0,21	0,21	0,81	0,03	0,3
RMSE	0,47	0,45	0,46	0,9	0,16	0,49
MedAE	0,1	0,11	0,26	0,2	0,11	0,16
R-squared	0,73	0,8	0,83	0,27	0,96	0,72
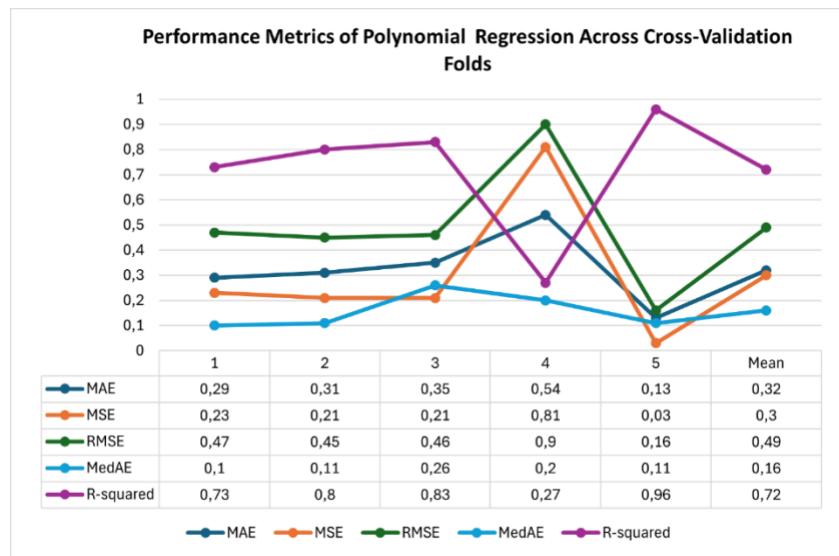
Figure 13: Performance measures in cross-validation folds of the polynomial regression model

Five-fold cross-validation results of the Polynomial Regression model show that MAE, MSE, RMSE, and MedAE values reach particularly high levels in the fourth fold, while the R^2 value varies between 0.27 and 0.96. This indicates that the model exhibits more sensitive and variable performance to data subsets. For example, the highest R^2 value (0.96) and very low error metrics in the fifth fold indicate that the data distribution in this fold provides an excellent fit to the model, while the increase in the error metrics in the fourth fold and the decrease in R^2

A Data-Driven Approach to Determining Safe Classroom Capacities During the Transition to Face-to-Face Education

to 0.27 indicate that the model is inadequate for some data subsets. When considering average metrics, the Polynomial Regression model generally exhibits acceptable performance on the dataset. However, it can produce more inconsistent results when nonlinear relationships are present. The average performance was lower than that of linear regression.

The results of the model developed with the support vector regression method are shown in **Figure 14**.

Performance Metrics of Support Vector Regression Across Cross-Validation Folds						
	1	2	3	4	5	Mean
MAE	0,28	0,46	0,39	0,38	0,21	0,34
MSE	0,23	0,43	0,26	0,48	0,1	0,3
RMSE	0,48	0,66	0,51	0,69	0,31	0,53
MedAE	0,1	0,19	0,27	0,2	0,12	0,18
R-squared	0,73	0,58	0,8	0,57	0,85	0,7
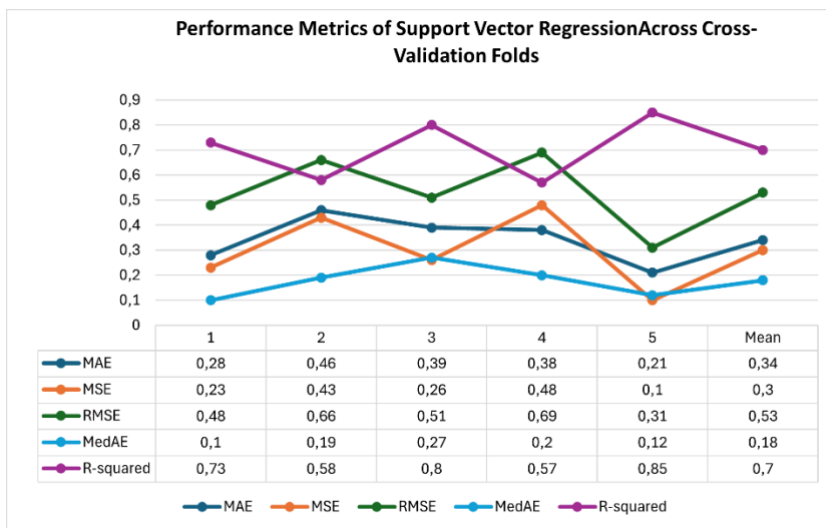
Figure 14: Performance measures in cross-validation folds of the support vector regression model

Five-fold cross-validation results of the Support Vector Regression model show that MAE, MSE, RMSE, and MedAE values vary significantly across folds, while R^2 varies between 0.57 and 0.85. Considering the average metrics, the Support Vector Regression model demonstrates stable and satisfactory performance on the dataset. However, despite offering a more flexible structure compared to linear and polynomial models, SVR's average performance remains relatively low. Particularly poor results were obtained in some folds (e.g., Fold 2 and Fold 4). This demonstrates that SVR is highly sensitive to hyperparameter selection and data distribution.

The results of the model developed with the decision tree regression method are shown in **Figure 15**.

306

JCoDe | Vol 6 No 2 | September 2025 | Tolerance in Computational Design | Diker, F., Erkan, İ.

Figure 15: Performance measures in cross-validation folds of the decision tree regression model
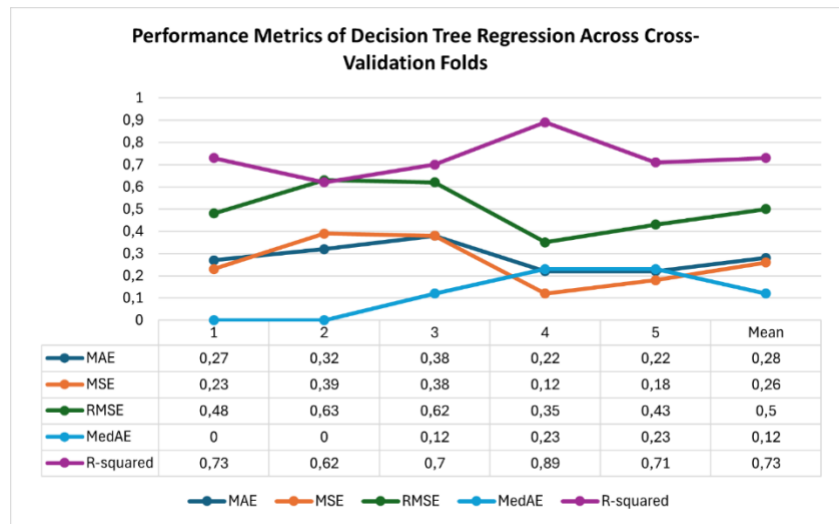
The five-fold cross-validation results of the Decision Tree Regression model show that MAE, MSE, RMSE, and MedAE values vary significantly across layers, with R^2 varying between 0.62 and 0.89. This suggests that the model experiences performance degradation in some layers. The fourth layer exhibits the highest R^2 value (0.89), while the error metrics drop to their lowest levels. Conversely, in the second layer, the increase in the error metrics and the decrease in R^2 to 0.62 indicate that the model performs less well on some data subsets. This result reflects the high-variance nature of decision trees. When average metrics are considered, the Decision Tree Regression model also demonstrates stable and acceptable performance on the dataset. Although decision trees offer a more flexible structure compared to linear models, their average performance remains relatively limited. Particularly weak results were obtained in Folds 2 and 3. This shows that the Decision Tree Regression model is quite sensitive to the hyperparameter selection and data distribution.

The results of the model developed with the random forest regression method are shown in **Figure 16**.

A Data-Driven Approach to Determining Safe Classroom Capacities During the Transition to Face-to-Face Education
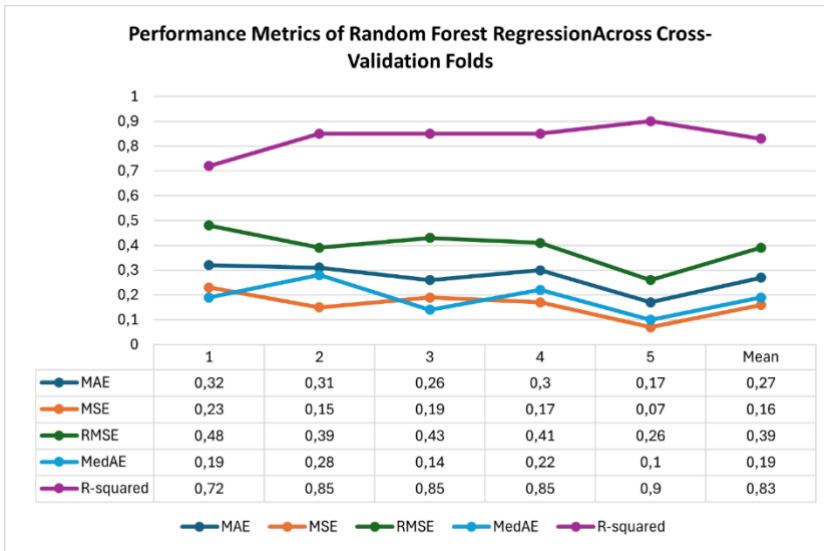
Figure 16: Performance measures in cross-validation folds of the random forest regression model

The 5-fold cross-validation results of the Random Forest Regression model show that MAE, MSE, RMSE, and MedAE values exhibit relatively less variability across layers, while the R² value ranges from 0.72 to 0.9. This demonstrates that the model generally achieves high accuracy and exhibits more consistent performance across layers. When average metrics are considered, the Random Forest Regression model demonstrates a balanced, reliable, and satisfactory performance on the dataset. The Random Forest Regression model demonstrated a more successful and stable performance compared to Decision Tree Regression. Thanks to the k-fold crossover method, Random Forest significantly reduces the risk of overfitting compared to single decision trees and produces more consistent results across different subsets.

The results of the model developed with the deep neural network regression method are shown in **Figure 17**.

308

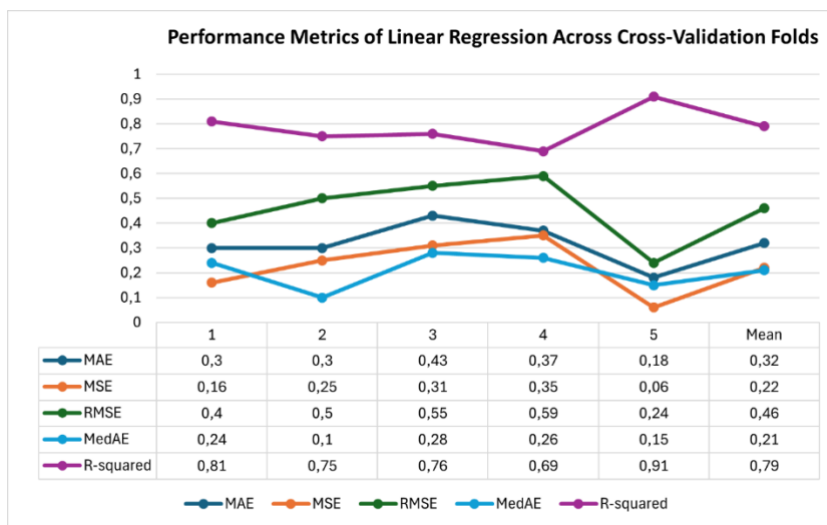JCoDe | Vol 6 No 2 | September 2025 | Tolerance in Computational Design | Diker, F., Erkan, İ.

Figure 17: Performance measures in cross-validation folds of the deep neural network regression model
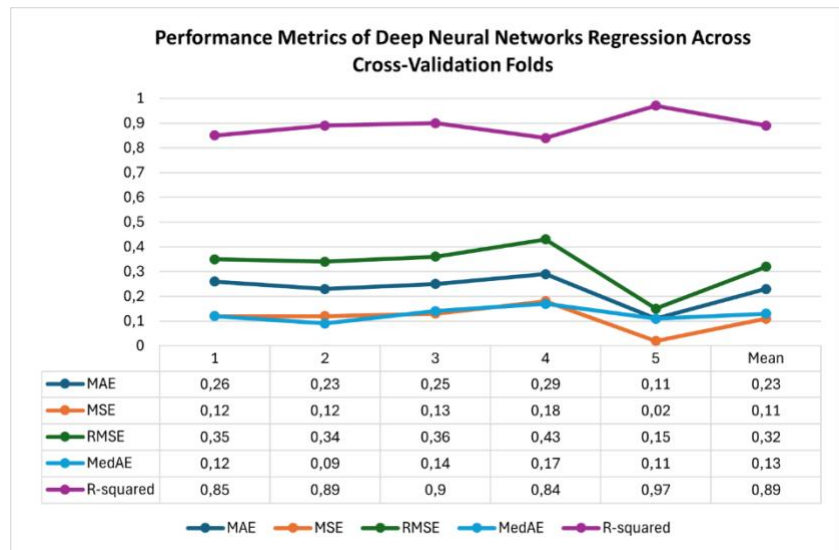
According to the 5-fold cross-validation results, the MAE, MSE, RMSE, and MedAE values of the Deep Neural Network Regression model show relatively less variability across layers. The R^2 value ranges between 0.84 and 0.97. This demonstrates that the model generally achieves high accuracy and exhibits consistent performance across layers. When average metrics are considered, the Deep Neural Network Regression model demonstrated stable, reliable, and satisfactory performance on the dataset. Capable of capturing complex relationships between variables, the model achieved more consistent results across different subsets thanks to its deep learning architecture. However, while performance was slightly lower in some layers, the overall trend was toward higher accuracy and lower errors.

Figure 18 illustrates the comparison of six regression models using the average performance across 5-fold cross-validation.

A Data-Driven Approach to Determining Safe Classroom Capacities During the Transition to Face-to-Face Education
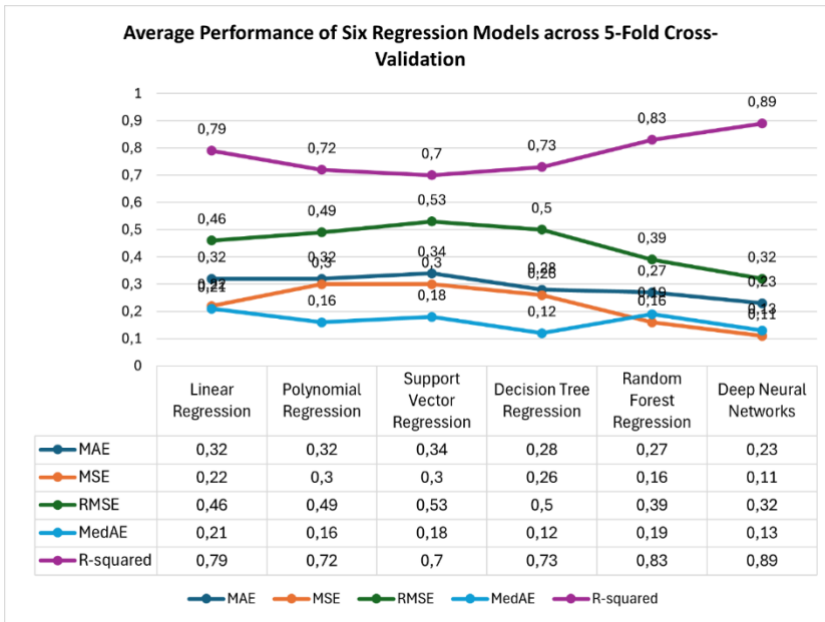
Figure 18: Comparison of six regression models based on the average results of 5-fold cross-validation

As a result, the Deep Neural Network Regression model demonstrated better and more consistent performance compared to classical regression methods. This clearly demonstrates that deep learning-based methods offer higher accuracy and generalizability due to their ability to capture nonlinear relationships. While the Random Forest Regression model also demonstrated consistent performance across layers, the Deep Neural Network Regression model stood out with its higher accuracy (especially in R²) and lower error metrics.

5. CONCLUSION

Some measures and restrictions have been made to be less affected and protected from the Covid 19 virus, which is a global epidemic. One of these measures was the closure of educational institutions and online training. In the process of gradually transitioning to normal life with developed vaccines, the trainings are gradually transitioning to face-to-face training. During this period, classroom capacity needed to be reduced. Classroom capacity should be evaluated not only in terms of physical space but also in terms of ventilation facilities that will ensure student safety during pandemic conditions. In this context, within the scope of the study, recommendation models were developed to determine the maximum number of students that primary school classrooms can accommodate in possible epidemic situations based on spatial parameters.

310

JCoDe | Vol 6 No 2 | September 2025 | Tolerance in Computational Design | Diker, F., Erkan, İ.

In this context, a model has been created by Fuzzy Logic method to evaluate the efficiency of existing primary school classrooms in terms of physical sizes. From the data obtained by examining the existing primary school classrooms, the area per person (m^2) in the classrooms, the ratio of the window area to the floor area and the ratio of the window area to the wall area and the efficiency of the classrooms in terms of physical sizes were obtained. According to these values obtained, it was determined how many students should be present in the classrooms. Due to the lack of sufficient windows according to classroom sizes in most existing classrooms, changing the area per person for each classroom according to classroom and window sizes, rather than the standard (4 m^2), will reduce the risk of virus transmission. In addition to the physical distance, the dimensions of the classrooms and row sizes should be determined by considering the minimum area per person.

To increase the generalizability and reliability of the models, a 5-fold cross-validation method was applied. This method divided the dataset into five equal parts. Each part served as test data, while the remaining four were used for training, and the results were average. This reduced the bias that could arise from a single training-test split, allowing the average performance of the models across different data splits to be evaluated. This approach reduces the risk of overfitting the model, particularly when working with limited data, and allows for more reliable comparisons.

According to five-fold cross-validation results, the Deep Neural Network regression model demonstrated the highest overall performance and consistency compared to conventional regression approaches. While the Random Forest regression model also exhibited relatively consistent performance across layers, the Deep Neural Network regression model outperformed the other methods with higher accuracy and lower error metrics. These findings demonstrate the ability of deep learning-based approaches to capture complex and nonlinear relationships in data and demonstrate higher generalizability compared to conventional regression models. Therefore, the Deep Neural Network regression model can be considered a more suitable method than other supervised learning algorithms for this prediction problem.

A Data-Driven Approach to Determining Safe Classroom Capacities During the Transition to Face-to-Face Education

During the gradual transition to face-to-face education following the COVID-19 pandemic, six different regression models were developed to estimate the maximum number of students required in classrooms, considering existing classroom sizes and window area. The study findings indicate that the Deep Neural Network method provides higher accuracy compared to other methods in estimating student numbers based on spatial parameters. However, rather than setting a definitive standard, the model developed here is considered a tool that serves as a recommendation for implementing necessary precautions in educational structures and reducing the spread of infectious diseases. In this respect, it is expected to guide decision-makers by providing quantitative input to the prepared guidelines. Furthermore, expanding the scope of the dataset could further enhance the model's performance and generalizability. The developed models are limited to data obtained only from primary school classrooms; therefore, studies at middle school, high school, and university levels will provide the opportunity to test the model's applicability at different educational levels. This methodology has the potential to be used not only to determine student capacity for a safe return to face-to-face education under pandemic conditions, but also to determine optimal class sizes in terms of student achievement, health, and spatial comfort in the post-pandemic period. In future studies, it is recommended to examine school typologies in different climatic zones, including more comprehensive spatial parameters (acoustics, lighting, indoor air quality, etc.) in the model, and verify with field applications.

Acknowledgements

Conflict of Interest Statement

The manuscript is entitled "A Data-Driven Approach to Determining Safe Classroom Capacities During the Transition to Face-to-Face Education" has not been published elsewhere and that it has not been submitted simultaneously for publication elsewhere.

Author Contribution

All authors contributed equally to this article.

312

JCoDe | Vol 6 No 2 | September 2025 | Tolerance in Computational Design | Diker, F., Erkan, İ.

References

Alsubaie, M. A. (2022). Distance education and the social literacy of elementary school students during the COVID-19 pandemic. *Heliyon*, *8*(7). https://doi.org/10.1016/j.heliyon.2022.e09811

American Institute of Architects. (2020, July 31). Re-occupancy assessment tool V3.0. American Institute of Architects. Retrieved July 11, 2021, from https://content.aia.org/sites/default/files/2020-08/ReOccupancy_Assessment_Tool_v3.pdf

Amir, L. R., Tanti, I., Maharani, D. A., Wimardhani, Y. S., Julia, V., Sulijaya, B., & Puspitawati, R. (2020). Student perspective of classroom and distance learning during COVID-19 pandemic in the undergraduate dental study program Universitas Indonesia. *BMC medical education*, *20*(1), 392. https://doi.org/10.1186/s12909-020-02312-0

Amirzadeh, M., Sobhaninia, S., Buckman, S. T., & Sharifi, A. (2023). Towards building resilient cities to pandemics: A review of COVID-19 literature. *Sustainable cities and society*, *89*, 104326. https://doi.org/10.1016/j.scs.2022.104326

Breiman, L. (2001). Random forests. *Machine learning*, *45*(1), 5-32. https://doi.org/10.1023/A:1010933404324

Dehghani, A. A., Movahedi, N., Ghorbani, K., & Eslamian, S. (2023). Decision tree algorithms. In *Handbook of hydroinformatics* (pp. 171-187). Elsevier. https://doi.org/10.1016/B978-0-12-821285-1.00004-X

DeKay, M., & Brown, G. Z. (2013). *Sun, wind, and light: architectural design strategies*. John Wiley & Sons.

Diker, F., & Erkan, İ. (2022). Fuzzy logic method in the design of elementary school classrooms. *Architectural Engineering and Design Management*, *18*(5), 739-758. https://doi.org/10.1080/17452007.2021.1910925

Gaisie, E., Oppong-Yeboah, N. Y., & Cobbinah, P. B. (2022). Geographies of infections: Built environment and COVID-19 pandemic in metropolitan Melbourne. *Sustainable cities and society*, *81*, 103838. https://doi.org/10.1016/j.scs.2022.103838

Gupta, M. M. (2021). Impact of Coronavirus Disease (COVID-19) pandemic on classroom teaching: Challenges of online classes and solutions. *Journal of education and health promotion*, *10*, 155. https://doi.org/10.4103/jehp.jehp_1104_20

Güzelci, O. Z., Şen Bayram, A. K., Alaçam, S., Güzelci, H., Akkuyu, E. I., & Şencan, İ. (2021). Design tactics for enhancing the adaptability of primary and

middle schools to the new needs of postpandemic reuse. *Archnet-IJAR: International Journal of Architectural Research*, *15*(1), 148-166. https://doi.org/10.1108/ARCH-10-2020-0237

Heiberger, R. M., & Neuwirth, E. (2009). Polynomial regression. In *R through excel: a spreadsheet interface for statistics, data analysis, and graphics* (pp. 269-284). Springer New York. DOI 10.1007/978-1-4419-0052-4 11

Hinton, G. E., & Salakhutdinov, R. R. (2006). Reducing the dimensionality of data with neural networks. *science*, *313*(5786), 504-507. https://doi.org/10.1126/science.1127647

Hinton, G., Deng, L., Yu, D., Dahl, G. E., Mohamed, A., & Jaitly, N. (2012). Deep neural networks for acoustic modeling in speech recognition: The shared views of four research groups. *IEEE Signal Processing Magazine*, *29*(6), 82–97. https://doi.org/10.1109/MSP.2012.2205597

Huang, C., Wang, Y., Li, X., Ren, L., Zhao, J., Hu, Y., Zhang, L., Fan, G., Xu, J., Gu, X., Cheng, Z., Yu, T., Xia, J., Wei, Y., Wu, W., Xie, X., Yin, W., Li, H., Liu, M., Xiao, Y., Gao, H., Guo, L., Xie, J., Wang, G., Jiang, R., Gao, Z., Jin, Q., Wang, J., & Cao, B. (2020). Clinical features of patients infected with 2019 novel coronavirus in Wuhan, China. *The Lancet, 395*(10223), 497–506. https://doi.org/10.1016/S0140-6736(20)30183-5

James, G., Witten, D., Hastie, T., & Tibshirani, R. (2013). *An introduction to statistical learning: with applications in R* (Vol. 103). Springer.

Karadag, I., Güzelci, O. Z., & Alaçam, S. (2023). EDU-AI: A twofold machine learning model to support classroom layout generation. *Construction Innovation*, *23*(4), 898-914. https://doi.org/10.1108/CI-02-2022-0034

Kavuncu, S. K. (2018). Makine öğrenmesi ve derin öğrenme: Nesne tanıma uygulaması [Master's thesis, Kırıkkale University, Institute of Science and Technology]. YÖK Tez Merkezi. https://tez.yok.gov.tr/UlusalTezMerkezi/giris.jsp

Keogh-Brown, M. R., Wren-Lewis, S., Edmunds, W. J., Beutels, P., & Smith, R. D. (2010). The possible macroeconomic impact on the UK of an influenza pandemic. *Health Economics*, *19*(11), 1345-1360. https://doi.org/10.1002/hec.1554

Li, J., & Che, W. (2022). Challenges and coping strategies of online learning for college students in the context of COVID-19: A survey of Chinese universities. *Sustainable Cities and Society*, *83*, 103958. https://doi.org/10.1016/j.scs.2022.103958

314

JCoDe | Vol 6 No 2 | September 2025 | Tolerance in Computational Design | Diker, F., Erkan, İ.

Liu, J., Liao, X., Qian, S., Yuan, J., Wang, F., Liu, Y., Wang, Z., Wang, F.-S., Liu, L., & Zhang, Z. (2020). Community transmission of severe acute respiratory syndrome coronavirus 2, Shenzhen, China, 2020. Emerging Infectious Diseases, 26(6), 1320–1323. https://doi.org/10.3201/eid2606.200239

Liu, Y., Wang, X., Song, C., Chen, J., Shu, H., Wu, M., Guo, S., Huang, Q., & Pei, T. (2023). Quantifying human mobility resilience to the COVID-19 pandemic: A case study of Beijing, China. *Sustainable Cities and Society, 89*, 104314. https://doi.org/10.1016/j.scs.2022.104314

Lordan, R., FitzGerald, G. A., & Grosser, T. (2020). Reopening schools during COVID-19. *Science*, *369*(6508), 1146-1146. https://doi.org/10.1126/science.abe5765

Mitchell, T. M. (1997). *Machine learning.* McGraw-Hill. Retrieved from https://www.cs.cmu.edu/~tom/files/MachineLearningTomMitchell.pdf [Date of access: 11.07.2021]

Mouratidis, K., & Papagiannakis, A. (2021). COVID-19, internet, and mobility: The rise of telework, telehealth, e-learning, and e-shopping. *Sustainable Cities and Society*, 74, 103182. https://doi.org/10.1016/j.scs.2021.103182

Naqa, I., & Murphy, M. J. (2015). What is machine learning? In I. El Naqa, R. Li, M. Murphy (Eds.), *Machine Learning in Radiation Oncology* (3-11). Springer International Publishing. https://doi.org/10.1007/978-3-319-18305-3_1

Neuwirth, L. S., Jović, S., & Mukherji, B. R. (2021). Reimagining higher education during and post-COVID-19: Challenges and opportunities. *Journal of Adult And Continuing Education*, *27*(2), 141-156. https://doi.org/10.1177/1477971420947738

Nicola, M., Alsafi, Z., Sohrabi, C., Kerwan, A., Al-Jabir, A., Iosifidis, C., ... & Agha, R. (2020). The socio-economic implications of the coronavirus pandemic (COVID-19): A review. *International journal of surgery*, *78*, 185-193. https://doi.org/10.1016/j.ijsu.2020.04.018

Samuel, A. L. (1959). Some studies in machine learning using the game of checkers. *IBM Journal of research and development*, *3*(3), 210-229. https://doi.org/10.1147/rd.33.0210

Suchetana, B., Rajagopalan, B., & Silverstein, J. (2017). Assessment of wastewater treatment facility compliance with decreasing ammonia discharge limits using a regression tree model. *Science of the Total Environment*, *598*, 249-257. https://doi.org/10.1016/j.scitotenv.2017.03.236

United Nations Educational, Scientific and Cultural Organization (UNESCO), (2020). *COVID-19 impact on Education*. Retrieved June 25, 2021, from

315

https://en.unesco.org/themes/education-emergencies/coronavirus-school-closures

Vapnik, V. N. (1997, October). The support vector method. In *International conference on artificial neural networks* (pp. 261-271). Berlin, Heidelberg: Springer Berlin Heidelberg. https://doi.org/10.1007/BFb0020166

World Health Organization (WHO). (2020). Coronavirus disease (COVID-19) advice for the public. Retrieved July 2, 2021, from https://www.who.int/emergencies/diseases/novel-coronavirus-2019/advice-for-public

Yetiş, C., & Kayılı, M. T. (2021). Covid-19 salgını: eğitim yapıları üzerinden yeniden kullanım değerlendirmesi. *Journal of Awareness*, *6*(2), 199-2114. https://doi.org/10.26809/joa.6.2.10

Yüksek Öğretim Kurulu (YÖK) (2020). Guide for the Development of Healthy and Clean Environments in Higher Education Institutions. Retrieved July 11, 2021, from https://eski.yok.gov.tr/Documents/Yayinlar/Yayinlarimiz/2020/yuksekogretim-kurumlarinda-saglikli-ve-temiz-ortamlarin-gelistirilmesi-kilavuzu.pdf

Yu, R., Ostwald, M. J., Gu, N., Skates, H., & Feast, S. (2022). Evaluating the effectiveness of online teaching in architecture courses. *Architectural Science Review*, *65*(2), 89-100. https://doi.org/10.1080/00038628.2021.1921689

316

JCoDe | Vol 6 No 2 | September 2025 | Tolerance in Computational Design | Diker, F., Erkan, İ.

Using Voronoi Diagrams and Space Syntax in Determining Emergency Assembly Areas: Bursa Karaman District

Gizem Özçidem Sümen[1], İlayda Şevval Alış[2], Göktürk Bostancı[3], Barış Mert Karasu[4], Özgür Ediz[5]

ORCID NO: 0009-0007-1930-0416[1], 0009-0002-9875-3547[2], 0009-0009-7983-3008[3], 0000-0002-0743-208X[4], 0000-0002-0486-8806[5]

[1,2,3,4,5] Bursa Uludağ University, Faculty of Architecture, Architecture Department, Bursa, Türkiye

The planning of safe assembly areas in disaster and emergency management processes is of paramount importance for ensuring public safety and minimizing risks. Particularly in regions undergoing rapid urbanization, the accurate identification of such areas is critical to mitigating chaos during disasters and expediting the post-disaster recovery process. This study evaluates the adequacy of existing emergency assembly areas within the boundaries of Karaman Neighborhood in Nilüfer District, Bursa, in terms of population density and accessibility. Furthermore, it proposes new assembly areas where deemed necessary.

The study employs a combination of Voronoi diagrams and space syntax methods. In the initial phase, a correlation between population density data and urban voids within Karaman Neighborhood was established. Using Voronoi diagrams, the influence areas of these voids were delineated based on appropriate accessibility distances. This analysis enabled the assessment of how effectively the urban voids accommodate the current population density and their spatial proximity to residential zones. In the subsequent phase, the accessibility levels of the proposed and existing assembly areas were analyzed through space syntax methods.

The findings indicate that the existing assembly areas in Karaman Neighborhood are insufficient in certain regions in terms of both population density and accessibility. The results derived from the Voronoi diagrams underscore the necessity of additional assembly areas, particularly in densely populated zones. Spatial analysis further reveals significant disparities in the accessibility levels of the existing urban voids, highlighting the need for their enhancement to meet the requirements of disaster preparedness effectively. The use of these two methods together in determining disaster assembly areas constitutes the novelty of the study.

317

Afet Toplanma Alanlarının Belirlenmesinde Voronoi Diyagramları ve Mekân Dizimi Kullanılması: Bursa Karaman Mahallesi Örneği

Gizem Özçidem Sümen[1], İlayda Şevval Alış[2], Göktürk Bostancı[3], Barış Mert Karasu[4], Özgür Ediz[5]

ORCID NO: 0009-0007-1930-0416[1], 0009-0002-9875-3547[2], 0009-0009-7983-3008[3], 0000-0002-0743-208X[4], 0000-0002-0486-8806[5]

[1,2,3,4,5] Bursa Uludağ Üniversitesi, Mimarlık Fakültesi, Mimarlık Bölümü, Bursa, Türkiye

Afet ve acil durum süreçlerinde güvenli toplanma alanlarının planlanması, toplumsal güvenliğin sağlanması ve risklerin en aza indirilmesi açısından büyük bir öneme sahiptir. Özellikle kentleşme sürecinin hız kazandığı bölgelerde, bu alanların doğru bir şekilde belirlenmesi hem afet anındaki kaosun azaltılması hem de toplumun afet sonrası toparlanma sürecinin hızlanması için kritik bir gerekliliktir. Bu çalışma, Bursa Nilüfer ilçesi Karaman Mahallesi sınırlarında yer alan mevcut afet toplanma alanlarının, olası bir afet durumunda nüfus yoğunluğu ve erişilebilirlik açısından yeterliliğini değerlendirerek gerekli görülen bölgelerde yeni toplanma alanları önermektedir. Araştırmada, algoritmik-üretken bir yöntem olan Voronoi diyagramları ve mekân dizimi yöntemleri birlikte kullanılmıştır. İlk aşamada, Karaman Mahallesi'nin nüfus yoğunluğu verileri ile kentsel boşluklar arasında bir ilişki kurulmuş ve Voronoi diyagramları aracılığıyla bu boşlukların her birinin uygun erişim mesafelerine göre etki alanları belirlenmiştir. Bu analiz, boşlukların mevcut nüfus yoğunluğunu ne derece kapsayabildiğini ve mahalledeki yerleşim alanlarına olan mesafelerini değerlendirmeyi mümkün kılmıştır. İkinci aşamada, önerilen alanların ve mevcut toplanma alanlarının erişilebilirlik seviyeleri mekân dizimi yöntemi kullanılarak incelenmiştir. Çalışma sonucunda, Karaman Mahallesi'ndeki toplanma alanlarının bazı bölgelerde nüfus yoğunluğu ve erişilebilirlik açısından yetersiz olduğu tespit edilmiştir. Voronoi diyagramları ile elde edilen bulgular, özellikle yoğun nüfuslu bölgelerde daha fazla toplanma alanına ihtiyaç duyulduğunu ortaya koymuştur. Mekân dizimi analizleri ise mevcut kentsel boşlukların erişilebilirlik seviyelerindeki farklılıkları göstermiş ve bu boşlukların iyileştirilmesi gerektiğini vurgulamıştır. Bu iki yöntemin afet toplanma alanlarının belirlenmesinde bir arada kullanılması çalışmanın yenilikçi tarafını oluşturmaktadır.

Anahtar Kelimeler: Afet toplanma alanı, Mekân dizimi, Voronoi diyagramı, Yapay zekâ

318

JCoDe | Cilt 6 Sayı 2 | Eylül 2025 | Hesaplamalı Tasarımda Tolerans | Özçidem Sümen, G., Alış, İ. Ş. Bostancı, G., Karasu, B. M., Ediz, Ö.

1. GİRİŞ (INTRODUCTION)

Mimarlık kavramının ortaya çıkışı insanlık tarihi kadar eskidir. Yeme ve içmenin yanı sıra barınmak da insanların temel gereksinimleri arasında yer almaktadır. Bu gereksinim, yıllar boyunca kültürel, teknolojik ve ekonomik koşullara göre başkalaşım geçirmiştir. Bu süreç günümüz dinamikleri kapsamında ele alındığında, özellikle sayısal teknolojilerin gelişmesi ile bambaşka ve daha önce karşılaşmadığımız çözüm önerilerine evrilmiştir. Literatürde yer alan ve geçmiş yüzyılı etkileyen mimarideki "seri üretim" (mass production) yaklaşımlarının, "kitlesel bireyselleştirme"ye (mass customization) dayalı çözümlere dönüşmesi günümüz mimarlığı açısından oldukça büyük bir önem taşımaktadır. Sayısal yaklaşımların ortaya çıkmasını tetiklemesi açısından "kitlesel bireyselleştirme"ye dayalı bu dönüşüm; mimarlık kuramı ve pratiği üzerinde günümüzde halen yeni tartışmaların platformu olmaya devam etmektedir. (Ediz vd., 2010). Bu kavramların ve uygulamalarının ortaya çıkmasından sonra farklı teknolojik gelişmelerle de dönüşüme uğrayan mimari tasarım-üretim ortamı günümüzde yalnızca estetik ve işlevsellik bağlamında değil, aynı zamanda toplumsal ve çevresel etkileri ile de ele alınmaktadır. Mimarlığın yapay çevrenin oluşmasındaki büyük rolü, bağlamda ve özellikle deprem gerçeği konusundaki toplumsal sorumluluğunun büyüklüğünü arttırmaktadır.

Sanayileşme ile hızlı, çarpık kentleşmenin ve yoğun göçün etkisi altında bulunan Bursa kenti deprem üretme riski en yüksek olan Kuzey Anadolu fay hattının etkisinde olması nedeniyle tarihi boyunca birçok kez deprem gerçeği ile yüzleşmiştir. Bu depremlerden kayıt altına alınan en etkilileri, 1855 Bursa depremleridir. Bu tarihe kadar Bursa'da 1143, 1327, 1418, 1463, 1555, 1674 ve 1705 yıllarında gerçekleşen depremler küçük çaplı olup büyük etkiler bırakmamışlardır fakat 1855 yılında gerçekleşen depremler kentte büyük yıkıma neden olmuştur. (Özcan, 2010). Bu depremler kentin gelişim yönünü ve planlanmasını doğrudan etkilenmiştir. Kent morfolojisinin değişimini takip edebilmek için Bursa'nın farklı dönemlerde hazırlanmış haritaları önemli kaynaklardır. 1855 Bursa depremlerinden sonra 1862 yılında Suphi Bey tarafından hazırlanan ''Bursa Şehri Harita-i Mufassalası''nda kentin batıya; Çekirge bölgesine doğru genişlediği ve bölgesel olarak daha düzenli bir kentleşme olduğu gözlemlenmektedir (Şekil 1).

319

Afet Toplanma Alanlarının Belirlenmesinde Voronoi Diyagramları ve Mekân Dizimi Kullanılması: Bursa Karaman Mahallesi Örneği
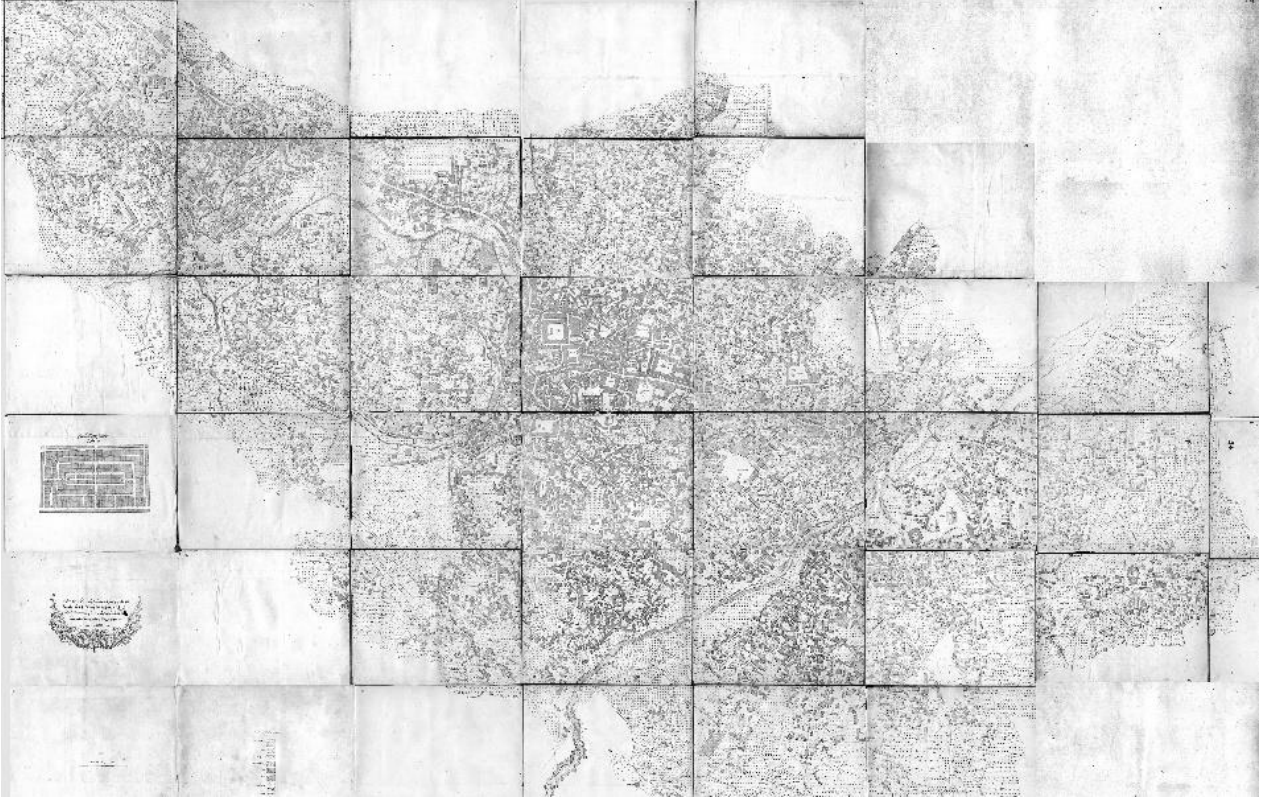
Günümüzde Bursa'da kentleşme, Uludağ eteklerinden ova içerisine kadar inmiştir. Kalın alüvyon zemin yapısına sahip olan bu alanların konut alanı olarak değerlendirilmesi tarihte büyük depremler üretmiş olan aktif fay hattı üzerinde bulunan bir şehir için çok risklidir (Akyol vd., 2002; Uyanık, 2006; Tabban, 2000). Bu sebeple, gelecekte gerçekleşebilecek olası depremler için kentte kusursuz işleyen bir afet yönetim programı uygulanmalıdır. Afet yönetim programlarının önemli bileşenlerinden birini de afet esnasında ve sonrasında güvenliği sağlayacak toplanma alanları oluşturmaktadır.

Deprem ve sel gibi ani ve yıkıcı doğal afetler sonrasında halkın toplanması için planlanan afet toplanma alanlarının etkin bir şekilde belirlenmesi hayati öneme sahiptir (Alexander, 2002; Cutter, 2003). Literatürde, bu alanların belirlenmesi için coğrafi bilgi sistemleri (CBS) tabanlı yöntemler sıklıkla kullanılmakta olup, voronoi diyagramları gibi geometrik modeller, afet toplanma alanlarının optimizasyonu ve erişilebilirlik analizleri için etkili bir araç olarak öne çıkmaktadır (Aurenhammer, 1991; Okabe vd., 2000). Voronoi diyagramları ayrıca üretken bir tasarım yaklaşımı olarak kentsel tasarım çalışmalarında

320

JCoDe | Cilt 6 Sayı 2 | Eylül 2025 | Hesaplamalı Tasarımda Tolerans | Özçidem Sümen, G., Alış, İ. Ş., Bostancı, G., Karasu, B. M., Ediz, Ö.

kullanılmaktadır (Davis, 2013; Nowak, 2015). Kentsel biçimlerin erişilebilirlik miktarlarının derecelendirilmesi ve değerlendirilmesinde space syntax (mekân dizimi) yöntemi, mekânsal biçimlenme ve insan hareketliliği arasındaki ilişkiyi anlamak açısından önemli bir katkı sağlamaktadır (Hillier ve Hanson, 1984; Karimi, 2012).

Bu çalışmada, voronoi diyagramları ile belirlenen afet toplanma alanlarının erişilebilirlik değerlerinin mekân dizimi yöntemi ile analiz edilmesi ve bu yöntemlerin afet yönetimi stratejilerine entegrasyonu üzerine bir yaklaşım önerilmektedir. Voronoi diyagramlarıyla önerilen afet toplanma alanlarının erişilebilirlik derecelerinin mekân dizimi yöntemiyle değerlendirmesi çalışmanın özgün yönünü oluşturmaktadır. Çalışma kapsamında sayısal yöntemlere dayalı bir kurgu ile algoritmik-üretken bir yöntem olan voronoi diyagramı yöntemi kullanılarak, Bursa Nilüfer ilçesi Karaman Mahallesi'nin mevcut afet toplanma alanlarını nüfus yoğunluğu ve erişilebilirlik parametreleri üzerinden değerlendirilerek olası afet durumunda yerleşik nüfusun daha kolay ulaşabileceği toplanma alanları önerilmiştir. Bu kapsamda ilk aşamada nüfus yoğunluğunun kentsel boşluklarla ilişkisini ve bu boşluklara olan erişim mesafelerini değerlendirmek için voronoi diyagramı kullanılmıştır. İkinci aşamada kentsel boşlukların erişilebilirlik seviyelerini değerlendirmek için mekân dizimi yöntemlerinden faydalanılmıştır. Çalışmada, voronoi diyagramları ile belirlenen afet toplanma alanlarının erişilebilirlik derecelerinin oldukça yüksek olduğu gösterilmiştir. Bu çalışmanın gelecekte toplanma alanlarının planlanmasında, afet ve acil durum sonrası yeniden yapılanmada sistemli ve bilimsel bir yaklaşım olarak kullanılabileceği öngörülmektedir.

2. AFET VE ACİL TOPLANMA ALANLARI KRİTERLERİ (CRITERIA FOR DISASTER AND EMERGENCY ASSEMBLY AREAS)

Kentsel alanlarda acil toplanma alanlarının seçimi, afet/acil durum anında ve hemen sonrasında insanların güvenliğinin ivedilikle sağlanabilmesi için büyük önem taşımaktadır. Günümüzde bir üst plan olarak uygulanan Türkiye Afet Müdahale Planı'nda, afet ve acil durumlarla ilgili müdahale süreçlerinde görev alacak ekiplerin ve koordinasyon birimlerinin görevleri tanımlanarak afet hazırlık, müdahale ve iyileşme aşamalarındaki eylem planlamasının esasları belirlenmiştir (Afet ve Acil Durum Yönetimi Başkanlığı [AFAD], 2014).

Afet Toplanma Alanlarının Belirlenmesinde Voronoi Diyagramları ve Mekân Dizimi Kullanılması: Bursa Karaman Mahallesi Örneği

Ancak bu plan kapsamında afet ve acil toplanma alanlarının oluşturulmasına yönelik kriterler yer almamaktadır. Literatürde Acil toplanma alanlarının belirlenmesinde beş temel kriter göz önünde bulundurulmaktadır (Aksoy vd., 2009; Japonya Uluslararası İşbirliği Ajansı [JICA] ve İstanbul Büyükşehir Belediyesi [İBB], 2002; Tarabanis ve Tsionas, 1999):

- Erişilebilirlik: Toplanma alanlarına ulaşımın her birey için kolay olması gerekmektedir. Bu doğrultuda, yapı adalarından toplanma alanlarına olan yürüme mesafesi en fazla 500 metre veya 15 dakika içinde tamamlanabilecek şekilde belirlenmelidir.

- Ana Yollarla Bağlantı: Toplanma alanlarının ana yollarla bağlantısının sağlanması önemlidir. Acil durumda kapanma riski olan yollar da dikkate alınarak, diğer toplanma alanlarıyla kesintisiz bir ulaşım ağı oluşturulmalıdır.

- Mülkiyet: Öncelikli olarak kamuya ait araziler toplanma alanı olarak seçilmelidir. Özel mülkiyette bulunan boş alanlar ve açık otoparklar ise erişilebilirlik, kullanım özellikleri, yol bağlantıları ve diğer toplanma alanlarıyla oluşturduğu bütünlük ile alan büyüklüğü göz önünde bulundurularak değerlendirilebilir. Ayrıca, mahallelerde bulunan kamu okulları ve cami gibi yapılar, sismik açıdan yeterli dayanıklılığa sahip olmaları durumunda toplanma alanı olarak kullanılabilir (JICA ve İBB, 2002).

- Kullanılabilirlik ve Çok Fonksiyonluluk: Toplanma alanı olarak, mevcut aktif yeşil alanlar arasında yer alan spor sahaları, mahalle ve semt parkları, çocuk oyun alanları, cep parkları, değerlendirilebilir. Ayrıca okul, bina, cami, hastane bahçeleri; boş araziler, halı sahalar ve açık otoparklar da uygun seçenekler arasındadır. Bu alanların en az 500 m² büyüklüğünde olması gerekmektedir (JICA ve İBB, 2002).

- Alansal Büyüklük: Her mahallede bir "Ön Tahliye Alanı" oluşturulması ve kişi başına en az 1,5 m² brüt alan ayrılması önerilmektedir (JICA ve İBB, 2002). Tarabanis ve Tsionas (1999) ise yapı adası ölçeğinde, toplanma alanlarında kişi başına düşen net kullanım alanının en az 2 m² olması gerektiğini belirtmiştir.

Bu kriterlerden yapılan çıkarımlara göre hizmet ettiği yerleşim yerlerine maksimum ulaşım mesafesi 500 m veya 15 dakika olan, minimum 500 m² büyüklüğünde, kişi başı 2 m² kullanım alanı şartını sağlayabilecek toplanma alanları voronoi diyagramı kullanılarak belirlenmeye

322

JCoDe | Cilt 6 Sayı 2 | Eylül 2025 | Hesaplamalı Tasarımda Tolerans | Özçidem Sümen, G., Alış, İ. Ş., Bostancı, G., Karasu, B. M., Ediz, Ö.

çalışılmıştır. Bu alanların erişim düzeyi de mekân dizimi yöntemiyle belirlenmiştir.

Ülke genelinde afet ve acil toplanma alanlarının belirlenmesinde çerçevesi net çizilmiş bir standartlar bütünlüğünün bulunmaması, belediyeler tarafından belirlenen toplanma alanlarının temel kriterlere göre kullanılabilirliğinin yeterli olmamasıyla sonuçlanmaktadır. Bu çalışmada afet ve acil toplanma alanlarının belirlenmesinde farklı bölgeler için uyarlanabilir, bilimsel bir model oluşturmak amaçlanmıştır.

3. KARAMAN MAHALLESİ (KARAMAN NEIGHBORHOOD)

Karaman mahallesi İzmir-Mudanya yolu arasında yer almaktadır. Köy olarak tarihi 1530 yılındaki kayıtlara kadar uzanmaktadır. 1926 yılında İhsaniye köyü ile birleştirilmiş ve 1987 yılında mahalle haline getirilmiştir (Kaplanoğlu, 2016). Bursa'nın eski mahallelerinden biri olan Karaman'da Nilüfer Belediyesi'nden alınan 2023 nüfus verilerine göre 5532 erkek, 5917 kadın olmak üzere 11449 kişi yaşamaktadır. Mahallenin en kalabalık yaş grubunu toplam 1642 kişi olmak üzere 65 yaş ve üzeri kişilerden oluşturmaktadır. Mahallenin 1985, 2010 ve 2024 kuş bakışı görüntüleri incelendiğinde, yerleşme biçimlerinin ne şekilde olduğuna dair bilgi edinilebilmektedir. Google Earth platformu üzerinden 1985 yılına ait kuş bakışı görüntüsü bulanık olsa da mahalledeki yerleşimlerin kuzey yönünden başladığı gözlemlenmektedir (Şekil 2).

Şekil 2: Karaman Mahallesi'nin soldan sağa; 1985, 2010 ve 2024 yıllarına ait uydu görüntüleri (Satellite images of Karaman Neighborhood, shown from left to right for the years 1985, 2010, and 2024) (Google Earth)

Mahallenin ilk yerleşiminin başladığı kuzey ve kuzey-batı bölgesinde yoğun bir yapılaşma gözlemlenmektedir. Bölgedeki yapılaşma şekli bitişik nizamdır. Sistemsiz yapılan araç parklarının araç ve yaya sirkülasyonunu zorlaştırdığı görülmektedir (Şekil 3).

323

Afet Toplanma Alanlarının Belirlenmesinde Voronoi Diyagramları ve Mekân Dizimi Kullanılması: Bursa Karaman Mahallesi Örneği

Mahallenin İzmir yolundan girişinde kalan güney bölgesinde ise daha geniş yollar, yeni ve ayrık nizam binalar gözlemlenmektedir. Kentsel dönüşüm projeleri daha çok bu alanda yoğunlaşmıştır **(Şekil 4)**.

Karaman Mahalle'si sınırları içerisinde Nilüfer Belediyesi'nin belirlediği 3 adet afet toplanma bölgesi bulunmaktadır. Bu alanlar; Karaman Dernekler Yerleşkesi, Canaydın İlköğretim Okulu ve Karaman Muhtarlığı halı sahasıdır. Bu 3 toplanma alanı haricinde mahalle sınırları dışarısında kalan fakat mahalleye hizmet edebilecek kadar yakında bulunan 2 adet daha afet toplanma alanı mevcuttur. Bu alanlar, İhsaniye Ihlamur Çocuk Parkı ve Esentepe Nedim Öztan İlköğretim Okulu'dur. Çalışma Karaman Mahallesi özelinde yapıldığı için mahalle sınırları dışında kalan toplanma alanları dikkate alınmamıştır **(Şekil 5)**.

324

JCoDe | Cilt 6 Sayı 2 | Eylül 2025 | Hesaplamalı Tasarımda Tolerans | Özçidem Sümen, G., Alış, İ. Ş., Bostancı, G., Karasu, B. M., Ediz, Ö.

Şekil 5: Mevcut acil durum toplanma alanları (Existing emergency assembly areas)

Mevcut toplanma alanlarının niteliğine bakıldığında kuzeyde yer alan toplanma alanı hem kapalı pazar alanı hem de dernekler yerleşkesi olarak kullanılan üç katlı binadan oluşmaktadır. Yakın çevresindeki yoğun yapılaşmanın yarattığı tehlike ve kapalı alandan oluşması sebebiyle bir toplanma alanı olarak güvenlik yönünden yeterli görülmemiştir. Aynı zamanda çevre yapılaşmadaki dar sokaklar ve sistemsiz araç parkları sebebiyle ulaşım yönünden de yeteriz bulunmuştur. Mahallenin güney batısında yer alan Canaydın İlköğretim okulu toplanma alanı ile Karaman muhtarlığına ait halı sahadan oluşan toplanma alanları sağladıkları açık alan miktarı yönünden daha nitelikli bulunmuştur **(Şekil 6, 7, 8).**

Şekil 6: Karaman Dernekler Yerleşkesi toplanma alanı (Karaman Dernekler Yerleşkesi assembly area)

Afet Toplanma Alanlarının Belirlenmesinde Voronoi Diyagramları ve Mekân Dizimi Kullanılması: Bursa Karaman Mahallesi Örneği

Şekil 7: Canaydın İlköğretim Okulu toplanma alanı (Canaydın Primary School assembly area)
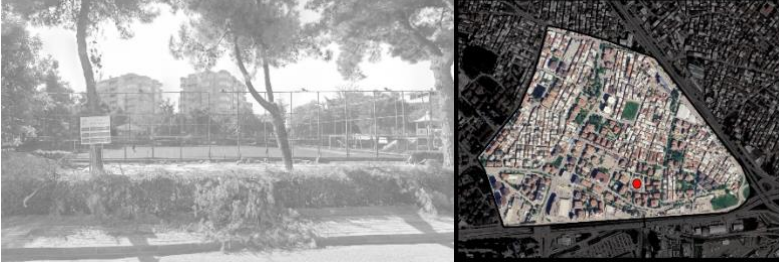
Şekil 8: Halı saha toplanma alanı (Football pitch assembly area)

Daha öncesinde Karamanköy olarak bilinen Karaman Mahallesi Nilüfer Bölgesi'nin en eski yerleşimlerinden birisidir. Mahallede bitişik nizam yapılaşma şeklini, çarpık kentleşme örneklerini, dar sokakları, kaçak katları, gözlemlerken aynı zamanda geniş sokakları, kentsel dönüşümü ve ayrık nizam yapılaşma şeklini de gözlemlemek mümkündür. Mahalle içerisinde bulunan afet toplanma alanları da dahil olmak üzere kuzey ve güney yönünde farklı yapılaşma karakteristikleri göstermiştir. Bu sebeplerle farklı dokuları içinde barındıran Karaman Mahallesi bu çalışmada kullanılmak için uygun bulunmuştur. Çalışma kapsamında Karaman Mahallesi ve bu mahalledeki toplanma alanları incelenmiş, mahalle voronoi diyagramları kullanılarak yapılaşma yoğunluklarına göre bölümlere ayrılmış ve her bölüm için ideal toplanma alanı önerileri geliştirilmiştir.

4. YÖNTEM (METHOD)

Bu çalışmada, yeni afet ve acil toplanma alanlarının belirlenmesi hedefiyle hesaplamalı bir yöntem olan voronoi diyagramı yaklaşımının uygulanması için MATLAB yazılımından faydalanılmıştır. OpenAI tarafından geliştirilen ChatGPT yapay zekâ aracı yardımıyla voronoi diyagramlarının üretilmesinde kullanılan algoritmalar oluşturulmuştur.

Voronoi diyagramları, bir düzlemi veya uzayı, belirli bir dizi noktaya (çekirdek) olan yakınlıklarına göre bölümlere ayıran temel bir geometrik yapıdır. Her bir bölge, o bölgedeki en yakın çekirdeğe ait olan noktaları içerir (Aurenhammer ve Klein, 2000).

326

JCoDe | Cilt 6 Sayı 2 | Eylül 2025 | Hesaplamalı Tasarımda Tolerans | Özçidem Sümen, G., Alış, İ. Ş., Bostancı, G., Karasu, B. M., Ediz, Ö.

Voronoi diyagramları, mimarlıkta estetik ve yapısal tasarımda geniş bir kullanım alanına sahiptir. Doğadan esinlenen bu desenler, cephe tasarımından yapısal optimizasyona, parametrik tasarımdan kentsel planlamaya kadar birçok alanda yenilikçi çözümler sunar. Bu diyagramlar, mimari tasarımda estetik ve işlevselliği bir araya getirerek, tasarımcılara geniş bir yaratıcı alan sağlar. Voronoi diyagramları, kentsel alanların ve konut alanlarının tasarımında da kullanılabilir. Bu diyagramlar, alanların zonlanmasında ve bölgesel planlamada etkili bir araç olarak kullanılabilir (Nowak, 2015).

Voronoi diyagramlarının, Karaman mahallesi bazında potansiyel toplanma alanlarının belirlenmesinde matematiksel bir yaklaşım olarak kullanılması çalışmanın temelini oluşturmaktadır.

4.1. Veri Toplama ve Hazırlık (Data Collection And Preparation)

Çalışma alanı olarak seçilen Bursa Nilüfer ilçesi Karaman Mahallesine ilişkin mevcut toplanma alanlarının nokta ve koordinatlarının yer aldığı kmz dosyasıyla 2023 yılı verilerine göre tüm mahalleyi kapsayan kadın, erkek ve toplam nüfus bilgisinin yer aldığı excel dosyası Nilüfer Belediyesi'nden temin edilmiştir. Toplanma alanlarının büyüklükleri, çevresindeki yapılaşma niteliği ve yoğunluğu, ana yollara uzaklığı Google Earth ve Google Maps kullanılarak incelenmiş gerekli görüldüğü takdirde yerinde ziyaret yapılarak bu alanların mevcut durumu belgelenmiştir. Toplanma alanlarını gösteren kmz dosyası Google Earth platformunda incelenmiş ve koordinatları daha sonra işlenmek üzere kaydedilmiştir.

4.2. Voronoi Diyagramlarının Oluşturulması (Creating Voronoi Diagrams)

Elde edilen veriler, yapay zekâ yardımıyla MATLAB yazılımı kullanılarak uygun bir biçimde düzenlenmiş ve araştırmanın temel yöntemi olan Voronoi diyagramları süreci için hazırlanmıştır. Öncelikle, Karaman Mahallesi sınırları içerisindeki mevcut toplanma alanlarının coğrafi koordinatları belirlenmiştir. Bu kapsamda, ilgili toplanma alanlarına ait boylam (longitude) ve enlem (latitude) değerleri bir dizi halinde MATLAB ortamında tanımlanmıştır.

Bu koordinatlar doğrultusunda uydu görüntüsü temin edilmiş ve yapay zekâ yardımı ile kodlanarak, çalışmada kullanılmak üzere MATLAB yazılımına entegre edilmiştir. Uydu görüntüsünün çalışma kapsamında doğru bir şekilde hizalanması ve coğrafi boyutlarının uyarlanabilmesi

327

Afet Toplanma Alanlarının Belirlenmesinde Voronoi Diyagramları ve Mekân Dizimi Kullanılması: Bursa Karaman Mahallesi Örneği

için, görüntünün boylam ve enlem aralıkları belirlenmiş ve bu aralıklar kodda sınır değerleri olarak tanımlanmıştır.

Voronoi diyagramlarının oluşturulması için MATLAB'ın voronoi fonksiyonu kullanılmıştır. Bu fonksiyon, belirlenen koordinatlara dayalı olarak geometrik bir bölgeleme yaparak, her bir toplanma alanının kapsama sınırlarını belirlemiştir. Diyagramlar, uydu görüntüsü üzerine görsel olarak yerleştirilmiş ve noktalar, ilgili toplanma alanlarını temsil edecek şekilde mavi renkli olarak görselleştirilmiştir (Şekil 9).
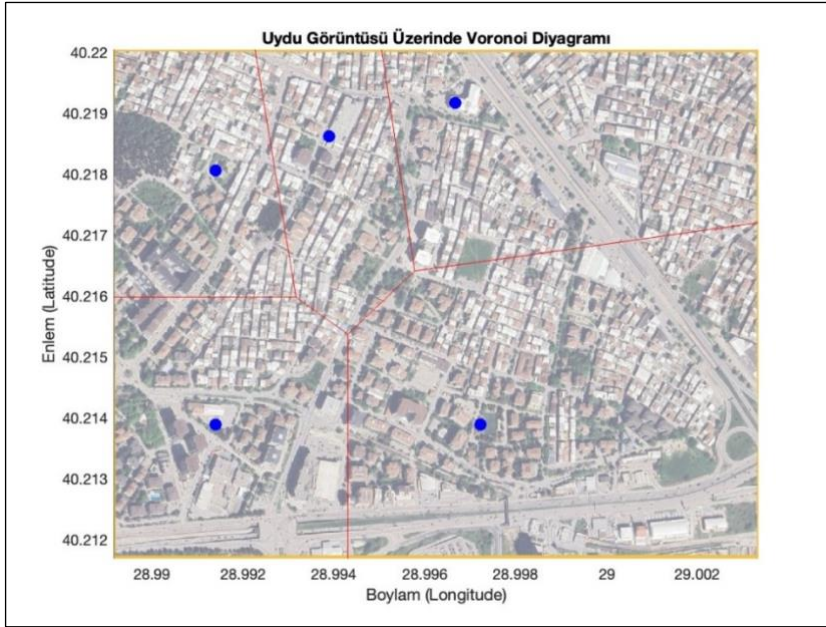
Şekil 9: Mevcut afet toplanma alanlarına göre çizilen voronoi diyagramı (Voronoi diagram drawn according to existing disaster assembly areas)

Bir sonraki aşamada ise mevcut toplanma alanlarını esas alan önceki analizden farklı olarak, Voronoi noktaları nüfusun yoğun olduğu bölgeler dikkate alınarak belirlenmiştir (Şekil 10). Burada ilk olarak analiz yapılacak bölgeyi tanımlamak için çalışma alanının sınırlarını belirleyen bir poligon sistemi oluşturulmuştur. Poligonun köşe noktalarının koordinatları (enlem ve boylam) kullanılarak MATLAB ortamında bir poligon şekli tanımlanmıştır. Bu poligon, analiz alanının sınırlarını ifade etmektedir.

Sonraki aşamada diyagramı oluşturmak için noktalar belirlenmiştir. Bu noktalar belirlenirken Karaman Mahallesi Google Earth uydu görüntüsü incelenerek yapılaşmanın yoğun göründüğü her bir alan için yaklaşık olarak o alanların merkezlerine denk gelecek noktalar işaretlenmiştir. Bu noktalar çalışma alanındaki potansiyel yoğunluk bölgelerini temsil

328

JCoDe | Cilt 6 Sayı 2 | Eylül 2025 | Hesaplamalı Tasarımda Tolerans | Özçidem Sümen, G., Alış, İ. Ş., Bostancı, G., Karasu, B. M., Ediz, Ö.

etmektedir. Bu noktaların koordinatları derece, dakika ve saniye formatında belirlenmiş ve daha sonra ondalık dereceye çevrilerek MATLAB ortamına tanımlanmıştır.

Voronoi diyagramları, MATLAB'ın voronoi fonksiyonu kullanılarak hesaplanmıştır. Bu işlem, belirlenen Voronoi noktalarından hareketle, her bir noktanın etkili kapsama alanını belirlemek amacıyla gerçekleştirilmiştir. Voronoi sınırlarının coğrafi bağlamda doğru şekilde görselleştirilmesi için MATLAB'ın coğrafi harita (geobasemap) altyapısı kullanılmış ve uydu görüntüsünü baz alan harita olarak seçilmiştir. MATLAB'ın geoplot ve geoscatter fonksiyonları, poligon sınırlarının, noktaların ve Voronoi kenarlarının uydu görüntüsü üzerinde coğrafi olarak doğru bir şekilde görselleştirilmesini sağlamıştır (Şekil 10). Çizim sırasında, Voronoi kenarlarının birden fazla segmenti, bir döngü (loop) kullanılarak coğrafi koordinatlar üzerinden çizilmiştir.

Şekil 10: Yoğun nüfus bölgelerine göre oluşturulmuş voronoi diyagramı (Voronoi diagram created in relation to high-density population areas)
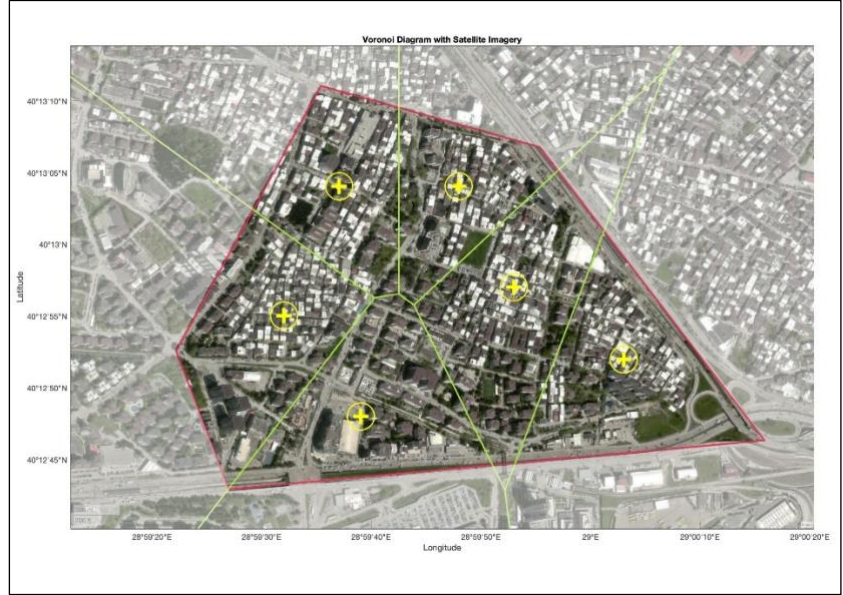
4.3. Mekân Dizimi Yöntemi (Space Syntax Method)

Çalışmada voronoi diyagramlarından elde edilen sonuçların erişilebilirlik parametresiyle ilişkisini test etmek için mekân dizimi analiz tekniğinden faydalanılmıştır. Mekân dizimi yaklaşımında bütünü oluşturan parçalarda meydana gelen bir değişimin bütünün yapısını değiştirdiği öne sürülmektedir. Şehirlerin barındırdığı geometrik düzen sonucu sahip olduğu morfolojik yapı konfigürasyon olarak tanımlanmaktadır. Mekân dizim kuramı, yerleşimlerin konfigürasyonel özelliklerinin

329

Afet Toplanma Alanlarının Belirlenmesinde Voronoi Diyagramları ve Mekân Dizimi Kullanılması: Bursa Karaman Mahallesi Örneği

bireylerin hareketleri, karşılaşmaları ve etkileşimleri üzerinde belirleyici bir etkiye sahip olduğunu öne sürmektedir. Mekân dizimi yaklaşımına göre, mekanların sosyal yapıları ile mekânsal konfigürasyonları arasında karşılıklı bir ilişki bulunmaktadır (Hillier, 2007; Hillier ve Hanson, 1984). Eksensel hat haritaları bir konfigürasyonun analiz edilebilmesi için gerçekleştirilmesi gereken ilk görev olarak tanımlanmaktadır (Oliveira, 2013). Eksensel bir harita oluşturmak için yollar, caddeler ve insanların hareket edebileceği kentsel boşluklar, en uzun görüş ve hareket hatları şeklinde çizilen eksensel çizgilerle modellenmektedir (Van Nes ve Yamu, 2021). Lee vd. (2023) tarafından gerçekleştirilen çalışmada, kentsel ölçekli mekân dizim araştırmalarının büyük çoğunluğunun eksensel hat analiz tekniğinin entegrasyon değerlerinin temel parametre olarak tercih edildiğini vurgulamaktadır. Global entegrasyon analizi, bir caddenin veya sokağın, kentsel sistemdeki diğer tüm cadde ve sokaklara olan erişilebilirlik miktarını nicel olarak ifade etmek için kullanılmaktadır (Hillier, 2007). Yüksek entegrasyon değeri eksensel hattın sistemdeki diğer hatlarla kurduğu ilişkinin kuvvetli olduğunu başka bir deyişle eksensel hattın erişilebilirlik derecesinin yüksek olduğunu ifade etmektedir. Literatürde mekân dizimi erişilebilirlik parametreleriyle insan hareketleri arasındaki paralel ilişkiyi ortaya koyan çalışmalar bulunmaktadır (Chang ve Penn, 1998; Chiu vd., 2020; Colaço ve Silva, 2023; Hillier vd., 1993; Penn vd., 1998). Çalışma kapsamında Karaman mahallesinin fiziksel yapısını ve afet toplanma alanlarının erişilebilirlik derecesini ortaya çıkarmak için mekân dizimi yönteminin entegrasyon parametresinden faydalanılmıştır.

5. BULGULAR VE TARTIŞMA (FINDINGS AND DISCUSSION)

Mahallede mevcutta 3 adet afet toplanma alanı ve 4 adet çadırkent alanı bulunmaktadır. "Erişilebilirlik" ölçütüne göre, 3 alandan da 500 m yarıçapında bir çemberler çizildiğinde bu çemberlerin tüm mahalleyi kapsadığı görülmüştür. Bu durum, yerleşim yerlerinden toplanma alanlarına mesafe açısından erişim kriterinin karşılandığını göstermektedir. "Yol akslarıyla bağlantı" kriteri açısından değerlendirildiğinde, Karaman Dernekler Yerleşkesi ve ilkokulun ana yollarla doğrudan bağlantısının bulunduğu, ancak halı sahanın böyle bir bağlantıya sahip olmadığı tespit edilmiştir. Halı sahanın en yakın ana yola olan mesafesi yaklaşık 100 metre olarak ölçülmüştür. Mülkiyet durumu incelendiğinde, üç alanın da belediye mülkiyetinde olduğu belirlenmiştir. Bu durum, toplanma alanlarının öncelikli olarak kamu

330

JCoDe | Cilt 6 Sayı 2 | Eylül 2025 | Hesaplamalı Tasarımda Tolerans | Özçidem Sümen, G., Alış, İ. Ş., Bostancı, G., Karasu, B. M., Ediz, Ö.

arazileri üzerinde belirlenmesi gerektiği yönündeki kriteri sağlamaktadır. "Kullanılabilirlik ve çok fonksiyonluluk" açısından yapılan incelemede, Karaman Dernekler Yerleşkesi'nin kapalı bir yapıdan oluştuğu ve açık alan içermediği için toplanma alanı olarak uygun olmadığı sonucuna varılmıştır. Buna karşın, ilkokul bahçesinin yaklaşık 3.850 m² büyüklüğünde engelsiz bir açık alan sunduğu ve minimum 500 m² büyüklük şartını sağladığı belirlenmiştir. Halı saha toplanma alanı da benzer şekilde yaklaşık 3.000 m² açık alanıyla minimum büyüklük kriterini karşılamaktadır.

Halı saha ve Canaydın İlköğretim Okulu daha nitelikli toplanma alanları olsa da çalışma kapsamında nüfusun toplanma alanlarında daha dengeli bir şekilde dağılabilmesi ve çadırkent alanları üzerindeki insan yükünün azaltılması için 2 yeni afet toplanma bölgesi önerilmiştir. Bu bölgeler; Selçuk Bahtiyar Parkı ve Seyit Onbaşı Parkı'dır. Üçüncü öneri için en uygun bölge, kuzeyde hem çadırkent hem de afet toplanma alanı olarak kullanılan Karaman Dernekler Yerleşkesi'ne alternatif olabilecek bir afet toplanma alanıdır. Fakat bu alanın halihazırda mezarlık olarak kullanılıyor olması sebebi ile çalışma kapsamına dahil edilmemiştir. Mahallenin bu bölgesindeki sıkışıklığına ve mevcut afet toplanma alanının aynı zamanda çadırkent alanı olarak kullanılmasına rağmen alternatif olarak uygun başka bir alan bulunamamıştır (Şekil 11).

Şekil 11: Mevcut çadırkent alanları kırmızı, mevcut toplanma alanları mavi ve önerilen toplanma alanları sarı renkle gösterilmiştir. (The existing tent city areas are indicated in red, the existing assembly areas in blue, and the proposed assembly areas in yellow.).
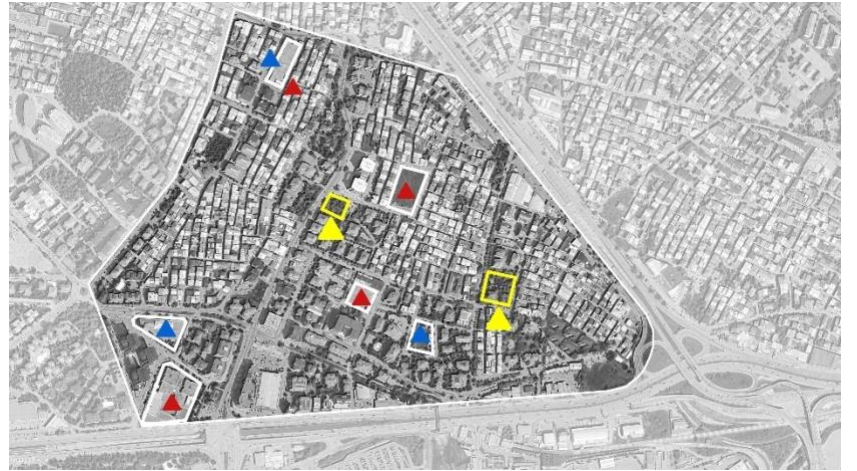
Çalışma kapsamında öncelikle Karaman Mahallesi'nin yoğun nüfus bölgeleri belirlenmiş ve sayısallaştırılmıştır. Bu ayrım, uydu görüntülerinden gözlemlenebilen yapılaşma yoğunluklarına göre yapılmıştır. Ardından, belirlenen bölgelerin tahmini merkez noktaları, koordinat sistemine göre düzenlenerek MATLAB ortamında Voronoi

diyagramlarının oluşturulması için temel veri seti olarak kullanılmıştır. Sonuçta oluşan diyagramdan yola çıkılarak "erişilebilirlik, mülkiyet, ana yollarla bağlantı, kullanılabilirlik ve çok fonksiyonluluk" ölçütleri dikkate alınarak mevcut toplanma alanlarına ek iki yeni toplanma alanı önerilmiştir. Alansal büyüklük kriteri, bölgesel nüfus verilerine ulaşılamadığı için her bir öneri toplanma alanı için değerlendirmeye alınamamıştır.

Voronoi diyagramı her hücrenin çekirdeğinden ortalama 500 m uzaklık mesafesindeki noktalarla oluşturulmuş ve çalışma alanını altı hücreye bölmüştür. Bir sınır çizgisini paylaşan iki hücrenin çekirdekleri bu sınır çizgisine aynı mesafede olmaktadır. Bu sayede sınır çizgilerinin üzerinde veya yakın alanlarında belirlenen yeni toplanma alanları her komşu bölgeye eşit mesafede yer alır. Aynı zamanda hücre içerisinde herhangi bir noktadan belirlenen toplanma alanlarına olan uzaklık 500 m'yi aşmamaktadır (Şekil 12).
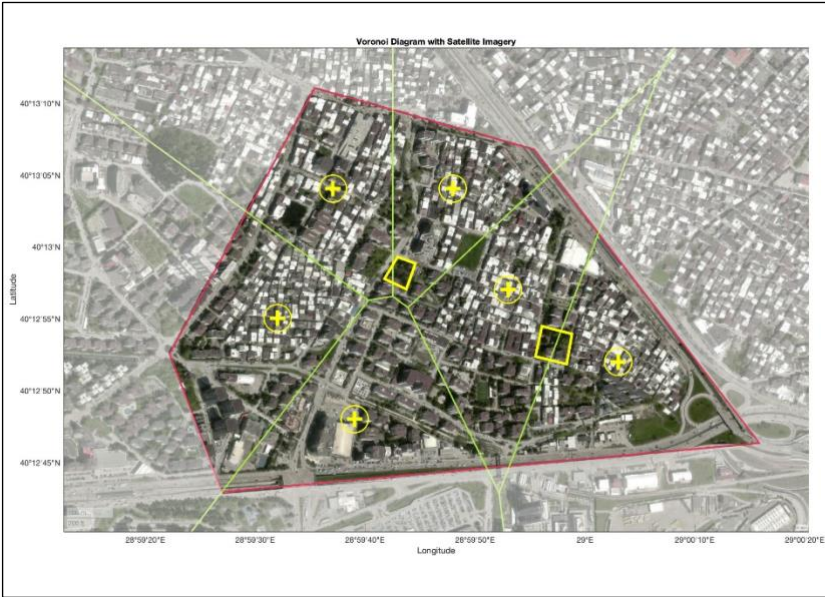
Şekil 12: Voronoi diyagramı ve önerilen toplanma alanları (Voronoi diagram and proposed assembly areas).

Belirlenen toplanma alanlarından ilki olan Selçuk Bahtiyar Parkı, voronoi diyagramında oluşan 5 hücrenin sınır çizgilerinin yakınında yer alması ve 5 hücreye de tek bir noktadan hizmet verebilecek olması sebebiyle önerilmiştir. Kamu mülkiyetinde bulunan alanın, Kükürtlü Caddesi ile doğrudan bağlantısı bulunmakta olup büyüklüğü 1540 m²'dir. Ayrıca, bu alanın belirlenmesinde etkili olan bir diğer faktör, parka yaklaşık 100'er metre mesafelerde bulunan ve Nilüfer Belediyesi tarafından belirlenen çadır kent alanlarıdır. Önerilen afet toplanma alanının, çadır kent

332

JCoDe | Cilt 6 Sayı 2 | Eylül 2025 | Hesaplamalı Tasarımda Tolerans | Özçidem Sümen, G., Alış, İ. Ş., Bostancı, G., Karasu, B. M., Ediz, Ö.

kurulması planlanan bölgelerin insan yükünü azaltma potansiyeline sahip olduğu düşünülmüştür.

(Şekil 13).

Şekil 13: Öneri afet toplanma alanı - Selçuk Bahtiyar Parkı
(Proposed disaster assembly area - Selçuk Bahtiyar Park)
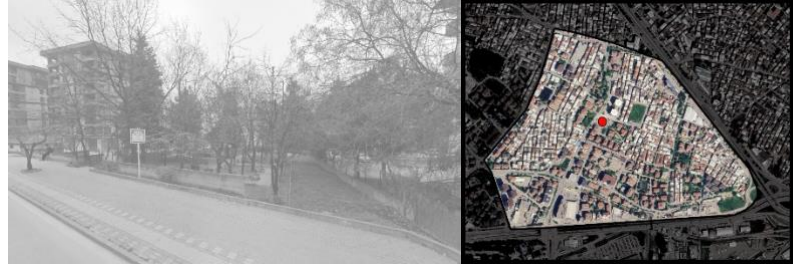
İkinci olarak belirlenen Seyit Onbaşı Parkı, voronoi diyagramına göre iki komşu hücrenin sınır çizgisi üzerinde yer alması ve iki hücre çekirdeğine eşit mesafede olması sebebiyle seçilmiştir **(Şekil 14).** Kamu mülkiyetinde olan park, Gürbüzler Caddesi ile doğrudan bağlantılıdır. İçerisinde tek katlı Karaman Sağlık Merkezi binası bulunsa da açık alanın büyüklüğü yaklaşık 850 m²'dir. Ayrıca, mevcut çadır kent alanlarına ortalama 250 metre mesafede yer alması, bu alanın seçiminde önemli bir kriter olmuştur. Bu alan seçilirken dikkat edilen diğer bir etken de İzmir yolu üzerinde bulunan benzin istasyonları olmuştur. Bu istasyonların varlığı olası bir depremde tehlike arz etmektedir. Bu sebeple önerilen toplanma alanının benzin istasyonları ile arasındaki mesafe göz önünde bulundurulmuştur.

Şekil 14: Öneri afet toplanma alanı – Seyit Onbaşı Parkı
(Proposed disaster assembly area – Seyit Onbaşı Park)

Çalışma kapsamında oluşturulan eksensel harita DepthmapX yazılımı aracılığıyla işlenerek sayısal veriler ve kırmızıdan maviye giden renk paletiyle temsil edilen grafik ifadesi elde edilmiştir **(Şekil 15).** Sıcak renkler (kırmızı, turuncu) daha yüksek değerleri ifade ederken soğuk renkler (mavi) ise düşük değerleri temsil etmektedir.

Eksensel hat haritasında en yüksek değerler "Y" ile belirtilmiştir. Karaman mahallesinin erişilebilirlik durumunun mevcut ve önerilen toplanma alanlarıyla ilişkisi **Şekil 15**'te gösterilmiştir. En yüksek değeri temsil eden Y1 eksensel hattı 2.29 entegrasyon değerine sahiptir. Bu hat ile ikinci en yüksek değer olan Y2 hattının kesişiminde önerilen ilk toplanma alanı (Ö1) yer almaktadır. Bu alan mahallenin topolojik merkezine yakın konumlanmasının yanı sıra voronoi diyagramlarında da nüfus ayrışma bölgelerinin sınırı olabilecek bir konumda yer almaktadır. Erişilebilir eksensel hatlar tarafından çevrelenmesi ve topolojik konumu Ö1 toplanma alanını olası bir afet durumunda kullanılması oldukça muhtemel bir alan haline getirmektedir.

Mevcut ikinci toplanma alanı (M2) yüksek entegrasyon değerine sahip hatlarla doğrudan ilişki kurmamasına rağmen en yüksek 3 erişilebilirlik değerine sahip hattın merkezinde konumlanmaktadır. Önerilen ikinci toplanma alanı (Ö2) en yüksek üçüncü entegrasyon değerine sahip hattın üzerinde yer almaktadır. Bu hattın yakın çevresinde ayrıca yüksek entegrasyon değerine sahip hatlar yer almaktadır. Mahallenin güney-batısında yer alan ilk toplanma alanının (M1), çevresinde ortalama üzerinde erişilebilirliğe sahip eksensel yollar bulunmaktadır. Mahallenin kuzey-batısında yer alan üçüncü toplanma alanı (M3) ise erişilebilirlik değeri oldukça düşük eksenel hatlarla çevrelenmiş bir konumdadır (**Şekil 15**). Mekân dizimi yönteminin erişilebilirlik parametresi verileri

334

JCoDe | Cilt 6 Sayı 2 | Eylül 2025 | Hesaplamalı Tasarımda Tolerans | Özçidem Sümen, G., Alış, İ. Ş., Bostancı, G., Karasu, B. M., Ediz, Ö.

değerlendirildiğinde önerilen toplanma alanlarının, mevcut toplanma alanlarından daha erişilebilir konumlarda bulunduğu gözlemlenmiştir. Çalışma kapsamında kentsel biçimlerin potansiyellerini ortaya koymaya yarayan hesaplamalı analiz yöntemlerinden voronoi diyagramları (Nowak, 2015) ve mekân dizimi (Hillier, 2007) yöntemi bir arada kullanılmıştır. Literatürde voronoi diyagramlarının afet toplanma alanlarının optimizasyonu ve erişilebilirlik değerlendirmelerinde kullanıldığı çalışmalar mevcuttur (Aurenhammer, 1991; Okabe vd., 2000). Fakat çalışma kapsamında önerilen voronoi diyagramları ve mekân dizimi yöntemlerinin bir arada kullanıldığı çalışmalara nadir rastlanmaktadır. Bu yöntemlerin toplanma alanlarının belirlenmesi ve belirlenen alanların erişilebilirlik derecelerinin test edilmesi amacıyla bir arada kullanımı çalışmanın özgün yönünü oluşturmaktadır. Voronoi diyagramları aracılığıyla "erişilebilirlik, ana yollarla bağlantı, mülkiyet durumu, kullanılabilirlik ve çok fonksiyonluluk" kriterleri dikkate alınarak Karaman mahallesi sınırlarında yer alan mevcut toplanma alanlarına ek iki yeni toplanma alanı önerilmiştir. Önerilen Selçuk Bahtiyar Parkı ve Seyit Onbaşı Parkı'nın mahalle ölçeğinde yapılan analizleri sonucu erişilebilirlik değerleri en yüksek eksensel hatlarla komşu oldukları gösterilmiştir (Şekil 15). Çalışma kapsamında afet toplanma alanlarının belirlenmesinde farklı hesaplamalı yöntemlerin birlikte kullanımının pozitif etkileri gösterilmiştir. Kentlerin sahip olduğu geometrik potansiyellerin ortaya koyulması amacıyla hesaplamalı yöntemlerden faydalanmanın, afet yönetim süreçlerini rasyonel bir alt yapıya dayandırmak için etkili bir araç olabileceği çalışma kapsamında ortaya koyulmuştur.

Özellikle 65 yaş üstü nüfus gibi dezavantajlı grupların afet durumlarında toplanma alanlarına erişimi büyük önem taşımaktadır. Yapılan analizler, önerilen yeni toplanma alanlarının mevcut alanlara kıyasla yaşlı nüfusun erişimini önemli ölçüde iyileştirdiğini göstermektedir. Örneğin, yüksek katlı ve yoğun yapılaşmanın olduğu bölgelerde, önerilen alanların daha merkezi ve erişilebilir konumlarda belirlenmesi, yaşlıların afet anında daha hızlı ve güvenli bir şekilde ulaşımını sağlamaktadır. Bu bulgular, özellikle kentsel alanlarda afet planlamasında dezavantajlı grupların ihtiyaçlarının daha etkin bir şekilde karşılanabileceğini ortaya koymaktadır. Çalışma kapsamında elde edilen sonuçların pratikte uygulanabilirliği ve yerel yönetimlerin bu alanları nasıl entegre edeceği gibi konuların gelecek çalışmalarda detaylı olarak incelenmesi önerilmektedir.

335

Afet Toplanma Alanlarının Belirlenmesinde Voronoi Diyagramları ve Mekân Dizimi Kullanılması: Bursa Karaman Mahallesi Örneği

6. SONUÇ (CONCLUSION)

Bu çalışmada, Bursa ili Karaman Mahallesi sınırlarında yer alan mevcut afet toplanma alanlarının konumları nicel yöntemler kullanılarak değerlendirilmiş ve olası afet durumunda nüfus ve erişilebilirlik verilerine dayanarak alternatif toplanma alanları önerilmiştir. Alternatif toplanma alanları önerilirken voronoi diyagramları ve mekân dizimi yönteminin erişilebilirlik parametresi bir arada kullanılarak afet toplanma alanlarının belirlenmesinde çok yönlü bir değerlendirme modeli önerilmiştir. Elde edilen bulgular, Karaman Mahallesi'nde mevcut afet toplanma alanlarının bir kısmının nüfus yoğunluğu ve erişilebilirlik açısından yetersiz olduğunu göstermektedir. Özellikle, mevcut alanların nüfus yoğunluğuna göre erişim mesafelerinin eşit bir dağılıma sahip olmadığı ve bazı yoğun nüfuslu bölgelerin toplanma alanlarının erişimde dezavantajlı olduğu tespit edilmiştir.

Bu çalışma kapsamında, alternatif afet toplanma alanlarının belirlenmesi için voronoi diyagramları ve belirtilen kriterler kullanılarak Selçuk Bahtiyar Parkı ve Seyit Onbaşı Parkı'nın uygun toplanma alanları olarak seçilmesi önerilmiştir. Mekân dizimi yönteminin entegrasyon parametresi kullanılarak yapılan analizler, belirlenen alanların Karaman mahallesi içindeki en erişilebilir eksensel hatlarla bağlantılı olduğunu ortaya koymuştur. Bu bulgular, söz konusu parkların afet durumlarında hızlı ve etkili bir şekilde erişilebilir olması açısından stratejik öneme sahip olduğunu göstermektedir. Alternatif toplanma alanları önerilirken voronoi diyagramları ve mekân dizimi yönteminin erişilebilirlik parametresi bir arada kullanılarak afet toplanma alanlarının belirlenmesinde çok yönlü bir değerlendirme modeli önerilmiştir. Çalışma, afet yönetimi planlamasında mekânsal analiz yöntemlerinin birlikte kullanımının önemini vurgulamakta ve benzer çalışmalar için bir metodolojik çerçeve sunmaktadır. Önerilen değerlendirme modeli, yalnızca Karaman Mahallesi ile sınırlı kalmamakta, farklı kentsel bağlamlarda da uygulanabilir bir yöntem sunmaktadır. Gelecekteki araştırmalarda, benzer yöntemlerin daha geniş ölçekli analizlerde kullanılmasının, afet yönetimi, kentsel dönüşüm ve planlama süreçlerine önemli bir katkı sağlayacağı düşünülmektedir.

336

JCoDe | Cilt 6 Sayı 2 | Eylül 2025 | Hesaplamalı Tasarımda Tolerans | Özçidem Sümen, G., Alış, İ. Ş., Bostancı, G., Karasu, B. M., Ediz, Ö.

Referanslar (References)

Afet ve Acil Durum Yönetimi Başkanlığı. (2014). *TAMP Türkiye Afet Müdahale Planı*. Afet ve Acil Durum Yönetimi Başkanlığı. https://www.afad.gov.tr/turkiye-afet-mudahale-plani

Aksoy, Y., Turan, A.Y. & Atalay, H. (2009). İstanbul Fatih İlçesi Yeşil Alan Yeterliliğinin Marmara Depremi Öncesi ve Sonrası Değerleri Kullanılarak İncelenmesi, *Uludağ Üniversitesi Mühendislik-Mimarlık Fakültesi Dergisi*, 14(2), 137-150. https://doi.org/10.17482/uujfe.30331

Akyol, N., Akıncı, A., & Eyidoğan, H. (2002). Site amplification of S-waves in Bursa City and its vicinity, Northwestern Turkey: Comparison of Different Approaches. *Soil Dynamics and Earthquake Engineering*, 22(7), 579-587. https://doi.org/10.1016/S0267-7261(02)00030-1

Alexander, D. (2002). *Principles of emergency planning and management.* Terra Publishing.

Aurenhammer, F. (1991). Voronoi diagrams—A survey of a fundamental geometric data structure. *ACM Computing Surveys (CSUR),* 23(3), 345-405. https://doi.org/10.1145/116873.116880

Aurenhammer, F., & Klein, R. (2000). Voronoi diagrams. In J. R. Sack, & J. Urrutia (Eds.), *Handbook of Computatioal Geometry* (201-290). North-Holland Publ Co. https://doi.org/10.1016/B978-0-444-82537-7.X5000-1

Chang, D. & Penn, A. (1998). Integrated Multilevel Circulation in Dense Urban Areas: The Effect of Multiple Interacting Constraints on the Use of Complex Urban Areas. *Environment and Planning B: Planning and Design*, 25(4), 507-538. https://doi.org/10.1068/b250507

337

Afet Toplanma Alanlarının Belirlenmesinde Voronoi Diyagramları ve Mekân Dizimi Kullanılması: Bursa Karaman Mahallesi Örneği

Chiu, Y.-H., Chuang, I.-T., & Tsai, C.-Y. (2020). Analyzing correlation of urban functionality and spatial configuration. *Environment and Planning B: Urban Analytics and City Science*, 0(11), 1-18. https://doi.org/10.1177/2399808320924673

Colaço, R. & Silva, J. d. (2023). Exploring the role of accessibility in shaping retail location using space syntax measures: A panel-data analysis in Lisbon, 1995–2010. *Environment and Planning B: Urban Analytics and City Science*, 50(5), 1345-1360. https://doi.org/10.1177/23998083221138570

Cutter, S. L. (2003). The vulnerability of science and the science of vulnerability. *Annals of the Association of American Geographers*, 93(1), 1-12. https://doi.org/10.1111/1467-8306.93101

Davis, D. (2013). *Modelled on software engineering: Flexible parametric models in the practice of architecture*. [Doctoral dissertation, RMIT University].https://www.danieldavis.com/papers/danieldavis_thesis.pdf

Ediz, Ö. M., Erbil, Y., & Akıncıtürk, E. N. (2010). Günümüz mimarlığının dinamikleri Iceberg in görünmeyen yüzü. *Mimarlık*, 47(354), 49-52. http://www.mimarlikdergisi.com/index.cfm?sayfa=mimarlik&DergiSayi=368&RecID=2438

Hillier, B. & Hanson, J. (1984). *The social logic of space*. Cambridge University Press. https://doi.org/10.1017/CBO9780511597237

Hillier, B., Penn, A., Hanson, J., Grajewski, T., & Xu, J. (1993). Natural movement: Or, configuration and attraction in urban pedestrian movement. *Environment & Planning B: Planning & Design*, 20, 29–66. https://doi.org/10.5694/j.1326-5377.1963.tb26584.x

Hillier, B. (2007). *Space is the machine: a configurational theory of architecture*. Space Syntax.

Japonya Uluslararası İş birliği Ajansı & İstanbul Büyükşehir Belediyesi (2002). *Türkiye Cumhuriyeti İstanbul İli Sismik Mikro-Bölgeleme Dahil Afet Önleme/Azaltma Temel Planı Çalışması Son Rapor Cilt V.* https://depremzemin.ibb.istanbul/uploads/prefix-jica-turkce-raporu-66a39c6e9b70d.pdf

Kaplanoğlu, R. (2016, Nisan 4). *Karamanköy Mahallesi*. Turkhaber.com.https://www.turkhaber.com/wiki/Karamankoy_Mahallesi-4492.html

Karimi, K. (2012). A configurational approach to analytical urban design: 'Space syntax' methodology. *Urban Design International*, 17(4), 297-318. https://doi.org/10.1057/udi.2012.19

Lee, J. H., Ostwald, M. J., & Zhou, L. (2023). Socio-Spatial Experience in Space Syntax Research: A PRISMA-Compliant Review. *Buildings*, 13(3), 644. https://doi.org/10.3390/buildings13030644

338

JCoDe | Cilt 6 Sayı 2 | Eylül 2025 | Hesaplamalı Tasarımda Tolerans | Özçidem Sümen, G., Alış, İ. Ş., Bostancı, G., Karasu, B. M., Ediz, Ö.

Nowak, A. (2015). Application of Voronoi diagrams in contemporary architecture and town planning. *Challenges of Modern Technology,6.*

Okabe, A., Boots, B., Sugihara, K., & Chiu, S. N. (2000). *Spatial tessellations: Concepts and applications of Voronoi diagrams*. Wiley. DOI:10.1002/9780470317013

Oliveira, V. (2013). Morpho: a methodology for assessing urban form. *Urban Morphology*, 17(1), 21–33. https://doi.org/10.51347/jum.v17i1.2885

Özcan, B. (2010). Bursa Depremleri (2 Mart - 12 Nisan 1855). *Güzel Sanatlar Enstitüsü Dergisi*, (5).

Penn, A., Hillier, B., Banister, D., & Xu, J. (1998). Configurational modelling of urban movement networks. *Environment and Planning B: Planning and Design*, 25(1), 59–84. https://doi.org/10.1068/b250059

Salt Research, Mühendishane-i Hümayun Archive. (1862). Retrieved January 5, 2025, from Salt Research: https://archives.saltresearch.org/handle/123456789/122041

Tabban, A. (2000). *Kentlerin Jeolojisi ve Deprem Durumu*. TMMOB Jeoloji Mühendisleri Odası.

Tarabanis, K. & Tsionas, I. (1999). Using network analysis for emergency planning in case of earthquake. *Transactions in GIS*, 3(2), 187–197. https://doi.org/10.1111/1467-9671.00015

Van Nes, A. & Yamu, C. (2021). *Introduction to Space Syntax in Urban Studies.* Springer International Publishing.

Uyanık, O. (2006). Sıvılaşır ya da Sıvılaşmaz Zeminlerin Yinelemeli Gerilme Oranına bir Seçenek. *Dokuz Eylül Üniversitesi Fen ve Mühendislik Dergisi*, 8(2), 79-91.

339

Afet Toplanma Alanlarının Belirlenmesinde Voronoi Diyagramları ve Mekân Dizimi Kullanılması: Bursa Karaman Mahallesi Örneği

340

JCoDe | Cilt 6 Sayı 2 | Eylül 2025 | Hesaplamalı Tasarımda Tolerans | Özçidem Sümen, G., Alış, İ. Ş., Bostancı, G., Karasu, B. M., Ediz, Ö.

Predicting Air Quality in İzmir Using Artificial Intelligence and IoT

Kübra Öztürk[1], Zuhal Can[2]

ORCID NO: 0009-0003-4368-9274, 0000-0002-6801-1334

[1] Eskişehir Osmangazi University, Faculty of Engineering and Architecture, Department of Computer Engineering, Eskişehir, Türkiye
[2] Eskişehir Osmangazi University, Faculty of Engineering and Architecture, Department of Computer Engineering, Eskişehir, Türkiye

Air pollution is a significant concern in Izmir, the third-largest city in Türkiye, with adverse impacts on public health and urban quality of life. Leveraging Internet of Things (IoT) monitoring, this study forecasts PM_{10} and SO_2 using machine learning, deep learning, and time-series models over 1996-2024. Our main contribution is a controlled, city-scale evaluation that isolates the role of extreme-value handling by creating three preprocessing variants for each pollutant (keep, cap, remove) and benchmarking four model families (SARIMA, SVR, LSTM, xLSTM) under a leakage-free, time-ordered train/validation/test protocol. To our knowledge, this is the first Izmir study that quantifies how peak treatment interacts with model choice to affect forecast accuracy, and that reports results in a way that directly supports operational planning. Results show that for PM_{10}, SARIMA often attains the lowest errors when peaks are capped or removed, while xLSTM provides competitive accuracy across all strategies. For SO_2, xLSTM consistently outperforms traditional methods under capped and kept conditions, yielding lower errors and higher explanatory power. By combining IoT-based monitoring with a rigorous modeling method and explicit sensitivity to peak processing, the study offers actionable guidance for air-quality management, informing traffic control, industrial regulation, and urban design decisions in Izmir.

341

JCoDe | Vol 6 No 2 | September 2025 | Tolerance in Computational Design| Öztürk, K., Can, Z.

Yapay Zeka ve IoT Kullanarak İzmir'deki Hava Kalitesinin Tahmini

Kübra Öztürk[1], Zuhal Can[2]

ORCID NO: 0009-0003-4368-9274, 0000-0002-6801-1334

[1] Eskişehir Osmangazi Üniversitesi, Mühendislik ve Mimarlık Fakültesi, Bilgisayar Mühendisliği Bölümü, Eskişehir, Türkiye
[2] Eskişehir Osmangazi Üniversitesi, Mühendislik ve Mimarlık Fakültesi, Bilgisayar Mühendisliği Bölümü, Eskişehir, Türkiye

Türkiye'nin üçüncü büyük şehri İzmir'de hava kirliliği, halk sağlığı ve kentsel yaşam kalitesi üzerinde olumsuz etkileri olan önemli bir endişe kaynağıdır. Nesnelerin İnterneti (IoT) izlemeyi kullanan bu çalışma, makine öğrenimi, derin öğrenme ve zaman serisi modelleri kullanarak 1996-2024 yılları arasında PM_{10} ve SO_2'yi tahmin etmektedir. Ana katkımız, her bir kirletici için üç ön işleme varyantı oluşturarak (tut, sınırla, kaldır) ve sızıntısız, zaman sıralı bir eğitim/doğrulama/test protokolü altında dört model ailesini (SARIMA, SVR, LSTM, xLSTM) kıyaslayarak aşırı değer işleme rolünü izole eden kontrollü, şehir ölçeğinde bir değerlendirmedir. Bilgimize göre, bu, tepe işleminin tahmin doğruluğunu etkilemek için model seçimiyle nasıl etkileşime girdiğini ölçen ve sonuçları doğrudan operasyonel planlamayı destekleyecek şekilde raporlayan ilk İzmir çalışmasıdır. Sonuçlar, PM_{10} için SARIMA'nın, tepe noktaları sınırlandırıldığında veya kaldırıldığında genellikle en düşük hatalara ulaştığını, xLSTM'nin ise tüm stratejilerde rekabetçi doğruluk sağladığını göstermektedir. SO_2 için ise xLSTM, sınırlandırılmış ve sabitlenmiş koşullar altında geleneksel yöntemlerden sürekli olarak daha iyi performans göstererek daha düşük hatalar ve daha yüksek açıklama gücü sağlamaktadır. IoT tabanlı izlemeyi titiz bir modelleme metodu ve tepe noktası işlemeye açık duyarlılıkla birleştiren çalışma, İzmir'de hava kalitesi yönetimi, trafik kontrolü, endüstriyel düzenlemeler ve kentsel tasarım kararlarına bilgi sağlamak için uygulanabilir rehberlik sunmaktadır.

342

JCoDe | Cilt 6 Sayı 2 | Eylül 2025 | Hesaplamalı Tasarımda Tolerans | Öztürk, K., Can, Z.

1. INTRODUCTION

Air pollution is a critical issue in urban environments, significantly affecting human health and the ecosystem. Izmir, the third-largest city in Türkiye, faces recurring air quality challenges, primarily due to industrial activities, dense traffic, and seasonal meteorological patterns that can exacerbate pollutant accumulation. Addressing these challenges is essential to safeguard public health and ensure a sustainable environment.

This study develops a city-scale forecasting workflow for İzmir using a combination of machine learning, deep learning, and time series analysis methods. Unlike prior works that focused solely on raw historical values, this study systematically incorporates extreme-value handling into the predictive workflow, creating three separate versions of each pollutant series, keep, cap, and remove, to assess how different preprocessing strategies influence model performance. By analyzing historical air quality data, the study seeks to provide valuable insights that can help public health authorities and policymakers mitigate potential risks. The findings can inform strategies such as traffic management and industrial regulation, improving air quality, and ensuring compliance with environmental standards.

The integration of IoT and artificial intelligence (AI) into air quality forecasting offers significant advantages in the design and implementation of environmental management systems. IoT-based sensor networks enable real-time, high-resolution monitoring of pollutant levels, while AI-driven models can process this continuous data stream to produce accurate and timely forecasts. Embedding these predictive capabilities into urban planning workflows allows decision-makers to proactively address emerging air quality issues, such as by adjusting traffic flows, optimizing industrial operations, or issuing early health advisories, before critical thresholds are exceeded.

In addition, coupling IoT infrastructure with AI forecasting models facilitates adaptive policy-making. For example, predictive alerts generated by AI can be integrated with smart city control systems to automatically trigger mitigation measures, such as activating air filtration in public spaces or modifying public transportation schedules. This real-time, feedback-driven approach not only improves response

speed but also helps optimize resource allocation, ultimately contributing to healthier and more sustainable urban environments.

Beyond short-term interventions, accurate air quality forecasts can also shape long-term urban design and planning decisions. Predictive insights can guide optimal building placement to minimize exposure in high-pollution corridors, inform the strategic allocation of green spaces to enhance natural air filtration, and support the development of sustainable architecture that incorporates passive ventilation and pollutant-shielding designs. By integrating forecasting data into master planning processes, cities can proactively design neighborhoods that balance density with environmental health considerations.

Furthermore, urban planners can leverage AI-driven air quality projections to evaluate the long-term impact of infrastructure projects, ensuring that new developments do not exacerbate pollution hotspots. This integration of environmental forecasting into architectural and landscape planning supports the creation of resilient, climate-adaptive, and livable urban spaces that protect public health while advancing sustainability goals.

The dataset utilized in this study includes air quality measurements for PM_{10} and SO_2, collected from 1996 to 2024 through IoT sensors. These measurements, sourced from the National Smart City Open Data Platform (Ulusav) and the Izmir Metropolitan Municipality, provide a comprehensive view of the air quality across multiple monitoring stations in Izmir. Monthly observations were aggregated into pollutant-specific time series for each preprocessing strategy, with temporal splits applied strictly in chronological order to avoid data leakage.

To predict future air pollution levels, the study employs four models: Support Vector Regression (SVR), Seasonal Autoregressive Integrated Moving Average (SARIMA), Long Short-Term Memory (LSTM), and Extended Long-Term Memory (xLSTM). The xLSTM architecture enhances LSTM by incorporating extended memory connections and adaptive gating mechanisms, improving its capacity to capture long-term dependencies in air quality trends. These models are evaluated using key performance metrics, including Mean Absolute Error (MAE), Mean Squared Error (MSE), Root Mean Squared Error (RMSE), and R^2 Score.

344

JCoDe | Vol 6 No 2 | September 2025 | Tolerance in Computational Design| Öztürk, K., Can, Z.

The results reveal that model performance varies by pollutant and preprocessing strategy. For PM_{10}, SARIMA often achieves the lowest errors under capped and removed peaks, whereas xLSTM delivers comparable accuracy with greater adaptability across strategies. For SO_2, xLSTM consistently outperforms traditional methods, particularly under capped and kept conditions, achieving lower error metrics and higher explanatory power. These findings underscore the potential of advanced machine learning models, especially xLSTM, in forecasting air quality and contributing to better environmental management in urban settings.

1.1. Contributions to Planning and Architectural Design

Beyond forecasting, we explicitly translate model outputs into design- and planning-ready artifacts and workflows. (i) Design-relevant framing: By testing three peak-handling policies (keep/cap/remove) across four model families, we treat outlier processing as a planning lever, showing how alternative regulatory and operational choices for peaks change forecast fidelity and, consequently, recommended interventions. (ii) Actionable products: We derive monthly risk bands with uncertainty envelopes and convert them into trigger-action rules for practice (e.g., adjusting street-canyon permeability and block porosity, temporally reallocating traffic/freight, or prioritizing green/blue infrastructure where dispersion is favored). (iii) Multi-scale guidance: We link forecast bands to block- and building-scale decisions, such as ventilation and filtration scheduling, façade/atrium strategies along high-exposure corridors, and the micro-siting of sensitive receptors (schools/clinics) to minimize long-term exposure. (iv) Toolchain integration and reproducibility: We provide a leakage-free, city-scale workflow that municipalities can embed into GIS dashboards and scenario planning to test design options under different peak policies and seasonal regimes. (v) Sustainability integration: Aligning ventilation/filtration duty cycles, traffic operations, and the siting and maintenance of green/blue infrastructure with forecasted exposure patterns delivers equal-or-greater air-quality benefits at lower energy and material intensity than uniform, calendar-based interventions; it also yields co-benefits such as reduced greenhouse-gas emissions (via demand-controlled ventilation and freight retiming) and mitigates maladaptation risks (e.g., over-canopying in narrow street canyons). Equity is addressed by prioritizing sensitive receptors using banded

forecasts. The artifacts align with municipal monitoring and verification cycles, supporting cost-effectiveness tracking (e.g., kWh saved, avoided vehicle-kilometers, filter-lifetime extension, and person-exposure-hours reduced).

2. LITERATURE REVIEW

In recent years, the integration of Internet-of-Things (IoT) technology into environmental-monitoring systems has gained significant attention. Researchers have developed a variety of IoT-based platforms to capture weather conditions and air-quality dynamics with high temporal resolution. Bernardes et al. (Bernardes et al., 2023) proposed a low-cost automated weather station for disaster monitoring, while Woo et al. (Woo et al., 2023) released WeatherChimes, an open-hardware package giving near-real-time access to on-site sensor data. Bolla et al. (Bolla et al., 2022) highlighted the importance of a robust IoT framework for efficient data collection, and Elbasi et al. (Elbasi et al., 2023) reviewed AI-enabled sensing networks for crops and leak detection. Singh et al. (Singh et al., 2022) demonstrated an intelligent irrigation system that responds adaptively to soil and weather inputs.

IoT innovation continues to expand. Ioannou et al. (Ioannou et al., 2021) combined wireless technologies and ARM-SoC to create a multi-purpose device, whereas Mabrouki et al. (Mabrouki et al., 2021) delivered a real-time climate platform. Ambildhuke and Banik (Ambildhuke & Banik, 2022) applied deep learning to a portable precipitation-forecasting device, and Karvelis et al. (Karvelis et al., 2020) offered an on-board solution for real-time weather prediction. Efforts to optimise energy consumption in remote stations include Leelavinodhan et al. (Leelavinodhan et al., 2021) and Mehmood et al. (Mehmood et al., 2023), while Lu et al. (Lu et al., 2023) introduced ThunderLock, a dual-microphone lightning localisation system.

Complementary work has explored data-fusion and hybrid-modelling strategies. Nie et al. (Nie et al., 2012) combined ARIMA and SVM for short-term load forecasting, Mohapatra and Subudhi (Mohapatra & Subudhi, 2022) demonstrated embedded data-collection modules, and Kaya et al. (Kaya et al., 2023) benchmarked anomaly-detection algorithms. Suresh et al. (Suresh et al., 2022) attained high F1-scores for IoT-driven irrigation. Jamil et al. (Jamil et al., 2021) presented a big-

346

JCoDe | Vol 6 No 2 | September 2025 | Tolerance in Computational Design| Öztürk, K., Can, Z.

data architecture for streaming IoT flows, Albuali et al. (Albuali et al., 2023) integrated machine-learning with automated weather stations, and Tsalikidis et al. (Tsalikidis et al., 2024) compared classical and deep models for traffic prediction under varying meteorology.

Deep-learning approaches now dominate many environmental-forecasting tasks. Yang et al. (Yang et al., 2022) fused dense vehicular IoT data with neural networks for city-scale PM-prediction; Yu et al. (Yu et al., 2021) combined LSTM with long-term meteorological archives for temperature forecasts. Roy (Roy, 2020) showed that hybrid CNN + LSTM structures boost horizon length, while Elsaraiti and Merabet (Elsaraiti & Merabet, 2021), Geng et al. (Geng et al., 2020), Atali et al. (Atali et al., 2022) and Aydin et al. (Aydin et al., 2021) documented performance gains for wind-speed and PM_{10} series.

Crucially, recent scholarship has begun to translate these sensing-and-forecasting advances into architectural and urban-planning practice. Bansal and Quan (Bansal & Quan, 2024) employed explainable machine learning on 1.4 million parcels to show how block geometry modulates heat-island intensity across Seoul, offering planners data-driven guidance on reflectivity and porosity. Synthesis papers on green infrastructure further warn that vegetative interventions may trap pollutants in narrow canyons if used indiscriminately, whereas carefully sited barriers and corridors can reduce near-road exposure (Vos et al., 2013), (Abhijith et al., 2017). These architecture- and planning-oriented studies bridge measurement, simulation, and design decision-making, providing pathways to couple forecasting outputs with street-canyon permeability, green/blue-infrastructure siting, and building-scale ventilation/filtration schedules within GIS-supported scenario workflows.

Recent work at the intersection of AI, urban form and sustainability further demonstrates design uptake. Patel et al. (Patel et al., 2023) linked deep-learning-derived morphology metrics to dispersion models. Wu et al. (Wu et al., 2023) applied GIS-CFD coupling for canyon ventilation. Multi-scale land-use regression by Wang et al. (Wang et al., 2024) connects neighbourhood density, greenery and $PM_{2.5}$ gradients, while Venter et al. (Venter et al., 2024) caution that indiscriminate greening can intensify street-level PM under calm conditions.

These studies collectively demonstrate not only the technical maturation of IoT-centric environmental monitoring and predictive modelling, but an emerging evidence base that positions air-quality data as a design lever in architecture and urban planning, linking sensor insight to façade tactics, corridor porosity, traffic orchestration and green-infrastructure siting in pursuit of healthier, more sustainable cities.

3. METHOD

The aim of this study is to carry out a local study with the air quality data of Izmir province, the third largest city of Turkey, and to make predictions about air quality for the future. The potential impact is significant, as it can alert health institutions and public-health authorities to possible risks, inform policies such as traffic management or regulation of industrial activities, and support industrial facilities or commercial enterprises in ensuring compliance with environmental regulations by reducing emissions under identified meteorological conditions.

3.1. Dataset

This study uses monthly air-quality observations for İzmir, Türkiye, spanning 1996-2024, compiled from the National Smart City Open Data Platform and the İzmir Metropolitan Municipality (İzmir Büyükşehir Belediyesi, 2024). The raw file may appear in a "long" layout, with columns equivalent to a date, a pollutant identifier, and a numeric measurement, or in a "wide" layout with pollutant names as columns (e.g., PM_{10}, SO_2). A schema-inference routine first normalizes header strings and detects the date and value fields. For long-format data, the pollutant identifier is mapped to pollutant names using {1: PM_{10}, 2: SO_2}, and the numeric measurement column is used directly as the measurement; for wide-format data, the columns labelled (or normalized to) PM_{10} and SO_2 are taken directly. Dates are parsed to a monthly index at month start (MS), rows with invalid dates are discarded, and the series are sorted chronologically. Where multiple stations or regions exist, measurements are aggregated by the monthly mean to obtain a single univariate series per pollutant. The resulting PM_{10} and SO_2 series are resampled onto a regular monthly grid; if a series contains fewer than 60 monthly points, it is excluded to preserve a meaningful temporal split.

348

JCoDe | Vol 6 No 2 | September 2025 | Tolerance in Computational Design| Öztürk, K., Can, Z.

To systematically assess the impact of extreme values, peak handling was incorporated as a controlled preprocessing factor rather than a one-off cleaning step. For each pollutant, three parallel versions of the monthly time series were generated. The first version ("keep") retained the original values without modification. The second version ("cap") applied winsorization based on Tukey's method (Tukey & others, 1977), which identifies potential outliers as observations lying more than 1.5 times the interquartile range (IQR) below the first quartile (Q_1) or above the third quartile (Q_3). The 1.5×IQR threshold is a conventional choice in statistical analysis because it offers a balanced compromise, sufficiently wide to avoid labeling normal variability as an outlier, yet narrow enough to capture anomalous spikes. In this version, values exceeding the calculated bounds were clipped to the nearest limit. The third version ("remove") used the same 1.5×IQR rule to detect outliers but removed these observations entirely from the series. Each version proceeded independently through the full modeling method, enabling a systematic evaluation of how alternative outlier treatments affect forecasting accuracy.

Each version proceeds independently through training and evaluation. For every (pollutant, peak-strategy) pair, the data are split strictly by time into training (70% earliest observations), validation (next 15%), and test (final 15%) with no shuffling. Summary statistics (sample size, start/end dates, mean, standard deviation) are computed per pollutant and retained for transparency.

3.2. Models

Four forecasting models were employed to evaluate air quality prediction performance: SARIMA, SVR, LSTM, and the proposed xLSTM. These models represent different methodological paradigms, ranging from traditional statistical time-series analysis to modern deep learning architectures.

The Seasonal AutoRegressive Integrated Moving Average (SARIMA) model extends the classical ARIMA framework by explicitly incorporating seasonal components, enabling it to capture recurring temporal patterns alongside non-seasonal autoregressive and moving average structures. The model is denoted as $\mathrm{SARIMA}(p, d, q) \times (P, D, Q)_s$ where p, d, and q represent the non-seasonal autoregressive

order, differencing order, and moving average order, respectively, while P, D, and Q represents the seasonal counterparts over a period s. Optimal hyperparameters for SARIMA were determined using a grid search on the training and validation sets, minimizing error metrics to ensure robust seasonal pattern extraction.

Support Vector Regression (SVR) was employed as a kernel-based machine learning model capable of capturing nonlinear relationships between predictors and the target variable. SVR maps input data into a high-dimensional feature space through a kernel function. In this study, the radial basis function (RBF) kernel, allowing the algorithm to fit a regression function that tolerates deviations within an ε-insensitive margin while penalizing larger errors through a regularization parameter C.Hyperparameters (C, ε, and kernel parameters) were tuned via cross-validation on the validation set.

The Long Short-Term Memory (LSTM) network, a recurrent neural network (RNN) variant, was chosen for its ability to model long-range temporal dependencies without suffering from vanishing or exploding gradients. The LSTM architecture employs gated mechanisms, input, forget, and output gates, to regulate information flow across time steps, enabling the network to retain relevant patterns while discarding noise. In this study, the LSTM model was trained using sequences of fixed-length input windows and optimized with the Adam optimizer, with hyperparameters such as the number of layers, hidden units, learning rate, and batch size determined empirically.

The proposed xLSTM model extends the standard LSTM by integrating additional exogenous features and architectural enhancements designed to improve predictive accuracy for environmental time-series data. In particular, xLSTM incorporates parallel convolutional layers to capture short-term local dependencies before feeding into the recurrent layers, allowing the model to exploit both short-term fluctuations and long-term trends. The architecture was trained using the same temporal input windows as the baseline LSTM, ensuring comparability, but its expanded feature extraction capacity allowed for improved adaptability across varying pollutant characteristics and peak-handling strategies.

350

JCoDe | Vol 6 No 2 | September 2025 | Tolerance in Computational Design| Öztürk, K., Can, Z.

All models were implemented in Python using established libraries, statsmodels for SARIMA, scikit-learn for SVR, and PyTorch for LSTM and xLSTM, and trained separately for each pollutant and peak-handling version of the dataset.

Design facing outputs are as follows. For each pollutant-strategy-model triplet, monthly forecasts are mapped to three risk bands with ±RMSE uncertainty envelopes and operationalized as triggers for planning and architectural design actions, including adjustments to street-canyon permeability and block porosity, the siting of green/blue infrastructure, and building ventilation/filtration scheduling. RMSE sets safety margins around thresholds, MAE characterizes routine operational tolerance, and R² is used to prefer the more stable model when RMSE is comparable.

3.3. Metrics

Model performance was quantitatively evaluated using four standard regression metrics: Mean Absolute Error (MAE), Mean Squared Error (MSE), Root Mean Squared Error (RMSE), and the coefficient of determination (R^2). These metrics were computed on the test set for each combination of pollutant, peak strategy, and model, ensuring that comparisons were made on unseen data without temporal leakage from the training or validation phases.

MAE (Mean Absolute Error): MAE measures the average magnitude of prediction errors, disregarding their direction, and is expressed in the same units as the target variable. It is calculated as **Equation 1**.

$$MAE = \frac{1}{n}\sum_{i=1}^{n}|y_i - \hat{y}_i| \tag{1}$$

where y_i is the observed value, $\hat{y}_i$ is the predicted value, and n is the number of observations. Lower MAE values indicate better predictive accuracy. MAE gives the average absolute forecast error in μg/m³ and serves as a practical "routine tolerance" for operations; because it weights small and large errors equally, we next consider MSE to explicitly penalize large misses and short-lived spikes.

MSE (Mean Squared Error): MSE captures the average squared difference between observed and predicted values, placing greater weight on larger errors due to squaring. It is given by **Equation 2**.

351

$$MSE = \frac{1}{n}\sum_{i=1}^{n}(y_i - \hat{y}_i)^2 \tag{2}$$

A lower MSE implies better model performance, but because errors are squared, this metric is more sensitive to outliers compared to MAE. MSE squares residuals, making the metric especially sensitive to peak errors; to regain interpretability in the original units while retaining this peak sensitivity, we take its square root as RMSE.

RMSE (Root Mean Squared Error): RMSE is the square root of the MSE and re-expresses the error magnitude in the same units as the target variable, which aids interpretability as shown in **Equation 3**.

$$RMSE = \sqrt{\frac{1}{n}\sum_{i=1}^{n}(y_i - \hat{y}_i)^2} \tag{3}$$

RMSE is especially useful when large errors are undesirable, as it penalizes them more heavily. A large RMSE means that the model's predictions deviate substantially from the actual values, indicating lower accuracy and poorer predictive performance. RMSE expresses typical error magnitude in µg/m³ and aligns with design/regulatory thresholds; however, similar RMSE values can mask differences in model fit, so we complement it with R^2 to assess variance explained and stability.

R² Score (Coefficient of Determination): R^2 assesses how well the model explains the variance of the observed data. It is defined as in **Equation 4**.

$$R^2 = 1 - \frac{\sum_{i=1}^{n}(y_i - \hat{y}_i)^2}{\sum_{i=1}^{n}(y_i - \bar{y}_i)^2} \tag{4}$$

where $\bar{y}$ is the mean of the observed values s. An R^2 value of 1 indicates perfect predictions, 0 implies the model is no better than predicting the mean, and negative values suggest performance worse than the mean. R^2 indicates how much of the observed variability the model captures and helps choose between models with comparable RMSE; in practice, we select the model that minimizes RMSE without degrading MAE and with the higher (non-negative) R^2.

352

JCoDe | Vol 6 No 2 | September 2025 | Tolerance in Computational Design| Öztürk, K., Can, Z.

4. FINDINGS

Table 1: Performance of SARIMA, SVR, LSTM, and xLSTM models for PM$_{10}$ and SO$_2$ under different peak-handling strategies.

Model	Target	Peaks	MAE	MSE	RMSE	R^2
SARIMA	PM10	cap	4.8329	40.7825	6.3861	0.3309
xLSTM	PM10	cap	5.0005	41.4338	6.4369	0.3202
LSTM	PM10	cap	5.1378	46.2691	6.8021	0.2409
SVR	PM10	cap	6.9383	66.3797	8.1474	-0.0891
SARIMA	PM10	keep	4.8313	41.3923	6.4337	0.3209
xLSTM	PM10	keep	5.16	42.4085	6.5122	0.3042
LSTM	PM10	keep	5.4779	50.868	7.1322	0.1654
SVR	PM10	keep	6.9828	66.7479	8.1699	-0.0951
LSTM	PM10	remove	5.167	39.5821	6.2914	0.3632
xLSTM	PM10	remove	5.2018	39.9601	6.3214	0.3572
SARIMA	PM10	remove	5.1383	48.5534	6.968	0.2189
SVR	PM10	remove	6.1585	54.9973	7.416	0.1153
SVR	SO2	cap	1.1941	2.4868	1.577	0.3004
xLSTM	SO2	cap	1.2894	2.6764	1.636	0.2471
LSTM	SO2	cap	1.5689	4.0212	2.0053	-0.1312
SARIMA	SO2	cap	1.7024	4.0525	2.0131	-0.14
xLSTM	SO2	keep	1.1376	2.2185	1.4895	0.3759
SVR	SO2	keep	1.3177	2.8654	1.6928	0.194
SARIMA	SO2	keep	1.6791	3.9729	1.9932	-0.1176
LSTM	SO2	keep	1.567	4.0986	2.0245	-0.1529
SVR	SO2	remove	1.2363	2.4462	1.564	0.2398
xLSTM	SO2	remove	1.2613	2.4695	1.5715	0.2325
SARIMA	SO2	remove	1.5407	3.9763	1.9941	-0.2357
LSTM	SO2	remove	1.6071	4.3793	2.0927	-0.3609

In this study, forecasts for PM$_{10}$ and SO$_2$ were generated using four models, SARIMA, SVR, LSTM, and the proposed xLSTM, under three different peak-handling strategies (cap, keep, and remove). Model

Predicting Air Quality in Izmir Using Artificial Intelligence and IoT

performance was evaluated using mean absolute error (MAE), mean squared error (MSE), root mean squared error (RMSE), and the coefficient of determination (R^2). The detailed results are presented in **Table 1**.

Air quality forecasting experiments were conducted using four models, SARIMA, SVR, LSTM, and the proposed xLSTM, across two pollutants (PM_{10} and SO_2) and three peak-handling strategies (cap, keep, remove). Model performances were evaluated using mean absolute error (MAE), mean squared error (MSE), root mean squared error (RMSE), and the coefficient of determination (R^2).

Figure 1 shows the time series comparison of actual and predicted PM_{10} concentrations for the xLSTM model under the cap strategy, illustrating that the model successfully tracks seasonal variations and most peak events, with deviations primarily during sharp changes.

For PM_{10} under the cap strategy, SARIMA achieved the lowest MAE (4.8329) and the lowest RMSE (6.3861), with an R^2 of 0.3309, indicating moderate explanatory power. The xLSTM model followed closely with an MAE of 5.0005 and an RMSE of 6.4369, delivering similar accuracy but slightly lower R^2 (0.3202). LSTM performed slightly worse than xLSTM (MAE 5.1378, RMSE 6.8021, R^2 0.2409), while SVR showed the weakest performance in this setting (MAE 6.9383, RMSE 8.1474, negative R^2 of -0.0891), suggesting poor generalization.

For PM_{10} with the keep strategy, SARIMA maintained a competitive MAE (4.8313) and RMSE (6.4337), outperforming the other methods in terms of absolute error. xLSTM remained the second-best performer, while LSTM and SVR exhibited larger errors and, in the case of SVR, a negative R^2, highlighting sensitivity to unaltered peaks.

Figure 2 presents the time series comparison of actual and predicted SO_2 concentrations for the xLSTM model under the cap strategy, showing that the predictions follow the general seasonal trend, with moderate discrepancies during high-variability periods.

354

JCoDe | Vol 6 No 2 | September 2025 | Tolerance in Computational Design| Öztürk, K., Can, Z.

Figure 1: Time series comparison of actual and predicted PM_{10} concentrations using the xLSTM model under the "cap" peak-handling strategy
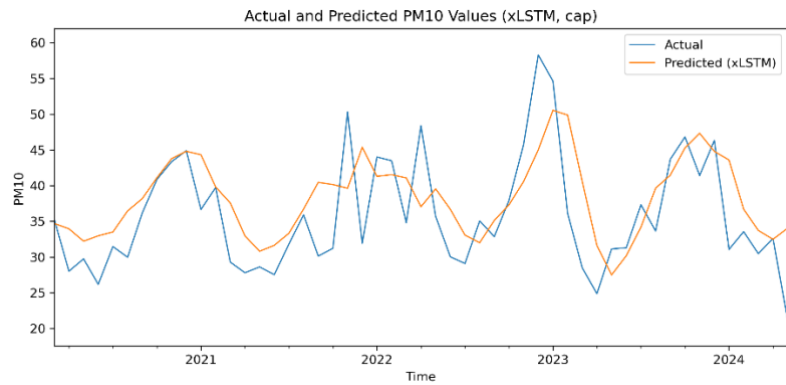
Figure 2: Time series comparison of actual and predicted SO_2 concentrations using the xLSTM model under the "cap" peak-handling strategy
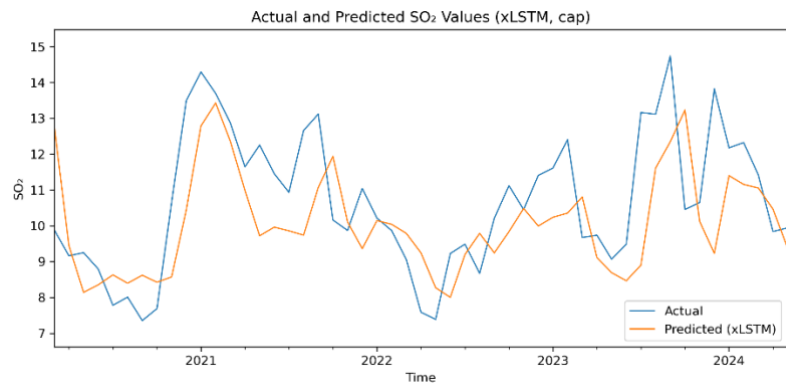
Under the remove strategy for PM_{10}, SARIMA again delivered strong results with the smallest MAE and RMSE values, indicating that traditional time-series modeling benefits from peak removal. xLSTM continued to outperform LSTM and SVR in most metrics, though SARIMA retained the top position overall for PM_{10} across all strategies. In contrast, SO_2 forecasting revealed a different dynamic. With the cap strategy, xLSTM consistently provided lower MAE and RMSE values compared to LSTM and SVR, while also maintaining a substantially higher R^2 than SARIMA, which performed poorly (negative R^2) in this setting. This suggests that the xLSTM's hybrid architecture is particularly effective at modeling capped SO_2 series.

For SO_2 under the keep strategy, both xLSTM and LSTM achieved comparable MAE and RMSE values, with xLSTM often holding a slight edge. SARIMA again struggled, indicating that raw peak variability hinders its performance. SVR showed moderate predictive ability but did not surpass the deep learning models.

When removing peaks from SO_2 data, the performance gap between models narrowed, but xLSTM maintained competitiveness, often ranking among the top two models in terms of error metrics. LSTM sometimes matched its performance, though R^2 values indicated that xLSTM tended to capture variance slightly better.

These results indicate that for PM_{10}, SARIMA remains a strong contender, particularly when peaks are removed or capped, while xLSTM delivers competitive accuracy with better adaptability across varying strategies. For SO_2, xLSTM generally outperforms traditional methods, especially under capped and kept peak strategies, reflecting its ability to integrate temporal dependencies and adapt to pollutant-specific characteristics. These findings underscore the importance of selecting both the appropriate modeling approach and peak-handling strategy based on the pollutant and data characteristics.

The ±RMSE risk bands are converted into simple design triggers that link forecasts to actions for streets, open-space elements, and buildings. When PM_{10} peaks are cap/remove, SARIMA's smaller error lets ventilation lanes remain as narrow as 2-3 m; with keep data, xLSTM's steadier forecasts guide short curb-lane closures during predicted high episodes. For SO_2, xLSTM bands under keep/cap point to calm-wind months, steering the timing and placement of porous tree belts and wetland aerators so they disperse rather than trap pollutants. At the building scale, a high-band signal prompts roughly a 20% cut in outdoor-air intake and earlier filter changes, while a low-band signal opens the door to night-purge ventilation for free cooling. A trigger activates only after the same band is exceeded for two consecutive months; the ±RMSE width sets the safety buffer and MAE marks everyday tolerance, so interventions respond to sustained risk.

5. APPLICATIONS TO URBAN PLANNING AND ARCHITECTURAL DESIGN

5.1. Translating Forecasts into Risk Bands and Triggers
Monthly PM_{10} and SO_2 forecasts are mapped to Low/Moderate/High bands with ±RMSE envelopes, forming a design-facing interface. Interventions trigger only when band exceedance persists ≥2 months. RMSE sets safety margins, MAE informs routine tolerance, and R^2 breaks ties. For PM_{10}, SARIMA supports tighter margins under

356

JCoDe | Vol 6 No 2 | September 2025 | Tolerance in Computational Design | Öztürk, K., Can, Z.

cap/remove, while xLSTM offers cross-strategy stability; for SO_2 (keep/cap), xLSTM provides more reliable banding.

5.2. Street-Canyon, Corridors, and Neighborhood Form

Bands guide corridor- and block-scale design during seasons of elevated residence time. High-band months motivate porosity/ventilation corridors, careful timing of works, and calibrated traffic operations. SARIMA enables narrow buffers for PM_{10} when peaks are controlled; xLSTM stabilizes guidance when preprocessing policies are fluid.

5.3. Building-Scale Strategies and Sensitive Receptors

Façade orientation, mixed-mode ventilation, and filtration scheduling align to bands and their envelopes: wider envelopes favor conservative intake and earlier maintenance; narrower envelopes allow relaxed setpoints. For receptors (schools/clinics), intake siting, protective planting, and advisories track monthly transitions; for SO_2, xLSTM bands target seasons more dependably.

5.4. Implementation Pathway and İzmir-Specific Guidance

The workflow integrates with municipal GIS to test scenarios against keep/cap/remove policies. In İzmir, PM_{10} under cap/remove pairs best with SARIMA for tight triggers, while stable playbooks reference xLSTM; SO_2 actions anchor to xLSTM. The approach links forecasting to design, prioritizing targeted, temporally adaptive interventions over uniform, calendar-based measures.

6. POTENTIAL, LIMITATIONS, AND BROADER IMPACTS

6.1. Potential

The workflow runs on routinely collected monitoring data, generates design-facing risk bands with uncertainty envelopes rather than opaque scores, and integrates directly with existing GIS dashboards to enable scenario planning and policy testing. Accordingly, it is lightweight and readily deployable for municipal adoption.

6.2. Limitations

Several constraints qualify the findings. First, monthly aggregation smooths diurnal extremes and may understate short-lived peaks. Second, key exogenous drivers (e.g., wind fields, traffic volumes) are not explicitly modeled, so causal attribution is outside the present

scope. Third, heterogeneous station coverage can bias area-wide means and introduce spatial representativeness errors. Fourth, external validation beyond İzmir is pending, and generalizability should be confirmed in cities with different meteorology, emission profiles, and monitoring density.

6.3. Broader Impacts

Forecast-guided siting and operations can reduce exposure inequities around sensitive receptors (schools, clinics), align with sustainability objectives through targeted, temporally adaptive ventilation and filtration, and help avoid maladaptive greening that traps pollutants in narrow street canyons. By coupling uncertainty-aware forecasts to design and operations, the approach enables more precise, lower-cost interventions that advance public health and urban sustainability.

7. CONCLUSION

This study presented a comprehensive framework for predicting air quality in İzmir, Türkiye, by combining Internet of Things (IoT) data streams with traditional statistical models and advanced deep learning architectures. Monthly observations of PM_{10} and SO_2 from 1996-2024 were processed under three distinct peak-handling strategies (cap, keep, remove) to systematically assess the influence of extreme values on predictive performance. Four forecasting models, SARIMA, SVR, LSTM, and the proposed xLSTM, were rigorously evaluated using MAE, MSE, RMSE, and R^2 on strictly time-ordered train, validation, and test splits, ensuring no temporal leakage.

The findings reveal that for PM_{10}, SARIMA remained highly competitive, particularly under capped and removed peak strategies, often achieving the lowest absolute errors. However, xLSTM provided accuracy close to SARIMA's best results while maintaining greater adaptability across varying preprocessing strategies. For SO_2, xLSTM consistently outperformed the other models under capped and kept peak conditions, delivering lower error metrics and higher explanatory power than traditional methods, which struggled with the pollutant's variability. These outcomes underscore that no single model dominates in all scenarios; instead, model selection should be pollutant- and preprocessing-specific.

358

JCoDe | Vol 6 No 2 | September 2025 | Tolerance in Computational Design| Öztürk, K., Can, Z.

The integration of advanced AI techniques such as xLSTM with IoT-enabled environmental monitoring offers clear practical benefits. Beyond public health and regulatory applications, accurate air quality forecasts can directly inform urban design and planning decisions.

By identifying pollution hotspots and predicting their temporal patterns, city planners can optimize building placement to minimize exposure, allocate green spaces strategically to act as natural air filters, and guide transportation network designs that reduce emission concentrations in residential areas. Furthermore, predictive insights can support sustainable architectural practices by enabling ventilation, façade, and material choices that mitigate the impact of expected air pollution levels. Ultimately, the proposed approach not only advances methodological rigor in air quality prediction but also contributes to healthier, more sustainable urban living environments. By temporally aligning interventions with forecasted exposure, rather than applying uniform, calendar-based measures, municipalities can achieve comparable or superior air-quality improvements with lower energy and material use, realize climate co-benefits through demand-controlled ventilation and traffic retiming, and avoid maladaptive greening that traps pollutants in narrow street canyons. The banded, design-facing outputs further support equity by directing protection to sensitive receptors (e.g., schools and clinics). Future work should couple this workflow with multi-objective optimization and lifecycle/health-impact assessment to jointly quantify exposure reduction, energy and carbon savings, and financial costs, thereby institutionalizing forecast-guided planning within sustainability and resilience frameworks.

Author Contribution

The study idea and research design were developed by Kübra Öztürk, data collection and analysis were conducted by Kübra Öztürk. The writing, writing and editing of the article were carried out jointly by Kübra Öztürk and Zuhal Can. Both authors read and approved the final version of the article.

References

Abhijith, K. V., Kumar, P., Gallagher, J., McNabola, A., Baldauf, R., Pilla, F., Broderick, B., Di Sabatino, S., & Pulvirenti, B. (2017). Air

pollution abatement performances of green infrastructure in open road and built-up street canyon environments: A review. *Atmospheric Environment, 162*, 71–86.

Albuali, A., Srinivasagan, R., Aljughaiman, A., & Alderazi, F. (2023). Scalable lightweight IoT-based smart weather measurement system. *Sensors, 23*(12), 5569. https://doi.org/10.3390/s23125569

Ambildhuke, G., & Banik, B. G. (2022). IoT-based portable weather station for irrigation management using real-time parameters. *International Journal of Advanced Computer Science and Applications, 13*(5), 267–278.

Atali, A., Eren, B., Erden, C., & Atali, G. (2022). LSTM derin öğrenme yaklaşımı ile hava kalitesi verilerinin tahmini: Sakarya örneği [Forecasting air quality data with an LSTM deep learning approach: The case of Sakarya]. *Academic Perspective Procedia, 5*(3), 477–484.

Aydin, S., Tasyürek, M., & Öztürk, C. (2021). Derin öğrenme yöntemi ile İç Anadolu Bölgesi ve çevresi hava kirliliği tahmini [Air pollution forecasting for Central Anatolia and surroundings using a deep learning method]. *Avrupa Bilim ve Teknoloji Dergisi / European Journal of Science and Technology, 29*, 168–173.

Bansal, P., & Quan, S. J. (2024). Examining temporally varying nonlinear effects of urban form on urban heat island using explainable machine learning: A case of Seoul. *Building and Environment, 247*, 110957.

Bernardes, G. F. L. R., Ishibashi, R., Ivo, A. A. S., Rosset, V., & Kimura, B. Y. L. (2023). Prototyping low-cost automatic weather stations for natural disaster monitoring. *Digital Communications and Networks, 9*(4), 941–956. https://doi.org/10.1016/j.dcan.2022.05.002

Bolla, S., Anandan, R., & Thanappan, S. (2022). Weather forecasting method from sensor-transmitted data for smart cities using IoT. *Scientific Programming, 2022*, 1426575. https://doi.org/10.1155/2022/1426575

Elbasi, E., Mostafa, N., AlArnaout, Z., Zreikat, A. I., Cina, E., Varghese, G., Shdefat, A., Topcu, A. E., Abdelbaki, W., Mathew, S., & Zaki, C. (2023). Artificial intelligence technology in the agricultural sector: A systematic literature review. *IEEE Access, 11*, 171–202. https://doi.org/10.1109/ACCESS.2022.3232485

Elsaraiti, M., & Merabet, A. (2021). A comparative analysis of the ARIMA and LSTM predictive models and their effectiveness for predicting

360

JCoDe | Vol 6 No 2 | September 2025 | Tolerance in Computational Design| Öztürk, K., Can, Z.

wind speed. *Energies, 14*(20), 6782.

Geng, D., Zhang, H., & Wu, H. (2020). Short-term wind speed prediction based on principal component analysis and LSTM. *Applied Sciences, 10*(13), 4416.

Ioannou, K., Karampatzakis, D., Amanatidis, P., Aggelopoulos, V., & Karmiris, I. (2021). Low-cost automatic weather stations in the Internet of Things. *Information, 12*(4), 146. https://doi.org/10.3390/info12040146

Izmir Metropolitan Municipality. (2024). Hava kalitesi ölçüm değerleri [Air quality measurement values] [Dataset]. Retrieved September 16, 2025, from https://ulasav.csb.gov.tr/dataset/35-hava-kalitesi-olcum-degerleri

Jamil, H., Umer, T., Ceken, C., & Al-Turjman, F. (2021). Decision-based model for real-time IoT analysis using big data and machine learning. *Wireless Personal Communications, 121*(4), 2947–2959. https://doi.org/10.1007/s11277-021-08857-7

Karvelis, P., Mazzei, D., Biviano, M., & Stylios, C. (2020). PortWeather: A lightweight onboard solution for real-time weather prediction. *Sensors, 20*(11), 3181. https://doi.org/10.3390/s20113181

Kaya, S. M., Isler, B., Abu-Mahfouz, A. M., Rasheed, J., & AlShammari, A. (2023). An intelligent anomaly detection approach for accurate and reliable weather forecasting at IoT edges: A case study. *Sensors, 23*(5), 2426. https://doi.org/10.3390/s23052426

Leelavinodhan, P. B., Vecchio, M., Antonelli, F., Maestrini, A., & Brunelli, D. (2021). Design and implementation of an energy-efficient weather station for wind data collection. *Sensors, 21*(11), 3831. https://doi.org/10.3390/s21113831

Lu, B., Wang, R., Qin, Z., & Wang, L. (2023). A practice-distributed thunder-localization system with crowd-sourced smart IoT devices. *Sensors, 23*(9), 4186. https://doi.org/10.3390/s23094186

Mabrouki, J., Azrour, M., Dhiba, D., Farhaoui, Y., & El Hajjaji, S. (2021). IoT-based data logger for weather monitoring using Arduino-based wireless sensor networks with remote graphical application and alerts. *Big Data Mining and Analytics, 4*(1), 25–32. https://doi.org/10.26599/BDMA.2020.9020018

Mehmood, A., Lee, K.-T., & Kim, D.-H. (2023). Energy prediction and optimization for smart homes with weather metric-weight coefficients. *Sensors, 23*(7), 3640. https://doi.org/10.3390/s23073640

Mohapatra, D., & Subudhi, B. (2022). Development of a cost-effective IoT-based weather monitoring system. *IEEE Consumer Electronics Magazine, 11*(5), 81–86. https://doi.org/10.1109/MCE.2021.3136833

Nie, H., Liu, G., Liu, X., & Wang, Y. (2012). Hybrid of ARIMA and SVMs for short-term load forecasting. *Energy Procedia, 16*, 1455–1460.

Patel, P., Kalyanam, R., He, L., Aliaga, D., & Niyogi, D. (2023). Deep learning-based urban morphology for city-scale environmental modeling. *PNAS Nexus, 2*(3), pgad027. https://doi.org/10.1093/pnasnexus/pgad027

Roy, D. S. (2020). Forecasting the air temperature at a weather station using deep neural networks. *Procedia Computer Science, 178*, 38–46.

Singh, D. K., Sobti, R., Jain, A., Malik, P. K., & Le, D.-N. (2022). LoRa-based intelligent soil and weather condition monitoring with Internet of Things for precision agriculture in smart cities. *IET Communications, 16*(5), 604–618. https://doi.org/10.1049/cmu2.12352

Suresh, P., Aswathy, R. H., Arumugam, S., Albraikan, A. A., Al-Wesabi, F. N., Hilal, A. M., & Alamgeer, M. (2022). IoT with evolutionary algorithm-based deep learning for smart irrigation system. *Computers, Materials & Continua, 71*(1), 1713–1728.

Tsalikidis, N., Mystakidis, A., Koukaras, P., Ivaškevičius, M., Morkūnaitė, L., Ioannidis, D., Fokaides, P. A., Tjortjis, C., & Tzovaras, D. (2024). Urban traffic congestion prediction: A multi-step approach utilizing sensor data and weather information. *Smart Cities, 7*(1), 233–253.

Tukey, J. W. (1977). *Exploratory data analysis*. Addison-Wesley.

Venter, Z. S., Hassani, A., Stange, E., Schneider, P., & Castell, N. (2024). Reassessing the role of urban green space in air pollution control. *Proceedings of the National Academy of Sciences, 121*(6), e2306200121.

Vos, P. E. J., Maiheu, B., Vankerkom, J., & Janssen, S. (2013). Improving local air quality in cities: To tree or not to tree? *Environmental Pollution, 183*, 113–122.

Wang, Z., Hu, K., Wang, Z., Yang, B., & Chen, Z. (2024). Impact of urban neighborhood morphology on PM2.5 concentration distribution at different scale buffers. *Land, 14*(1), 7.

Woo, W., Richards, W., Selker, J., & Udell, C. (2023). WeatherChimes:

362

JCoDe | Vol 6 No 2 | September 2025 | Tolerance in Computational Design| Öztürk, K., Can, Z.

An open IoT weather station and data sonification system. *HardwareX, 13,* e00402. https://doi.org/10.1016/j.ohx.2023.e00402

Wu, Q., Wang, Y., Sun, H., Lin, H., & Zhao, Z. (2023). A system coupling GIS and CFD for atmospheric pollution dispersion simulation in urban blocks. *Atmosphere, 14*(5), 832.

Yang, J., Yu, M., Liu, Q., Li, Y., Duffy, D. Q., & Yang, C. (2022). A high spatiotemporal resolution framework for urban temperature prediction using IoT data. *Computers & Geosciences, 159*, 104991. https://doi.org/10.1016/j.cageo.2021.104991

Yu, M., Xu, F., Hu, W., Sun, J., & Cervone, G. (2021). Using long short-term memory (LSTM) and Internet of Things (IoT) for localized surface temperature forecasting in an urban environment. *IEEE Access, 9*, 137406–137418.

364

JCoDe | Vol 6 No 2 | September 2025 | Tolerance in Computational Design| Öztürk, K., Can, Z.

Circular Built Environment During the Digital Age: A Systematic Review

Burcu Kısmet Conk[1], Meryem Birgül Çolakoğlu[2]

ORCID NO: 0000-0002-7690-9953[1], 0000-0002-9690-7488[2]

[1] Beykoz University, Faculty of Engineering and Architecture, Department of Architecture, Istanbul, Türkiye
[2] Istanbul Technical University, Faculty of Architecture, Department of Architecture, Istanbul, Türkiye

As the effects of the Industrial Revolution have significantly contributed to global climate change and the studies reveal that by 2050, the world's energy demand will double while fossil fuel reserves are projected to deplete. To mitigate the risks associated with exceeding the 1.5°C global warming threshold, international organizations, including the United Nations, as well as governments and NGOs, are implementing strategies aimed at achieving carbon neutrality by mid-century. One such approach involves transitioning from the "take-make-waste" model of the linear economy to the circular economy (CE), which operates on principles of "make-use-reuse-recycle." The AECO (Architecture-Construction-Engineering-Operation) industry, a key driver of global economic activity, plays a central role in this transformation by rethinking and restructuring the AECO industry to align with CE principles. This study examines the intersection of circular economy principles and the built environment through the lens of Industry 4.0. A systematic literature review combining descriptive and bibliometric analysis, covering publications from 2016 to 2024 from Scopus and Web of Science (WoS), was conducted using keywords related to CE, the built environment, and digital technologies. Structuring the review is processed through PRISMA and selecting the literature is strengthened by Quality Assessment (QA). The analysis, performed with VOSviewer, highlights key trends, thematic connections, and potential areas for future research. Continuous and significant increase in number of publications obtained since 2016. United Kingdom, Netherlands and Italy were the leading countries in this research area. "Sustainability" is the pioneering journal in this field with highest number of publications and citations. Digital technologies such as building information modeling (BIM), blockchain, and the Internet of Things (IoT) have emerged as powerful tools to support CE implementation. By enabling resource optimization, reducing waste, and enhancing lifecycle assessments, these technologies facilitate the adoption of sustainable practices within the AECO sector. These studies underscore the importance of advancing frameworks like life cycle assessment (LCA) and cradle-to-cradle (C2C) to support circular transitions in the built environment. Furthermore, the results demonstrate the increasing momentum and global interest in leveraging digitalization to achieve sustainability goals in the sector. This study offers valuable insights for academics, industry professionals, and policymakers by mapping the current state of CE research in the AECO industry and identifying emerging trends. It emphasizes the need for comprehensive frameworks and strategic roadmaps to enable the circular transition of the AECO sector. Future research should focus on deepening interdisciplinary collaboration and integrating CE with related sustainability concepts to enhance understanding and accelerate implementation. By doing so, the AECO industry can make significant contributions toward global carbon neutrality and sustainable development goals.

Keywords: Circular economy, Built environment, Architecture, Bibliometric analysis, Sustainability.

365

JCoDe | Vol 6 No 2 | September 2025 | Tolerance in Computational Design | Kısmet Conk, B., Çolakoğlu, M. B.

Dijital Çağda Yapılı Çevrede Döngüsellik: Sistematik Analiz

Burcu Kısmet Conk[1], Meryem Birgül Çolakoğlu[2]

ORCID NO: 0000-0002-7690-9953[1], 0000-0002-9690-7488[2]

[1] Beykoz Üniversitesi, Mühendislik ve Mimarlık Fakültesi, Mimarlık Bölümü, İstanbul, Türkiye
[2] İstanbul Teknik Üniversitesi, Mimarlık Fakültesi, Mimarlık Bölümü, İstanbul, Türkiye

Küresel iklim değişikliğinin etkilerini azaltmak için Birleşmiş Milletler ve diğer uluslararası kuruluşlar ile hükümetler ve STK'lar, özellikle 2050 yılına kadar karbon nötrlüğü sağlamayı hedefleyen stratejiler geliştirmektedir. Bu stratejilerden biri, lineer ekonomi modelinden ("al-yap-at") döngüsel ekonomi modeline ("üret-kullan-yeniden kullan-geri dönüştür") geçiştir. Mimarlık-İnşaat-Mühendislik-Operasyon (AECO) sektörü, küresel ekonomik faaliyetlerin temel itici gücü olarak, döngüsel ekonomi ilkelerine uyum sağlamak amacıyla yeniden yapılandırılmalıdır. Bu çalışma, döngüsel ekonomi ve yapılı çevre arasındaki ilişkiyi dijitalleşme perspektifinden incelemektedir. 2016-2024 dönemindeki yayınları kapsayan sistematik bir literatür taraması, Scopus ve Web of Science (WoS) veri tabanlarında "döngüsel ekonomi", "yapılı çevre" ve "dijital teknolojiler" anahtar kelimeleri kullanılarak gerçekleştirilmiştir. Literatür araştırmasının yapısı PRISMA yöntemiyle şekillendirilmiş, çalışmaların analizlere dahil edilmesi ise Kalite Değerlendirmesi ile gerçekleşmiştir. Analizler, Excel ve VOSviewer yazılımıyla yapılmış ve günümüzdeki eğilimler, anahtar kelimeler, tematik bağlantılar ve gelecekteki araştırma alanları belirlenmiştir. 2016 yılından itibaren bu alandaki çalışmaların sürekli ve artan ivme ile arttığı tespit edilmiştir. Aynı zamanda Birleşik Krallık, Hollanda ve İtalya bu araştırma alanının önde gelen ülkeleridir. "Sustainability" bu alanda en çok yayın yapılan ve atıf alan dergidir. BIM, blockchain ve IoT gibi dijital teknolojiler, kaynak optimizasyonu, atık azaltımı ve yaşam döngüsü değerlendirmelerini iyileştirerek sürdürülebilir uygulamaların benimsenmesini desteklemektedir. Çalışma, AECO sektöründe döngüsel geçişi desteklemek için kapsamlı çerçeve ve stratejik yol haritalarının gerekliliğini vurgulamaktadır. Aynı zamanda da bulguların tartışılması kısmında farklı döngüsel ekonomi tanımlamaları analiz edilmiş, döngüsel ekonomi ile bağlantılı olan kavramlar ve anahtar kelimeler ortaya konmuştur. Bu çalışma, döngüsel ekonomi alanında akademisyenler, sektör uzmanları ve politika yapıcılar için değerli bilgiler sunmakta, sektörün karbon nötrlüğü ve sürdürülebilir kalkınma hedeflerine katkı potansiyelini ortaya koymaktadır.

366

1. INTRODUCTION

Since the Industrial Revolution, rapid urbanization, overpopulation, destruction of nature and energy consumption based on fossil fuels has caused global climate change (European Commission, 2015). The effects of climate change appear as fires, floods, water and agricultural crises throughout the world. In addition, it is predicted that most of the fuel resources will be depleted by 2050, but the energy need will double (European Commission, 2020). With an aim of achieving carbon neutrality by 2050 to avoid the catastrophic effects of a 1.5°C of climate change, governments, global institutions like United Nations (UN), and NGOs (non-governmental organizations) are developing action plans and key strategies. Allan Kneese indicated that resources are not endlessly renewable, mentioning the circular economy for the first time in 1988 (Kneese, 1988). It is found crucial to transform from the linear economy model based on the "take-make-waste" logic, which has spread all over the world with the rapid development of technology, especially since the second half of the 20th century, to the circular economy model based on the "make-use-reuse-recycle" system to minimize the impact of climate change. Additionally, according to the studies, linear economic models have ignored the economy-environment interrelationships (Eberhardt et al., 2020; Kirchherr and van Santen, 2019; Zhuang et al., 2023).

To achieve a circular economy, a holistic approach to sustainable thinking and practice needs to be integrated into all disciplines, including Architecture-Construction-Engineering-Operation (AECO) industry. AECO industry which has one of the largest global market sizes has to be redesigned and reorganised considering the carbon neutrality strategies. In addition, AECO industry are responsible for more than 40% of global CO_2 emissions and almost quarter of it derives from the embodied carbon of the constructions (World Green Building Council, 2019) including materials-related, transport-related and equipment-related. Furthermore, one-third of the total waste is also produced by the AEC industry (IEA, 2019). In this regard, it is crucial to rethink and redesign AECO industry, its processes and components by integrating circular economy principles. Circular thinking aims to transform the processes and products to reach UN's Sustainable Development Goals (SDGs) (UN SDG, 2019). The key aims of the circular economy are to obtain material efficiency, minimize waste and optimize energy usage.

To achieve the circular economy, innovative technologies should be adopted to the AECO industry. As it is mentioned in the study of Olawumi et al. (2022) digital technologies support facilitates the implementation of sustainability practices in the built environment.

The purpose of this paper is to investigate how circular economy has emerged as a key research area for AECO industry to reach sustainable development targets and what is the role of digitalization in this transformation. This study utilises descriptive and bibliometric analysis to find major areas and intersections between CE, AECO, and digitalization which will provide significant insights for researchers, and policymakers. This paper adopts the visualization analysis method based on the theory of bibliometrics to reveal the development trend and future research directions of the circular & digital transition. The research questions addressed in this study are:

Q1. What is the current situation of the subject in the literature?

Q2. What research topics are being discussed within this subject?

Q3. How can CE be defined with AECO?

Q4. What are the related research areas?

Q5. What are the limitations of current research and practices on CE?

2. METHODOLOGY

This chapter aims to present the status quo of involvement of digitalization in circular economy (CE) research, as the methodological flow chart as illustrated in **Figure 1**. A quantitative research method has been adopted. Methodology started with the identification of the research problem according to the trends in CE affected by emerging immersive technologies along with a systematic literature review.

Figure 1: Methodological flow chart of the systematic review. (by Authors).
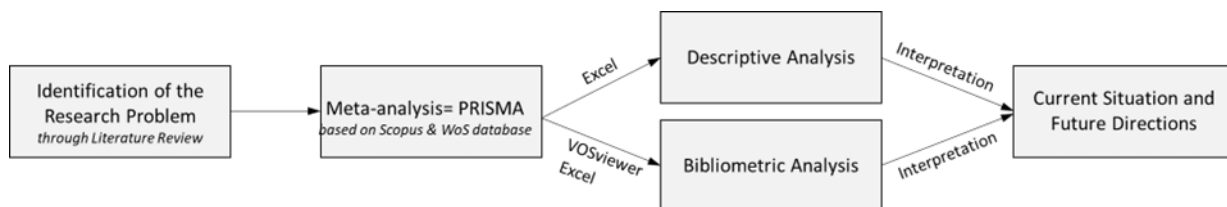
To organize the systematic literature review (SLR), the PRISMA (Preferred Reporting Items for Systematic Reviews and Meta-Analyses)

368

JCoDe | Vol 6 No 2 | September 2025 | Tolerance in Computational Design | Kısmet Conk, B., Çolakoğlu, M. B.

meta-analysis flow diagram of Page et al. (2020) was adopted thanks to the advantages which were mentioned in the study of Shahruddin and Zairul (2020), such as identifying large databases of scientific literature through keyword and search strategies, screening inclusion and exclusion criteria and conducting eligibility process to analyse the data from the studies. To validate the findings of the SLR and to evaluate the sources according to quality, and relevant to the research question, Quality Assessment (QA) is utilised. Evaluating the validity of the included sources is an integral component of the SLR. In addition, Kitchanham et al. (2009), Kitchanham et al. (2015), Petersen et al. (2015), Yang et al. (2021), Amin et al. (2021) and Usman et al. (2023) mentioned the necessity of QA in SLR studies.

In this study, PRISMA provided an examination of data from several independent studies of CE and related domain to determine overall situation and trends. QA provided assessing study quality to proceed in SLR. A typical QA instrument is a checklist consisting of multiple factors that need to be evaluated for the studies. Yet, there is no one standard QA method, a quality checklist usually designed for a particular study could be derived from factors and the checklist is generally based on "Yes or No" type answers. **Figure 2** explains the conducting systematic reviews and data collection process through the PRISMA approach; and **Table 1** lists the QA criteria customized in this study as an inclusion-exclusion criteria. Q1–Q3 journal quartiles were chosen as they offer a standardized, field-normalized indicator of publication quality, widely used in research assessments (Bornmann et al., 2012; SCImago, 2024; Waltman et al., 2013). Quartile rankings were preferred over raw citation counts because articles published recently (e.g., within the last year) have had less time to accumulate citations compared to those published 8–10 years ago, making quartiles a more time-independent and standardized measure of journal quality.

QA Criteria	
1.	The paper is published in a Q1, Q2 or Q3 journal or Scopus - WoS indexed conference proceeding.
2.	The paper is available in full text.
3.	The paper is written in English.
4.	The paper is related to 'Engineering' or 'Multidisciplinary' area in Scopus – WoS.
5.	The paper is related to urban/ building / construction domain.
6.	The paper links digitalization topics into CE.

Table 1. Inclusion-exclusion criteria for QA.

The literature sample was retrieved from Scopus and Web of Science (WoS) databases. Scopus and WoS are considered to be the world's largest and reliable peer-review databases (Guz and Rushchitsky, 2009; Aghaei Chadegani et al., 2013). The keywords were utilized in the literature search: TITLE-ABS-KEY ("circular economy" OR "circularity) AND ("architecture" OR "construction" OR "built environment" OR "urban" OR "city") AND ("digital" OR "smart" OR "industry 4.0" OR "innovation" OR "digitalization" OR "technology" OR "platform" OR "automation"). The combined sets of keywords were 70 as result of "2 x 5 x 7". Accordingly, the first retrieval resulted in the identification of 189 publications, 106 from Scopus and 83 from Web-of-Science (WoS). The period selected for review was from 2016 to the end of December 2024.

The identification phase included the removal of duplicated publications, and 5 publications were excluded in this phase. The screening phase included removal of the same publications and filtering process according to certain criteria: articles in the English language and with full text available were considered in this study. Also, not related subject areas were excluded. In addition, other documents rather than article, conference paper, book, book chapter and review were removed. The number of excluded papers was 32, and 152 papers were continued to screen through title and abstract. In total, 20 papers were not retrieved because of lack of focus on urban/ building / construction related domain and also some of them were related to food, agriculture, water, material, chemistry, supply-chain and sensors. The number of publications assessed for eligibility was 132. According to criteria in screening, a total number of 52 papers were removed in two steps; 132 papers continued to the PRISMA protocol. The inclusion phase provided additional criteria as studies' aims and relations to the related topic were analysed in detail. In this phase, 3 papers were removed. At the end of the PRISMA protocol and QA, 129 papers remained. Later on, analyses were applied to these 129 papers. This PRISMA and QA based methodological process is shown in **Figure 2**.

370

JCoDe | Vol 6 No 2 | September 2025 | Tolerance in Computational Design | Kısmet Conk, B., Çolakoğlu, M. B.
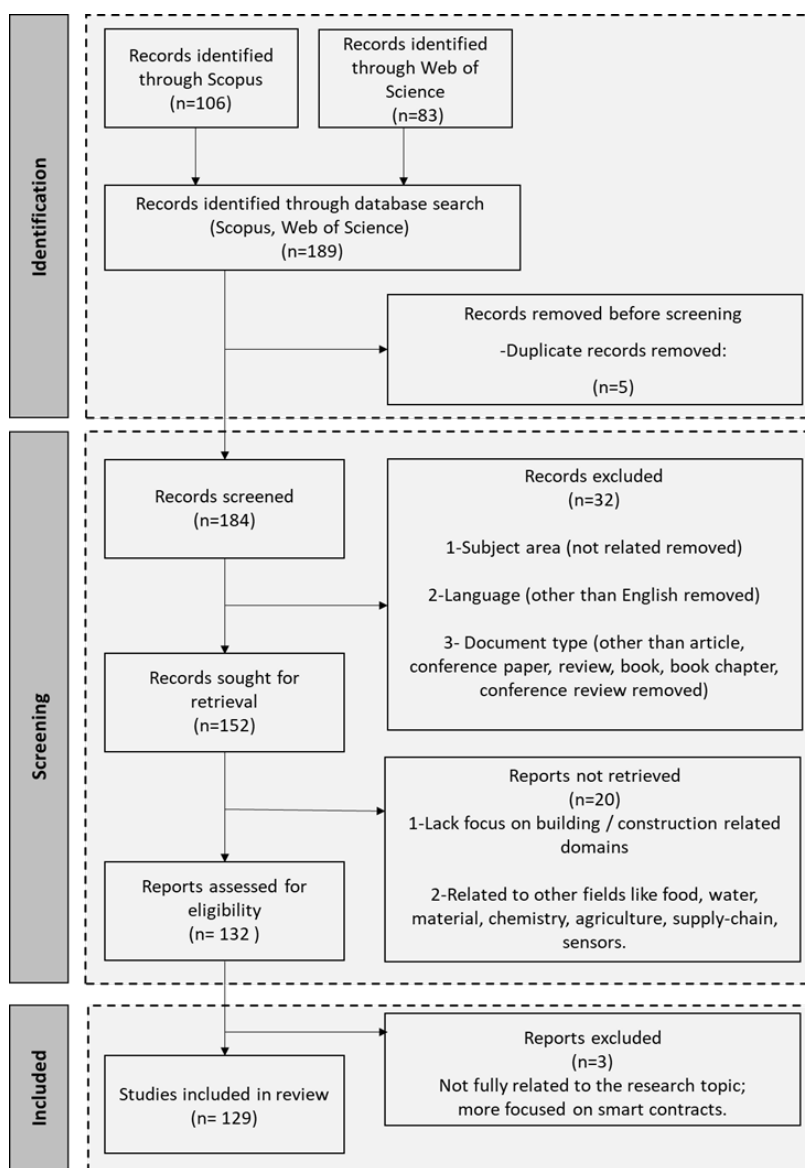
Figure 2: Research method for articles retrieval based on meta-analysis: PRISMA 2020. (by Authors).

The methodology of analyses was based on descriptive and bibliometric analysis to understand and state the current relations between CE, built environment and digitalization. Descriptive analyses presented an overview of the included papers in which Excel software was used to generate graphs. Bibliometric analyses employed the analyses through Excel and VOSviewer software focusing on the co-occurrence of keywords, country-based, source and citation analyses. Bibliometric analysis of scientific research has been considered one of the most common methods to evaluate the research performance of academicians, universities and even countries as well as academic journals (Konur, 2012). VOSviewer was selected as bibliometric

Circular Built Environment During the Digital Age: A Systematic Review

network software to construct and visualize bibliometric maps from the databases.

3. RESULTS

Results of descriptive and bibliometric analyses are presented, respectively.

3.1 Descriptive Analyses

Descriptive analyses are the process of using current and previous data to identify trends and relationships. It is a sort of data research that supports in describing, demonstrating, or summarizing data points so current and future patterns may develop.

3.1.1. Publications throughout the years

It is clear in the data that the concept of CE in built environment through digitalization gaining momentum. **Figure 3** shows the number of publications by year, demonstrating the growth of this field since 2016. During the past 8 years (2016–2024), the number of publications related to CE in built environment domain has increased by 43 times. Since 2017 considerable growth was seen. Only 6,9 % (19) of eligible papers were published before 2020, indicating rapid growth in related studies. 72% of papers were published during the last three years, in 2022, 2023 and 2024. Overall, it is obvious to state a growing trend in the number of publications for the near future.
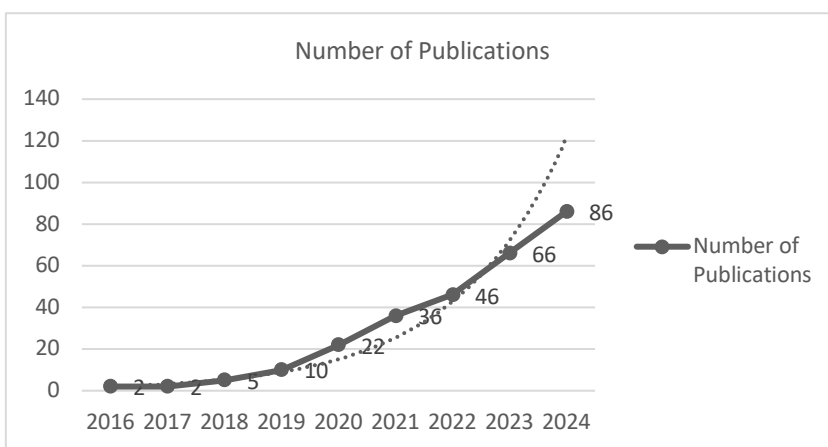
Figure 3: Number of publications per year. (by Authors).

372

JCoDe | Vol 6 No 2 | September 2025 | Tolerance in Computational Design | Kısmet Conk, B., Çolakoğlu, M. B.

3.1.2. Publications by country

Figure 4 illustrates the publications classified by the 40 countries of origin between January 2016 and December 2024. This diversity in various geographic distributions suggests a global interest in the technological transformation of construction management. Articles from the United Kingdom (48) are at the forefront of this new field, which accounts for 17.4% of all publications. Next comes the Netherlands and Italy with 45 publications, and these are followed by China (27), Germany (27), USA (22), Australia (20), and Austria (14). Turkey has 3 publications and all of them were published in 2023.
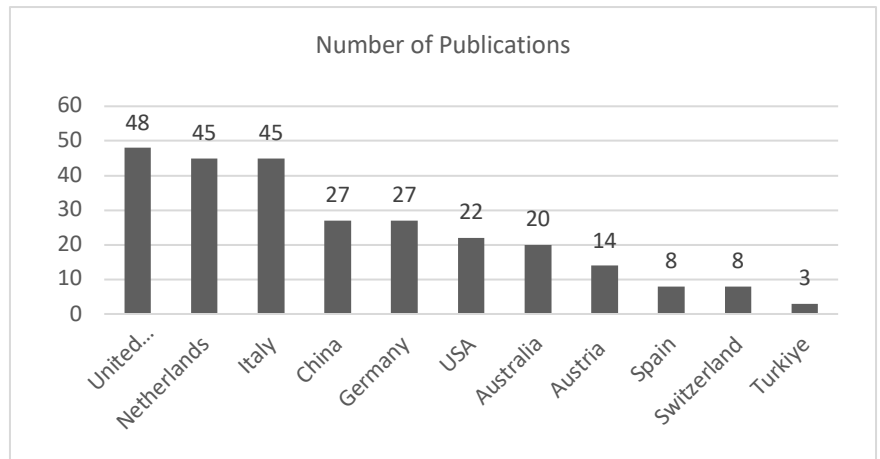
Figure 4: Number of publications per country. (by Authors).

3.2 Bibliometric Analyses

The bibliometric analysis was applied to map the scientific retrieved data for evaluation of themes, dynamic aspects of data and processing a wide range of information (Tijssen and Van Raan, 1994; Cobo et al., 2011; Khan et al., 2021). Moreover, it provides impact measurement of journals and articles, institutes, countries, subjects and keywords, which delivers the indicators for policy management across the subject removing subjectivity issues among the pieces of literature (Hammersley, 2001; Khan et al., 2021). VOSviewer generates visual scientific landscapes about academic publications, researchers, organizations, countries, keywords or terms based on co-authorship, co-occurrence, citation, bibliographic coupling or co-citation and counts the number of links and the total strength of those links to prepare for a graphical network visualization (Van Eck and Waltman, 2010; Laengle et al., 2018). In this study, bibliometric analyses include the co-occurrence of keywords, citations, sources and the countries active in the targeted research by VOSviewer.

Circular Built Environment During the Digital Age: A Systematic Review

3.2.1. Co-occurrence of keywords bibliometric analysis

The mapping of co-occurrence of keywords indicates the frequency of appearance of study topics in one paper and the interrelatedness among topics (Jin et al., 2018). **Figure 5** provides an insight into the selected data from the eligibility phase of the PRISMA protocol, demonstrating the important keywords in the literature. The differentiation in the grayscale of keywords denotes their interconnections while circles' sizes denote their weights. The larger the circle of an item, the higher the weight in the network. The distance attribute says the relatedness among the keywords, which is in terms of co-occurrence linkage. Therefore, if two keywords are close, the connection between them is stronger. Keywords co-occurrence provides the mental map of research topics in the field and facilitates the researchers to identify the relation between those keywords. Moreover, this mapping helps to identify the clusters and frequency of keywords addressed, which paves the way to fill in the gaps for future studies.

Figure 5: Co-occurrence of keywords analysis.

374

JCoDe | Vol 6 No 2 | September 2025 | Tolerance in Computational Design | Kısmet Conk, B., Çolakoğlu, M. B.

The keywords which are the same in meaning but different in spelling are also combined. For instance, "ce" and "circular economy"; "building" and "buildings"; "sustainable" and "sustainability"; "BIM", "bim" and "building information modelling" and "building information model" are merged. Since circular economy, sustainability and built environment have larger circles, respectively, they have a higher weight than the other keywords for the network. In addition, CR is the most connected keyword in construction management with 58 occurrences. Built environment and sustainability both have the second frequency of usage (14) and are followed by construction, resource efficiency, BIM, digitalization and waste management. Total link strengths are shown in **Table 2.**

Keyword	Occurrences	Total Link Strength
Circular economy	58	106
Built environment	14	42
Sustainability	14	42
Construction	11	30
Resource efficiency	8	21
BIM	6	13
Digitalization	6	19
Waste management	4	8
Adaptive reuse	3	12
Buildings	3	11
Reuse	3	10
Industry 4.0	3	9

Table 2. Total link strengths of the Keywords Analysis.

3.2.2. Citation bibliometric analysis

This analysis highlights the most notable academic contributions to research on the circular economy (CE) within the built environment. Certain authors have specialized in CE research, producing influential articles. **Table 3** provides further details on the most frequently cited articles, including the authors' names, full source titles, and total citation counts. Among them, Dervishaj, A. And Gudmundsson, K. have played a leading role in advancing CE concepts in the AECO industry with 6 publications, The article with the highest citations is about waste management. The second and third most cited works circular economy strategies and transition frameworks. The fourth article discusses circular building industry, while the fifth focuses on energy efficiency and circular economy.

Table 3. Author-Source-Citation analysis

Paper	Title	Citations
Esmaeilian, B., Wang, B., Lewis, K., Duarte, F., Ratti, C., Behdad, S. (2018).	The future of waste management in smart and sustainable cities: A review and concept paper	219
Bonsu, N.O. (2020).	Towards a circular and low-carbon economy: Insights from the transitioning to electric vehicles and net zero economy	95
Gravagnuolo, A., Angrisano, M., Girard, Girard, L.F. (2019)	Circular economy strategies in eight historic port cities: Criteria and indicators towards a circular city assessment framework	95
Joensuu, T., Edelman, H., Saari, A. (2020).	Circular economy practices in the built environment	86
Gan, V.J.L., Lo, I.M.C., Ma, J., Tse, K.T., Cheng, J.C.P., Chan, C.M. (2020).	Simulation optimisation towards energy efficient green buildings: Current status and future trends	71
Shojaei, A., Ketabi, R., Razkenari, M., Hakim, H., Wang, J. (2021).	Enabling a circular economy in the built environment sector through blockchain technology	63
Heisel, F., Rau-Oberhuber, S. (2020).	Calculation and evaluation of circularity indicators for the built environment using the case studies of UMAR and Madaster	60
Çetin, S., De Wolf, C., Bocken, N. (2021).	Circular digital built environment: An emerging framework	53
Hoosain, M.S., Paul, B.S., Ramakrishna, S. (2020).	The impact of 4ir digital technologies and circular thinking on the United Nations sustainable development goals	50

3.2.3. Source bibliometric analysis

Research results are usually shared and communicated in multiple published journals and conferences. In this study, the source journals of the collected documents were identified by VOSviewer and presented in **Figure 6.** In total, 66 different sources published the selected papers. This information signifies that this topic is highly popular among current researchers and conferences. "IOP Conference Series: Earth and Environmental Science (EES)" is the leading conference series. Of papers, 13 are published from these conferences during the selected period. "Sustainability" is the pioneering international journal in this research area with 12 papers. "Journal of Cleaner Production" is the second leading conference with 9.

In addition, "Automation in Construction", "Buildings", "Resources, Conservation and Recycling" and "Smart and Sustainable Built Environment" are retrieved from the principal journals for this particular subject.
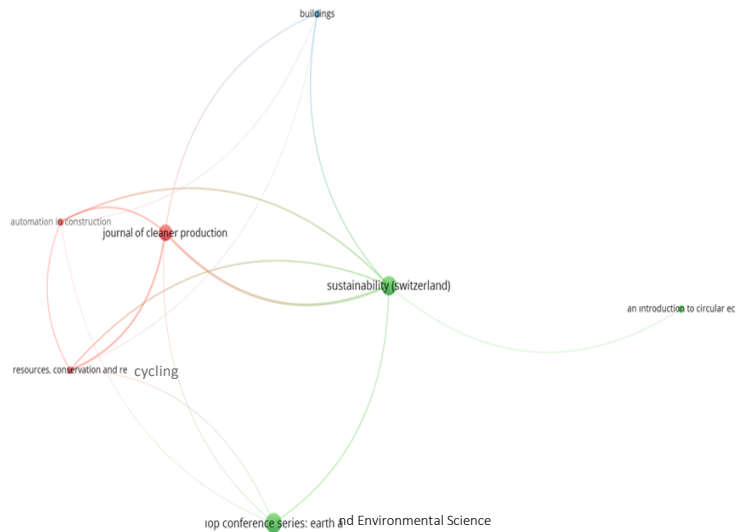
376

JCoDe | Vol 6 No 2 | September 2025 | Tolerance in Computational Design | Kısmet Conk, B., Çolakoğlu, M. B.

Figure 6: Source analysis.

4. DISCUSSION

In this study, the results of analyses have been discussed in terms of circular economy definitions, and circular economy related concepts. Based on the co-occurrence of keywords analysis, classification of keywords is generated whether there are about CE definitions and strategies or CE-related research areas, as shown in **Figure 7**. Thanks to the VOSviewer, keywords from similar or interrelated research areas are illustrated closer to each other. Also, interrelations between these keywords are linked to each other, allowing quicker interpretations.

For the further discussion in this study, CE definitions are investigated along with key theoretical perspectives; whereas CE-related concepts evaluated considering the relation with circularity and digitalization. These indicate the effective research areas of CE, which can help experts to conduct further research in this domain.
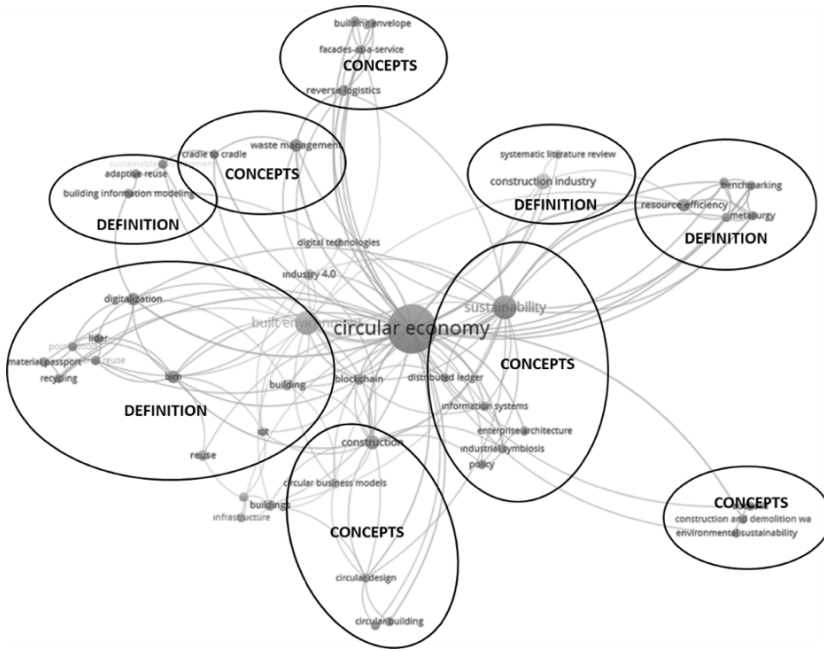
Circular Built Environment During the Digital Age: A Systematic Review

Figure 7: Classification of keywords into topics.

4.1. Circular Economy Definitions

This study highlights the most notable academic contributions to research on the circular economy (CE) within the built environment. The circular economy system offers a significant opportunity to reduce the consumption of primary materials, thereby conserving material resources and lowering the carbon footprint (EMF, 2013). In the literature, the concepts of the circular economy and circularity have been defined in various ways (Kirchherr et al., 2017). Kirchherr et al. (2017), after analysing 114 different definitions of the circular economy, identified the terms "reduce," "reuse," and "recycle," along with their various combinations, as the common elements across all definitions. The circular economy can be described as a business model and system design that is restorative and regenerative. By replacing the concept of life cycle and end-of-life with the principles of reuse and recycling, it aims to achieve sustainable processes (EMF, 2014). EMF and McKinsey (2015) have developed ReSOLVE Framework as a strategic approach in integrating sustainability and social responsibility into decision-making and business models. ReSOLVE (EMF and McKinsey, 2015) evaluates the systems according to six parameters: Regenerate, Share, Optimize, Loop, Virtualize and Exchange. UN Environmental Programme (UNEP, 2020) and Kirchherr et al. (2017) have defined circular economy strategies with 9Rs: Rethink, Refuse, Reduce, Reuse, Repair, Refurbish, Remanufacture, Repurpose and

378

JCoDe | Vol 6 No 2 | September 2025 | Tolerance in Computational Design | Kısmet Conk, B., Çolakoğlu, M. B.

Recycle. UNEP has developed conceptual context network and business model based on these 9Rs (UNEP, 2020). Three main concepts are named as Reduce, Reuse and Recycle in EU (2021) 's Circular Economy Action Plan (CEAP). According to EU (2023), circular economy has defined with 8Rs: Redesign, Refuse, Reduce, Reuse, Repair, Refurbish, Remanufacture, Repurpose. This strategy has ignored recycling as it will be the last choice. Doughnut economy (Raworth, 2017) evaluates rethinking the purpose and targets of economic activity, by systemic thinking to achieve social justice and ecological balance. A great deal of focus in the circular economy field is on the management of materials and ensuring that resource cycles are closed, in a similar way that occurs in natural ecosystems, where water and nutrients are continuously cycled. This approach has also studied in the literature throughout the years as "closed loops" or "closing the loop". Metabolic (2019) has developed "Seven Pillars of the Circular Economy" concept and defined these seven pillars as follows: materials are cycled at continuous high value, energy is based on renewable sources, water resources are extracted and cycled sustainably biodiversity is supported and enhanced through human activity, human society and culture are preserved, health and wellbeing of humans and other species are structurally supported and human activities maximize generation of societal value.

4.2. Circular Economy related Concepts

Considering the literature and systematic analysis, various concepts related to circular economy have defined. These are Cradle-to Cradle, Industrial Ecology, Closed Loop, Regenerative Design, Performance Economy, Biomimicry, Green Economy, Blue Economy and (Bio-Based Economy. Additionally, Sustainability is the most frequently used term related to circular economy. To understand and reveal the current situation of CE and these concepts within the digitalization, further bibliometric search is conducted.

The **Table 4** highlights the intersection of digital technologies with various circularity-related concepts by showcasing the number of publications and the most relevant keywords associated with each concept. Among the identified themes, "sustainability + digital" emerges as the most extensively studied, with 7,280 publications. This reflects the growing integration of digital tools in promoting sustainability, encompassing topics such as digital transformation,

innovation, and sustainable development. Following this, "life cycle/life cycle assessment (LCA) + digital" and "closed loop + digital" also demonstrate substantial research interest, with 6,328 and 5,688 publications respectively. These themes emphasize the role of digital technologies in lifecycle analysis, product design, and closed-loop control systems, underscoring their relevance to sustainable production and resource management.

**Table 4.** Bibliometric search series through different keywords.

Keywords	Number of Publications	Most Relevant Keywords
sustainability + digital	7280	Sustainability, sustainable development, digital storage, digital transformation, innovation
life cycle / life cycle assesment / lca + digital	6328	Life cycle, digital storage, information management, digital twin, product design
closed loop + digital	5688	Digital control systems, closed loop, controllers, discrete time control systems, digital storage
performance economy + digital	1863	Digital storage, digital economy, digital transformation, economics, sustainable development
circular economy + digital	703	Circular economy, sustainability, sustainable development, industry 4.0, life cycle
green economy + digital	643	Digital economy, china, sustainable development, green economy, digital storage
retrofit + digital	519	Retrofitting, digital storage, energy efficiency, energy utilization, buildings
regenerative design + digital	263	Digital storage, regenerative braking, analog to digital conversion, integrated circuits, energy efficiency
cradle to cradle / C2C + digital	235	Life cycle, digital storage, environmental impact, LCA, sustainable development
industrial ecology + digital	188	Ecology, industrial ecology, digital storage, ecosystems, sustainable development
biomimicry + digital	36	Biomimicry, design, digital fabrication, architectural design, 3D printing

Themes such as "performance economy + digital" (1,863 publications) and "circular economy + digital" (703 publications) focus on the economic and systemic aspects of integrating digital solutions. The term "performance economy" aligns with sustainable development and economic transformation, while "circular economy" links directly to concepts like Industry 4.0 and life cycle management. Lower publication numbers in categories like "green economy + digital" (643), "retrofit + digital" (519), and "regenerative design + digital" (263) suggest these areas may be emerging fields, gaining traction as

380

JCoDe | Vol 6 No 2 | September 2025 | Tolerance in Computational Design | Kısmet Conk, B., Çolakoğlu, M. B.

sustainability efforts evolve. Similarly, "cradle to cradle (C2C) + digital" (235), "industrial ecology + digital" (188), and "biomimicry + digital" (36) represent niche but significant research directions. These concepts emphasize environmental impact, sustainable ecosystems, and innovative design approaches, particularly through digital fabrication and 3D printing.

The keywords associated with each category underline the diverse applications of digital technologies in advancing sustainability goals. They range from digital storage and control systems to cutting-edge tools like digital twins, which facilitate information management and system optimization. This diversity reflects the broad potential for digital innovations to transform sustainability practices across various sectors. **Figure 8** discusses the major subject areas related to the terminology and concepts.

Figure 8: Major subject areas related to the terminology.
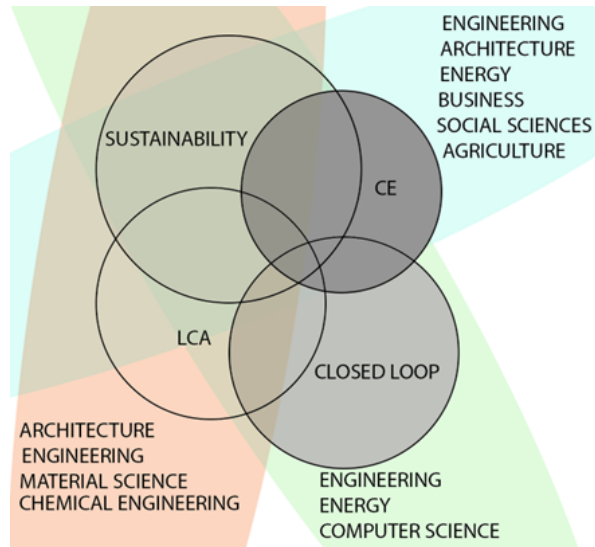
The relatively low number of publications (703) combining "circular economy + digital" in the table may be attributed to several factors. One explanation could be the novelty of integrating digital technologies into CE practices. While CE principles have gained considerable attention in recent years, leveraging tools such as blockchain for material tracking, artificial intelligence for optimizing resource flows, or digital twins for circular design is still an emerging area of research. As such, it remains less established compared to more generalized topics like "sustainability + digital" or "life cycle assessment (LCA) + digital." Another contributing factor is the complexity of applying CE principles

Circular Built Environment During the Digital Age: A Systematic Review

at scale. Unlike broader sustainability topics, CE research often focuses on specific material loops, product lifecycles, or business models, which naturally narrows the scope. Furthermore, implementing circular economy systems requires systemic change across industries, often involving coordination between policymakers, manufacturers, and consumers. This interdisciplinary nature and the need for collaboration can pose challenges to rapid research advancements. In addition, the adoption of digital tools to support CE is highly dependent on technological infrastructure and policy frameworks, which vary across regions and industries. The lack of widespread standardization and alignment may also contribute to the limited volume of research in this area.

Despite the current disparity, the **Table 4** and **Figure 8** suggests that CE research involving digital technologies is advancing, as indicated by keywords such as "sustainability," "life cycle," and "Industry 4.0." These terms underscore the growing recognition of digital tools as enablers of circular strategies. As industries increasingly adopt innovative technologies to support circular systems, the number of publications in this field is expected to grow, reflecting the critical role of digital transformation in achieving a circular economy.

5. CONCLUSION

The aim of this study is to investigate how circular economy and built environment research have emerged as key topics for sustainable development during the Industry 4.0. This study acts as a systematic literature review, using descriptive and bibliometric analysis to reveal the current situation, connections and intersections between CE and built environment research, which will provide significant insights to the area. This study uses mapping knowledge on CE in the built environment research area between 2016 and 2024 by employing VOSviewer to generate the bibliometric analysis. This systematic literature review does not only describe the current state of the research, but also investigates new trends and prospective areas for future directions which ends in contributing to the literature. By utilising PRISMA, the structure of the review is shaped and the accuracy of the review and sources are tested with QA criteria.

382

JCoDe | Vol 6 No 2 | September 2025 | Tolerance in Computational Design | Kısmet Conk, B., Çolakoğlu, M. B.

The main contribution of this study is providing reliable and latest theoretical knowledge along with investigating the CE-related research areas on digital & circular potentials in the AECO industry.

Several key insights can be drawn from this study. Firstly, multidisciplinary research of CE and built environment, which has been significantly accelerating since 2016, indicates that circular transition of the built environment should be studied for further investigation and has significant potential contributions in real life applications. As the number of publications has been continuously increased during the last eight years, this trend indicates the strength and growing interest in the topic. Secondly, sustainability is the most connected keyword in CE research, which is followed by resource efficiency, BIM and digitalization. Thirdly, circular built environment studies are mostly related to BIM, blockchain and IoT as components of Industry 4.0 in terms of digitalization pillar. Another significant finding, UK, Netherlands and Italy are at the forefront of this domain followed by China and Germany. The journal-wise distribution of the selected articles indicated that most papers have been published Sustainability, and Esmaeilian et al. are the most cited authors about "waste management in cities" study. Consequently, the results of analyses have been discussed in terms of circular economy definitions and circular economy related terms. Especially, its relation with sustainable development, LCA and C2C should be studied deeply.

The findings of this study reveal valuable information for researchers, practitioners and policymakers, allowing them to gain an in-depth understanding of CE in AECO industry. The main contribution of this work is providing reliable and latest theoretical knowledge along with investigating the future potentials on CE for the AECO industry. Theoretical key implications are; being up-to-date review on CE within the AECO industry, providing detailed insight about circular economy, its definitions, its strategies and similar research areas. Practical key implications are; being a latest study that presents the current situation, key topics, papers and authors to follow; addressing the future direction of the digital & circular transition by mentioning the related technologies and discussing the related concepts. The study provides transparent and detailed review for AECO experts especially to be used in circular transformation or circular implementations.

The findings of this study suggest that combining circularity with similar knowledge concepts will contribute to a deeper understanding and quicker implementation. On the other hand, this study limited the databases with Scopus and WoS, for the further studies, grey literature can be included. Moreover, only sources in English language are taken into account, in this regard, the study excludes the rest. Future research can focus on the integration of frameworks and strategic roadmaps as robust circular transition of the built environment and the AECO industry.

Acknowledgement

Conflict of Interest Statement

The manuscript is entitled "Circular Built Environment During the Digital Age: A Systematic Review" has not been published elsewhere and that it has not been submitted simultaneously for publication elsewhere.

Author Contribution

All authors contributed equally to this article.

References

Aghaei Chadegani, A., Salehi, H., Yunus, M. M., Farhadi, H., Fooladi, M., Farhadi, M., & Ale Ebrahim, N. (2013). A comparison between two main academic literature collections: Web of Science and Scopus databases. *Asian Social Science, 9*(5), 18–26. https://doi.org/10.5539/ass.v9n5p18

Amin, Z., Ali, N. M., & Smeaton, A. F. (2021). Attention-based design and user decisions on information sharing: A thematic literature review. *IEEE Access, 9,* 88255–88273. https://doi.org/10.1109/ACCESS.2021.3087740

Bonsu, N. O. (2020). Towards a circular and low-carbon economy: Insights from the transitioning to electric vehicles and net zero economy. *Journal of Cleaner Production, 256,* https://doi.org/10.1016/j.jclepro.2020.120659

Bornmann, L., Mutz, R., & Daniel, H. D. (2012). A reliability-generalization study of journal impact factors. Journal of the American Society for Information Science and Technology, 63(2), 389–393.

384

JCoDe | Vol 6 No 2 | September 2025 | Tolerance in Computational Design | Kısmet Conk, B., Çolakoğlu, M. B.

Cobo, M.J., López-Herrera, A.G., Herrera-Viedma, E. and Herrera, F. (2011). An approach for detecting, quantifying, and visualizing the evolution of a research field: a practical application to the Fuzzy Sets Theory field. *Journal of Informetrics*, 5, 146-166.

Çetin, S., De Wolf, C., & Bocken, N. (2021). Circular Digital Built Environment: An Emerging Framework. *Sustainability*, 13(11). https://doi.org/10.3390/su13116348.

Eberhardt, L. C. M., van Stijn, A., Rasmussen, F. N., Birkved, M., & Birgisdottir, H. (2020). Towards circular life cycle assessment for the built environment: A comparison of allocation approaches. *IOP Conference Series: Earth and Environmental Science, 588*(3), 032026. https://doi.org/10.1088/1755-1315/588/3/032026

Ellen MacArthur Foundation (EMF). (2013). *Towards the circular economy, opportunities for the consumer goods sector,* 2. Retrieved October 26, 2024, from https://www.werktrends.nl/app/uploads/2015/06/Rapport_McKinseyTowards_A_Circular_Economy.pdf

Ellen MacArthur Foundation (EMF). (2014). *Towards the circular economy Vol. 3: Accelerating the scale-up across global supply chains.* Ellen MacArthur Foundation. Retrieved October 26, 2024, from https://emf.thirdlight.com/file/24/cDm30tVcyxPQsxcD10AcOo2GK/Towards%20the%20circular%20economy%20Vol%203%3A%20Accelerating%20the%20scale-up%20across%20global%20supply%20chains.pdf

Ellen MacArthur Foundation (EMF) & McKinsey. (2015). *Growth within: A circular economy vision for a competitive Europe.* Ellen MacArthur Foundation. Retrieved February 20, 2025, from https://emf.thirdlight.com/link/8izw1qhml4ga-404tsz/@/preview/1?o

Esmaeilian, B., Wang, B., Lewis, K., Duarte, F., Ratti, C., & Behdad, S. (2018). The future of waste management in smart and sustainable cities: A review and concept paper. *Waste Management, 81,* 177–195. https://doi.org/10.1016/j.wasman.2018.09.047

European Commission. (2015, December 2). *Closing the loop: Commission adopts ambitious new Circular Economy Package* [Press release]. European Commission Press Corner. Retrieved February 20, 2025, from https://ec.europa.eu/commission/presscorner/detail/en/memo_15_6204

European Union (EU). (2023, December 1). Circular economy: Definition, importance and benefits. European Parliament. Retrieved February 11, 2025, from

https://www.europarl.europa.eu/topics/en/article/20151201STO05
603/circular-economy-definition-importance-and-benefits

European Union (EU). (2021, March 11). *A new Circular Economy Action Plan: For a cleaner and more competitive Europe.* European Commission. Retrieved February 11, 2025, from https://environment.ec.europa.eu/strategy/circular-economy-action-plan_en

Gan, V. J. L., Lo, I. M. C., Ma, J., Tse, K. T., Cheng, J. C. P., & Chan, C. M. (2020). Simulation optimisation towards energy efficient green buildings: Current status and future trends. *Journal of Cleaner Production, 262,* 120012. https://doi.org/10.1016/j.jclepro.2020.120012

Gravagnuolo, A., Angrisano, M., & Fusco Girard, L. (2019). Circular Economy Strategies in Eight Historic Port Cities: Criteria and Indicators Towards a Circular City Assessment Framework. *Sustainability*, 11(13), 3512. https://doi.org/10.3390/su11133512.

Guz, A. N., & Rushchitsky, J. J. (2009). Scopus: A system for the evaluation of scientific journals. *International Applied Mechanics, 45*(4), 351–362. https://doi.org/10.1007/s10778-009-0189-4

Hammersley, M. (2001). On 'systematic' reviews of research literature: a 'narrative' response to Evans and Benefield. *British Educational Research Journal,* 27, 543-554. https://doi.org/10.1080/01411920120095726

Heisel, F. & Rau-Oberhuber, S. (2020). Calculation and evaluation of circularity indicators for the built environment using the case studies of UMAR and Madaster. *Journal of Cleaner Production*, 243.

Hoosain, M. S., Paul, B. S., & Ramakrishna, S. (2020). The Impact of 4IR Digital Technologies and Circular Thinking on the United Nations Sustainable Development Goals. *Sustainability,* 12(23). https://doi.org/10.3390/su122310143

International Energy Agency (IEA). (2019). *2019 Global Status Report for Buildings and Construction: Towards a zero-emissions, efficient and resilient buildings and construction sector.* World Green Building Council. Retrieved January 10, 2025, from https://www.worldgbc.org/sites/default/files/2019%20Global%20Status%20Report%20for%20Buildings%20and%20Construction.pdf

Jin, R.Y., Gao, S., Cheshmehzangi, A. & Aboagye-Nimo, E. (2018). A holistic review of off-site construction literature published between 2008 and 2018. *Journal of Cleaner Production*, 202, 1202-1219.

Joensuu, T., Edelman, H. & Saari, A. (2020). Circular economy practices in the built environment. *Journal of Cleaner Production*, 276. https://doi.org/10.1016/j.jclepro.2020.124215.

386

JCoDe | Vol 6 No 2 | September 2025 | Tolerance in Computational Design | Kısmet Conk, B., Çolakoğlu, M. B.

Khan, A., Sepasgozar, S., Liu, T., & Yu, R. (2021). Integration of BIM and immersive technologies for AEC: A scientometric-SWOT analysis and critical content review. *Buildings, 11*(3), 126. https://doi.org/10.3390/buildings11030126

Kirchherr, J., Reike, D., & Hekkert, M. (2017). Conceptualizing the circular economy: An analysis of 114 definitions. *Resources, Conservation and Recycling, 127,* 221–232. https://doi.org/10.1016/j.resconrec.2017.09.005

Kirchherr, J., & van Santen, R. (2019). Research on the circular economy: A critique of the field. *Resources, Conservation and Recycling, 151,* 104480. https://doi.org/10.1016/j.resconrec.2019.104480

Kirchherr, J., Yang, N.N., Schulze-Spüntrup, F., Heerink, M.J. & Hartley, K. (2023). Conceptualizing the Circular Economy (Revisited): An Analysis of 221 Definitions. *Resources, Conservation and Recycling, 194,* https://doi.org/10.1016/j.resconrec.2023.107001

Kitchenham, B., Brereton, O.P., Budgen, D., Turner, M., Bailey, J. & Linkman, S. (2009). Systematic literature reviews in software engineering–a systematic literature review. *Information and software technology*, *51*(1), 7-15. https://doi.org/10.1016/j.infsof.2008.09.009

Kitchenham, B. A., Budgen, D., & Brereton, P. (2015). *Evidence-based software engineering and systematic reviews.* CRC press.

Kneese, A. V. (1988). The economics of natural resources. *Population and Development Review, 14*(2), 281–309. https://doi.org/10.2307/1973579

Metabolic. (2019, October 15). *Seven pillars of the circular economy.* Metabolic. Retrieved February 11, 2025, from https://www.metabolic.nl/news/the-seven-pillars-of-the-circular-economy/

Olawumi, T., Chan, D. W. M., Ojo, S., & Yam, M. C. H. (2022). Automating the modular construction process: A review of digital technologies and future directions with blockchain technology. *Journal of Building Engineering, 46,* 103720. https://doi.org/10.1016/j.jobe.2021.103720

Page, M. J., McKenzie, J. E., Bossuyt, P. M., Boutron, I., Hoffmann, T. C., & Mulrow, C. D. (2021). The PRISMA 2020 statement: An updated guideline for reporting systematic reviews. *BMJ, 372,* n71. https://doi.org/10.1136/bmj.n71

Petersen, K, Vakkalanka, S. & Kuzniarz, L. (2015). Guidelines for conducting systematic mapping studies in software engineering: An update. *Information and Software Technology,* 64, 1-18. https://doi.org/10.1016/j.infsof.2015.03.007

Raworth, K. (2017). *Doughnut economics: Seven ways to think like a 21st-century economist.* Chelsea Green Publishing. Retrieved February 11, 2025, from https://www.chelseagreen.com/product/doughnut-economics/

SCImago. (2024). Journal Rankings. Retrieved from https://www.scimagojr.com

Shahruddin, S. and Zairul, M. (2020). BIM requirements across a construction project lifecycle: a PRISMA-compliant systematic review and meta-analysis. *International Journal of Innovation, Creativity and Change,* 12,569-590. https://www.ijicc.net/images/vol12/iss5/12529_Shahruddin_2020_E_R2.pdf

Shojaei, A., Ketabi, R., Razkenari, M., Hakim, H., & Wang, J. (2021). Enabling a circular economy in the built environment sector through blockchain technology. *Journal of Cleaner Production*, 294. https://doi.org/10.1016/j.joi.2012.11.011

Tijssen, R. J. W., & van Raan, A. F. J. (1994). Mapping changes in science and technology: Bibliometric co-occurrence analysis of the R&D literature. *Evaluation Review,* *18*(1), 98–115. https://doi.org/10.1177/0193841X9401800110

United Nations (UN) Environment Programme (UNEP). (2020). *Building circularity.* UNEP. Retrieved May 11, 2024, from https://buildingcircularity.org/

United Nations (UN) Habitat. (2020). *World cities report 2020: The value of sustainable urbanization.* Nairobi, Kenya: UN-Habitat. Retrieved May 10, 2024, from https://unhabitat.org/World%20Cities%20Report%202020

United Nations (UN) Sustainable Development Goals (SDG). (2019). *Sustainable development goals: Guidelines.* UN. Retrieved May 10, 2024, from https://www.un.org/sustainabledevelopment/wp-content/uploads/2019/01/SDG_Guidelines_AUG_2019_Final.pdf

Usman, M., Ali, N., & Wohlin, C. (2023). A quality assessment instrument for systematic literature reviews in software engineering. *e-Informatica Software Engineering Journal,* *17*(1), 1–26. https://doi.org/10.37190/e-Inf230105

388

JCoDe | Vol 6 No 2 | September 2025 | Tolerance in Computational Design | Kısmet Conk, B., Çolakoğlu, M. B.

Van Eck, N. J., & Waltman, L. (2010). Software survey: VOSviewer, a computer program for bibliometric mapping. *Scientometrics, 84,* 523–538. https://doi.org/10.1007/s11192-009-0146-3

Yang, L., Zhang, H., Shen, H., Huang, X., Zhou, X., Rong, G. & Shao, D. (2021). Quality Assessment in Systematic Literature Reviews: A Software Engineering Perspective. *Information and Software Technology*, 130. https://doi.org/10.1016/j.infsof.2020.106397

Waltman, L., van Eck, N. J., van Leeuwen, T. N., & Visser, M. S. (2013). Some modifications to the SNIP journal impact indicator. *Journal of Informetrics,* *7*(2), 272–285. https://doi.org/10.1016/j.joi.2012.11.011

World Green Building Council. (2019, September 23). *World Green Building Week 2019.* World Green Building Council. Retrieved February 21, 2025, from https://worldgbc.org/wgbw19/

Zhuang, G.L., Shih, S.G. & Wagiri, F. (2023). Circular economy and sustainable development goals: Exploring the potentials of reusable modular components in circular economy business model. *Journal of Cleaner Production*, 414, https://doi.org/10.1016/j.jclepro.2023.137503.

390

JCoDe | Vol 6 No 2 | September 2025 | Tolerance in Computational Design | Kısmet Conk, B., Çolakoğlu, M. B.